



This is a digital copy of a book that was preserved for generations on library shelves before it was carefully scanned by Google as part of a project to make the world's books discoverable online.

It has survived long enough for the copyright to expire and the book to enter the public domain. A public domain book is one that was never subject to copyright or whose legal copyright term has expired. Whether a book is in the public domain may vary country to country. Public domain books are our gateways to the past, representing a wealth of history, culture and knowledge that's often difficult to discover.

Marks, notations and other marginalia present in the original volume will appear in this file - a reminder of this book's long journey from the publisher to a library and finally to you.

Usage guidelines

Google is proud to partner with libraries to digitize public domain materials and make them widely accessible. Public domain books belong to the public and we are merely their custodians. Nevertheless, this work is expensive, so in order to keep providing this resource, we have taken steps to prevent abuse by commercial parties, including placing technical restrictions on automated querying.

We also ask that you:

- + *Make non-commercial use of the files* We designed Google Book Search for use by individuals, and we request that you use these files for personal, non-commercial purposes.
- + *Refrain from automated querying* Do not send automated queries of any sort to Google's system: If you are conducting research on machine translation, optical character recognition or other areas where access to a large amount of text is helpful, please contact us. We encourage the use of public domain materials for these purposes and may be able to help.
- + *Maintain attribution* The Google "watermark" you see on each file is essential for informing people about this project and helping them find additional materials through Google Book Search. Please do not remove it.
- + *Keep it legal* Whatever your use, remember that you are responsible for ensuring that what you are doing is legal. Do not assume that just because we believe a book is in the public domain for users in the United States, that the work is also in the public domain for users in other countries. Whether a book is still in copyright varies from country to country, and we can't offer guidance on whether any specific use of any specific book is allowed. Please do not assume that a book's appearance in Google Book Search means it can be used in any manner anywhere in the world. Copyright infringement liability can be quite severe.

About Google Book Search

Google's mission is to organize the world's information and to make it universally accessible and useful. Google Book Search helps readers discover the world's books while helping authors and publishers reach new audiences. You can search through the full text of this book on the web at <http://books.google.com/>

B 1,298,230

PROPERTY OF
*University of
Michigan
Libraries*

1817

ARTES SCIENTIA VERITAS

1

2



ARTIFICIAL ELECTRIC LINES

McGraw-Hill Book Company

Publishers of Books for

Electrical World	The Engineering and Mining Journal
Engineering Record	Engineering News
Railway Age Gazette	American Machinist
Signal Engineer	American Engineer
Electric Railway Journal	Coal Age
Metallurgical and Chemical Engineering	Power

ARTIFICIAL ELECTRIC LINES

THEIR THEORY, MODE
OF CONSTRUCTION AND USES

BY

A. E. KENNELLY, A. M., Sc. D.

PROFESSOR OF ELECTRICAL ENGINEERING, HARVARD UNIVERSITY AND
THE MASSACHUSETTS INSTITUTE OF TECHNOLOGY; DIRECTOR
RESEARCH DIVISION OF ELEC. ENG. DEPT.; PAST PRESIDENT,
AM. INST. ELEC. ENGRS.; PAST PRESIDENT, ILLUM.
ENG. SOC.; PAST PRESIDENT, INST. RADIO
ENGRS.; GENL. SECY., INT. ELEC.
CONGRESS, ST. LOUIS

FIRST EDITION

McGRAW-HILL BOOK COMPANY, Inc.

239 WEST 39TH STREET. NEW YORK

LONDON: HILL PUBLISHING CO., LTD.

6 & 8 BOUVERIE ST., E. C.

1917



COPYRIGHT, 1917, BY THE
MCGRAW-HILL BOOK COMPANY, INC.

THE MAPLE PRESS, YORK PA

PREFACE

Artificial lines are now in practical use in various electrical industries; namely, in telegraphy, telephony, railway-track signalling and power transmission. The principles, construction and tests of such lines are therefore important industrially.

Artificial lines have already found their way, and are continuing to find their way, into the laboratories of engineering colleges, as aids to the class-room studies of electric transmission and distribution. The laboratory-class student who actually measures, in the concrete, the electric behavior of such lines, has a great advantage over the student who merely studies the same phenomena, in the abstract, out of a book. Moreover, to a student who may be apt to apply Ohm's law too generally, the fact that the current entering a line, under a constant impressed alternating e.m.f., is frequently greater when the distant end is freed, than when the distant end is grounded, is apt to come as a paradox and shock. A few tests on an alternating-current artificial line may quickly exorcise the mystery. The properties and utilities of engineering-laboratory artificial lines are therefore important educationally.

The engineering theory of artificial lines is far simpler in hyperbolic functions than in any other quantitative terms. Hyperbolic functions form the natural solution of the fundamental differential equations which all lines in the steady state necessarily obey. It is therefore important to develop the engineering theory of artificial lines in the direction of greatest simplicity. There is need. Engineering literature in the past contains some terrible examples of complexity in the non-hyperbolic theory of the subject.

In applied mathematics, generalized trigonometry is of enormous importance. Circular trigonometry has hitherto claimed almost exclusive consideration. A plea should be made for the beauty, simplicity and serviceability of hyperbolic trigonometry, in those regions where it naturally dominates.

It is the hope and purpose of this book to serve as a text-book on artificial lines for engineering-laboratory students, and also as a reference book for students of electric transmission generally.

The subject matter is a recent development of part of the contents of the author's earlier book on "The Application of Hyperbolic Functions to Electrical Engineering Problems." Some of the propositions offered here rest upon demonstrations already presented there.

A complete analysis and study of the behavior of electric lines would naturally include both transient and steady-state phenomena. The work here presented is restricted almost entirely to the phenomena of the steady state. For this reason, no attempt has been made to discuss the transient phenomena which occur on the artificial lines used in duplex telegraphy.

The author desires to express his indebtedness to the New England Telephone and Telegraph Co. and to the General Railway Signal Co. and Mr. C. F. Estwick for pictures and data of their artificial lines, also to Mr. H. F. Dodge, S. B., M. I. T., for assistance in preparing illustrations throughout the book; also to Mr. P. L. Alger, A. M., S. B., M. I. T., for assistance in the computations presented in Figs. 178 and 179, and to Mr. C. W. Whitall, S. B., M. I. T., for assistance in the tests; also to Dr. F. A. Wolff of the Bureau of Standards, for suggestions.

The author in this text is also under obligations to the writings and publications of many scientists and engineers whose names would make too long a list to permit of attempting an enumeration; but particularly to Heaviside and Fleming.

It is hoped that the book may serve as a stimulus to the study of the electrical phenomena of line conductors, a grand, absorbing, and practically most important subject.

A. E. K.

CAMBRIDGE, MASS.,
March, 1917.

CONTENTS

	PAGE
PREFACE	v
CHAPTER	
I. Descriptive Outline of Artificial Lines, Their Early History, and Their Uses	1
II. Elementary Trigonometrical Relations Applying to Real and Artificial Lines	6
III. Trigonometrical Properties of Real Continuous-current Lines .	15
IV. The Steady State Differential Equation of a Uniform Real Line	24
V. Impedance, Admittance and Power of a Smooth Line at Any Point	48
VI. Lumpy Artificial Lines	55
VII. Equivalent Circuits of a Smooth Line	89
VIII. The Design, Construction and Tests of Continuous-current Artificial Lines	101
IX. Complex Quantities and Alternating-current Quantities . . .	113
X. Fundamental Properties of Alternating-current Real Lines . .	141
XI. Fundamental Properties of Alternating-current Artificial Lines	164
XII. Design and Construction of Artificial Alternating-current Lines	196
XIII. Tests of Alternating-current Artificial Lines	219
XIV. Composite Lines	240
XV. Quarter-wave and Half-wave Lines	288
XVI. Regularly Loaded Lines	300
XVII. Various Types of Artificial Lines	309
XVIII. Miscellaneous Uses of Artificial Lines	316
APPENDIX A. List of Important Trigonometrical Formulas with Cir- cular and Hyperbolic Equivalents	323
APPENDIX B. Propositions Relating to Alternating Continued Fra- ctions	327
List of Symbols Employed	335
INDEX	343

1

ARTIFICIAL ELECTRIC LINES

CHAPTER I

DESCRIPTIVE OUTLINE OF ARTIFICIAL LINES, THEIR EARLY HISTORY, AND THEIR USES

An artificial electric line is a model line constructed of such materials, dimensions, and parts, so connected, that it shall at certain assigned terminals, be the electrical counterpart of a corresponding imitated real electric line. When the artificial line is connected to suitable terminal apparatus, such as a generator at one end, and a motor at the other, the voltage, current and power, at its assigned terminals, will be respectively the same as the corresponding quantities on the imitated real line, similarly connected to the same terminal apparatus.

The principal purpose of an artificial line is thus to furnish an electric model of a corresponding real line; so that the electrical behavior of the real line can be imitated by the model, in a manner suitable for either demonstration or observation in the laboratory. Not only may the electrical behavior of a projected real line be predetermined from observations on its model in the laboratory; but the behavior of an existing long real line may also be measured much more conveniently on a laboratory model, than is possible from simultaneous measurements at distant points on the real line.

The behavior investigated may relate either to the steady state of electric flow over the line, or to the transient states of electric flow, during disturbances. Since, however, the steady state is much the easier to examine, and is much more thoroughly understood in the present state of engineering knowledge, we shall confine ourselves, in the main, to the study of the steady states of artificial and real lines.

Artificial lines may be divided into two general types, namely:

1. Smooth lines, or lines in which the linear constants are distributed smoothly and uniformly throughout. Thus a smooth a.c. artificial line would have its resistance, inductance, capaci-

tance and leakance all intimately associated and continuously distributed.

2. Lumpy lines, or lines in which the linear constants are connected in successive lumps or localized units. Thus a lumpy a.c. artificial line would have alternate lumps of conductor impedance and dielectric admittance; *i.e.*, alternate reactors in series and condensers in shunt.

Smooth artificial lines have the advantage of being capable of imitating the electric conditions of real lines for all frequencies and transient conditions. Lumpy artificial lines have the advantages of being much simpler, more compact, more durable, cheaper and easier to construct. They react differently, however, to different frequencies; so that either some correction, or some examination for assurance, is necessary to make certain that the electrical behavior of a lumpy line is applicable to the real line imitated.

The theory of both real and artificial lines in the steady state naturally finds expression in hyperbolic functions. With the aid of these functions all the essential formulas are brief, easy and difficult to forget. Without them, the expressions to a like degree of precision are lengthy, ponderous and hard to remember. Examples of the contrast between hyperbolic and non-hyperbolic formulas will be presented, as occasion may serve, in the following pages.*

Historical Outline of Artificial Lines.—The artificial line of series resistance and shunt capacitance first came into use as an

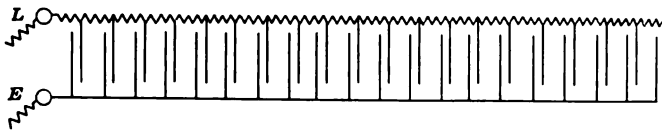


FIG. 1.—Varley artificial submarine cable of 1862.

adjunct of duplex submarine-cable telegraphy. In its first form it was a lumpy line with alternate lumps of resistance and capacitance, as represented in Fig. 1. A similar artificial line for duplex telegraphy was also employed by J. B. Stearns.

In a later form, introduced by Messrs. H. A. Taylor and Alex. Muirhead, the artificial line for duplex submarine-cable tele-

* In particular, see page 163, at the end of Chapter X.

† C. F. VARLEY, British Patent No. 3,453 of 1862.

raphy was a smooth line* in which resistance and capacitance were distributed uniformly together, as shown in Fig. 2. The construction employed for effecting the distribution of resistance and capacitance is indicated in Fig. 3. The first or upper electrode sheet of each paraffined paper layer is cut out into the form of a grid of such dimensions that the resistance of the strip between its ends *A* and *B* is such as should be associated with the

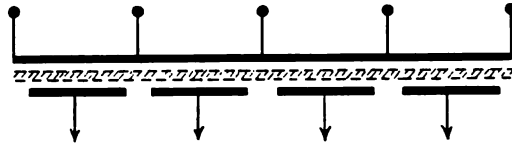


FIG. 2.—Muirhead smooth artificial cable of 1875.

capacitance of the condenser. The second or opposing sheet electrode remains uncut. All the upper sheets in each box are then connected in series, and all the lower sheets in parallel.

In the ordinary duplex system of land-line telegraphy, only a very crude model of the real line needs to be embodied in the artificial line, because the duplex balance is so crude, and the receiving instrument so relatively insensitive to imperfections of balance. In the duplex system as applied to long submarine cables, however, the siphon recorder, or other receiver used, is relatively very sensitive to feeble current changes; so that a high degree of electrical symmetry is required between the artificial and real cables at and near the sending ends. That is, the artificial cable must imitate the real cable closely, not only in steady states, but also throughout a large class of unsteady or transient states. A lumpy artificial line is, therefore, likely to be serviceable for submarine long-cable duplex balances only at a certain electrical distance from the sending end. Close to the sending end, it is important to have the artificial cable smooth and in close imitation of the real cable. Beyond the design of the artificial cable so as to attain the required degree of electrical imitation, the operation of duplex-cable telegraphy

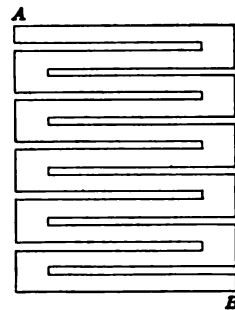


FIG. 3.

* H. A. TAYLOR and ALEX. MUIRHEAD, British Patent No. 684 of 1875.

did not demand a knowledge of the quantitative relations of artificial lines in the steady state.

An artificial line with distributed resistance, inductance and capacitance was constructed by Prof. M. I. Pupin in 1898, and

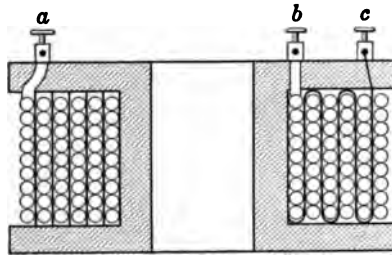


FIG. 4.—Longitudinal section of one coil of Pupin line containing resistance inductance and capacitance in association.

measurements on it were published by him in 1899.* The sections of this line consisted of coils of insulated wire having tinfoil sheets between the layers. These tinfoil sheets, connected together, formed one plate of a condenser, the other plate of which

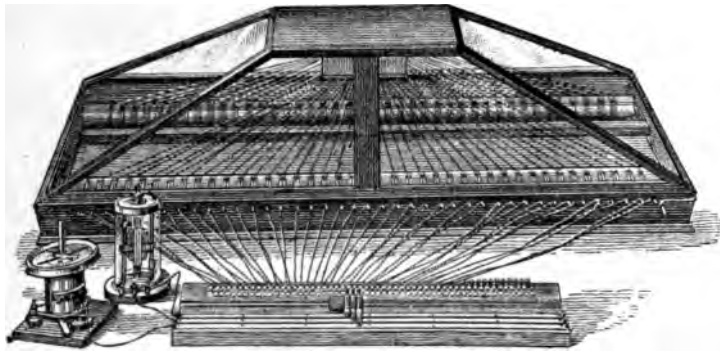


FIG. 5.—Section of an artificial line at Columbia University containing alternate lumps of inductive resistance and capacitance.

was formed by the insulated wire. A longitudinal section of one coil is shown in Fig. 4. One assemblance of coils into an artificial line is shown in Fig. 5.

A smooth artificial power-transmission line with distributed

* "Propagation of Long Electrical Waves," by M. I. PUPIN, *Trans. A. I. E. E.*, March, 1899, vol. xvi, pp. 93-142.

resistance, inductance and capacitance is described in the A. I. E. E. *Transactions* for 1912,* as having been installed at Union College, Schenectady. Its electrical length is stated as being 130 miles (209 km.) of a one-wire line of No. 1 A.W.G. copper wire, with resistance 93.6 ohms, inductance 0.3944 henry and capacitance 1.135 mf. The wire, No. 8 A.W.G. copper, was wound on glass cylinders, in 240 turns per cylinder. On the inside of each such tube was a tinfoil layer forming the grounded side of the condenser. There were about 400 of these wound



FIG. 6.—Unit tube of smooth artificial power line.

glass tubes. Each tube was about $4\frac{1}{2}$ ft. (1.37 m.) long, and 6 in. (15 cm.) in diameter, weighed complete some 40 lb. (18 kg.), and represented about 0.5 km. (0.3 mile) of the imitated line. The tubes were mounted on wooden racks, each about 9 ft. (2.74 m.) long, by $4\frac{1}{2}$ ft. (1.37 m. wide) and 8 ft. (2.44 m.) high, occupying about 324 cu. ft. (9.15 cu. m.) and holding 100 tubes. The total space occupied was thus about 1,300 cu. ft. (36.8 cu. m.) with over 7,000 lb. (3,180 kg.) of copper wire. A unit tube is illustrated in Fig. 6. Such a line is particularly well adapted for the study of very rapid transient phenomena.

* "Design, Construction and Test of an Artificial Transmission Line," by J. H. CUNNINGHAM, *Trans. A. I. E. E.*, February, 1911, vol. xxx, part 1, pp. 245-256.

CHAPTER II

ELEMENTARY TRIGONOMETRICAL RELATIONS APPLYING TO REAL AND ARTIFICIAL LINES

Before commencing the study of the electrical properties of artificial lines, it is important to define certain fundamental trigonometrical relations.

Real Circular Angles.—Let a radius-vector OP , Fig. 7 start, with center fixed at O , from an initial position OA , of unit length, on the reference line OX , and with its free end P on the circle APB defined by

$$x^2 + y^2 = 1 \quad (\text{units of length})^2 \quad (1)$$

and sweep over or describe the circular sector AOP , in the positive or counter-clockwise direction. Then the circular angle of the sector AOP is determined by the area of the sector AOP , and may be expressed in circular radians. We may for convenience construct a negative sector AOp , equal in area but opposite in direction, to the sector AOP . Then the magnitude of the circular angle AOP , in circular radians, will be numerically equal to the area of the double sector POp . In the case represented in Fig. 7, the radius OA of the circle being say 1 in., the shaded double sector is drawn to enclose an area of 1 sq. in., and the angle of the circular sector AOP is, therefore, 1 circ. radian. A positive circular angle is one which is described from the initial line OA in the positive or counter-clockwise direction of rotation. A negative circular angle, on the other hand, is described in the negative or clockwise direction. Circular angles may be reckoned from 0 to either + or - infinity; but for practical purposes they are usually limited to 360° (2π radians or $\frac{1}{2}$ quadrants), excess revolutions being ignored.

Real Hyperbolic Angles.—Let a radius-vector OP , Fig. 8, start with center fixed at O , from an initial position OA , of unit length, on the reference axis OX , and with its free end P on the rectangular hyperbola, pAP , defined by

$$x^2 - y^2 = 1 \quad (\text{units of length})^2 \quad (2)$$

sweep over or describe the hyperbolic sector AOP , in the positive or counter-clockwise direction. Then the hyperbolic angle of the sector AOP is determined by the area of the sector AOP , and may be expressed in *hyperbolic radians*. We may, for convenience, construct a negative sector AOp , equal in area but opposite in direction, to the sector AOP . Then the magnitude of the hyperbolic angle AOP , in hyperbolic radians, will be numerically equal to the area of the double sector POp . In the case represented in Fig. 8, the radius OA of the hyperbola being say 1 in., the shaded double area is drawn to enclose an area of 1

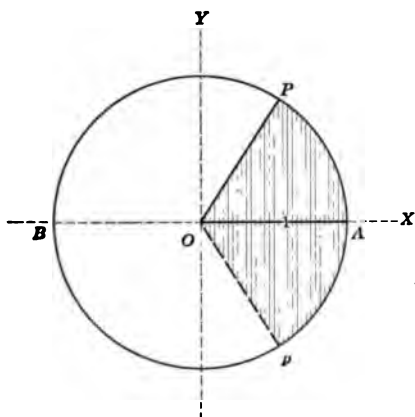


FIG. 7.—Circular angle.

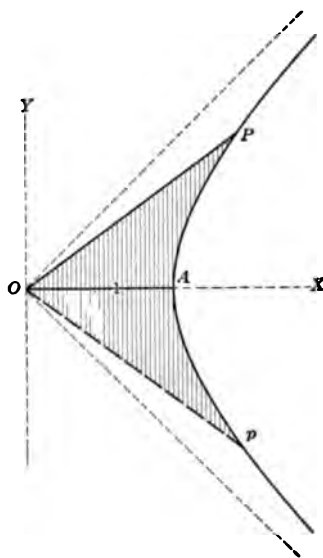


FIG. 8.—Hyperbolic angle.

sq. in., and the angle of the hyperbolic sector AOP is therefore 1 hyp. radian.

A positive hyperbolic angle is one which is described from the initial line OA in the positive or counter-clockwise direction of rotation. A negative hyperbolic angle, on the other hand, is described in the negative or clockwise direction. Hyperbolic angles extend from zero to either + or - infinity.

Common Properties of Real Circular and Hyperbolic Angles.—It will be evident from the foregoing, that, in radian measure, the magnitudes of circular and hyperbolic angles are similarly defined with reference to the area of circular and hyperbolic sec-

tors. A number of such geometrical analogies may be presented between circular and hyperbolic angles. One only may be noticed here; namely, that if the free end P of the radius-vector OP , Fig. 7, describes a very small circular arc ds , the magnitude of the very small circular angle thereby described is

$$d\beta = \frac{ds}{\rho} = \frac{ds}{1} = ds \quad \text{circ. radians} \quad (3)$$

where ρ is the unit length of the constant circular radius-vector OP . Similarly, if the free end P of the radius vector OP , Fig. 8, describes a very small hyperbolic arc ds , the magnitude of the very small hyperbolic angle thereby described is

$$d\theta = \frac{ds}{\rho} \quad \text{hyp. radians} \quad (4)$$

where ρ is the instantaneous length of the hyperbolic radius-vector OP .* The total circular or hyperbolic angle described in passing from one position to another of the radius-vector is, therefore,

$$\beta = \theta = \int \frac{ds}{\rho} \quad \text{radians} \quad (5)$$

but whereas ρ is constant in the circular case, it is variable in the hyperbolic case. In fact, if β is the circular angle and θ the hyperbolic angle of the hyperbolic segment AOP in Fig. 8,

$$\rho = \sqrt{\sec 2\beta} = \sqrt{\cosh 2\theta} \quad \text{units of length} \quad (6)$$

Thus, if we consider the case represented in Fig. 8, of a hyperbolic angle of 1 radian, the circular angle β of the aperture AOP is 0.65088 circ. radian, or $37^\circ 17' 33.67''$. The secant of $74^\circ 35' 07''$ is 3.762196, which is also the cosine of 2 hyperbolic radians. The radius-vector ρ in Fig. 8, therefore, has a length of

$$\sqrt{3.762196} = 1.93964$$

units, the unit being represented by the length OA .

Numerical Values of the Sines, Cosines and Tangents of Real Circular and Hyperbolic Angles.—Figs. 9 and 10 represent respectively a certain positive circular angle AOP , and a certain positive hyperbolic angle apo . The radius OA of the circle, and

* For a demonstration of (4), see Appendix L of "The Application of Hyperbolic Functions to Electrical Engineering Problems."

oa of the hyperbola, are each equal to unit length. In Fig. 10, os and os' are the asymptotes of the hyperbola, or the two straight lines, each inclined 45° with the radius oa , which the hyperbola continually approaches but never meets. Then, if we consider only numerical magnitudes, and ignore directions in the plane, we may find the sine, cosine and tangent of the two angles compared, β and θ respectively, by following the same construction in each case.

To Find the Numerical Value of the Sine.—From the free end of the radius-vector, drop a perpendicular on the initial radius. The length of this perpendicular measures the sine of the circular or hyperbolic angle. In Fig. 9, it is $\sin \beta = PQ$. In Fig. 10, it is $\sinh \theta = pq$. The sine of a real circular angle cannot exceed unity, and changes sign twice per revolution. The sine of a positive real hyperbolic angle is always positive, and may range from 0 to $+\infty$.

To Find the Numerical Value of the Cosine.—The intercept on the initial line OA , between the origin and the perpendicular let fall from the free end of the radius-vector, measures the cosine of the circular or hyperbolic angle. In Fig. 9, it is $\cos \beta = OQ$. In Fig. 10, it is $\cosh \theta = oq$. The cosine of a real circular angle cannot exceed unity, and changes sign twice per revolution. The cosine of a real hyperbolic angle cannot be less than unity, and is always positive. It ranges between $+1$ and $+\infty$.

To Find the Numerical Value of the Tangent.—Carry a perpendicular from the end of the initial radius (reversed for circular angles between $\frac{\pi}{2}$ and $\frac{3\pi}{2}$) up to the radius-vector or its production. The length of this perpendicular measures the tangent of the circular or hyperbolic angle. In Fig. 9, it is $\tan \beta = AT$. In Fig. 10, it is $\tanh \theta = at$. The tangent of a real circular angle may range between 0 and $\pm \infty$. It changes sign twice per revolution. The tangent of a positive real hyperbolic angle varies between 0 and $+1$.

The rules for finding the numerical values of the same trigonometrical functions of negative angles are identical. Thus taking AOP' and $ap'o$ as the negative circular and hyperbolic angles, QP' and qp' are their respective sines, OQ and oq their respective cosines, AT' and at' their respective tangents. In

either case, the sine of a negative angle is the negative of the sine of the same angle positive; the cosine of a negative angle is the same as the cosine of the same angle positive; the tangent of a negative angle is the negative of the tangent of the same angle positive.

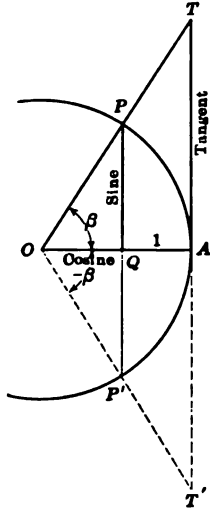


FIG. 9.—Constructions for the sine, cosine and tangent of a circular angle.

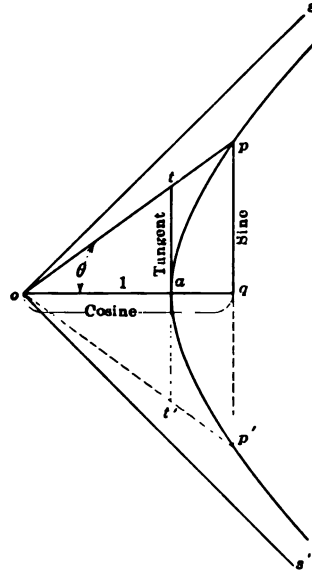


FIG. 10.—Constructions for the sine, cosine and tangent of a hyperbolic angle.

Fig. 11 shows the graphs of the sines, cosines and tangents of positive real circular and hyperbolic angles. The circular angles are expressed in *quadrant measure* and the hyperbolic angles in hyperbolic radian measure.

Reduction of Formulas from Circular to Hyperbolic Trigonometry.—From (482) and (483), we may write

$$\cos \beta = \cosh j\beta = \cosh (-j\beta) = \cosh \theta \quad \text{numeric} \quad (7)$$

if we assign to θ the value $\theta = -j\beta$, and similarly,

$$\sin \beta = -j \sinh j\beta = j \sinh (-j\beta) = j \sinh \theta \quad \text{numeric} \quad (8)$$

also

$$\tan \beta = -j \tanh j\beta = j \tanh (-j\beta) = j \tanh \theta \quad \text{numeric} \quad (9)$$

Any such identity involving circular functions in circular

trigonometry can be reduced to a corresponding identity in hyperbolic trigonometry, by substituting $\cosh \theta$ for $\cos \beta$, $j \sinh \theta$ for $\sin \beta$, and $j \tanh \theta$ for $\tan \beta$.

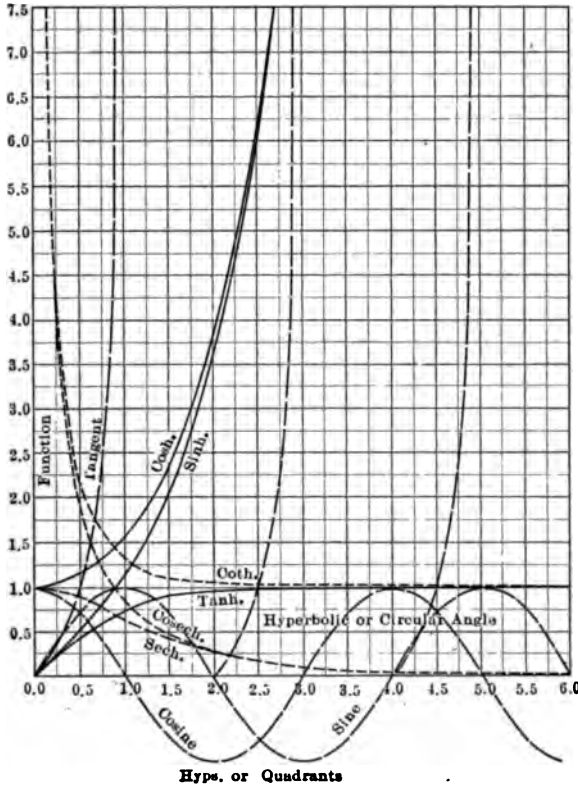


FIG. 11.—Graphs of circular and hyperbolic functions.

Thus, taking the well-known identity in circular trigonometry:

$$\cos^2 \beta + \sin^2 \beta = 1 \quad (10)$$

we have

$$\cosh^2 \theta + j^2 \sinh^2 \theta = 1$$

or

$$\cosh^2 \theta - \sinh^2 \theta = 1 \quad (11)$$

which is the corresponding hyperbolic identity. Again,

$$\sin(\beta_1 + \beta_2) = \sin \beta_1 \cos \beta_2 + \cos \beta_1 \sin \beta_2 \quad (12)$$

whence

$$j \sinh(\theta_1 + \theta_2) = j \sinh \theta_1 \cosh \theta_2 + \cosh \theta_1 \cdot j \sinh \theta_2$$

$$\text{or } \sinh(\theta_1 + \theta_2) = \sinh \theta_1 \cosh \theta_2 + \cosh \theta_1 \sinh \theta_2 \quad (13)$$

Similarly,

$$\cos(\beta_1 + \beta_2) = \cos \beta_1 \cos \beta_2 - \sin \beta_1 \cdot \sin \beta_2 \quad (14)$$

whence

$$\begin{aligned} \cosh(\theta_1 + \theta_2) &= \cosh \theta_1 \cosh \theta_2 - j \sinh \theta_1 \cdot j \sinh \theta_2 \\ \text{or } \cosh(\theta_1 + \theta_2) &= \cosh \theta_1 \cosh \theta_2 + \sinh \theta_1 \sinh \theta_2 \end{aligned} \quad (15)$$

In this manner, any transformation formula involving sines, cosines or tangents in circular trigonometry, can be immediately converted into the corresponding formula of hyperbolic trigonometry; so that it is not necessary to learn independently the formulas of hyperbolic trigonometry, in order to deal quantitatively with real or artificial electric lines.

A list of circular and hyperbolic formulas is given in Appendix A, for reference.

Geometrical Interpretation of the Exponentials $e^{j\beta}$ and $e^{-j\beta}$.—
If we expand $e^{j\beta}$ by Maclaurin's theorem, we obtain

$$e^{j\beta} = 1 + j\beta + \frac{(j\beta)^2}{2!} + \frac{(j\beta)^3}{3!} + \frac{(j\beta)^4}{4!} + \frac{(j\beta)^5}{5!} + \dots \quad \text{numeric} \quad (16)$$

$$\begin{aligned} &= 1 + j\beta - \frac{\beta^2}{2!} - \frac{j\beta^3}{3!} + \frac{\beta^4}{4!} + \frac{j\beta^5}{5!} - \dots \quad \text{numeric} \\ &= \left(1 - \frac{\beta^2}{2!} + \frac{\beta^4}{4!} - \dots\right) + j\left(\beta - \frac{\beta^3}{3!} + \frac{\beta^5}{5!} - \dots\right) \\ &= \cos \beta + j \sin \beta \quad \text{numeric} \quad (17) \end{aligned}$$

Thus if we construct, as in Fig. 12, $\cos \beta + j \sin \beta$, we obtain a plane vector or complex quantity OP , of unit length, making a circular angle β radians with the initial radius OA . The exponential $e^{j\beta}$, applied to any numerical quantity, thus leaves the numerical value of that quantity unchanged, but rotates it about the origin through a positive angle of β radians. Similarly, $e^{-j\beta} = \cos \beta - j \sin \beta$; so that OP' , Fig. 12, would represent such a quantity. The coefficients $e^{j\beta}$ and $e^{-j\beta}$ therefore modify only the polar circular angle, or "slope" of the quantity to which they are applied, and may be regarded as twisting operators. If β is taken large enough, the operator $e^{\pm j\beta}$ may cause the operand to be rotated many times about the origin in the plane of reference.

An exponential of the form $e^{j\omega t}$, where t is an elapsed time in

seconds, is a rotor which causes the operand to rotate positively about the origin in the plane of reference at the velocity of ω radians per sec. Similarly, $\epsilon^{-j\omega t}$ is a rotor in the clockwise or negative direction.

Geometrical Interpretation of the Exponentials ϵ^θ and $\epsilon^{-\theta}$.— If (Fig. 13) we draw the Cartesian axes OX, OY through the origin O , in the plane of reference XOY , and draw through a point A , whose coördinates are $x = 1, y = 1$, a rectangular hyperbola of radius OA , having OX and OY as asymptotes, then a radius-vector OP , starting from the initial position OA , with one end fixed at O , sweeping with its free end P in the positive direction

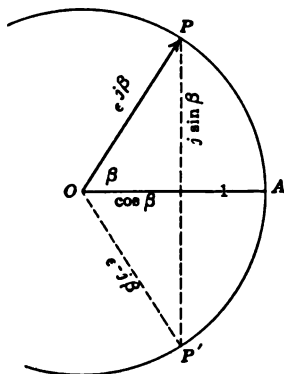


FIG. 12.—Graphical representation of the exponential $\epsilon^{\pm j\beta}$ in relation to an angle of $\pm\beta$ circular radians.

over the hyperbola, will describe a *hyperbolic angle* θ , measured by the area through which it has swept. The projection p of P , on the Y axis, will then measure ϵ^θ units of length from O . In Fig. 13, the successive positions of P for hyperbolic angles, differing by 0.1 hyp. radian, are indicated on the curve up to $\theta = 1.2$ hyps., with the corresponding exponentials ϵ^θ indicated on OY .

Similarly, if the radius-vector, starting from OA moves clockwise or negatively along the curve $AP'Q'$, describing an angle $-\theta$ hyp. radians, the corresponding projection p' on OY will be $Op' = \epsilon^{-\theta}$ units from O .

An exponential $\epsilon^{\pm\theta}$, may thus be interpreted as the *orthogonal**

* An orthogonal projection is defined as a projection made perpendicularly to the line or plane of projection.

projection of the free end of a radius-vector which has described a hyperbolic angle $\pm \theta$ radians.

Again, an exponential $e^{\pm at}$, where t is an elapsed time in seconds, may be interpreted as the orthogonal projection of the

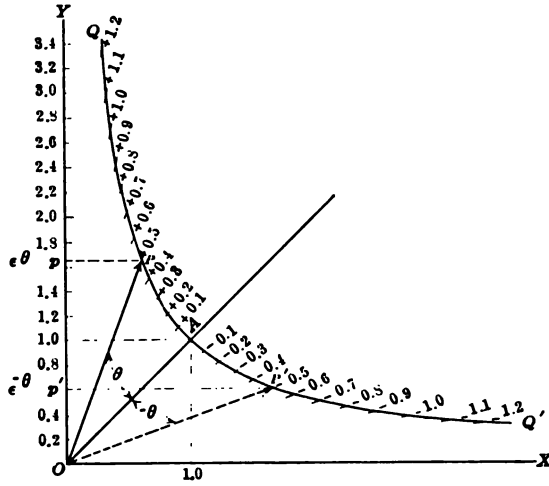


FIG. 13.

free end of a radius-vector moving over a rectangular hyperbola, with uniform angular velocity a hyp. radians per sec. describing equal areas in equal times.

CHAPTER III

TRIGONOMETRICAL PROPERTIES OF REAL CONTINUOUS-CURRENT LINES

Every c.c.* line, operated in the steady state, possesses two essential electrical properties, namely: (1) conductor resistance, and (2) dielectric leakance. Uniform c.c. lines have constant *linear resistance*, *i.e.*, constant conductor resistance in ohms per mile, or per kilometer, or other selected linear unit; and also constant *linear leakance*; *i.e.*, constant insulation leakance in mhos per mile, per kilometer, etc. Strictly speaking, in no actual line are these *linear constants* ever completely uniform. The resistance of equal lengths of conductor are never precisely equal, if only owing to accidental variations of temperature; or of conductor diameter; or of material quality. The dielectric leakance is still more liable to vary, over a certain range, along a line, if only owing to variations of temperature, humidity, dimensions and quality of the insulator. Nevertheless, if we consider any section of actual line having uniform dimensions and structure, we may, if the line is not defective or faulty, regard it as though it possessed a certain average linear resistance and average linear leakance. The more nearly the line conforms to these average values, the more nearly should its actual electric behavior conform to the behavior computed on the basis of the said averages. Unless we are entitled to assume some average linear constants from statistical knowledge of the line, we are debarred from making any logical quantitative estimate of the line's behavior. If the line is *composite*, *i.e.*, if it consists of a plurality of successive sections, each having its own linear constants, the behavior of the line can be predicated by taking each section into separate account (see Chapter XIV). If the line is discontinuous, in the sense of having a uniform section or sections, except at particular points where definite deviations or loads occur, such as an inserted resistance, or a known applied leak, then the effects of

*The contraction c.c. stands for continuous-current and a.c. for alternating-current.

these loads can be taken into separate account (see also Chapter XIV).

Hyperbolic Angle of a Line.—Consider the case of a single uniform line of length L km., such as is represented in Fig. 14, having a total actual aggregate conductor resistance of $R = Lr$ ohms, where r is the linear resistance in ohms per wire kilometer, also a total actual aggregate dielectric leakance of $G = Lg$ mhos, where g is the linear leakance. The number of leaks may be regarded as very great, and sufficiently uniform, so that the leakance of each or any particular kilometer of line is substantially constant at g mhos. Then the line will subtend or contain a

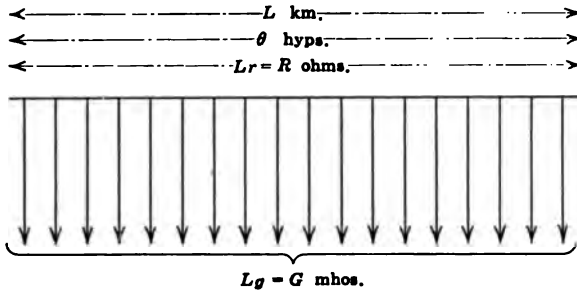


FIG. 14.—Diagram of a smooth single-wire line.

hyperbolic angle, θ , as is demonstrated in the next chapter, and which is defined by the relation

$$\theta = L\sqrt{rg} = L\alpha = \sqrt{RG} \quad \text{hyp.* radians } \angle \quad (18)$$

Here the *linear hyperbolic angle* of the line is

$$\alpha = \sqrt{rg} \quad \frac{\text{hyp. radians}}{\text{km.}} \angle \quad (19)$$

α is also called the *attenuation constant*, or the *propagation constant* of the line. It should be noted that the unit of length does not affect the value of θ . In other words, the angle subtended by any uniform line is independent of the unit of length; but the attenuation constant α is directly dependent on the unit of length; so that if r and g are respectively the resistance and leakance of the line per wire mile, then α will be 1.609 times larger than if r

* The angle sign \angle is appended to the unit of this and other following formulas to indicate that although, in the c.c. case, the units are essentially real, yet they may be regarded as complex or plane vector units in the general a.c. case.

and g are taken with reference to the wire kilometer. On the other hand, the angle θ of a line increases directly as its length, whereas the linear hyperbolic angle α is a characteristic of a given type of uniform line and has the same value whether the line is long or short.

As an example, let us take the case of a line of $L = 200$ km. (124.3 miles), $r = 4$ ohms per wire km. ($6.437 \Omega/\text{w.m.}$) and $g = 10^{-6}$ mho per wire km. ($1.609 \times 10^{-6} \text{ U/w.m.}$). Then $\alpha = \sqrt{4 \times 10^{-6}} = 0.002$ hyp. per km. This is the linear hyperbolic angle, or the attenuation constant. The angle subtended by the whole line ($R = 800$ ohms, $G = 2 \times 10^{-4}$ mho) is $\theta = \sqrt{800 \times 2 \times 10^{-4}} = 0.4$ hyp. radian, which is also equal to the length multiplied by the linear hyperbolic angle.

Significance of the Term Linear Hyperbolic Angle or Attenuation Constant.—A physical interpretation which may be placed upon α , the linear hyperbolic angle of the line, is that when the line is very long, either the current or the voltage, at the end of any selected kilometer length, is $\epsilon^{-\alpha}$ of that existing at the beginning of that kilometer length. In other words, the linear attenuation factor is the numeric $\epsilon^{-\alpha}$. If V is the potential in volts at any point on the line, in the steady state, then the potential 1 km. further along the line in the direction of flow of energy is $V_1 = V\epsilon^{-\alpha}$ volts. Similarly, the current being I amp. at the same point, the current 1 km. further on is $I_1 = I\epsilon^{-\alpha}$ amp. If, as is necessarily the case in practice, the value of α is small with respect to unity, since

$$\epsilon^{-\alpha} = 1 - \alpha + \frac{\alpha^2}{2!} - \frac{\alpha^3}{3!} + \dots \quad \text{numeric } \angle \quad (20)$$

we may, for most practical purposes, neglect the term $\frac{\alpha^2}{2!}$ and all its successors,

$$\text{so that} \quad V_1 = V(1 - \alpha) \quad \text{volts } \angle \quad (21)$$

$$\text{and} \quad I_1 = I(1 - \alpha) \quad \text{amp. } \angle \quad (22)$$

Thus, in the case considered, $\alpha = 0.002$ and

$$V_1 = V(1 - 0.002) = 0.998V \text{ volts,}$$

or the voltage falls by 0.2 per cent., or 0.002 per unit, in each kilometer of line length. The linear hyperbolic angle is thus the perunitage of attenuation, of either voltage or current, in a line

that is so long that there is no appreciable reflection from the distant end. If the line is short, the steady-state linear attenuation factor will, in general, differ from α . In such a case the *actual linear attenuation factor* differs from the *normal linear attenuation factor* $\epsilon^{-\alpha}$.

Normal Attenuation Factor.—A line of large real hyperbolic angle θ is necessarily a line of large attenuation, or one in which the current received at the distant delivery end is very weak with respect to the current at the generator end. If the line is grounded at the receiving end through a resistance equal to the “surge resistance” (see page 45), then the attenuation of voltage and of current will be $\epsilon^{-L\alpha} = \epsilon^{-\theta}$; so that if the potential and current at the generating end A are respectively V_A and I_A , the values at the receiving end, B , will be

$$V_B = V_A \epsilon^{-\theta} \quad \text{volts } \angle \quad (23)$$

and
$$I_B = I_A \epsilon^{-\theta} \quad \text{amp. } \angle \quad (24)$$

The ratio $\epsilon^{-\theta} = \epsilon^{-L\alpha}$ of received to generated voltage or current is called the *normal attenuation factor* of the line. In the case considered, this normal attenuation factor is $\epsilon^{-0.4} = 0.6703$; so that the percentage value of the generated current and voltage received at the distant end is 67.03; or the perunitage value 0.6703. The normal attenuation factor of a line may, therefore, be defined as equal to the perunitage value of the generated current or voltage received at the distant end of the line, when the line is grounded through its normal surge resistance. If the line is actually grounded through a resistance other than the surge resistance, the actual attenuation factors of voltage and current V_B/V_A and I_B/I_A , respectively, will, in general, differ from each other and from the normal attenuation factor $\epsilon^{-\theta}$.

Surge Resistance.—A uniform line of linear conductor resistance r ohms per wire km., and linear dielectric leakance g mhos per wire km., possesses a surge resistance r_0 which is the square root of their ratio

$$r_0 = \sqrt{\frac{r}{g}} \quad \text{ohms } \angle \quad (25)$$

This resistance is not affected by the length of the uniform line. If we consider a length L km. of the line, having a total conductor resistance $R = Lr$ ohms, and a total dielectric leakance $G =$

Lg mhos, the square root of their ratio will still be the surge resistance

$$r_0 = \sqrt{\frac{R}{G}} = \sqrt{\frac{Lr}{Lg}} = \sqrt{\frac{r}{g}} \quad \text{ohms } \angle \quad (26)$$

This resistance has been called various names by various writers, such as the "characteristic resistance," the "natural resistance," or the "iterative resistance." Any of these terms may be used. The term surge resistance has the advantages of brevity and distinctiveness. It was first applied* as meaning that resistance which a line automatically offers to its surges or free oscillations at the high-frequency limit, see formula (371). A physical meaning may be given to the term by noticing that, as will be shown later, the resistance which a uniform wire of indefinitely great length offers, between the home end and ground, is always equal to the surge resistance r_0 , whether the distant end is free, grounded or in any intermediate condition, assuming that the line is devoid of e.m.f. before applying the measuring apparatus. But although the surge resistance may conveniently be defined as the resistance offered by an infinite length of the uniform line considered, it should be remembered that any finite length of the line possesses a surge resistance, and the same surge resistance in all parts. Another way of presenting the same fact is that if for any length of the uniform line considered, we take the conductor resistance $R = Lr$, and the resistance corresponding to the total leakance $G = Lg$, then calling this equivalent leak resistance

$$R' = \frac{1}{G} \quad \text{ohms } \angle \quad (27)$$

the surge resistance will always be the geometrical mean of R and R' , or

$$r_0 = \sqrt{R \cdot R'} \quad \text{ohms } \angle \quad (28)$$

If the length L is great, the value of R will be large and that of R' small; while, on the contrary, if the length is short, R' will be large and R small; but their geometrical mean r_0 will not change.

Moreover, if the uniform line of any length L km. be successively freed and grounded at the distant end, its resistance to ground as measured at the home end will be say R_1 and R_2 ohms respectively. Then, as we shall see later, the geometrical mean

* "Surges in Transmission Circuits" by A. E. KENNELLY, *Electrical World*, Nov. 23, 1901, vol. xxxviii, No. 21, pp. 847-849.

of these two resistances, if correctly measured, will always be equal to the surge resistance r_0 ohms, no matter what the length of line; or

$$r_0 = \sqrt{R_f \cdot R_g} \quad \text{ohms } \angle \quad (29)$$

Single-wire and Two-wire Lines in Relation to α , θ and r_0 .—

We have hitherto considered only single-wire d.c. real lines using ground return, such as those used in ordinary wire telegraphy. We shall now examine two-wire lines forming a metallic circuit, such as are used in ordinary wire telephony.

In Fig. 15 a two-wire or metallic circuit is indicated as being voltageed at one end with an e.m.f. E_{11} , volts at battery terminals, and being loaded at the other end with a resistance R_{11} , ohms. A single kilometer length of this circuit $ab b'a'$ is selected from this line circuit for examination. Let the linear resistance of this

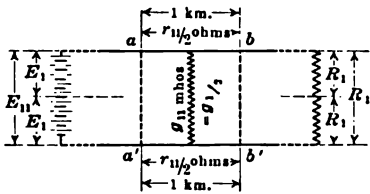


FIG. 15.—Two-wire line with metallic circuit.

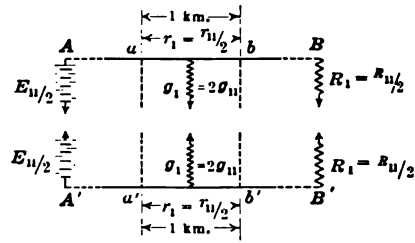


FIG. 16.—Two-wire line divided into two single-wire lines, each with perfect ground return circuit.

pair of wires be r_{11} ohms per loop km., and let the linear leakage be g_{11} mhos per loop km. Then, if the system is completely symmetrical, it is clear that there will be zero potential at the middle of the battery, and also at the middle of the load resistance. No electrical change can be made in the system by connecting either or both of these zero-potential points to ground. If they are both perfectly grounded, the system may properly be divided, as in Fig. 16, into two entirely separate and equal parts, AB and $A'B'$, each employing perfect ground-return circuit. The terminal voltage at A and also at A' will be $E_1 = E_{11}/2$; while the terminal receiving-end load resistance at B and also at B' , Fig. 16, will be $R_1 = R_{11}/2$. In the selected kilometer of Fig. 16 there will be in each circuit a conductor resistance of $r_1 = r_{11}/2$ ohms; while the leakage to ground will be $g_1 = 2g_{11}$ mhos, since two

equal conductances in series produce a total conductance one-half of either taken singly.

The linear hyperbolic angle of either ab or $a'b'$ in Fig. 16 will be $\sqrt{r, g}$, radians per km.; while that of the loop kilometer $abb'a'$ in Fig. 15 will be

$$\alpha_{,,} = \sqrt{r_{,,} g_{,,}} = \sqrt{2r, \cdot \frac{g,}{2}} = \sqrt{r, g,} = \alpha, \text{ radians per km. } \angle \quad (30)$$

It is evident that the linear hyperbolic angle will be the same whether reckoned on a loop-kilometer or on a wire-kilometer basis.

As an example, a two-wire line may be considered having a linear resistance $r_{,,} = 10$ ohms per loop km., and a linear leakance $g_{,,} = 4 \times 10^{-7}$ mho per loop km. Then, if the system were split into halves as in Fig. 16, we should have two ground-return systems in each of which the linear resistance was $r, = 5$ ohms per wire km., and a linear leakance $g, = 8 \times 10^{-7}$ mho per wire km. The linear hyperbolic angle on the two-wire basis would then be $\alpha_{,,} = \sqrt{10 \times 4 \times 10^{-7}} = 0.002$ radian per loop km.; while on the single-wire basis it would be $\alpha, = \sqrt{5 \times 8 \times 10^{-7}} = 0.002$ radian per wire km. It is evident that the linear hyperbolic angle would be the same for either case.

It, therefore, follows that since

$$\theta_{,,} = L\alpha_{,,} = L\alpha, = \theta, \quad \text{hyp. radians } \angle \quad (31)$$

the total hyperbolic angle θ subtended by a uniform two-wire line is the same as that subtended by either of the two single-wire lines into which it might be resolved.

If we form the surge resistance of the two-wire line based on formula (26) with the data for 1 loop km. we have

$$r_{0,,} = \sqrt{\frac{r_{,,}}{g_{,,}}} = \sqrt{\frac{2r,}{\left(\frac{g,}{2}\right)}} = 2\sqrt{\frac{r,}{g,}} = 2r_{0,} \quad \text{ohms } \angle \quad (32)$$

from which it appears that the surge resistance of a two-wire line is just double that of either of its single-wire components. This simple relation is easily borne in mind, if we notice that the two-wire circuit of Fig. 15 has twice the terminal e.m.f. of either component single-wire circuit of Fig. 16; so that with twice the terminal voltage the same current would flow through the doubled

surge resistance of Fig. 15 as with the single voltage and single surge resistance of Fig. 16.

In the case considered, the two-wire surge resistance would be

$$r_{0,,} = \sqrt{4 \times 10^{-7}} = 5,000 \quad \text{ohms}$$

while the single-wire surge resistance of each component circuit in Fig. 16 would be

$$r_0 = \sqrt{8 \times 10^{-7}} = 2,500 \quad \text{ohms}$$

We, therefore, conclude that when a two-wire circuit is under consideration, it is a matter of indifference whether we form the angle θ and surge resistance r_0 of the line from either loop-kilometer or from wire-kilometer constants, provided we adhere to one or the other set throughout. The values of θ and of α for the line will be the same in either case. The value of r_0 will bear a simple and self-evident 2 to 1 relation. Since, however, single wires are easier to represent and to carry in the mind than double wires, we shall continue to discuss only single-wire lines with perfect-ground or zero-potential return circuit, on the understanding that the results obtained are immediately applicable to two-wire or metallic-circuit lines. As for three-wire three-phase circuits, they are very commonly treated in single-wire star-branch single-phase components for general analysis; so that the single-wire mode of representation conveniently applies to them also. Since there is no numerical distinction between θ , and $\theta_{,,}$ or between α , and $\alpha_{,,}$, we shall drop these subscripts, and employ only the symbols θ and α . Similarly, we shall continue to use r_0 in preference to $r_{0,,}$ for the surge resistance of a single-wire uniform line.

Fundamental Constants of a Real Line.—In the theory of electric lines, the line angle θ with its linear value $\theta/L = \alpha$, as well as the surge resistance r_0 are to be regarded as the fundamental constants; while the resistance and leakance of the line, together with their linear values, are secondary constants which readily follow. Thus

$$r = \alpha r_0 \quad \text{ohms per wire km. } \angle \quad (33)$$

$$g = \alpha/r_0 \quad \text{mhos per wire km. } \angle \quad (34)$$

also

$$R = \theta r_0 \quad \text{ohms } \angle \quad (35)$$

$$G = \theta/r_0 \quad \text{mhos } \angle \quad (36)$$

Having postulated the relations between these fundamental constants of a real line, we shall proceed in the next chapter to demonstrate these relations in the theory of real lines, as a preliminary step to demonstrating their corresponding relations to the theory of artificial lines.

CHAPTER IV

THE STEADY-STATE DIFFERENTIAL EQUATION OF A UNIFORM REAL LINE

The Fundamental Differential Equations.—The differential equations of potential and current on a real uniform line, in the steady a.c. state, were given by Heaviside, with their algebraic solutions, in 1887; although the solutions offered were very lengthy and unserviceable.* The following presentation relates to the c.c. case, but applies also to the a.c. case, when the mathematical reasoning is extended from real to complex quantities, in a manner to be considered later.

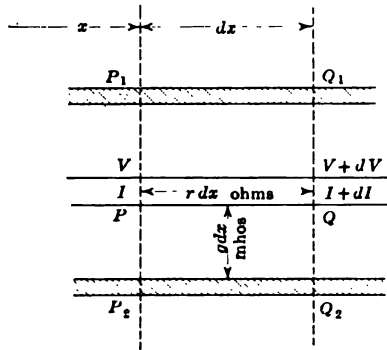


FIG. 17.—Longitudinal section of an element of leaky conductor.

Fig. 17 represents the longitudinal section of a short length of single-wire uniform cable conductor, with a metallic conductor PQ insulated from the grounded metallic sheath P_1Q_1, P_2Q_2 . Two neighboring parallel planes P_1P_2, Q_1Q_2 , dx km. apart, cutting across the cable perpendicularly, are indicated by the dotted lines. The plane P_1P_2 is at a distance x km. from the origin of the line on the left hand, not shown on the drawing. The plane Q_1Q_2 is therefore at a distance of $x + dx$ km. from the origin. The electrical conditions at the origin, and at the distant right-

* *The Electrician*, London, January-February, 1887; Reprinted in "Electrical Papers" by OLIVER HEAVISIDE, London, 1892, vol. ii, pp. 247-250.

hand end, of the line are not known, but the potential of the conductor PQ is V volts, at the point P , with respect to ground. The current in the conductor is also I amp. at the point P . This current is flowing from P to Q , or in the direction of increasing x .

Then the potential at Q will be $V + dV$ volts. The reason for the change of voltage in dx is the drop of potential in the conductor impedance. If r be the linear conductor impedance (linear resistance in the d.c. case), in ohms per kilometer, the resistance of the element of conductor is $r \cdot dx$ ohms \angle , and the change in potential from P to Q will be:

$$dV = - Ir \cdot dx \quad \text{volts } \angle \quad (37)$$

or
$$\frac{dV}{dx} = - Ir \quad \frac{\text{volts}}{\text{km.}} \angle \quad (38)$$

The current at P , or at x km. from the origin, being given at I amp., the current at Q , or $x + dx$, will be $I + dI$ amp. The current will change between P and Q , owing to dielectric leakage. If g be the linear admittance of the dielectric in mhos per kilometer (a real leakance in the d.c. case), the total leakance of the element PQ will be $g \cdot dx$ mhos \angle , and the change of current in dx is

$$dI = - Vg \cdot dx \quad \text{amp. } \angle \quad (39)$$

$$\frac{dI}{dx} = - Vg \quad \frac{\text{amp.}}{\text{km.}} \angle \quad (40)$$

If we differentiate (38) and (40), each with respect to x , we obtain

$$\frac{d^2V}{dx^2} = - r \frac{dI}{dx}, \quad \frac{\text{volts}}{\text{km.}^2} \angle \quad (41)$$

and
$$\frac{d^2I}{dx^2} = - g \frac{dV}{dx} \quad \frac{\text{amp.}}{\text{km.}^2} \angle \quad (42)$$

Substituting (40) in (41), and (38) in (42), we find

$$\frac{d^2V}{dx^2} = gr \cdot V \quad \frac{\text{volts}}{\text{km.}^2} \angle \quad (43)$$

and
$$\frac{d^2I}{dx^2} = gr \cdot I \quad \frac{\text{amp.}}{\text{km.}^2} \angle \quad (44)$$

Graphical Relations.—Equations (38) and (40) show that if we plot, for any d.c. case, the voltage and the current as ordi-

nates, against the distance x as abscissas, in the manner indicated in Fig. 18, where V, V is the curve of potential and I, I the curve of current along the line, then if the gradients of these curves are plotted, as in the broken curves, the gradient of V , or $\frac{dV}{dx}$, is the same, when taken to a suitable scale of ordinates, as the I, I curve negated, and similarly for the gradient of I . These relations must hold, in view of (38) and (40), whatever

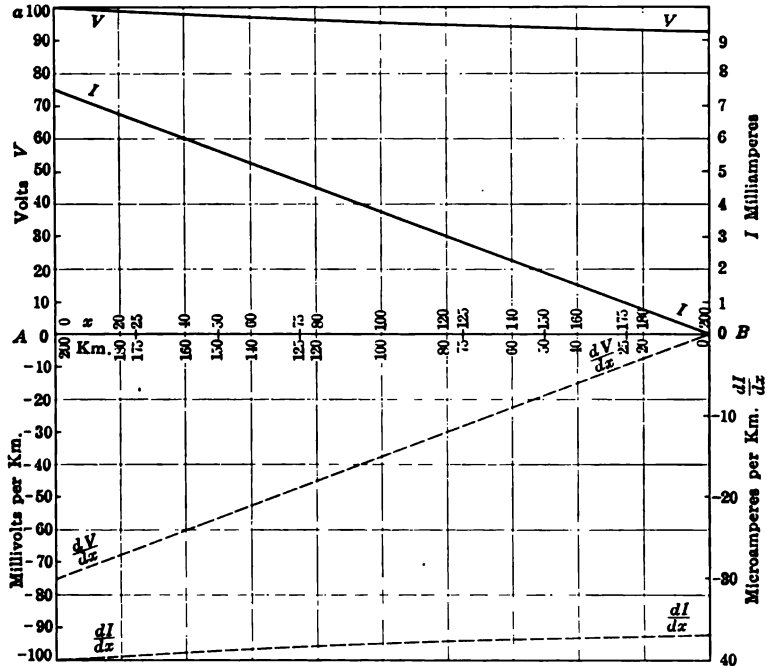


FIG. 18.—Graphs of potential and current and their gradients.

may be the terminal conditions of the line considered. Moreover, if we plot the gradient of the $\frac{dV}{dx}$ curve, or $\frac{d^2V}{dx^2}$, we reproduce the V curve to a suitably selected scale, and if we plot the gradient of the $\frac{dI}{dx}$ curve, or $\frac{d^2I}{dx^2}$, we reproduce the I curve to another particular scale.

In the case represented by Fig. 18, a single-wire uniform line of length $L = 200$ km. (124.3 miles), is freed at the distant end, and connected at the home end $x = 0$, to a potential $V_0 = + 100$

volts, supplied by a storage battery, whose negative pole is grounded. The linear constants of the line are $r = 10$ ohms per wire km. (16.09 ohms per wire mile), and $g = 0.4 \times 10^{-6}$ mho per wire km. (0.6436×10^{-6} mho per wire mile). The total resistance of the conductor is thus 2,000 ohms, and the total leakance 0.08×10^{-3} mho, corresponding to a line angle $\theta = 0.4$ hyp. radian, an attenuation constant $\alpha = 0.002$ hyp. radian per km., and a surge resistance $r_0 = 5,000$ ohms.

TABLE I
Particulars Relating to a Line of $\theta = 0.4$ Hyp. and $r_0 = 5,000$ Ohms Freed at Far End

x km.	L_2 km.	θ_2 hyps.	$\cosh \theta_2$	$\sinh \theta_2$	V volts	I amp.	$\frac{dV}{dx}$ volts km.	$\frac{dI}{dx}$ amp. km.	$\frac{d^2V}{dx^2}$ volts km. ²	$\frac{d^2I}{dx^2}$ amp. km. ²
0	200	0.40	1.08107	0.41075	100.000	7.5990	75.990	40.000	400.00	30.396
25	175	0.35	1.06188	0.35719	98.225	6.6081	66.081	39.290	392.90	26.432
50	150	0.30	1.04534	0.30452	96.695	5.6337	56.337	38.678	386.78	22.535
75	125	0.25	1.03141	0.25261	95.406	4.6734	46.734	38.163	381.63	18.693
100	100	0.20	1.02007	0.20134	94.357	3.7247	37.247	37.743	377.43	14.899
125	75	0.15	1.01127	0.15056	93.543	2.7854	27.854	37.417	374.17	11.142
150	50	0.10	1.00500	0.10017	92.964	1.8531	18.531	37.185	371.85	7.412
175	25	0.05	1.00125	0.05002	92.616	0.9254	9.254	37.047	370.47	3.702
200	0	0.00	1.00000	0.00000	92.501	0.0000	0.000	37.000	370.00	0.000

The preceding table shows the values of the voltage, current, and their respective gradients, at various distances along the line. Distances x km. from the home end appear in the first column, with corresponding distances L_2 from the far end, in the second column.

Fig. 18 gives the graphs of the values contained in the last six columns. The voltage curve, or catenary VV , falls from 100 at A , to 92.501 at B . The descending or negative gradient, dV/dx , of V , is given by the broken ascending line marked $\frac{dV}{dx}$, which commences at -75.99 millivolts per km. at A , and ends in zero at B . This curve is the image, or negative counterpart, of the I, I curve of current, which falls from 7.599 milliamper. at A , to zero at the open end B . The lowest and broken curve, marked $\frac{dI}{dx}$, is the graph of the gradient of I and is the image or negative counterpart of the V curve.

If we plot the values of $\frac{d^2I}{dx^2}$ from the last column of Table I, in Fig. 18, *i.e.*, the gradient of $\frac{dI}{dx}$, we should reproduce the I, I current curve, provided that we take the full ordinate Aa , as 40×10^{-9} amp. per km.² Similarly, if we plot $\frac{d^2V}{dx^2}$ from the preceding column of the table, or the gradient of $\frac{dV}{dx}$, we should reproduce the potential curve, provided that we take the full ordinate as 400 microvolts per km.². The change of scale is represented by the factor gr in (43) and (44).

Expressing (38) and (40) in words, we may say that on any uniform c.c. line, in the steady state, whatever the terminal conditions may be, *the voltage and current at any point are always so related that the local gradient of the one is proportional to the local value of the other.* Moreover, including the disclosures of (43) and (44), at any point, the gradient of the gradient, of the potential or the current, either one, is always proportional to the local value of the same. If the current I , say, falls in a certain distance to one-half, the gradient of the potential falls likewise to one-half, and the gradient of the gradient of I also falls to one-half, in the same distance. We shall see that corresponding conditions apply in the a.c. case.

Overhead Aerial Lines with Their Multiple Segregated Leaks.—

The type of cable conductor indicated in Fig. 17 may be regarded as having continuously distributed leakance, such as is contemplated and required in the reasoning of equations (37) to (44). In the case of an overhead aerial-line conductor, such as a telegraph wire, supported on insulators, spaced say 25 to the kilometer, or 40 to the statute mile, it is evident that the leakance is no longer strictly continuous, but occurs in little lumps 40 m. apart, and that these individual leaks are usually far from being all alike. However, actual tests show that except where faults or localized leak-disturbances interfere with the law of averages, an aerial-line conductor normally behaves substantially as though it had strictly continuous leakance. In other words, the deviation from theory in the observed properties of a not very short line, due to lumpiness, is ordinarily insignificant, when the lumps of leakance are only a few dekameters apart.

Primitive Equations, or Complete Solutions of the Fundamental Differential Equations.—Equations (43) and (44) are

the essential and fundamental differential equations for V and I on a uniform line in the steady state. Being of the second order, we must expect that the complete solution of either one will contain two arbitrary constants, to meet the terminal conditions of any particular case. Moreover, since these two equations are identical in form, their solutions must also be identical in form. Taking (43), the solution is*

$$V = A_v \cosh (\sqrt{gr} \cdot x) + B_v \sinh (\sqrt{gr} \cdot x) \quad \text{volts } \angle \quad (45)$$

where V is the potential at point x ; while A_v and B_v are the two arbitrary voltage constants. In view of (19), this may be written

$$V = A_v \cosh \alpha x + B_v \sinh \alpha x \quad \text{volts } \angle \quad (46)$$

Or, we may use the transformation of (506), Appendix A, and put

$$V = A'_v \cosh (\alpha x + \Delta') = A''_v \sinh (\alpha x + \Delta'') \quad \text{volts } \angle \quad (47)$$

Either (46) or (47) may be regarded as the complete solution of the fundamental differential equation (43), and, by differentiating either twice, we can obtain (43). In (46), we have V expressed as the sum of two hyperbolic functions, each involving an arbitrary or condition-satisfying coefficient. In (47), we have V expressed as a single hyperbolic function with one arbitrary coefficient; but the hyperbolic angle includes another arbitrary constant, which is a condition-satisfying hyperbolic angle. In c.c. cases, there is usually but little choice between these two forms of the primitives (46) and (47); but in a.c. cases, we shall see that (47) is ordinarily the easier to compute with.

From the type identity of (43) and (44), we may infer that there is a corresponding pair of equivalent solutions of (44), namely:

$$I = A_i \cosh \alpha x + B_i \sinh \alpha x \quad \text{amp. } \angle \quad (48)$$

or

$$I = A'_i \cosh (\alpha x + \Delta_i) = A''_i \sinh (\alpha x + \Delta_{i'}) \quad \text{amp. } \angle \quad (49)$$

where I is the current at any point x along the line, A_i , B_i , A'_i , and A''_i are condition-satisfying currents in amperes; while Δ_i and $\Delta_{i'}$ are condition-satisfying hyperbolic angles.

Another form of primitive equation which satisfies the funda-

* O. HEAVISIDE, "Electromagnetic Theory," 1893, vol. i, p. 451.

mental differential equation (43), and which may be obtained by transformation from either (46) or (47) is

$$V = A''_v \epsilon^{\alpha x} + B''_v \epsilon^{-\alpha x} \quad \text{volts } \angle \quad (50)$$

with a similar expression for I ; but except in the case of indefinitely long lines, or of ordinary lines behaving as such, by being grounded through a load equal to their surge resistance; this exponential form does not lend itself to computation so well as the hyperbolic forms.

Evaluation of the Arbitrary Constants in the Primitive Equations.—The assignment of particular values to the arbitrary constants in the primitive equations (45) to (50), in order to meet a given set of terminal conditions, ordinarily requires that both the current and the potential shall be given at one end of the

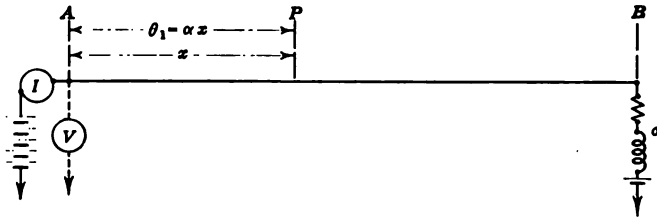


FIG. 19.—Line loaded at the motor end. The potential and current at the generator end are given.

line. If we consider a line AB , Fig. 19, we may suppose that A is the *generator end*, and B the *motor end* of the line; so that, in the steady state, electrical energy shall flow from A to B . In order, therefore, to reduce any of the primitive equations (45) to (50) to a definite arithmetical basis, we need, in general, to know either V_A and I_A , the potential and current at A ; or else V_B and I_B , the potential and current at B . While, theoretically, it would suffice to have one of these data from the A end, and the other from the B end, yet, from a practical standpoint, this would be an unlikely condition. Although two terminal data from one end, therefore, are sufficient for the evaluation of the two arbitrary constants of any of the primitive equations (45) to (50), yet we shall see that if we know the terminal motor load; *i.e.*, the impedance at the receiving end B , only one other datum, say the potential or current at either A or B , is needed for the complete solution of the case.

Evaluation from Data at the Generator End.—Taking first the case where the A -end potential and entering current I_A are given, let AB , Fig. 19, be any uniform single-wire line, with an impressed potential of V_A volts at A , as observed by voltmeter V , and with any load whatever of σ ohms at B . This load may also contain any steady counter e.m.f. Let the steady current entering the line at A observed on the ammeter I be I_A amp. then let the voltage be required at the point P , distant x km. from A . The uniform linear constants r and g of the line are supposed to be known; so that the linear angle α hyp. radians per km. is found by (19). Then the angular distance of the position P from A is $\theta_1 = \alpha x$ hyp. radians. We may therefore, write the primitive equation (46) in the form

$$V_P = A_v \cosh \theta_1 + B_v \sinh \theta_1 \quad \text{volts } \angle \quad (51)$$

Since the distance x is here quite arbitrary, we may assign to it the particular value $x = 0$, which means moving the point P up to the end A , where the potential is V_A volts by hypothesis, and the distance angle $\theta_1 = 0$; so that we have:

$$V_A = A_v \cosh 0 + B_v \sinh 0 \quad \text{volts } \angle \quad (52)$$

But $\cosh 0 = 1$, and $\sinh 0 = 0$; so that $A_v = V_A$, and if this happens when $x = 0$, it is evident that it must happen in (51) for any value of x . Hence, rewriting (51)

$$\begin{aligned} V_P &= V_A \cosh \theta_1 + B_v \sinh \theta_1 \\ &= V_A \cosh \alpha x + B_v \sinh \alpha x \end{aligned} \quad \text{volts } \angle \quad (53)$$

If we differentiate (53) with respect to x , we have

$$\begin{aligned} \frac{dV_P}{dx} &= \alpha V_A \sinh \alpha x + \alpha B_v \cosh \alpha x \\ &= \alpha V_A \sinh \theta_1 + \alpha B_v \cosh \theta_1 \end{aligned} \quad \begin{array}{l} \text{volts} \\ \text{km.} \end{array} \angle \quad (54)$$

and substituting (38)

$$-I_P r = \alpha V_A \sinh \theta_1 + \alpha B_v \cosh \theta_1 \quad \begin{array}{l} \text{volts} \\ \text{km.} \end{array} \angle \quad (55)$$

where I_P is the current strength at the selected point P . If, as before, we move P up to A , so as to make $x = 0$, and $\theta_1 = 0$, I_P becomes I_A and

$$-I_A r = \alpha V_A \sinh 0 + \alpha B_v \cosh 0 \quad \begin{array}{l} \text{volts} \\ \text{km.} \end{array} \angle \quad (56)$$

whence
$$B_v = -I_A \frac{r}{\alpha} \quad \text{volts } \angle \quad (57)$$

or by (33)
$$= -I_A r_0 \quad \text{volts } \angle \quad (58)$$

or B_v is the drop in potential produced by the entering current in resistance equal to r_0 ; so that rewriting (51), we have:

$$\begin{aligned} V_P &= V_A \cosh \theta_1 - I_A r_0 \sinh \theta_1 \\ &= V_A \cosh \alpha x - I_A r_0 \sinh \alpha x \quad \text{volts } \angle \quad (59) \end{aligned}$$

This formula expresses the potential V_P at any point P , along the line, distant θ_1 hyp. radians from the generator end, in terms of V_A , I_A , and line constants.

Similarly, from (48), we have for the current in the line at the point P :

$$I_P = A_i \cosh \alpha x + B_i \sinh \alpha x = A_i \cosh \theta_1 + B_i \sinh \theta_1 \quad \text{amp. } \angle \quad (60)$$

Taking $x = 0$, and $\theta_1 = 0$, this places P at A and makes $I_P = I_A$;

so that
$$I_A = A_i \cosh 0 + B_i \sinh 0 \quad \text{amp. } \angle \quad (61)$$

whence
$$A_i = I_A \quad \text{amp. } \angle \quad (62)$$

a condition which must hold for all values of x , and rewriting (60), we obtain

$$I_P = I_A \cosh \alpha x + B_i \sinh \alpha x = I_A \cosh \theta_1 + B_i \sinh \theta_1 \quad \text{amp. } \angle \quad (63)$$

Differentiating with respect to x , it follows that:

$$\begin{aligned} \frac{dI_P}{dx} &= \alpha I_A \sinh \alpha x + \alpha B_i \cosh \alpha x \\ &= \alpha I_A \sinh \theta_1 + \alpha B_i \cosh \theta_1 \quad \frac{\text{amp.}}{\text{km.}} \angle \quad (64) \end{aligned}$$

and by (40)

$$-gV_P = \alpha I_A \sinh \theta_1 + \alpha B_i \cosh \theta_1 \quad \text{amp. } \angle \quad (65)$$

where V_P is the potential at the selected point P . If we move P to A so that $x = 0$ and $\theta_1 = 0$, $V_P = V_A$, and

$$\begin{aligned} -gV_A &= \alpha I_A \sinh 0 + \alpha B_i \cosh 0 \quad \text{amp. } \angle \quad (66) \\ &= 0 + \alpha B_i \end{aligned}$$

or
$$B_i = -\frac{g}{\alpha} V_A \quad \text{amp. } \angle \quad (67)$$

Substituting (34),
$$B_i = -\frac{V_A}{r_0} \quad \text{amp. } \angle \quad (68)$$

so that rewriting (60) and (63)

$$\begin{aligned}
 I_P &= I_A \cosh \alpha x - \frac{V_A}{r_0} \sinh \alpha x \\
 &= I_A \cosh \theta_1 - \frac{V_A}{r_0} \sinh \theta_1 \quad \text{amp. } \angle \quad (69)
 \end{aligned}$$

This formula expresses the current strength I_P at any point P along the line, distant θ_1 hyp. radians from the generator end, in terms of V_A , I_A and line constants.

As an example, let us take the case of the line referred to in Table I and Fig. 19. Here the observed impressed terminal potential is $V_A = 100$ volts, and the terminal entering current $I_A = 7.599 \times 10^{-3}$ amp. The surge resistance of the line is

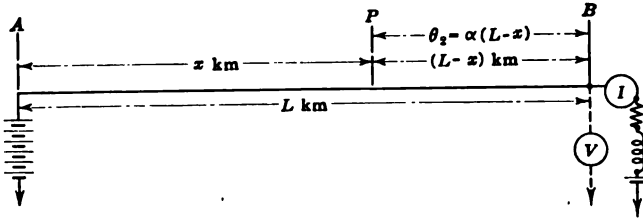


FIG. 20.—Line voltage at A and loaded at B . The potential and current at the B end are observed.

$r_0 = 5,000$ ohms. Then the potential at a point P , 50 km. from A , and, therefore, removed from A by an angular distance of 0.1 hyp. radian, is by (59)

$$\begin{aligned}
 V_P &= 100 \cosh 0.1 - 7.599 \times 10^{-3} \times 5 \times 10^3 \times \sinh 0.1 \\
 &= 100 \times 1.00500 - 37.995 \times 0.10017 \\
 &= 100.500 - 3.806 = 96.694 \text{ volts.}
 \end{aligned}$$

The current strength at the same point is also by (69)

$$\begin{aligned}
 I_P &= 7.599 \times 10^{-3} \cosh 0.1 - \frac{100}{5,000} \sinh 0.1 \\
 &= 7.599 \times 10^{-3} \times 1.00500 - 0.020 \times 0.10017 \\
 &= 7.637 \times 10^{-3} - 2.0034 \times 10^{-3} = 5.6336 \times 10^{-3} \quad \text{amp.}
 \end{aligned}$$

The above values are in close conformity with those given in Table I, which were computed in a somewhat different way.

Evaluation from Data at the Motor End.—If the potential and current are observed at the B end of the line, V_B and I_B respectively, as indicated in Fig. 20, then we may reckon the distance $(L - x)$ km. from B toward A , and take

$$\theta_2 = (L - x) \quad \text{hyp. radians } \angle \quad (70)$$

as the hyperbolic angular distance of the point P and B .

We may then rewrite (46)

$$\begin{aligned} V_P &= A_v \cosh \alpha(L - x) + B_v \sinh \alpha(L - x) \\ &= A_v \cosh \theta_2 + B_v \sinh \theta_2 \quad \text{volts } \angle \quad (71) \end{aligned}$$

If now we bring the point P into coincidence with B , so that

$$\begin{aligned} x &= L \text{ and } \theta_2 = 0, V_P = V_B \\ \text{and} \quad V_B &= A_v \cosh 0 + B_v \sinh 0 \quad \text{volts } \angle \quad (72) \end{aligned}$$

$$\text{or} \quad A_v = V_b$$

We therefore rewrite (71)

$$\begin{aligned} V_P &= V_B \cosh \alpha(L - x) + B_v \sinh \alpha(L - x) \\ &= V_B \cosh \theta_2 + B_v \sinh \theta_2 \quad \text{volts } \angle \quad (73) \end{aligned}$$

If we differentiate this with respect to increasing x , we have, by (38),

$$\begin{aligned} \frac{dV_P}{dx} &= -V_B \alpha \sinh \alpha(L - x) - B_v \alpha \cosh \alpha(L - x) \\ &= -V_B \alpha \sinh \theta_2 - B_v \alpha \cosh \theta_2 = -I_P r \frac{\text{volts}}{\text{km.}} \angle \quad (74) \end{aligned}$$

Bringing P up to B once more, with $\theta_2 = 0$, $I_P = I_B$

$$V_B \alpha \sinh 0 + B_v \alpha \cosh 0 = I_B r \frac{\text{volts}}{\text{km.}} \angle \quad (75)$$

$$\text{whence} \quad B_v = I_B \frac{r}{\alpha} = I_B r_0 \quad \text{volts } \angle \quad (76)$$

Consequently (46) becomes in the general case:

$$\begin{aligned} V_P &= V_B \cosh \alpha(L - x) + I_B r_0 \sinh \alpha(L - x) \\ &= V_B \cosh \theta_2 + I_B r_0 \sinh \theta_2 \quad \text{volts } \angle \quad (77) \end{aligned}$$

Similarly, to find the current I_P we may rewrite (48), and, in the same way as before, obtain:

$$\begin{aligned} I_P &= I_B \cosh \theta_2 + \frac{V_B}{r_0} \sinh \theta_2 \\ &= I_B \cosh \alpha(L - x) + \frac{V_B}{r_0} \sinh \alpha(L - x) \quad \text{amp. } \angle \quad (79) \end{aligned}$$

As an example, we may consider the case represented in Fig.

21, of a line AB , 150 km. in length, with 100 volts impressed at A , and the B end grounded through a resistance $\sigma = 1,000$ ohms. The linear constants are $r = 4$ ohms/wire km. and $g = 10^{-6}$ mho/wire km. To these correspond the values $\alpha = 0.002$ hyp./wire km., $\theta = 0.3$ hyp. and $r_0 = 2,000$ ohms. In this case, the receiving end potential V_B is 60.446 volts, and the receiving-end current I_B is 60.446 milliamp. Starting with these data, and taking a point P 50 km. from B , $\theta_2 = 0.1$ hyp. radian, we have by (77)

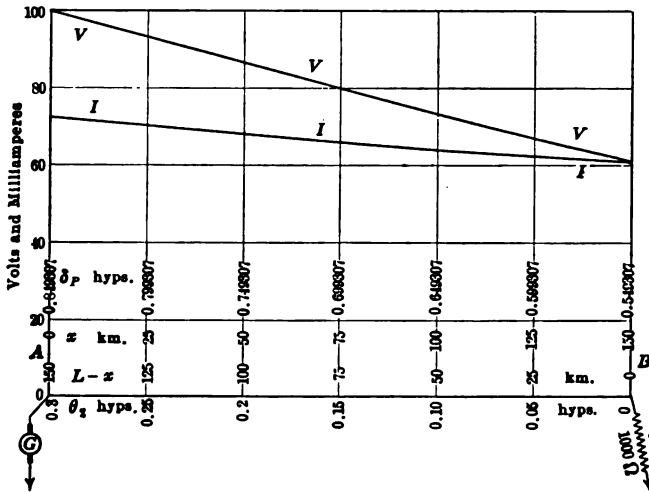


FIG. 21.—Case of a line with $\theta = 0.3$ hyp. and $r_0 = 2000$ ohms, grounded at B through a resistance σ of 1000 ohms and with an impressed potential of 100 volts at A .

$$\begin{aligned} V_P &= 60.446 \cosh 0.1 + 60.446 \times 10^{-3} \times 2 \times 10^3 \sinh 0.1 \\ &= 60.446 \times 1.00500 + 120.892 \times 0.10017 \\ &= 60.748 + 12.109 = 72.857 \text{ volts.} \end{aligned}$$

Similarly, by (78)

$$\begin{aligned} I_P &= 60.446 \times 10^{-3} \cosh 0.1 + \frac{60.446}{2,000} \sinh 0.1. \\ &= 60.446 \times 10^{-3} \times 1.00500 + 30.223 \times 10^{-3} \times 0.10017 \\ &= (60.748 + 3.027)10^{-3} = 63.775 \times 10^{-3} \text{ amp.} \end{aligned}$$

The distributions of potential and current over the line are given in Table II.

TABLE II

Particulars relating to a Line *AB* of $\theta = 0.3$ hyp. and $r_0 = 2,000$ ohms grounded at *B* through $\sigma = 1,000$ ohms, and with an impressed potential at *A* of 100 volts

I	II	III	IV	V	VI	VII	VIII	IX	X
<i>x</i> km.	<i>L-x</i> km.	θ_2 hyps.	$\cosh \theta_2$	$\sinh \theta_2$	V_P volts	I_P amp.	$\frac{\delta_P}{\theta_2 + \theta'}$ hyps.	$\cosh \delta_P$	$\sinh \delta_P$
						$\times 10^{-3}$			
0	150	0.30	1.04534	0.30452	100.000	72.390	0.84931	1.38287	0.95516
25	125	0.25	1.03141	0.25261	92.884	69.980	0.79931	1.33683	0.88719
50	100	0.20	1.02007	0.20134	85.998	67.743	0.74931	1.29411	0.82142
75	75	0.15	1.01127	0.15056	79.329	65.677	0.69931	1.25464	0.75771
100	50	0.10	1.00500	0.10017	72.857	63.775	0.64931	1.21831	0.69590
125	25	0.05	1.00125	0.05002	66.568	62.033	0.59931	1.18502	0.63583
150	0	0.00	1.00000	0.00000	60.446	60.446	0.54931	1.15470	0.57735

Degradation to Ohm's Law in the Case of Negligible Leakage.—If we take formulas (53) and (59) with (57), we have for the potential V_P at any point *P*,

$$V_P = V_A \cosh L_1\alpha - I_A \frac{r}{\alpha} \sinh L_1\alpha \quad \text{volts } \angle \quad (80)$$

where $\alpha = \sqrt{rg}$, according to (19).

If now the linear leakance becomes extremely small, so that we may virtually take $g = 0$, it follows that $\alpha = 0$, and that $L_1\alpha = 0$. Hence,

$$V_P = V_A \cosh 0 - I_A r \frac{\sinh L_1\alpha}{\alpha} \quad \text{volts } \angle \quad (81)$$

We know from tables, or from elementary hyperbolic trigonometry, that $\cosh 0 = 1$, and it is evident from (475) of Appendix A that

$$\sinh L_1\alpha = L_1\alpha + \frac{(L_1\alpha)^3}{3!} + \frac{(L_1\alpha)^5}{5!} + \dots \quad \text{numeric } \angle \quad (82)$$

so that, when $L_1\alpha$ becomes indefinitely small, $\frac{\sinh L_1\alpha}{\alpha}$ tends to the limit L_1 .

Formula (80) thus becomes when

$$V_P = V_A - I_A L_1 r \quad \text{volts } \angle \quad (83)$$

which is the ordinary Ohm's law value of V_P , in terms of the terminal potential V_A and the IR drop from *A* to *P*.

Again, taking (69) and remembering that $r_0 = \alpha$ when $g = 0$, we obtain for the leakanceless condition:

$$I_P = I_A \cosh 0 - \frac{V_A}{\alpha} \sinh 0 \quad \text{amp. } \angle \quad (84)$$

$$= I_A \quad \text{amp. } \angle \quad (85)$$

which expresses the constancy of current along the line.

Similarly, taking (79) with (76), we have, when $g = 0$,

$$V_P = V_B \cosh 0 + I_B r \frac{\sinh \alpha(L-x)}{\alpha} \quad \text{volts } \angle \quad (86)$$

$$= V_B + I_B r (L-x) \quad \text{volts } \angle \quad (87)$$

which is the corresponding Ohm's law value of V_P in terms of V_B and the IR drop from P to B . The formula (79) for current similarly degrades to

$$I_P = I_B \quad \text{amp. } \angle \quad (88)$$

General Solution in Terms of Position Angles.—If a line AB , having a surge resistance r_0 , see (26), and subtending θ hyp. radians in accordance with (18), is grounded at B , through a terminal impedance of σ ohms, and receives an impressed voltage at A , so that electrical energy flows in the steady state from A to B , then the series load, being devoid of lateral leakance, has no hyperbolic angle in itself, but the end B of the line, immediately connected thereto, acquires a hyperbolic position angle δ_B of θ' hyp. radians, defined by the condition:

$$\tanh \theta' = \frac{\sigma}{r_0} \quad \text{numeric } \angle \quad (89)$$

Having assigned the position angle δ_B of the end B in this way, the position angle* of the end A is:

$$\delta_A = \theta + \theta' \quad \text{hyps. } \angle \quad (90)$$

and at any intermediate point P , distant θ_2 hyps. from B , by (70), the position angle is:

$$\delta_P = \theta_2 + \theta' \quad \text{hyps. } \angle \quad (91)$$

In words, *the position angle of a point P , distant θ_2 hyp. radians from the energy-receiving end B , is always found by adding to θ_2*

* "On Electric Conducting Lines of Uniform Conductor and Insulation Resistance in the Steady State," by A. E. KENNELLY, *Harvard Engineering Journal*, vol. ii, pp. 135-168, May, 1903.

the angle θ' , subtended at B by the terminal load σ . Position angles are of great importance in the electrical computations of steady-state lines, either with alternating or continuous currents.

Formula for Potential in Terms of the Position Angle.—The formula which expresses the potential at any point P of a line in terms of the position angle of P , belongs to the type (47), and may be derived by direct transformation either from (59) or from (77). We may proceed to obtain it from the latter.

$$V_P = V_B \cosh \theta_2 + I_B r_0 \sinh \theta_2 \quad \text{volts } \angle \quad (92)$$

$$= V_B \cosh \theta_2 + \frac{V_B}{\sigma} r_0 \sinh \theta_2 \quad \text{volts } \angle \quad (93)$$

$$= V_B \left(\cosh \theta_2 + \frac{r_0}{\sigma} \sinh \theta_2 \right) \quad \text{volts } \angle \quad (94)$$

and from (89) this is

$$V_P = V_B (\cosh \theta_2 + \coth \theta' \sinh \theta_2) \quad \text{volts } \angle \quad (94a)$$

using (506) Appendix A,

$$= V_B \sqrt{\coth^2 \theta' - 1} \sinh (\theta_2 + \tanh^{-1} \tanh \theta') \quad \text{volts } \angle \quad (94b)$$

$$= V_B \frac{1}{\sinh \theta'} \sinh (\theta_2 + \theta') \quad \text{volts } \angle \quad (94c)$$

$$= V_B \frac{\sinh \delta_P}{\sinh \theta'} \quad \text{volts } \angle \quad (95)$$

and
$$\frac{V_P}{V_B} = \frac{\sinh \delta_P}{\sinh \delta_B} \quad \text{numeric } \angle \quad (96)$$

If we take P at A , where $\delta_P = \delta_A = \theta + \theta'$

$$\frac{V_A}{V_B} = \frac{\sinh \delta_A}{\sinh \delta_B} \quad \text{numeric } \angle \quad (97)$$

and dividing (96) by (97),

$$\frac{V_P}{V_A} = \frac{\sinh \delta_P}{\sinh \delta_A} \quad \text{numeric } \angle \quad (98)$$

In general, if at any reference point C on the line, which may or may not be a terminal, we happen to know the potential V_C , and the position angle δ_C , then the potential V_P at any other point P of the line having a position angle δ_P is obtainable from

$$\frac{V_P}{V_C} = \frac{\sinh \delta_P}{\sinh \delta_C} \quad \text{numeric } \angle \quad (99)$$

which we can express in language, by saying that *the potentials*

of any and all points of a line are as the sines of the corresponding position angles; so that, knowing the distribution of position angles, any single observed potential suffices for the determination of the entire potential distribution.

In the case where the line is grounded directly at B , or $\sigma = 0$, $\delta_B = 0$, $\delta_A = \theta$, and $\delta_P = \theta_2$.

In the case of a line freed at B , $\sigma = \alpha$, $\delta_B = j \frac{\pi}{2}$, and (96) becomes by (502)

$$V_P = V_B \cosh \theta_2 \quad \text{volts } \angle \quad (100)$$

$$\text{and} \quad V_B = V_A / \cosh \theta = V_A \operatorname{sech} \theta \quad \text{volts } \angle \quad (101)$$

As an example of (98), we may take the case presented in Fig. 21 and Table II, where $\sigma = 1,000$ ohms, $r_0 = 2,000$ ohms, and $\tanh \theta' = 0.5$; whence by Tables, $\theta' = \delta_B = 0.549307$ hyp. At a position P , 50 km. from B , $\theta_2 = 0.1$ hyp., and $\delta_P = \theta_2 + \theta' = 0.649307$ hyp. The position angle at A where $V_A = 100$ volts, is $\delta_A = \theta + \theta' = 0.849307$ hyp. Consequently,

$$\frac{V_P}{100} = \frac{\sinh 0.649307}{\sinh 0.849307} = \frac{0.69590}{0.95516} = 0.72857$$

$$\text{or} \quad V_P = 72.857 \text{ volts.}$$

Formula for Current in Terms of the Position Angle.—The formula which expresses the current strength in the line at any assigned point P , in terms of the position angle δ_P belongs to the type (49), and may be derived by direct transformation from either (69) or (79). We may select the latter.

$$I_P = I_B \cosh \theta_2 + \frac{V_B}{r_0} \sinh \theta_2 \quad \text{amp. } \angle \quad (102)$$

$$= I_B \left(\cosh \theta_2 + \frac{\sigma}{r_0} \sinh \theta_2 \right) \quad \text{amp. } \angle \quad (103)$$

$$= I_B (\cosh \theta_2 + \tanh \theta' \sinh \theta_2) \text{ by (89)} \quad \text{amp. } \angle \quad (104)$$

$$= I_B \sqrt{1 - \tanh^2 \theta'} \cdot \cosh(\theta_2 + \tanh^{-1} \tanh \theta') \text{ by (506)} \quad \text{amp. } \angle \quad (105)$$

$$= I_B \frac{1}{\cosh \theta'} \cdot \cosh(\theta_2 + \theta') \quad \text{amp. } \angle \quad (106)$$

$$= I_B \frac{\cosh \delta_P}{\cosh \delta_B} \quad \text{amp. } \angle \quad (107)$$

$$\frac{I_P}{I_B} = \frac{\cosh \delta_P}{\cosh \delta_B} \quad \text{numeric } \angle \quad (108)$$

If we move the point P up to A , where $\delta_P = \delta_A = \theta + \theta'$, and $I_P = I_A$,

$$\frac{I_A}{I_B} = \frac{\cosh \delta_A}{\cosh \delta_B} \quad \text{numeric } \angle \quad (109)$$

Dividing (108) by (109)

$$\frac{I_P}{I_A} = \frac{\cosh \delta_P}{\cosh \delta_A} \quad \text{numeric } \angle \quad (110)$$

Finally, if at any datum point, say C , on the line, where the position angle is δ_C and the current I_C are known, we obtain:

$$\frac{I_P}{I_C} = \frac{\cosh \delta_P}{\cosh \delta_C} \quad \text{numeric } \angle \quad (111)$$

In language, *the current strengths at any and all points along the line are as the cosines of the corresponding position angles.*

As an example, we may find the current at the point selected in the last case 50 km. from B , in the line shown at Fig. 21, where $\delta_P = 0.649307$ hyp., the current at A being given as $I_A = 72.3896 \times 10^{-3}$ amp.

Here

$$72.3896 \times 10^{-3} = \frac{\cosh 0.649307}{\cosh 0.849307} = \frac{1.21831}{1.38287} = 0.881003$$

or

$$I_P = 63.7754 \times 10^{-3} \text{ amp.}$$

In the particular case, when the line is grounded at B , or $\sigma = 0$, $\theta' = 0$, and $\delta_B = 0$, so that $\delta_A = \theta$, and $\delta_P = \theta_2$; whence

$$\frac{I_P}{I_A} = \frac{\cosh \theta_2}{\cosh \theta} \quad \text{numeric } \angle \quad (112)$$

Case When $\sigma > r_0$.—In the c.c. case, there is no difficulty in applying the position-angle formulas (99) and (109), so long as σ is distinctly less than r_0 ; but in the opposite case, when the terminal load σ is distinctly greater than r_0 , we are faced with the condition $\theta' = \tanh^{-1} \left(\frac{\sigma}{r_0} \right)$, or

$$\tanh \theta' = \frac{\sigma}{r_0} = k \quad \text{numeric } (112a)$$

a number greater than unity, which is an impossible condition, so long as θ' , σ and r_0 , are all real quantities.

Table III gives the values of $\tanh \theta$ and $\coth \theta$ for various hyperbolic angles. Referring to columns I and II, it is clear that as θ increases from 0 to ∞ , $\tanh \theta$ increases from 0 to 1. If, however,

TABLE III.—TANGENTS AND ANTITANGENTS

I θ	II $\tanh \theta$	III $\coth \theta$	IV θ	V $\tanh \theta$	VI $\coth \theta$
0	0	∞	$0 + j\frac{\pi}{2}$	∞	0
0.5	0.4621	2.1640	$0.5 + j\frac{\pi}{2}$	2.1640	0.4621
1.0	0.7616	1.3130	$1.0 + j\frac{\pi}{2}$	1.3130	0.7616
1.5	0.9052	1.1048	$1.5 + j\frac{\pi}{2}$	1.1048	0.9052
2.0	0.9640	1.0373	$2.0 + j\frac{\pi}{2}$	1.0373	0.9640
2.5	0.9866	1.0136	$2.5 + j\frac{\pi}{2}$	1.0136	0.9866
3.0	0.9951	1.0050	$3.0 + j\frac{\pi}{2}$	1.0050	0.9951
.....
∞	1.0000	1.0000	$\infty + j\frac{\pi}{2}$	1.0000	1.0000

we use formula (504), Appendix A, we obtain the entries in columns IV and V. That is, if we add $j\frac{\pi}{2}$ to any real number its tangent is greater than unity, and is equal to the cotangent of that real number. Thus $\tanh\left(1.0 + j\frac{\pi}{2}\right) = 1.313 = \coth 1.0$.

In fact, as we increase θ from $\left(0 + j\frac{\pi}{2}\right)$ to $\left(\infty + j\frac{\pi}{2}\right)$, the tangent decreases from ∞ to 1. The same conditions are indicated graphically in Fig. 22. In order to solve (89) for θ' when σ/r_0 exceeds unity, we have only to find in tables the real angle whose cotangent is equal to σ/r_0 , and then add $j\frac{\pi}{2}$ to that angle. Since

$\frac{\pi}{2}$, in circular radians, is the same as 90° , or one circular quadrant, it follows that any receiving-end load σ , greater than the surge impedance r_0 of the line, involves position angles having an imaginary circular quadrant, of the type $\delta_p = \delta'_p + j\frac{\pi}{2}$ hyps.

When we come to apply (99) to a line having a super-surge-impedance load, we must use formula (502), Appendix A, thus:

$$\frac{V_P}{V_C} = \frac{\sinh \delta_P}{\sinh \delta_C} = \frac{\sinh(\delta'_P + j\frac{\pi}{2})}{\sinh(\delta'_C + j\frac{\pi}{2})} = \frac{j \cosh \delta'_P}{j \cosh \delta'_C} = \frac{\cosh \delta'_P}{\cosh \delta'_C}$$

numeric (113)

Similarly (111) becomes by (503), Appendix A,

$$\frac{I_P}{I_C} = \frac{\cosh \delta_P}{\cosh \delta_C} = \frac{\cosh(\delta'_P + j\frac{\pi}{2})}{\cosh(\delta'_C + j\frac{\pi}{2})} = \frac{j \sinh \delta'_P}{j \sinh \delta'_C} = \frac{\sinh \delta'_P}{\sinh \delta'_C}$$

numeric (114)

TABLE IV

Particulars relating to a line AB of $\theta = 0.3$ hyp., and $r_0 = 2,000$ ohms, grounded at B through $\sigma = 4,000$ ohms, and with an impressed potential at A of 100 volts

I	II	III	IV	V	VI	VII	VIII	IX	X
x km.	$L - x$ km.	θ_2 hyp.	$\cosh \theta_2$	$\sinh \theta_2$	V_P volts	I_P amp.	$\delta_P = \theta_2 + \theta'$ hyp.	$\cosh \delta_P$	$\sinh \delta_P$
						$\times 10^{-3}$	$\times j$		$\times j$
0	150	0.30	1.04534	0.30452	100.000	34.535	0.849307 + $j\frac{\pi}{2}$	0.95516	1.38287
25	125	0.25	1.03141	0.25261	96.671	32.078	0.799307 + $j\frac{\pi}{2}$	0.88719	1.33683
50	100	0.20	1.02007	0.20134	93.582	29.700	0.749307 + $j\frac{\pi}{2}$	0.82142	1.29411
75	75	0.15	1.01127	0.15056	90.727	27.396	0.699307 + $j\frac{\pi}{2}$	0.75771	1.25464
100	50	0.10	1.00500	0.10017	88.100	25.162	0.649307 + $j\frac{\pi}{2}$	0.69590	1.21831
125	25	0.05	1.00125	0.05002	85.693	22.990	0.599307 + $j\frac{\pi}{2}$	0.63583	1.18502
150	0	0.00	1.00000	0.00000	83.500	20.875	0.549307 + $j\frac{\pi}{2}$	0.57735	1.15470

The effect, therefore, of a super-surge-impedance load at B , is to introduce imaginary quadrants into the position angles along the line, and to interchange the use of sines and cosines in the general formulas for potential and current, so far as relates to the real components of the position angles.

As an example, we may take the case of the line AB last considered (Table II and Fig. 21) with 100 volts at A , but grounded at B , Fig. 23, through $\sigma = 4,000$ ohms. The numerical particulars of this case are presented in Table IV. Here $\tanh \theta' = 4,000/2,000 = 2.0$; whence $\theta' = 0.549307 + j\frac{\pi}{2}$ hyp. The position angle at any point P is found by adding θ_2 for that point

to θ' . Such values are given in column VIII. The currents are then as the cosines and the potentials as the sines of these complex position angles, and are respectively as the sines and cosines of their real parts, as will be seen by comparing Tables II and IV. The values of V_P and I_P appear in columns VI and VII respectively. They may also be computed from formulas (77) and (79), using the data of columns IV and V.

At the point $x = 25$ km., or $\theta_2 = 0.25$ hyp., the position angle $\delta_P = 0.799307 + j\frac{\pi}{2}$, and the potential, by (113), is

$$\begin{aligned} V_P &= 100 \times \frac{\sinh \left(0.799307 + j\frac{\pi}{2} \right)}{\sinh \left(0.849307 + j\frac{\pi}{2} \right)} \\ &= 100 \times \frac{\cosh 0.799307}{\cosh 0.849307} = 100 \times \frac{1.33683}{1.38287} \\ &= 96.671 \text{ volts.} \end{aligned}$$

Again, since the current I_B at B is V_B/σ amp., the current at $x = 25$ km. becomes, by (114)

$$\begin{aligned} I_P &= I_B \frac{\cosh \left(0.799307 + j\frac{\pi}{2} \right)}{\cosh \left(0.549307 + j\frac{\pi}{2} \right)} \\ &= 0.020875 \times \frac{j0.88719}{j0.57735} = 0.032078 \text{ amp.} \end{aligned}$$

It is remarkable that in a.c. cases, the question as to whether the terminal-load impedance is greater or less than the surge impedance, has no significance and, as we shall see, has never to be considered. In this respect, the a.c. case is easier to deal with than the c.c. case.

Case of $\sigma = r_0$. The Virtually Infinite Line.—

In the particular case when the load at the motor end has a resistance equal to the surge resistance of the line, the hyperbolic functions expressing the potential and current distributions reduce, as we shall see, to exponentials.

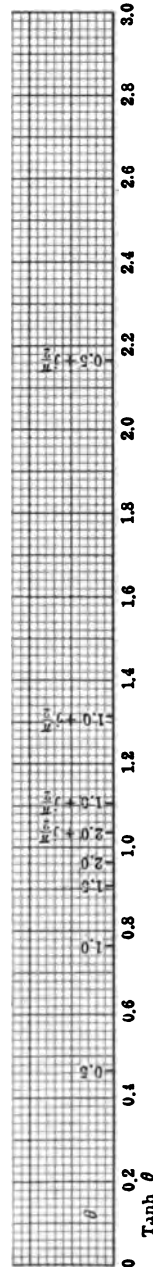


FIG. 22.—Value of real hyperbolic angles θ and their corresponding tangents.

The position angle at B is then defined by (89),

$$\tanh \theta' = \frac{r_0}{r_0} = 1 \quad \text{numeric} \quad (115)$$

The solution of which is $\theta' = \alpha$. Entering (98) with this value of θ' , we have

$$\frac{V_P}{V_A} = \frac{\sinh \delta_P}{\sinh \delta_A} = \frac{\sinh (\theta_2 + \alpha)}{\sinh (\theta + \alpha)} \quad \text{numeric} \quad (116)$$

$$= \frac{\sinh \theta_2 \cosh \alpha + \cosh \theta_2 \sinh \alpha}{\sinh \theta \cosh \alpha + \cosh \theta \sinh \alpha} \quad \text{numeric} \quad (117)$$

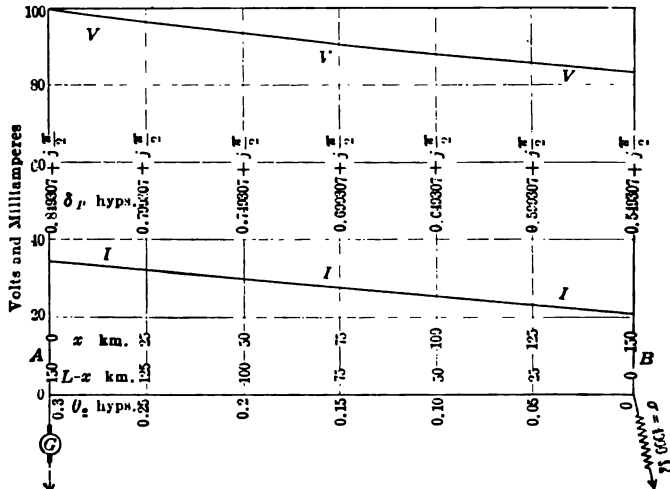


FIG. 23.—Case of a line with $\theta = 0.3$ hyp. and $r_0 = 2000$ ohms grounded at B through a resistance 0 of 4000 ohms, and with an impressed potential of 100 volts at A .

But $\sinh \alpha = \cosh \alpha$, and we may assume that since the same infinity occurs in both numerator and denominator, we may divide throughout by $\sinh \alpha$; so that

$$\frac{V_P}{V_A} = \frac{\sinh \theta_2 + \cosh \theta_2}{\sinh \theta + \cosh \theta} = \frac{e^{\theta_2}}{e^{\theta}} = e^{-(\theta - \theta_2)} = e^{-\theta_1} \quad \text{numeric} \quad \angle \quad (118)$$

$$V_P = V_A e^{-\theta_1} = V_A e^{-L_1 \alpha} = V_A \frac{\cosh \theta_1 - \sinh \theta_1}{2} \quad \text{volts} \quad \angle \quad (119)$$

It is evident that the potential falls from A toward B according to a simple exponential law. It also follows immediately from either (97) or (119) that

$$V_P = V_B e^{\theta_2} = V_B \epsilon^{L_2 \alpha} = V_B \frac{\cosh \theta_2 + \sinh \theta_2}{2} \quad \text{volts } \angle \quad (120)$$

Similarly, the fundamental equation for current strength (110) becomes

$$I_P = I_A \epsilon^{-\theta_1} = I_A \epsilon^{-L_1 \alpha} = I_A \cdot \frac{\cosh \theta_1 - \sinh \theta_1}{2} \quad \text{amp. } \angle \quad (121)$$

$$= I_B \epsilon^{\theta_2} = I_B \epsilon^{L_2 \alpha} = I_B \cdot \frac{\cosh \theta_2 + \sinh \theta_2}{2} \quad \text{amp. } \angle \quad (122)$$

This type of simple exponential attenuation, peculiar either to an infinitely long line, or to a finite line which has been made vir-

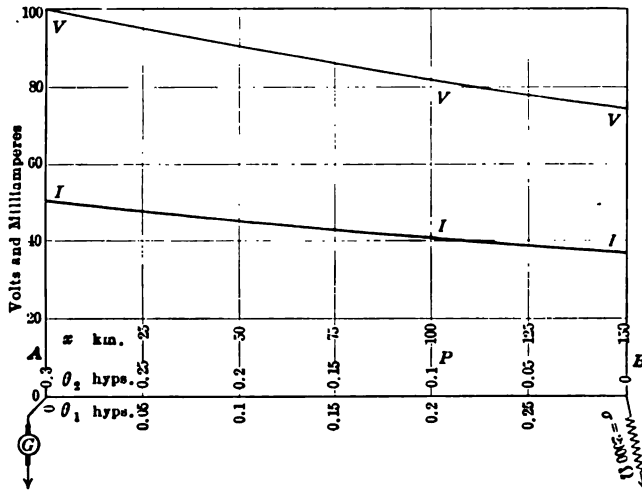


FIG. 24.—Case of a line with $\theta = 0.3$ hyp. and $r_0 = 2000$ ohms grounded at B through a resistance $0 = 2000$ ohms and with an impressed potential of 100 volts at A . Exponential case.

tually infinite, *i.e.*, to behave like a portion of an infinite line by surge-impedance loading at B , is called *normal attenuation*. The *normal attenuation factor* of a line L km. long is $\epsilon^{-L\alpha}$. Both the potential and current on such a line undergo normal attenuation.

As an example, we may take the case of the line already considered ($L = 150$ km., $\alpha = 0.002$ hyp./km., $\theta = 0.3$ hyp., $r_0 = 2,000$ ohms), and with an impressed potential of 100 volts at A . If this line is grounded at B through a surge-impedance load $\sigma = r_0 = 2,000$ ohms, we find the conditions set forth in Table V and Fig. 24.

If we seek the potential at P , 100 km. from A , we have $\theta_1 =$

0.2, $\epsilon^{-0.2} = 0.818731$, and $V_P = 81.8731$ volts. The current at P is similarly $50 \times 10^{-3} \times 0.818731 = 40.9866 \times 10^{-3}$ amp.

Single Values of Either Potential or Current Needed in Certain Cases.—It has already been pointed out, in connection with formulas (45) to (50), that since the fundamental differential equation (43) for potential is of the second order, two condition-

TABLE V

Particulars relating to a line AB of $\theta = 0.3$ hyp. and $r_0 = 2,000$ ohms, grounded at B through $\sigma = 2,000$ ohms, and with an impressed potential at A of 100 volts. Exponential case. Virtually infinite line.

x km.	θ_1 hyps.	θ_2 hyps.	$\epsilon^{-\theta_1}$	V_P volts	I_P milliamp.
0	0.00	0.30	1.000000	100.0000	50.0000
25	0.05	0.25	0.951229	95.1229	47.5615
50	0.10	0.20	0.904837	90.4837	45.2419
75	0.15	0.15	0.860708	86.0708	43.0354
100	0.20	0.10	0.818731	81.8731	40.9866
125	0.25	0.05	0.778801	77.8801	38.9400
150	0.30	0.00	0.740818	74.0818	37.0409

satisfying or arbitrary constants must be forthcoming, if a numerical solution is to be obtained. Similar conditions apply also to solutions for current strength. In certain cases, however, only one such arbitrary constant is needed, when the conditions are such as to imply the second arbitrary constant. Thus, if a line AB is known to be grounded at B , this condition is equivalent to establishing one arbitrary constant; so that only one other arbitrary constant, such as a potential, or a current, needs to be given, in order to determine the complete distributions of voltage and current over the line, using (99) and (111), with $\theta' = 0$. The single necessary quantity to obtain the complete solutions may be either a potential or a current, at some particular point on the line. The potential at B is, however, in this case, an insufficient datum, because we know that this potential must be zero, and no new datum is provided by offering the gratuitous information that $V_B = 0$.

Similarly, if the line is freed at B , the same formulas (99) and (111) will serve to evaluate the complete distribution, if we re-

member that $\theta' = j\frac{\pi}{2}$ hyps., and have one independent datum given, of a potential or a current at an assigned position.

Moreover, if the terminal load at B is given in the form of an actual or equivalent resistance σ , we know the terminal position angle $\delta_B = \theta'$, by (89), and can then evaluate the entire potential-current system from a single independent datum.

The transition from the potential to the current distribution, or *vice versa*, usually requires a knowledge of the impedance offered by the line, and this will be considered in the next chapter.

CHAPTER V

IMPEDANCE, ADMITTANCE AND POWER OF A SMOOTH LINE AT ANY POINT

It is evident that if we consider any line, having a steady distribution of potential and current, the ratio, at each and every point, of the potential to the current is equal, in the general case, to the impedance (in the d.c. case, to the resistance) of the line at and beyond that point, in the direction of the flow of energy. In other words, if at any point P , of a single line, AB , the potential with respect to ground is V_P volts, and the current is I_P amp., then their ratio $V_P/I_P = R_P$ ohms. If the line were cut at the point P , and the end toward B were connected to a Wheatstone bridge or other resistance-measuring apparatus, R_P would be the resistance measured to ground, including the effects of the distributed conductor resistance, the distributed dielectric leakance and the terminal load, if any, at B . Similarly, and reciprocally, the ratio I_P/V_P would be the admittance G_P in the general case (the conductance in the c.c. case) of the line, at and beyond P , as measured from P to ground.

If we divide (99) by (111), we obtain

$$\frac{R_P}{R_C} = \frac{\tanh \delta_P}{\tanh \delta_C} \quad \text{numeric } \angle \quad (123)$$

or, in words, *the impedance at and beyond any point of a line varies as the hyperbolic tangent of the position angle*. If we know the distribution of position angles and the impedance at any point C , such as the home end or the far end, then we can find at once the impedance offered at and beyond any or all other points of the line. Similarly, dividing (111) by (99) we have

$$\frac{G_P}{G_C} = \frac{\coth \delta_P}{\coth \delta_C} \quad \text{numeric } \angle \quad (124)$$

or *the line admittances are as the cotangents of the position angles*. Formulas (123) and (124) express general laws of smooth lines.

For example, consider the line of hyperbolic angle $\theta = 0.3$ hyp. and $r_0 = 2,000$ ohms, grounded at B , through 1,000 ohms,

as represented in Fig. 21. The following Table, No. VI, shows, in connection with Fig. 25, the values of x , $(L - x)$, θ_2 , δ_P , $\tanh \delta_P$, $\coth \delta_P$, R_P and G_P .

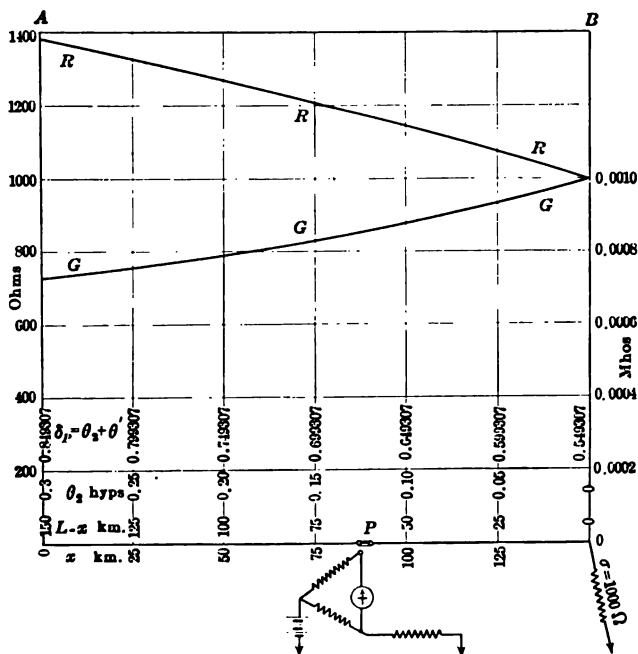


FIG. 25.—Diagram showing changes of resistance and conductance along the line AB of $\theta = 0.3$ hyps. and $r_0 = 2000$ ohms, grounded at B through 1000 ohms. A Wheatstone bridge is indicated as ready to connect to the section PB at P .

TABLE VI

Values of Line Resistance and Conductance at various Points along a Line of $\theta = 0.3$ hyps., and $r_0 = 2,000$ ohms, grounded at B through $\sigma = 1,000$ ohms

I x km.	II $L - x$ km.	III θ_2 hyps.	IV θ' hyps.	V $\delta_P = \theta_2 + \theta'$ hyps.	VI $\tanh \delta_P$	VII $\coth \delta_P$	VIII R_P ohms	IX G_P mhos
0	150	0.30	0.549307	0.849307	0.69071	1.4478	1,381.4	0.7239
25	125	0.25	0.799307	0.66368	1.5068	1,327.4	0.7534
50	100	0.20	0.749307	0.63473	1.5754	1,269.5	0.7877
75	75	0.15	0.699307	0.60393	1.6559	1,207.9	0.8280
100	50	0.10	0.649307	0.57121	1.7507	1,142.4	0.8754
125	25	0.05	0.599307	0.53656	1.8637	1,073.1	0.9319
150	0	0.00	0.549307	0.5000	2.0000	1,000.0	1.0000

Here the line resistance is 1,000 ohms at B where $\delta_B = 0.549307$ hyp.; so that entering (123) with these values of R_C and δ_C respectively, we obtain the values recorded in column VIII. Similarly, entering (124) with $G_C = 1.0 \times 10^{-3}$, and $\delta_C = 0.549307$ hyp., we obtain the values of line conductance recorded in column IX. Manifestly the numerical values of R_P and G_P , at any point x , should be mutually reciprocal.

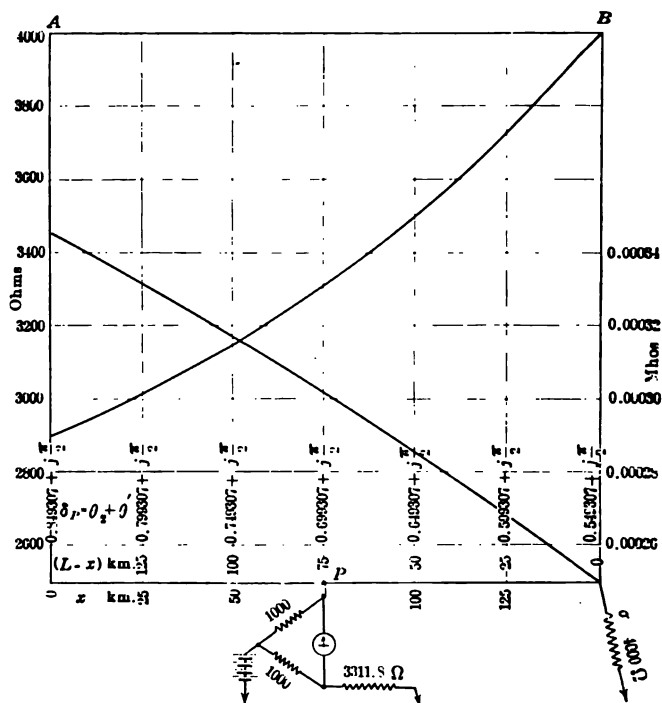


FIG. 26.—Diagram showing change of resistance and conductance along the line AB of $\theta = 0.3$ hyp. and $r_0 = 2000$ ohms, grounded at B through 4000 ohms. A Wheatstone bridge is indicated as connected to the section PB at B . Rising curve for resistance, falling curve conductance.

As another example, consider the same line grounded at B through the super-surge impedance of 4,000 ohms. In this case, as we have already seen, the position angles from B to A all contain one imaginary quadrant, or $j \frac{\pi}{2}$ radians. Referring to formula (504), Appendix A, it is to be observed that this extra imaginary quadrant virtually exchanges the tangent and cotan-

gent of the real component. We thus obtain the values contained in Table VII and Fig. 26.

TABLE VII

Values of Line Resistance and Conductance at various points along a line of $\theta = 0.3$ hyp. and $r_0 = 2,000$ ohms, grounded at B through $\sigma = 4,000$ ohms

I x km.	II $L - x$ km.	III θ_1 hyps.	IV θ' hyps.	V $\delta_P = \theta_1 + \theta'$ hyps.	VI $\tanh \delta_P$	VII $\coth \delta_P$	VIII R_P ohms	IX G_P mhos
0	150	0.30	$0.549307 + j\frac{\pi}{2}$	$0.849307 + j\frac{\pi}{2}$	1.4478	0.69071	2,895.6	0.34536
25	125	0.25	$0.799307 + j\frac{\pi}{2}$	1.5068	0.66368	3,013.6	0.33184
50	100	0.20	$0.749307 + j\frac{\pi}{2}$	1.5754	0.63473	3,150.8	0.31737
75	75	0.15	$0.699307 + j\frac{\pi}{2}$	1.6559	0.60393	3,311.8	0.30196
100	50	0.10	$0.649307 + j\frac{\pi}{2}$	1.7507	0.57121	3,501.4	0.28560
125	25	0.05	$0.599307 + j\frac{\pi}{2}$	1.8637	0.53656	3,727.4	0.26828
150	0	0.00	$0.549307 + j\frac{\pi}{2}$	2.0000	0.50000	4,000.0	0.25000

Taking Tables VI and VII together, as well as Figs. 25 and 26, we may safely conclude that when a line is grounded through an infra-surge-resistance load at the far end, the line resistance falls as we approach that end, while the line conductance reciprocally rises. On the other hand, when the line is grounded at the far end through a super-surge-resistance load, the line resistance rises as we approach that end; while the line conductance reciprocally falls. A glance at Table V will likewise show that in the intermediate case, when a line is grounded at the distant end through a surge-resistance load, the line resistance neither rises nor falls, but remains constant all along the line.

Line Resistance in the Unsteady and Steady States.—If we took up the consideration of the transient building up of potential and current along a line prior to the establishment of the steady state,* we should see that any line having a surge impedance of r_0 ohms, offers this resistance at any point to each single advancing electric wave in the unsteady state; so that if V_P is the instantaneous potential at point P , the instantaneous current in that wave is

* See Chapter VI of "The Application of Hyperbolic Functions to Electrical Engineering Problems"; also Chapter III of FLEMING's "The Propagation of Electric Currents in Telephone and Telegraph Conductors."

$$I_P = \frac{V_P}{r_0} = V_P g_0 \quad \text{amp. } \angle \quad (125)$$

where g_0 is the surge admittance, the reciprocal of the surge impedance. But any outgoing wave tends to be reflected, when reaching the end of the line toward which it moves. After as many of these successive reflections have taken place as need to be taken into consideration when watching for the establishment of the steady state, the effect on the outgoing stream, of all the superposed reflections of current, is to change the resistance at any point of the line to

$$R_P = r_0 \tanh \delta_P \quad \text{ohms } \angle \quad (126)$$

or
$$G_P = g_0 \coth \theta_P \quad \text{mhos } \angle \quad (127)$$

so that the final current strength becomes

$$I_P = V_P G_P = V_P \cdot g_0 \cdot \coth \delta_P = V_P \cdot g_0 / \tanh \delta_P \quad \text{amp. } \angle \quad (128)$$

Here the factor $\tanh \delta_P$ covers all the effects of reflected waves to infinity in number and time. If the line is so long that no reflected waves ever come back from the distant end, then the initial surge resistance r_0 remains the final line resistance at any and every point, as in the case presented in Table V and Fig. 24.

Sending-end Impedance.—The line impedance at A the sending or generator end, in the steady state, whatever load there may be at the receiving or motor end, is called the sending-end impedance R_A (in an a.c. case Z_A), and by (126) it is

$$R_A = r_0 \tanh \delta_A \quad \text{ohms } \angle \quad (129)$$

In the particular case when the line is grounded at the motor end, so that $\sigma = 0$, and $\theta' = 0$, $\delta_A = \theta$, and

$$R_{\theta A} = r_0 \tanh \theta \quad \text{ohms } \angle \quad (130)$$

In the particular case when the line is freed at the motor end, so that $\sigma = \alpha$, and $\theta' = j \frac{\pi}{2}$, $\delta_A = \theta + j \frac{\pi}{2}$, and

$$R_{jA} = r_0 \coth \theta \quad \text{ohms } \angle \quad (131)$$

Receiving-end Impedance.—The ratio of the potential V_A at the generator end to the current I_B at the motor end, is defined as the "receiving-end impedance" R_l (in the a.c. case Z_l)

$$R_l = \frac{V_A}{I_B} \quad \text{ohms } \angle \quad (132)$$

The receiving-end impedance is, therefore, the impedance which the line appears to offer to an observer of the current at the receiving end, who is informed of the voltage at the sending end.

Using (126), if the line is loaded at B with an impedance σ , such that $\delta_B = \theta' = \tanh^{-1} \left(\frac{\sigma}{r_0} \right)$,

$$I_B = \frac{V_B}{r_0 \tanh \delta_B} = \frac{V_A}{\sinh \delta_A} \cdot \frac{\sinh \delta_B}{r_0 \tanh \delta_B} = \frac{V_A}{\sinh \delta_A} \cdot \frac{\cosh \delta_B}{r_0} \quad \text{amp. } \angle \quad (133)$$

and

$$R_l = \frac{V_A}{I_B} = \frac{r_0 \sinh \delta_A}{\cosh \delta_B} = \frac{r_0 \sinh (\theta + \theta')}{\cosh \theta'} \quad \text{ohms } \angle \quad (134)$$

$$= r_0 \sinh \theta + \sigma \cosh \theta \quad \text{ohms } \angle \quad (135)$$

In the particular case when the line is grounded directly at B , $\sigma = 0$, $\theta' = 0$, $\delta_B = 0$, $\delta_A = \theta$

$$R_l = r_0 \sinh \theta \quad \text{ohms } \angle \quad (136)$$

which is a simple but important formula. As an example, a line of $\theta = 1.2$ hyps. and $r_0 = 1,500$ ohms, is grounded at B through $\sigma = 1,000$ ohms. The angle subtended by this load is $\theta' = \tanh^{-1} \left(\frac{1,000}{1,500} \right) = 0.80472 = \delta_B$. The receiving-end impedance, by (134), is then $1,500 \sinh 2.00472 / \cosh 0.80472 = 1,500 \times 3.6446 / 1.34164 = 4,074.8$ ohms. By (135), it would be $1,500 \sinh 1.2 + 1,000 \cosh 1.2 = 1,500 \times 1.50946 + 1,000 \times 1.81066 = 4,074.8$ ohms. The current strength at the receiving end from say 100 volts impressed at the sending end, would then be $100 / 4,074.8 = 0.02454$ amp.

Power in the Steady State at Any Point along the Line.—If we know the potential V_P and current I_P at a point P on the line in the steady state, the power at the point, *i.e.*, the rate at which electrical energy is carried past P to the rest of the line beyond, is

$$P_P = V_P I_P \quad \text{volt-amp. } (137)$$

and this is ordinarily the most convenient method of determining the power at P . We may nevertheless ascertain the power as a function of the position angle of a point on the line as follows: By (99) and (111)

$$\frac{P_P}{P_C} = \frac{V_P I_P}{V_C I_C} = \frac{\sinh \delta_P}{\sinh \delta_C} \cdot \frac{\cosh \delta_P}{\cosh \delta_C} = \frac{\sinh 2\delta_P}{\sinh 2\delta_C} \quad \text{numeric (138)}$$

so that, in language, *the volt-amperes at any point vary as the sine of twice the position angle* (see (383)).

As an example, we may consider the line represented in Fig. 38, of $\theta = 1.75868$ hyps. and $r_0 = 1,436.1$ ohms, 100 km. long, and grounded at the far end through 750 ohms resistance. Having given that the distant-end potential is $V_B = 11.931$ volts, and the distant-end current $11.931/750 = 0.015908$ amp., with a delivered power of $11.931 \times 0.015908 = 0.1898$ watt; also that the distant-end position angle is $\delta_C = 0.57941$ hyp., required the power at a point P , 20 km. from the distant end, where the position angle is 0.93114 hyp.

Here

$$\frac{P_P}{0.1898} = \frac{\sinh (2 \times 0.93114)}{\sinh (2 \times 0.57941)} = \frac{\sinh 1.86228}{\sinh 1.15882} = \frac{3.1416}{1.43615} = 2.1875$$

so that $P_P = 2.1875 \times 0.1898 = 0.4152$ watt (139)

CHAPTER VI

LUMPY ARTIFICIAL LINES

Lumpy artificial lines have already been described in Chapter I. They may be classified both in regard to the number of their main wires, and in regard to the nature of their terminal elements.

Classification According to Number of Main Wires.—Artificial lines are one-wire, two-wire, or three-wire, according to the

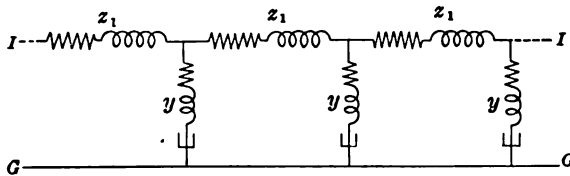


FIG. 27.—Diagram of connections between series and shunt elements in a single-wire artificial line.

number of their main-line conductors. A typical one-wire lumpy line is indicated, in part of its length at Fig. 27. Here z_1, z_1, z_1 are three equal sections or lumps of line impedance, (in c.c. cases, resistance). y, y, y are three equals leak of admittance (in c.c. cases conductance), all connected to the common

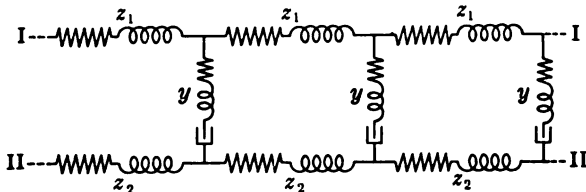


FIG. 28.—Diagram of connections between series and shunt elements in a two-wire artificial line.

ground wire, or neutral connection $G G$. The type of impedance z , and the type of leak admittance y , depend on the line to be imitated. Thus, z may be a pure resistance, or a reactance coil, or a condenser, or any combination of such elements, and similarly for y . Single-wire lines, in practice, are characteristic of wire telegraphy.

A typical two-wire artificial line is shown, in part of its length, at Fig. 28. Here there are three sections, each having equal impedances $z_1 z_1 z_1$ in one line, and similarly equal impedances $z_2 z_2 z_2$ in the other line. Between the corresponding lumps of opposite line impedances are branched the equal leak admittances $y y y$. Two-wire lines, in practice, are characteristic of wire telephony.

A typical four-wire artificial line is similarly shown in Fig. 29, for three sections. $z_1 z_1 z_1$ are three equal impedances in line I, $z_2 z_2 z_2$ three similar equal impedances in line II, $z_3 z_3 z_3$ in line III. Leak admittances $y_1 y_1 y_1$, $y_2 y_2 y_2$, $y_3 y_3 y_3$, are tapped off between corresponding line lumps of impedance to the ground wire or neutral connection $G G$. Three-wire lines, and four-wire lines, in practice, are characteristic of three-phase a.c. systems.

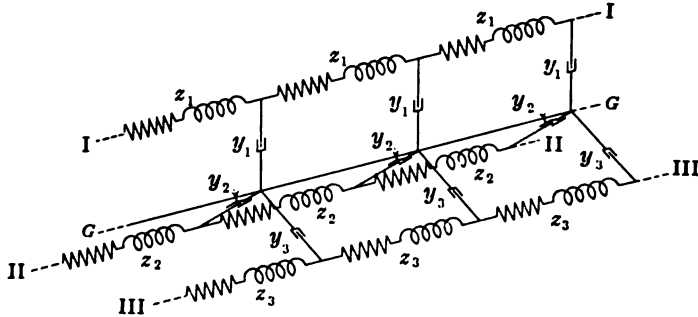


FIG. 29.—Diagram of connections between series and shunt elements in a four-wire three-phase artificial line.

In theory, it is unnecessary to employ any except one-wire artificial lines; because any symmetrical two-wire or three-wire system can always be subdivided into a like number of virtually independent single-wire systems. We shall, therefore, study only the theory of single-wire artificial lines, on the understanding that the results can be readily applied to either two-wire or three-wire artificial lines.

Classification According to Terminal Elements.—Artificial lines which terminate in half-lumps of line impedance, are called *T* lines; while those which terminate in half-lumps of leak admittance are called *H* lines.

If r be the line impedance per section (ohms \angle) and g the leak admittance per section (mhos \angle), then if the leak g is applied at the middle of the line section as in Fig. 30, the section is called a

T section, as is suggested by the diagram. If on the other hand, the leak g is divided into two half-leaks, each of $g/2$ mhos; and one half-leak is applied at each end of the line impedance section r , as shown in Fig. 31, the section is called a *II* section, as is also suggested by the diagram.

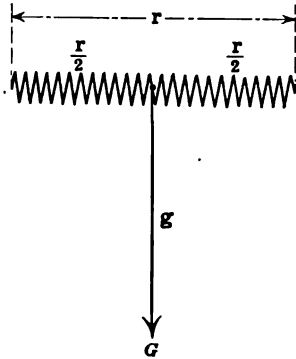


FIG. 30.—*T* section, comprising two equal-series elements and a leak or shunt element between them.

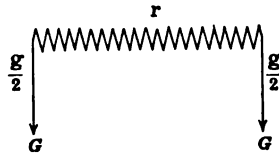


FIG. 31.—*II* section, comprising one-series element with a leak or shunt element at each end.

If a number of *T* sections are connected in series, the result is a simple alternation of r and g lumps except at the terminals, where half-sections, $r/2$, of line impedance supervene. Thus Fig. 32 shows an artificial line of four *T* sections. The sum total

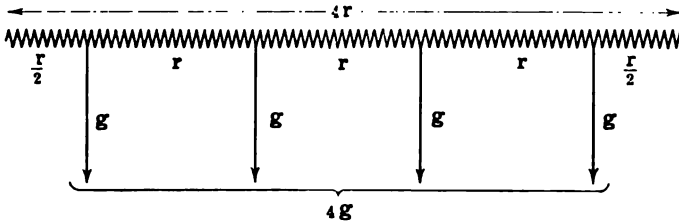


FIG. 32.—Four-section *T* line.

of all the line impedances is $4r$ ohms, and the sum total of the leak admittances is $4g$ mhos.

If, on the other hand, a number of *II* sections are connected in series, the result is a simple alternation of r and g lumps, except at terminals, where half-sections of leak admittance supervene. Thus Fig. 33 shows an artificial line of four *II* sections. The

sum total of all the line impedances is $4r$ ohms, and the sum total of all the leak admittances is $4g$ mhos.

Away from the ends, there is no necessary difference between a T line and a Π line. The distinction lies in the terminal elements only. Each type has, as we shall see, its own relative advantages and disadvantages.

We shall also see that each T section, or Π section, of artificial line subtends a certain hyperbolic angle θ radians. A line of n sections then subtends a total angle of $\Theta = n\theta$ hyps. A T line or a Π line also possesses a surge impedance r_0 ohms, which is independent of the number of sections.

The natural line which a given artificial line imitates, and to which it corresponds, has the same angle Θ and surge impedance r_0 as the artificial line. The first problem which presents itself,

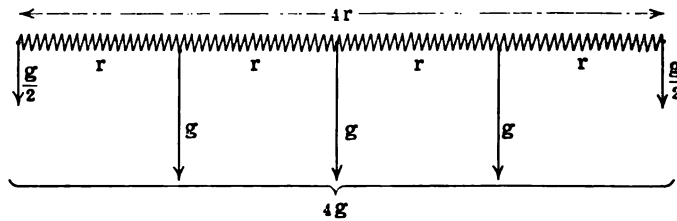


FIG. 33.—Four-section Π line.

therefore, in considering an artificial line of a given number of T or Π sections, each having definite lumps of line impedance and leak admittance, is the determination of its total line angle Θ hyps. and its surge impedance r_0 ohms.

First Approximation to the Section Angle θ and Surge Impedance r_0 of a T or Π Section.—If a single uniform smooth line has a total conductor resistance of R ohms, and a total dielectric leakance of G mhos, then we know from (18) and (26) that its line angle is

$$\theta = \sqrt{RG} \quad \text{hyps. } \angle \quad (140)$$

and its surge impedance

$$r_0 = \sqrt{R/G} \quad \text{ohms } \angle \quad (141)$$

In the same way, ignoring the lumpiness of the leaks in an artificial line section, having a line resistance r ohms, and a section leak of g mhos (Figs. 30 to 34), the uncorrected section angle will be

$$\theta_a = \sqrt{rg} \quad \text{apparent hyps. } \angle \quad (142)$$

whether the section be a T or a Π section. Likewise, the surge impedance will be

$$r_0 = \sqrt{r/g} \text{ apparent ohms } \angle \quad (143)$$

The total uncorrected angle of a line of n such sections will then be

$$\Theta_a = n \sqrt{rg} \text{ apparent hyps. } \angle \quad (144)$$

and the surge resistance of the line

$$r_0 = \sqrt{r/g} \text{ apparent ohms } \angle \quad (145)$$

These values require to be corrected for lumpiness. The lumpiness errors tend to increase, the larger and fewer the line sections.

There are two ways of arriving at the lumpiness corrections of θ and r_0 in an artificial line. One is to solve the problem by *continued fractions*. The other is to find the "equivalent" T or Π

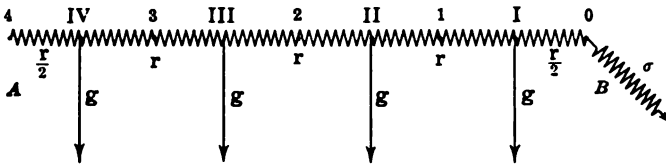


FIG. 34.—Four-section T line grounded at motor end B through a load of σ ohms.

of a section. The two methods are mutually illustrative, and we shall consider both, reserving the second method for the next chapter.

Impedance of a T Line Grounded through a Load at the Far End.—Let us consider a line of T sections, four of which are indicated in Fig. 34, grounded at B through an impedance of σ ohms \angle . Each section has a line impedance of r ohms \angle , and a leak of admittance of g mhos \angle . Required the impedance offered by this line at and beyond any section junction; *i.e.*, at the N th junction. At, but not including leak I, the impedance beyond I to ground at B is

$$R_I = \frac{r}{2} + \sigma = m \text{ ohms } \angle \quad (146)$$

Converting this impedance into an admittance,

$$G_I = \frac{1}{m} \text{ mhos } \angle \quad (147)$$

Adding to this the leak admittance at 1, of g mhos, we have for the total admittance at I, leak included,

$$G'_I = g + \frac{1}{m} \quad \text{mhos } \angle \quad (148)$$

Converting this into an impedance, the impedance at and beyond I is

$$R'_I = \frac{1}{g + \frac{1}{m}} \quad \text{ohms } \angle \quad (149)$$

Shifting the point of observation back to leak II, the impedance there, excluding that leak, is (see Appendix B)

$$R_{II} = r + \frac{1}{g + \frac{1}{m}} = 1/F_2(r, g) \frac{1}{m} \quad \text{ohms } \angle \quad (150)$$

Or as an admittance,

$$G_{II} = \frac{1}{r + \frac{1}{g + \frac{1}{m}}} = F_2(g, r) \frac{1}{m} \quad \text{mhos } \angle \quad (151)$$

Adding in leak II,

$$G'_{II} = g + \frac{1}{r + \frac{1}{g + \frac{1}{m}}} = 1/F_3(g, r) \frac{1}{m} \quad \text{mhos } \angle \quad (152)$$

Or, as an impedance at and including leak II,

$$R'_{II} = \frac{1}{g + \frac{1}{r + \frac{1}{g + \frac{1}{m}}}} = F_3(g, r) \frac{1}{m} \quad \text{ohms } \angle \quad (153)$$

Proceeding in this way along the line, we find that the impedance at leak N , including that leak, may be expressed as a terminally loaded alternating continued fraction (see Appendix B) of the type $F_n(g, r) \frac{1}{m}$, n , being an odd number, and connected with the leak number N by the relation

$$n = 2N - 1 \quad \text{numeric } \angle \quad (154)$$

At the section junction N next behind leak N (having the same numeral in arabic), the impedance at and beyond, will be

$$R_N = \frac{r}{2} + R'_N = \frac{r}{2} + F_{n,(\mathbf{g},r)} \quad \text{ohms } \angle \quad (155)$$

Turning to (563) Appendix B, this is found to be:

$$R_N = \sqrt{\frac{r}{g}} \cdot \cosh v \cdot \tanh \{(n, + 1) v + v'\} \quad \text{ohms } \angle \quad (156)$$

where by (546)

$$v = \sinh^{-1} \left(\frac{\sqrt{rg}}{2} \right) \quad \text{hyps. } \angle \quad (157)$$

and, by (553)

$$v' = \tanh^{-1} \left(\frac{m \sqrt{\frac{g}{r}} - \sinh v}{\cosh v} \right) = \tanh^{-1} \left(\frac{m \sqrt{\frac{g}{r}} - \frac{\sqrt{rg}}{2}}{\cosh v} \right) \quad \text{hyps. } \angle \quad (158)$$

In (156), it is evident from (143), that $\sqrt{r/g}$ is a first-approximation surge impedance, which we may denote by r'_0 , that is

$$r'_0 = \sqrt{\frac{r}{g}} \quad \text{ohms } \angle \quad (159)$$

Thus

$$R_N = r'_0 \cosh v \cdot \tanh \{(n, + 1)v + v'\} \quad \text{ohms } \angle \quad (160)$$

where

$$\begin{aligned} v' &= \tanh^{-1} \left(\frac{m - \frac{\sqrt{rg}}{2}}{r'_0 \cosh v} \right) = \tanh^{-1} \left(\frac{\frac{r}{2} + \sigma - \frac{\sqrt{rg}}{2}}{r'_0 \cosh v} \right) \\ &= \tanh^{-1} \left(\frac{\sigma}{r'_0 \cosh v} \right) \quad \text{hyps. } \angle \quad (161) \end{aligned}$$

When $\sigma = 0$, $v' = 0$; when $\sigma = r_0$, $v' = \alpha$; when $\sigma = \alpha$, $v' = j \frac{\pi}{2}$.

v' is wholly real from $\sigma = 0$ to $\sigma = r_0$, and contains an imaginary quadrant or $j \frac{\pi}{2}$, from $\sigma = r_0$ to $\sigma = \alpha$. Moreover, from (142), it is evident that v is the angle whose sine is the uncorrected angle $\frac{\theta_a}{2}$ of a half-section. That is a half-section having a line resistance of $r/2$ ohms \angle , and a half-leakance of $g/2$ ohms \angle would subtend, ignoring lumpiness, an apparent angle

$$v_a = \frac{\theta_a}{2} = \sqrt{\frac{r}{2} \cdot \frac{g}{2}} \quad \text{apparent hyps. } \angle \quad (162)$$

If, therefore, we define the surge impedance of the artificial

$$T \text{ line as } r_0 = r'_0 \cosh v \quad \text{ohms } \angle \quad (163)$$

(160) reduces to

$$R_N = r_0 \tanh (2Nv + v') = r_0 \tanh \left\{ 2Nv + \tanh^{-1} \left(\frac{\sigma}{r_0} \right) \right\} \\ \text{ohms } \angle \quad (164)$$

where

$$\sinh v = \sqrt{\frac{r}{2}} \cdot \frac{g}{2} = v_a; \text{ or } v = \sinh^{-1} v_a \quad \text{numeric } \angle \quad (165)$$

which connects the true and apparent semi-section angles. Further, if we write

$$\theta' = \delta_B = \tanh^{-1} \left(\frac{\sigma}{r_0} \right) \quad \text{hyps. } \angle \quad (166)$$

$$\theta = 2v \quad \text{hyps. } \angle \quad (167)$$

$$\delta_N = N\theta + \delta_B = \Theta + \delta_B \quad \text{hyps. } \angle \quad (168)$$

$$\text{This becomes } R_N = r_0 \tanh (N\theta + \delta_B) = r_0 \tanh \delta_N \\ \text{ohms } \angle \quad (169)$$

which is identical with formula (126) correspondingly developed for smooth lines.

If then we form the angle subtended by a section as

$$\theta = 2 \sinh^{-1} \frac{\sqrt{rg}}{2} = 2v \quad \text{hyps. } \angle \quad (170)$$

and form the surge impedance of the section or line by

$$r_0 = \sqrt{\frac{r}{g}} \cdot \cosh v \quad \text{ohms } \angle \quad (171)$$

in accordance with (163), and finally determine the angle subtended by the load in position angle at B , by (166), it follows that *the impedance at and beyond any junction of a T line is the same as at the corresponding position angle of a smooth line of the same Θ and r_0 , loaded at B with the same σ .* The line impedance at and beyond each junction of the T line will correspond precisely with that at the corresponding position angle on the conjugate smooth line. Away from junctions, of course, the correspondence must cease, owing to the lumpiness of the T line.

If the terminal load σ exceeds r_0 , then, as in (112a) and (89), an

imaginary quadrant, or $j \frac{\pi}{2}$, will appear in $\theta' = \delta_B$, which will replace tangents by cotangents in the application of (169). We shall see that this distinction disappears in a.c. cases, and (166) applies universally.

Formulas (170) and (171) are thus the corrections for the lumpiness of a T line.

As an example, we may take (see Fig. 35) the five-section T line shown in Fig. 38, loaded at the motor end with $\sigma = 750$ ohms. Here $r = 500$ ohms, and $g = 0.00025$ mho. The first-approximation section angle is, therefore, $\sqrt{500 \times 0.00025} = \sqrt{0.125} = 0.35355$ hyp., and the first-approximation surge impedance $r'_0 = \sqrt{\frac{500}{0.00025}} =$

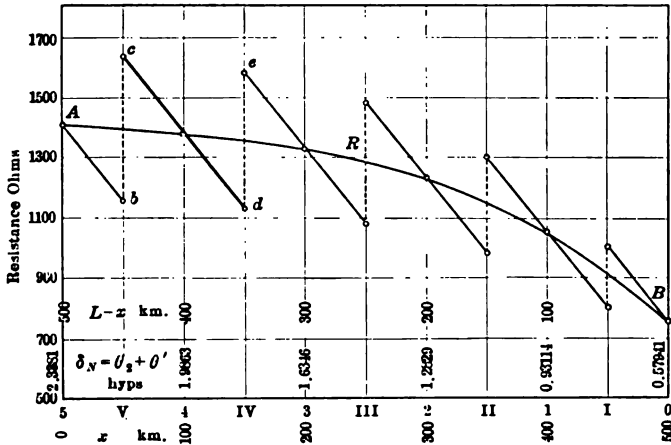


FIG. 35.—Line resistance at and beyond leaks and junctions of loaded T line, and at corresponding position angles on the conjugate smooth line. See Fig. 38.

$\sqrt{2,000,000} = 1,414.2$ ohms. The corrected section angle is, by (170), $\theta = 2 \sinh^{-1} \frac{0.35355}{2} = 0.35174$ hyp. The corrected surge impedance is, by (171), $r_0 = 1,414.2 \times \cosh 0.17587 = 1,436.1$ ohms. The angle subtended by the load is also, by (166), $\theta' = \tanh^{-1} \left(\frac{750}{1,436.1} \right) = 0.57941$ hyp. If we add θ' to $N\theta$, we obtain the position angles of the junctions shown in Fig. 35. At each junction, the resistance is given by (169). The resistance commences at 750 ohms for junction 0, rises steadily to 1,000

ohms by leak I; then falls, owing to the effect of the leak to 800 ohms; then rises to 1,050 ohms at junction 1, and so on, following the set of zigzag straight lines indicated. The conjugate smooth line of 1.7587 hyps. and surge impedance 1,436.1 ohms, loaded at *B* with 750 ohms, would offer a continuous line resistance from point to point, following formula (126), which corresponds exactly to (169) at section junctions, as shown by the continuous curve *ARB* in Fig. 35. It is evident that each and every point of an active smooth lines possesses a corresponding position angle δ_P ; but an artificial line can be said to have position angles only at its junctions and mid-sections.

At and excluding the *N*th leak, the line impedance is, from (150)

$$R_N = r'_0 \frac{\sinh \{(2N - 1)v + v'\}}{\cosh \{(2N - 2)v + v'\}} = r_0 \frac{\sinh \delta_N \operatorname{sech} v}{\cosh \delta_{N-1}} \text{ ohms } \angle \quad (172)$$

while at and including the *N*th leak, the line impedance falls by (153) to

$$R'_N = r'_0 \frac{\sinh \{(2N - 1)v + v'\}}{\cosh \{(2N)v + v'\}} = r_0 \frac{\sinh \delta_N \operatorname{sech} v}{\cosh \delta_N} \text{ ohms } \angle \quad (173)$$

Thus, at and including leak *III* in Fig. 38, the line impedance would be

$$1,414.2 \times \frac{\sinh (5 \times 0.17587 + 0.57941)}{\cosh (6 \times 0.17587 + 0.57941)} = 1,414.2 \frac{\sinh 1.45875}{\cosh 1.63462} = 1,080.9 \text{ ohms}$$

Potentials at Leaks and Junctions.—The law of distribution of potential over a smooth line in the steady state, is, as we have seen, directly as the sines of position angles, and the distribution of line impedance directly as the tangents of position angles.

We have also found in (169), that the latter law of impedance is true for *T* lines at junction points. This suggests that the former law of potential may also hold true for such junction points. The following is, however, a demonstration of this proposition.

Let V_N be the potential at junction *N* (volts \angle),

V_N be the potential at adjacent downside leak *N* (volts \angle),

R_N be the line impedance at junction *N* (ohms \angle).

Numerically $N = N$.

Then

$$\begin{aligned} \frac{V_N}{V_N} &= \frac{R'_N}{R_N} = \frac{r'_0 \sinh \{(2N-1)v + v'\}}{\cosh (2Nv + v')} \\ &= \frac{1}{\cosh v} \frac{\sinh \{(2N-1)v + v'\}}{\sinh (2Nv + v')} \quad \text{numeric } \angle \quad (174) \end{aligned}$$

and

$$\begin{aligned} \frac{V_{N-1}}{V_N} &= \frac{R_{N-1}}{R_N} = \frac{r'_0 \cosh v \cdot \tanh \{2(N-1)v + v'\}}{r'_0 \frac{\sinh \{(2N-1)v + v'\}}{\cosh \{2(N-1)v + v'\}}} \\ &= \cosh v \frac{\sinh \{2(N-1)v + v'\}}{\sinh \{(2N-1)v + v'\}} \quad \text{numeric } \angle \quad (175) \end{aligned}$$

thus

$$\frac{V_{N-1}}{V_N} = \frac{\sinh \{2(N-1)v + v'\}}{\sinh (2Nv + v')} = \frac{\sinh \delta_{N-1}}{\sinh \delta_N} \quad \text{numeric } \angle \quad (176)$$

That is the potentials at successive junctions are as the sines of the position angles, and if this is true for successive junctions, it must be true for all the junctions.

Line Currents at Junctions.—Since at T -line junctions, the potentials are directly as the sines of the position angles, and the line impedances as the tangents of the same, it may almost be inferred that the line currents at junctions are as the cosines of the position angles. The following, however, is a demonstration of the proposition.

Let I_N be the line current at junction N (amperes \angle),

I_{N-1} be the line current at junction $N-1$ (amperes \angle),

$N = N$ be the number of the leak between them (177)

Then

$$\begin{aligned} \frac{I_{N-1}}{I_N} &= \frac{G_N}{G'_N} = \frac{r'_0 \sinh \{(2N-1)v + v'\}}{1 \cdot \cosh (2Nv + v')} \\ &= \frac{r'_0 \sinh \{(2N-1)v + v'\}}{\cosh \{2(N-1)v + v'\}} = \frac{\cosh \delta_{N-1}}{\cosh \delta_N} \quad \text{numeric } \angle \quad (178) \end{aligned}$$

Since the cosine proposition applies for any pair of adjoining junctions, it must apply to all of the junctions. *The current at a junction is thus the same as at the corresponding point on the conjugate smooth line.*

Powers at Junctions.—Since, just as in smooth lines, the potentials at T -line junctions are as the sines of the position angles, and the currents as the cosines of the same, it follows, as with

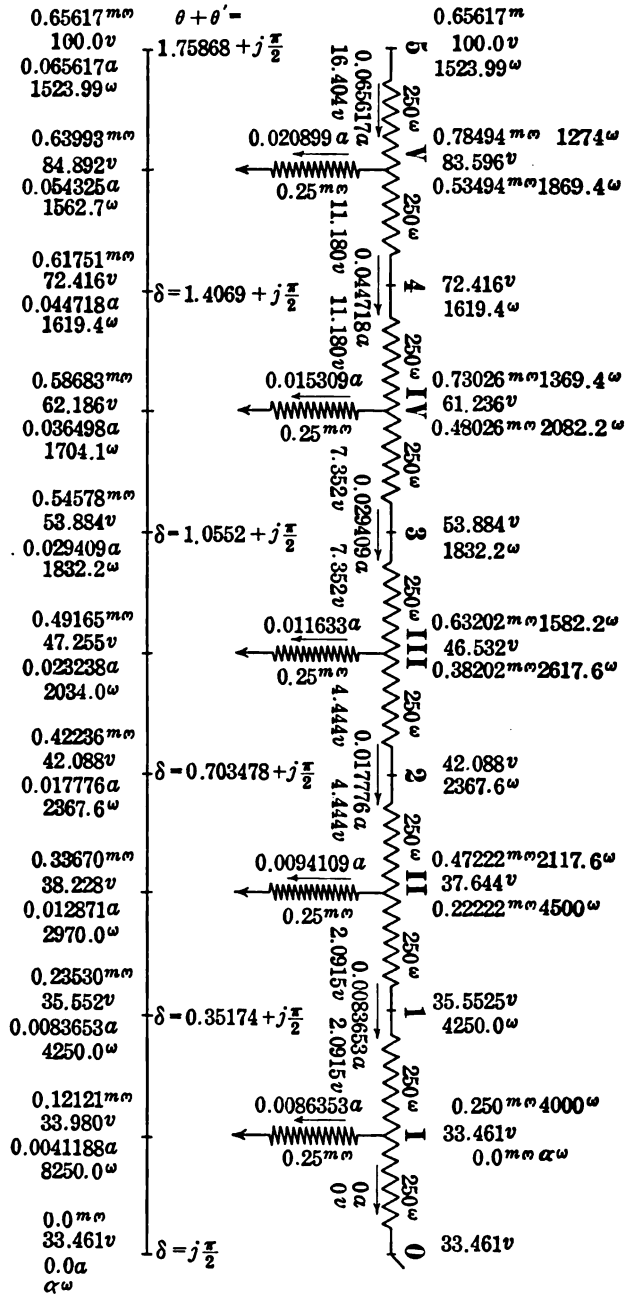


FIG. 36.—Five section T line freed at motor end, and its conjugate smooth line.

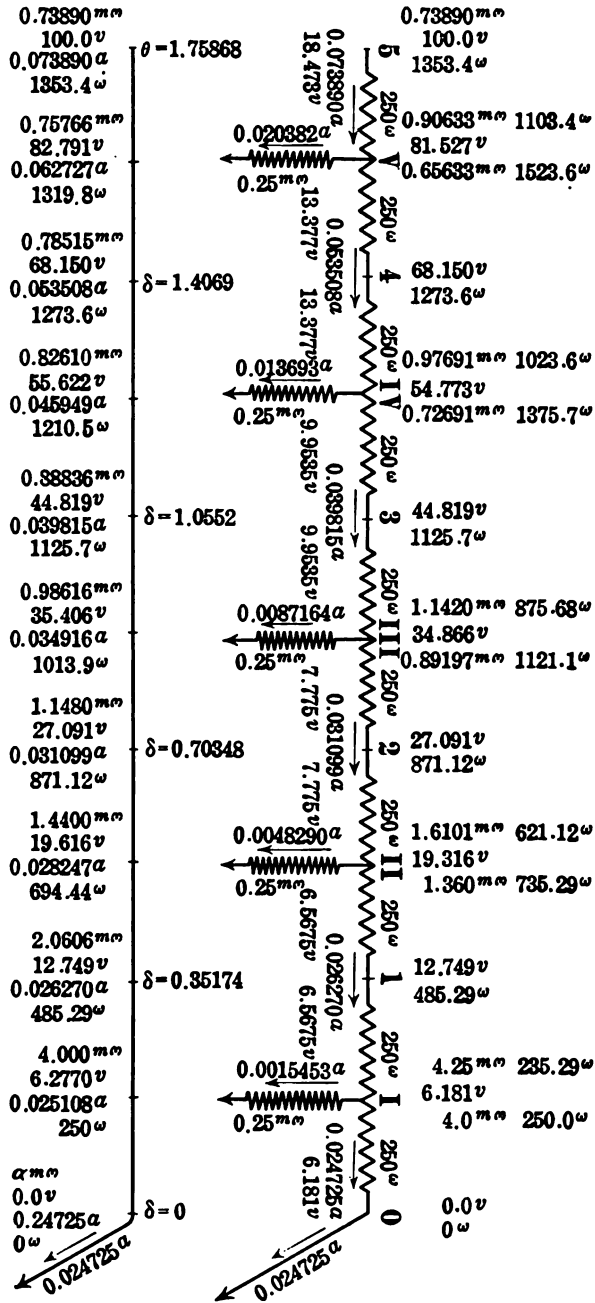


FIG. 37.—Five-section T line grounded at motor end, and its conjugate smooth line.

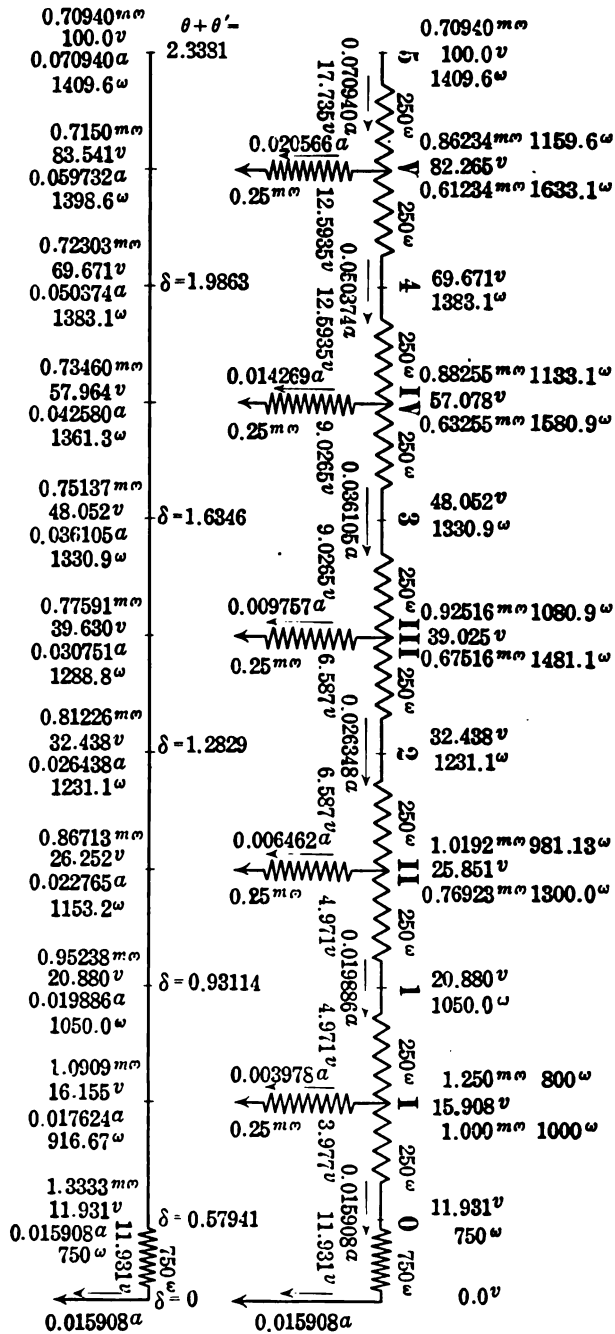


FIG. 38.—Five-section T line loaded at motor end, and its conjugate smooth line.

(138), that their product the voltamperes, and in d.c. cases the powers, at T-line junctions, are as the sines of twice the position angles.

Summary of Facts Concerning a T Line.—All of the immediately foregoing propositions concerning line impedance, potential, current and power on a line, loaded at its motor end with any impedance up to infinity, can be expressed by the proposition that a T line has, at its junctions, all of the electrical properties of its conjugate smooth line. In other words, a T line is the exact counterpart of its equivalent smooth, or conjugate line, if we confine consideration to its junctions and terminals. Away from junctions and terminals, the electrical conditions may be very different from those at corresponding points on the conjugate line.

Abundant examples of these propositions may be found in Figs. 36, 37 and 38, which give the distributions of potential

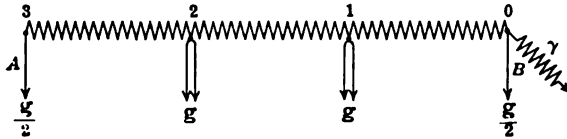


FIG. 39.—Three-section Π line grounded at motor end B through a load of conductance γ mhos.

current, conductance and resistance over the five-section T line already considered, as well as over its conjugate smooth line, for $\sigma = 0$, $\sigma = \alpha$, and $\sigma = 750$ ohms.

Impedance of a Π Line Grounded through a Load at the Far End.—Let us consider a Π line of N sections, three of which are indicated in Fig. 39, grounded at B through an admittance of γ mhos \angle . Each section has a line impedance of r ohms \angle and a total leak admittance of g mhos \angle . Required the admittance and impedance offered by this line at and beyond any section junction; i.e., at the N th junction and between the two leaks there.

At junction 0 or terminal B , the admittance to ground is

$$G'_0 = \frac{g}{2} + \gamma = \mu \quad \text{mhos } \angle \quad (179)$$

Converting this into an impedance at 0

$$R'_0 = \frac{1}{\mu} \quad \text{ohms } \angle \quad (180)$$

Shifting the measuring point to 1, but excluding the double leak there,

$$R_1 = r + \frac{1}{\mu} \quad \text{ohms } \angle \quad (181)$$

Converting this into an admittance,

$$G_1 = \frac{1}{r + \frac{1}{\mu}} \quad \text{mhos } \angle \quad (182)$$

Adding in the two leaks at 1

$$G'_1 = g + \frac{1}{r + \frac{1}{\mu}} = 1/F_2(\mathbf{g}, \mathbf{r}) \quad \text{mhos } \angle \quad (183)$$

Converting this into total impedance at 1

$$R_1 = \frac{1}{g + \frac{1}{r + \frac{1}{\mu}}} = F_2(\mathbf{g}, \mathbf{r}) \quad \text{ohms } \angle \quad (184)$$

Shifting the measuring point to 2, but excluding the double leak there,

$$R_2 = r + \frac{1}{g + \frac{1}{r + \frac{1}{\mu}}} = 1/F_3(\mathbf{r}, \mathbf{g}) \quad \text{ohms } \angle \quad (185)$$

or

$$G_2 = \frac{1}{r + \frac{1}{g + \frac{1}{r + \frac{1}{\mu}}}} = F_3(\mathbf{r}, \mathbf{g}) \quad \text{mhos } \angle \quad (186)$$

Adding the leaks at 2,

$$G'_2 = g + \frac{1}{r + \frac{1}{g + \frac{1}{r + \frac{1}{\mu}}}} = 1/F_4(\mathbf{g}, \mathbf{r}) \quad \text{ohms } \angle \quad (187)$$

or,

$$R'_2 = \frac{1}{g + \frac{1}{r + \frac{1}{g + \frac{1}{r + \frac{1}{g + \frac{1}{r + \frac{1}{\mu}}}}}}} = F_4(g, r) \frac{1}{\mu} \quad \text{ohm } \angle \quad (188)$$

Shifting the measuring point to 3, but excluding the leak there,

$$R_3 = r + \frac{1}{g + \frac{1}{r + \frac{1}{g + \frac{1}{r + \frac{1}{\mu}}}}} = 1/F_5(r, g) \frac{1}{\mu} \quad \text{ohms } \angle \quad (189)$$

or,

$$G_3 = \frac{1}{r + \frac{1}{g + \frac{1}{r + \frac{1}{g + \frac{1}{r + \frac{1}{\mu}}}}} = F_5(r, g) \frac{1}{\mu} \quad \text{mhos } \angle \quad (190)$$

Terminating the line at 3 with a single leak $g/2$

$$G''_3 = \frac{g}{2} + F_5(r, g) \frac{1}{\mu} \quad \text{mhos } \angle \quad (191)$$

It is evident, from the above, that measuring from any junction N , between its two leaks,

$$G''_N = \frac{g}{2} + F_{2N-1}(r, g) \frac{1}{\mu} \quad \text{mhos } \angle \quad (192)$$

Applying formula (563), Appendix B, to this, we have:

$$G''_N = \sqrt{\frac{g}{r}} \cdot \cosh v \cdot \tanh (2Nv + v') \quad \text{mhos } \angle \quad (193)$$

where

$$v = \sinh^{-1} \frac{\sqrt{gr}}{2} \quad \text{hyp. } \angle \quad (194)$$

and

$$v' = \tanh^{-1} \left(\frac{\mu \sqrt{\frac{r}{g}} - \sinh v}{\cosh v} \right) = \tanh^{-1} \left(g''_0 \frac{\gamma_{2N-1}}{\cosh v} \right) \quad \text{hyp. } \angle \quad (195)$$

Since $\sqrt{g, r}$ is of the nature of a surge admittance, we may denote it by g'' , and (163) becomes:

$$G''_N = g''_0 \cosh r + \tanh 2Nr - r' \quad \text{mhos } \angle \quad (196)$$

If we take $g_0 = g''_0 \cosh r \quad \text{mhos } \angle \quad (197)$

$$G''_N = g_0 \tanh 2Nr - r' \quad \text{mhos } \angle \quad (198)$$

where

$$r' = \tanh^{-1} \left(\frac{r}{g_0} \right) = \tanh^{-1} \left(\frac{r_0}{r} \right) \quad \text{hypos. } \angle \quad (199)$$

This is the counterpart of formula (164) for a Π line. If the line is grounded at B through any impedance less than r_0 , (199) will be uninterpretable for real values, unless we make

$$r'' = r' - j\frac{\pi}{2} \quad \text{hypos. } \angle \quad (200)$$

when (198) becomes

$$G''_N = g_0 \coth 2Nr - r'' = g_0 \coth \delta_N \quad \text{mhos } \angle \quad (201)$$

r'' will then be the position angle at junction O , or B , $2Nr$ will be the angular distance of junction N from B , hence at junction N

$$\delta_N = 2Nr - r'' \quad \text{hypos. } \angle \quad (202)$$

and

$$R''_N = r_0 \tanh (2Nr + r'') = r_0 \tanh \delta_N \quad \text{ohms } \angle \quad (203)$$

which agrees with (126) and (169). Consequently, *the impedance at and beyond any junction of a Π line is the same as at the corresponding position angle of the smooth line having the same Θ , r_0 and σ , the measurement being made between the two leaks of that junction.* When $\sigma = 0$, $r'' = 0$; when $\sigma = r_0$, $r'' = \alpha$; when $\sigma = \alpha$, $r'' = j\frac{\pi}{2}$. From $\sigma = 0$ to $\sigma = r$, r'' is real. From $\sigma = r_0$ to $\sigma = \alpha$, r'' contains $j\frac{\pi}{2}$.

The angle subtended by a Π section is the same as that subtended by a T section of the same line impedance r and leak admittance g ; namely, see (170).

$$\theta = 2 \sinh^{-1} \left(\frac{\sqrt{rg}}{2} \right) = 2r \quad \text{hypos. } \angle \quad (204)$$

The surge admittance g_0 of a Π line is formed from its apparent surge admittance $\sqrt{g, r}$ in the same way that the surge impedance

r_0 of a T line is formed from its apparent surge impedance $\sqrt{r/g}$; viz., by using the factor $\cosh v$; or

$$g_0 = \sqrt{\frac{g}{r}} \cdot \cosh v = g''_0 \cosh v \quad \text{mhos } \angle \quad (205)$$

whence

$$r_0 = r''_0 / \cosh v = r''_0 \operatorname{sech} v \quad \text{ohms } \angle \quad (206)$$

where r''_0 is the apparent surge impedance $\sqrt{r/g}$ of a section of Π line.

The lumpiness correction factor for the section angle of a Π line is thus identical with that for the section angle of a T line; but the

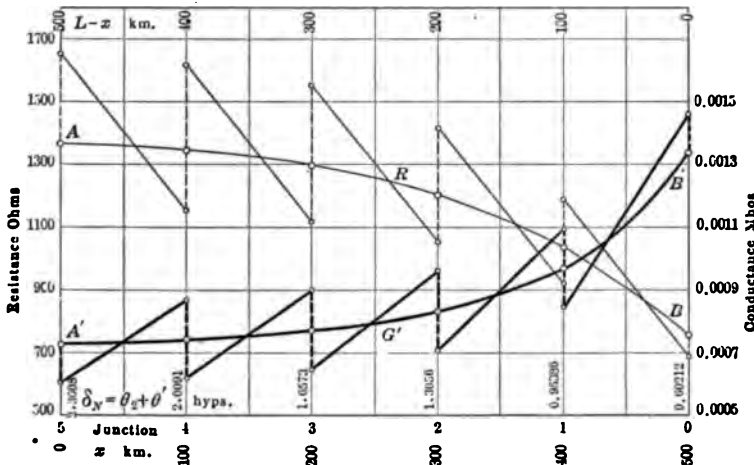


FIG. 40.—Line impedance and admittance at and beyond junctions of a loaded Π line, as well as at corresponding position angles of the conjugate smooth line.

correction factor ($\operatorname{sech} v$) for the surge impedance of a Π line is the reciprocal of that for the surge impedance of a T line ($\cosh v$).

Fig. 40 gives the graphs of line impedance and admittance for the case of the five-section loaded Π line of Fig. 44. The section line impedance is $r = 500$ ohms, and leakance $g = 0.00025$ mho. The uncorrected or apparent surge impedance is $r''_0 = \sqrt{500/0.00025} = \sqrt{2,000,000} = 1,414.2$ ohms. The uncorrected or apparent section angle is $\sqrt{500 \times 0.00025} = \sqrt{0.125} = 0.35355$ hyp. The corrected section angle is, by (184), $\theta = 2 \sinh^{-1} \left(\frac{\sqrt{0.125}}{2} \right) = 2 \sinh^{-1} 0.17678 = 2 \times 0.175868 = 0.351736$

hyp., and the angle subtended by the whole line is 1.75868 hyps. The corrected surge impedance is, by (206), $1,414.2/\cosh 0.175868 = 1,392.6$ ohms. The load of 750 ohms at B subtends an angle of $\theta' = \tanh^{-1} (750/1,392.6) = 0.60212$ hyp., which added to the successive values of θ_s at junctions, gives the position angles δ_N at junctions. The line resistance then varies as the tangent, and the line conductance as the cotangent, of these angles.

In Fig. 40, the curve ARB follows the line resistance of the conjugate line, having $\Theta = 1.7587$ hyps. and $r_0 = 1,392.6$ ohms. Such a line would possess a total conductor resistance, by (35), of $1.7587 \times 1,392.6 = 2,449$ ohms, and a total leakage, by (36), of $1.7587 \div 1,392.6 = 1.263 \times 10^{-3}$ mho; whereas the artificial line has an aggregate line resistance of 2,500 ohms, and a total leakage of 1.25×10^{-3} mho. The zigzag line connecting A and B follows the line resistance over the Π line. If measured

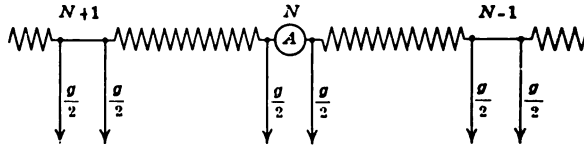


FIG. 41.—Diagrammatic representation of a Π line with double leaks at each junction for the insertion of an ammeter A between successive sections.

between the leaks at each junction, the resistance coincides with the corresponding points on the curve ARB . The heavy black curve $A'G'B'$ follows the graph of line conductance, along the conjugate line, and, at any point thereof, is the reciprocal of the corresponding value on the curve ARB . The zigzag heavy line, oscillating about $A'G'B'$, follows the line conductance over the Π line.

The curve ARB follows (203), and $A'G'B'$ (201), at all points along the conjugate line. At section junctions, the oscillating values on the Π line fall into coincidence with these smooth curves, provided that the measurements are made between the two leaks of a junction, as indicated in Fig. 41. In practice, it is customary to merge these two leaks $g/2$ into one of g mhos, as in Fig. 33. In such a case the agreement of line resistance and conductance at junctions is only realizable arithmetically.

Line Admittance and Impedance on Each Side of a Π Junction.—Theoretically, as above considered, the line impedance or

admittance as measured at any junction of a line should be taken from a point where the two leaks, each of $g/2$ mhos \angle , are supposed to be applied at that junction. Since, in practice, these two leaks are ordinarily merged, it is important to consider the line admittance on each side of a junction.

Let G_N be the admittance on the down-energy or motor side of junction N (mhos \angle) and G'_N the corresponding admittance on the up side (mhos \angle) including the leak at N ; so that

$$G'_N = g + G_N \quad \text{mhos } \angle \quad (207)$$

Then, by (186) and (190),

$$G_N = F_{2N-1}(\mathbf{r}, \mathbf{g})_{\frac{1}{\mu}} = \sqrt{\frac{\mathbf{g}}{\mathbf{r}}} \frac{\sinh \{(2N-1)v + v'\}}{\cosh (2Nv + v')} \text{ mhos } \angle \quad (208)$$

and by (556) this is

$$= \sqrt{\frac{\mathbf{g}}{\mathbf{r}}} \frac{\cosh \{(2N-1)v + v''\}}{\sinh (2Nv + v'')} = \sqrt{\frac{\mathbf{g}}{\mathbf{r}}} \frac{\cosh (\delta_N - v)}{\sinh \delta_N} \text{ mhos } \angle \quad (209)$$

where

$$v' = \tanh^{-1} \left(\frac{\gamma_i}{g_0} \right), \quad v'' = \tanh^{-1} \left(\frac{\sigma}{r_0} \right) \text{ hyps. } \angle \quad (210)$$

and

$$v = \sinh^{-1} \left(\frac{\sqrt{\mathbf{r}\mathbf{g}}}{2} \right) \text{ hyps. } \angle \quad (211)$$

so that

$$R_N = 1/G_N = r''_0 \frac{\sinh \delta_N}{\cosh (\delta_N - v)} = r_0 \frac{\sinh \delta_N \cosh v}{\cosh (\delta_N - v)} \text{ ohms } \angle \quad (212)$$

Again, by (187),

$$G'_N = 1/F_{2N}(\mathbf{g}, \mathbf{r})_{\frac{1}{\mu}} = 1/\sqrt{\frac{\mathbf{r}}{\mathbf{g}}} \frac{\cosh (2Nv + v')}{\sinh \{(2N+1)v + v'\}} \text{ mhos } \angle \quad (213)$$

$$= \sqrt{\frac{\mathbf{g}}{\mathbf{r}}} \frac{\sinh \{(2N+1)v + v'\}}{\cosh (2Nv + v')} \text{ mhos } \angle \quad (214)$$

by (557) and (562)

$$= \sqrt{\frac{\mathbf{g}}{\mathbf{r}}} \frac{\cosh \{(2N+1)v + v''\}}{\sinh (2Nv + v'')} = \sqrt{\frac{\mathbf{g}}{\mathbf{r}}} \frac{\cosh (\delta_N + v)}{\sinh \delta_N} \text{ mhos } \angle \quad (215)$$

and

$$R'_N = 1/G'_N = r''_0 \frac{\sinh \delta_N}{\cosh (\delta_N + v)} = r_0 \frac{\sinh \delta_N \cosh v}{\cosh (\delta_N + v)} \text{ ohms } \angle \quad (216)$$

The reciprocals of (209) and (215) give, in (212) and (216), the corresponding line impedances on each side of junction N .

As an example, we may take the case of the Π line shown in Fig. 44, loaded at its motor end with $\sigma = 750$ ohms, or $\gamma = 1.3333 \times 10^{-3}$ mho. Required the admittance on each side of leak 2.

Here

$$\delta_N = 1.30559, \delta_N - v = 1.12972, \delta_N + v = 1.48146.$$

$$G_N = \frac{1}{1,414.2} \frac{\cosh 1.12972}{\sinh 1.30559} = 0.00070691 \text{ mho}, R_N = 1,414.6 \text{ ohms}$$

and

$$G'_N = \frac{1}{1,414.2} \frac{\cosh 1.48146}{\sinh 1.30559} = 0.00095691 \text{ mho}, R'_N = 1,045.0 \text{ ohms}.$$

The arithmetical mean of these admittances is 0.00083191 mho, which is the admittance at the corresponding point on the conjugate smooth line, or the admittance as measured between leaks at junction 2.

Arithmetical Mean of Line Admittance on Each Side of a Junction.—If we apply formula (509) of Appendix A to (208) and (215) we obtain

$$\begin{aligned} \frac{G_N + G'_N}{2} &= \sqrt{\frac{g}{r}} \frac{\cosh(\delta_N + v) + \cosh(\delta_N - v)}{2 \sinh \delta_N} = g''_0 \frac{\cosh \delta_N \cosh v}{\sinh \delta_N} \\ &= g''_0 \cosh v \cdot \coth \delta_N = g_0 \coth \delta_N = G''_N \quad \text{mhos } \angle \quad (217) \\ &= g''_0 \cosh v \cdot \coth \delta_N = g_0 \coth \delta_N = G''_N \quad \text{mhos } \angle \quad (218) \end{aligned}$$

which, by (201), is the line admittance at junction N between leaks, or at the corresponding position angle on the conjugate smooth line. This is also evident from (192) and (207).

Consequently, *the arithmetical mean of the line admittances on each side of a junction (their plane vector mean in an a.c. case) is equal to the admittance between leaks at the junction, or to the admittance at the corresponding position angle of the conjugate smooth line.*

Potentials at Π -line Junctions.—If V_N is the potential at junction N (volts \angle), and V_{N-1} is the potential at junction $N - 1$, then it is evident that the ratio of these potentials is the ratio of the line impedance on the down side of N to the line impedance on the up side of $N - 1$. Hence

$$\frac{V_{N-1}}{V_N} = \frac{G_N}{G'_{N-1}} = \frac{\cosh(\delta_N - v) \sinh \delta_N}{\cosh(\delta_{N-1} + v) \sinh \delta_{N-1}} \quad \text{numeric } \angle \quad (219)$$

But

$$\delta_{N-1} + v = \delta_N - v \quad \text{hyp. } \angle \quad (220)$$

so that

$$\frac{V_{N-1}}{V_N} = \frac{\sinh \delta_{N-1}}{\sinh \delta_N} \quad \text{numeric } \angle \quad (221)$$

or the potentials at Π -line junctions are as the sines of their position angles, and therefore the same as at the corresponding position angles of the conjugate smooth line.

Line Currents at Π -line Junctions.—Since the potential V_N at any section junction has been shown to be the same as at the corresponding position angle on the similarly loaded conjugate smooth line, and the line admittance G'_N between leaks at that junction is the same as at the corresponding conjugate-line position angle, it follows that the line current $I_N = V_N G'_N$, between leaks at that junction, is also the same as at the corresponding conjugate-line position angle. If, as usual, there is only one leak at the junction, then the arithmetical mean of the line currents on each side of this leak is equal to the line current at the corresponding conjugate-line position angle.

Summary of Facts Concerning a Π Line.—All of the preceding propositions concerning a line, loaded at its motor end with any impedance up to infinity, can be included in the statement that a Π line has at its junctions all of the electrical properties of its conjugate smooth line, on the assumption that the leaks at those junctions are double, and the measurements are made between them, as in Fig. 41.

If the leaks at junctions are single, then this correspondence of electrical properties is complete in regard to potential and power; but involves arithmetical mean values (a.c. plane-vector means) in regard to current, and line admittance.

Figs. 42, 43 and 44 represent the distributions of potential, current, conductance and resistance over the five-section Π line already considered, and over its conjugate smooth line, for $\sigma = 0$, $\sigma = \alpha$, and $\sigma = 750$ ohms respectively. All of the numerical values indicated are obtainable either by the hyperbolic-function formulas above stated, or by direct Ohm's law computation.

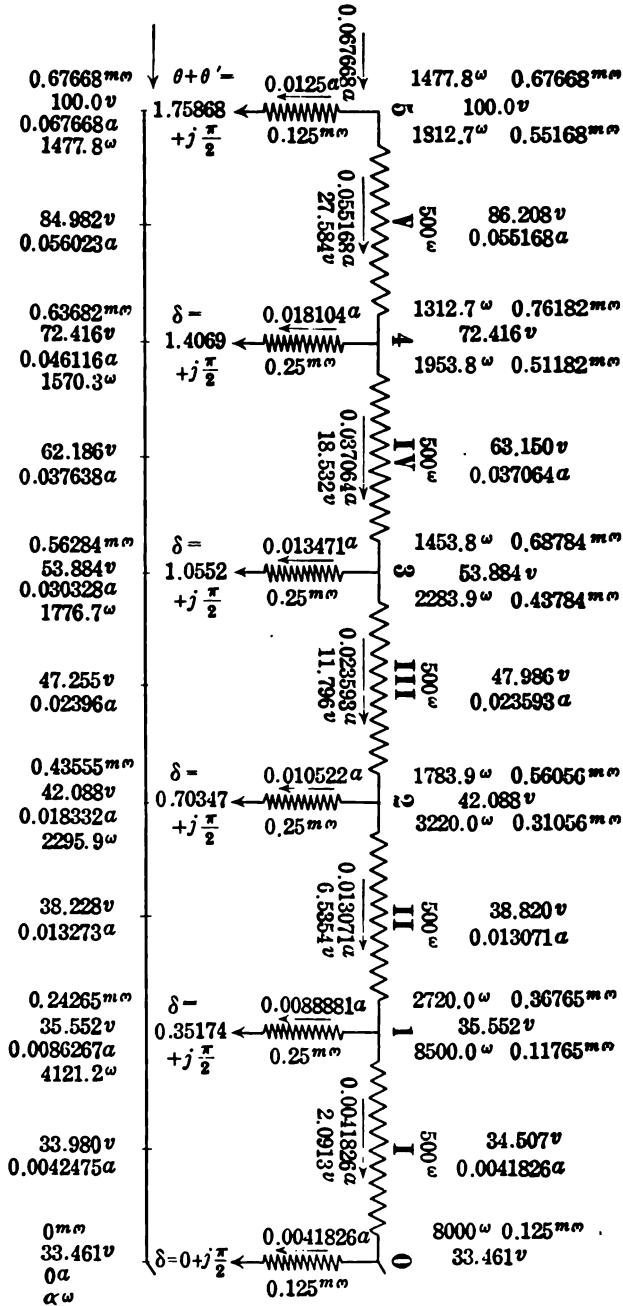


FIG. 42.—Five-section Π line freed at motor end, and its conjugate smooth line.

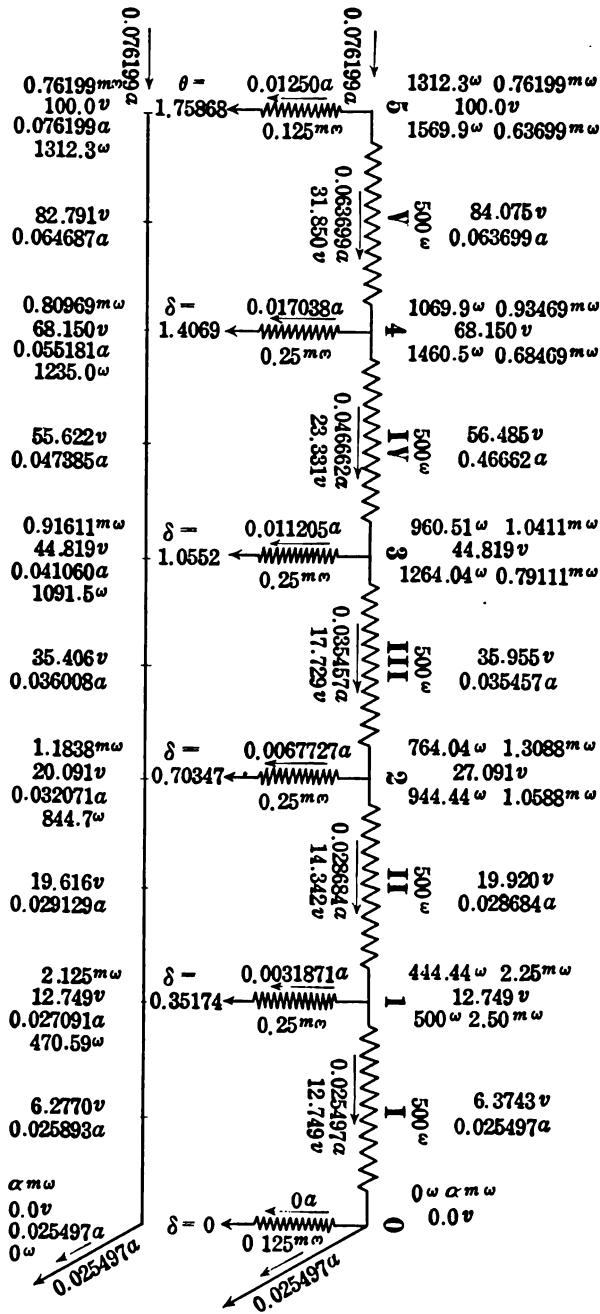


FIG. 43.—Five-section II line grounded at motor end, and its conjugate smooth line.

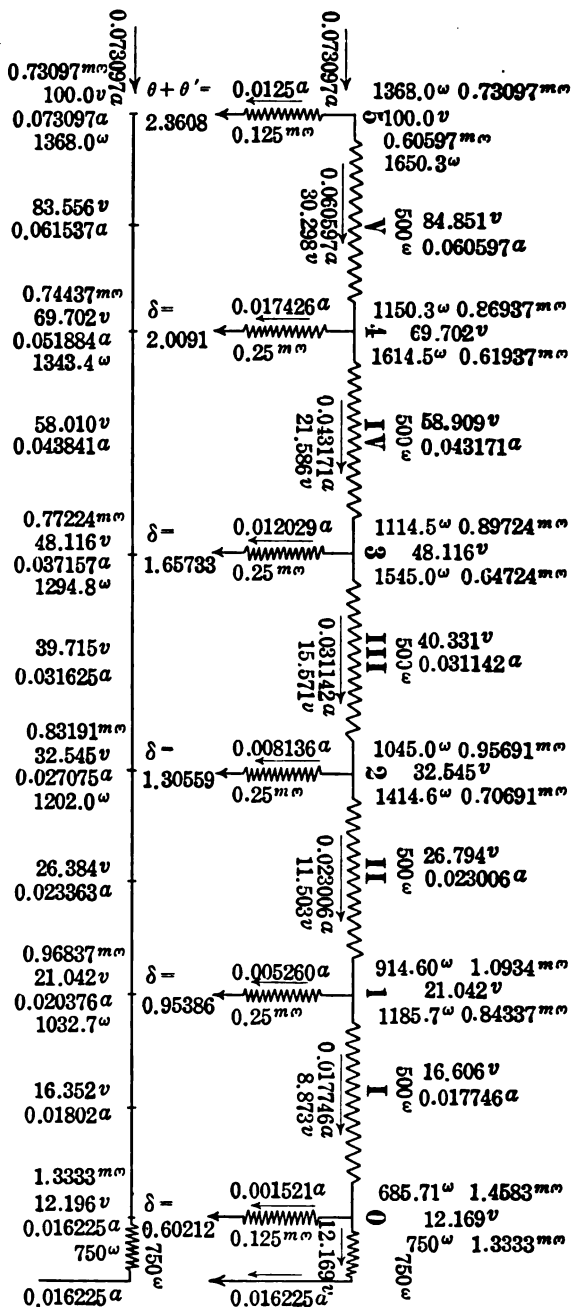


FIG. 44.—Five-section II line loaded at motor end, and its conjugate smooth line.

Properties of T Lines at Mid-sections.—We have already seen that the electrical properties of T and Π lines at section junctions coincide with those of corresponding points on the similarly loaded conjugate smooth lines; but there are also certain electrical correspondences at mid-section points which may be usefully considered.

Potentials at T-line Mid-sections.—Let V_N be the potential at mid-section N ; *i.e.*, at the leak on the down energy side of junction N , and where the potential is V_N volts \angle . Then

$$\begin{aligned} \frac{V_N}{V_N} = \frac{R'_N}{R_N} &= \frac{r'_0 \frac{\sinh \{(2N-1)v + v'\}}{\cosh (2Nv + v')}}{r'_0 \cosh v \cdot \tanh (2Nv + v')} \\ &= \frac{1}{\cosh v} \cdot \frac{\sinh \{(2N-1)v + v'\}}{\sinh (2Nv + v')} \quad \text{numeric } \angle \quad (222) \end{aligned}$$

$$= \frac{1}{\cosh v} \frac{\sinh \delta_N}{\sinh \delta_N} \quad \text{numeric } \angle \quad (223)$$

If we denote by V_{cN} the potential at the corresponding mid-section position on the conjugate smooth line, where the position angle is δ_N hyps. \angle , then

$$V_N = \frac{V_{cN}}{\cosh v} = V_{cN} \cdot \operatorname{sech} v \quad \text{volts } \angle \quad (224)$$

That is the potential at the mid-section of a T line is the potential at the corresponding mid-section point of the conjugate smooth line, multiplied by the secant of the half-section angle v .

As an example, the potential at leak III or mid-section 3 of the T line in Fig. 37 is found from the position angle at this point, $\delta_{III} = 0.87934$ hyp. The potential at this point on the conjugate smooth line is by (98), $V_{cIII} = 100 \frac{\sinh 0.87934}{\sinh 1.75868} = 35.406$ volts. The semi-section angle $v = \theta/2 = 0.175868$, $\operatorname{sech} v = 0.98474$; so that $V_{III} = 35.406 \times 0.98474 = 34.866$ volts.

Line-current at T-line Mid-sections.—We have already seen (178) that the current I_N at junction N may be written

$$I_N = I_C \cdot \frac{\cosh \delta_N}{\cosh \delta_C} \quad \text{amp. } \angle \quad (225)$$

and similarly at junction $N-1$

$$I_{N-1} = I_C \cdot \frac{\cosh \delta_{N-1}}{\cosh \delta_C} \quad \text{amp. } \angle \quad (226)$$

where I_c is the known current at some point on the conjugate line, or some other junction on the T line, where the position angle is δ_c . At a mid-section, the current in the line suddenly drops from I_N to I_{N-1} , owing to the presence of the leak. If we define the mid-section current I_N as the arithmetical mean of these two, then

$$I_N = \frac{I_c}{\cosh \delta_c} \cdot \frac{\cosh \delta_N + \cosh \delta_{N-1}}{2} \quad \text{amp. } \angle \quad (227)$$

But

$$\delta_N = \delta_N + v \text{ and } \delta_{N-1} = \delta_N - v; \text{ so that by (509),}$$

$$I_N = \frac{I_c}{\cosh \delta_c} \cdot \cosh \delta_N \cdot \cosh v \quad \text{amp. } \angle \quad (228)$$

But the actual line current at position angle δ_N on the conjugate smooth line is

$$I_{cN} = \frac{I_c}{\cosh \delta_c} \cdot \cosh \delta_N \quad \text{amp. } \angle \quad (229)$$

so that

$$I_N = I_{cN} \cosh v \quad \text{amp. } \angle \quad (230)$$

The T -line mid-section current is thus equal to the line current at the corresponding point of the conjugate smooth line, multiplied by the cosine of the semi-section angle v .

Power at T-line Mid-sections.—It follows from (224) and (230) that the power $V_N \cdot I_N$ in volt-amperes at any mid-section is equal to the power at the corresponding point on the conjugate smooth line. (See (383).)

Line Impedance at T-line Mid-sections.—Dividing (224) by (230) we obtain

$$R_N = R_{cN} \operatorname{sech}^2 v \quad \text{ohms } \angle \quad (231)$$

The particulars concerning T -line mid-sections and their corresponding conjugate-line points are indicated in Fig. 45. It will be seen that the agreement is complete at section junctions, but is incomplete at mid-sections.

Properties of Π Lines at Mid-sections.—The electrical conditions at Π -line mid-sections are related to those at corresponding conjugate-line points in a similar but inverse manner to those already found for T lines.

Potential at Π -line Mid-sections.—Since the potential at junction N is the same as at the point on the similarly loaded conjugate smooth line, whose position angle is δ_N hyps., we have, by (221),

$$V_N = \frac{V_c}{\sinh \delta_c} \cdot \sinh \delta_N \quad \text{volts } \angle \quad (232)$$

$$V_{N-1} = \frac{V_c}{\sinh \delta_c} \cdot \sinh \delta_{N-1} \quad \text{volts } \angle \quad (233)$$

where V_c is the potential at a point whose position angle is δ_c .
Then

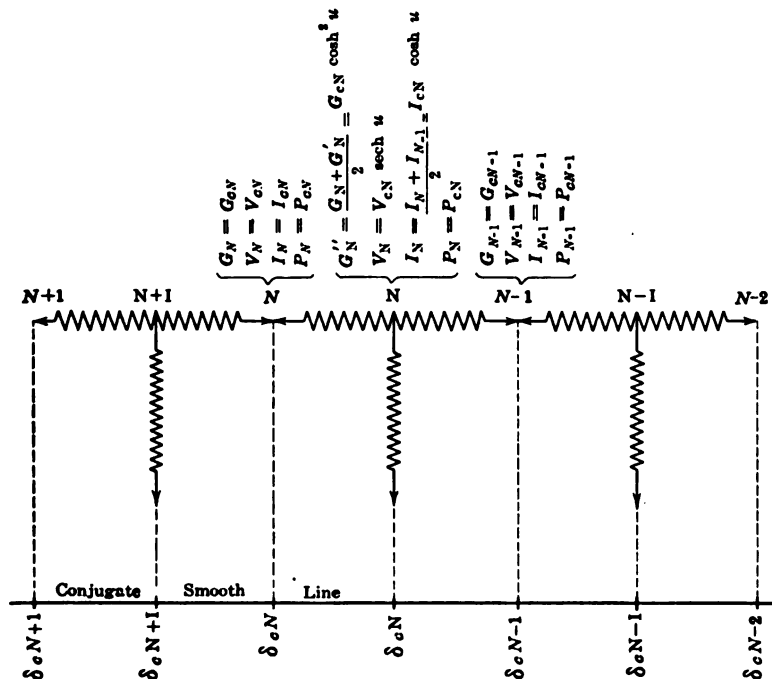


FIG. 45.—Electrical conditions at junctions and midsections of a T line and at corresponding points on the conjugate smooth line.

$$V_N = \frac{V_N + V_{N-1}}{2} = \frac{V_c}{\sinh \delta_c} \cdot \frac{\sinh \delta_N + \sinh \delta_{N-1}}{2} \quad \text{volts } \angle \quad (234)$$

$$= \frac{V_c}{\sinh \delta_c} \cdot \frac{\sinh (\delta_N + v) + \sinh (\delta_N - v)}{2} \quad \text{volts } \angle \quad (235)$$

$$= \frac{V_c}{\sinh \delta_c} \cdot \sinh \delta_N \cdot \cosh v = V_{c,N} \cosh v \quad \text{volts } \angle \quad (236)$$

Thus the potential at a Π -line mid-section is equal to the potential at the corresponding conjugate-line point, multiplied by the cosine of the semi-section angle. In other words, the potential at a Π -line mid-section is always factored as much greater than that at the

corresponding conjugate-line point, as the potential at the similar *T*-line mid-section is factored less, the one being $V_{\mathbf{N}} \cosh v$, and the other $V_{\mathbf{N}} \cosh v = V_{\mathbf{N}} \operatorname{sech} v$.

Line Impedance and Admittance at Π -line Mid-sections.—

If we denote the line impedance at mid-section **N** by $R_{\mathbf{N}}$, we have by (236)

$$\begin{aligned} R_{\mathbf{N}} &= R_s - \frac{r}{2} = \frac{1}{G_s} - \frac{r}{2} = \frac{r}{\sqrt{g}} \frac{\sinh \delta_{\mathbf{N}}}{\cosh \delta_{\mathbf{N}} - r} - \frac{r}{2} \quad \text{ohms } \angle \quad (237) \\ &= \frac{r}{\sqrt{g}} \frac{\sinh \delta_{\mathbf{N}}}{\cosh \delta_{\mathbf{N}} - r} - \frac{\sqrt{rg}}{2} \\ &= r'' \frac{\sinh \delta_{\mathbf{N}} - r}{\cosh \delta_{\mathbf{N}}} - \sinh r \\ & \qquad \qquad \qquad \text{ohms } \angle \quad (238) \end{aligned}$$

$$= r'' \tanh \delta_{\mathbf{N}} \cosh v = r_0 \tanh \delta_{\mathbf{N}} \cosh^2 v = R_{\mathbf{N}} \cosh^2 v \quad \text{ohms } \angle \quad (239)$$

The line resistance at a Π -line mid-section is therefore equal to the line resistance at the corresponding conjugate-line point, multiplied by the square of the cosine of the semi-sectional angle.

The line admittance at mid-section **N** is the reciprocal of $R_{\mathbf{N}}$ or

$$G_{\mathbf{N}} = g'' \coth \delta_{\mathbf{N}} \operatorname{sech} v = g_0 \coth \delta_{\mathbf{N}} \operatorname{sech}^2 v = G_{\mathbf{N}} \operatorname{sech}^2 v \quad \text{ohms } \angle \quad (240)$$

Line Current at Π -line Mid-sections.—From the preceding equations (236) and (240), it follows at once that

$$I_{\mathbf{N}} = V_{\mathbf{N}} \cosh v \angle G_{\mathbf{N}} \operatorname{sech}^2 v = V_{\mathbf{N}} G_{\mathbf{N}} \operatorname{sech} v \text{ amp. } \angle \quad (241)$$

$$= I_{\mathbf{N}} \operatorname{sech} v \quad \text{amp. } \angle \quad (242)$$

or the line current at mid-section **N** (or anywhere in this line section) is equal to the line current at the conjugate-line point corresponding to **N**, multiplied by the secant of the semi-section angle v .

Line Power at Π -line Mid-sections.—It follows directly, from (236) and (242), that the power in the Π line at a mid-section, or the rate in joules per second at which energy is being carried past this point, is

$$P_{\mathbf{N}} = V_{\mathbf{N}} \cdot I_{\mathbf{N}} = V_{\mathbf{N}} \cosh v \cdot I_{\mathbf{N}} \operatorname{sech} v = V_{\mathbf{N}} \cdot I_{\mathbf{N}} = P_{\mathbf{N}} \quad \text{watts } (243)$$

That is, the line volt-amperes at any Π -line mid-section is equal to

the volt-amperes at the corresponding conjugate-line point. (See (383)).

Hence in any *T* line or *Π* line, the power agrees with that at corresponding conjugate-line points at terminals, at section junctions, and, so far as concerns the volt-amperes, at mid-sections.

As an example, consider the power at mid-section II in Fig. 44. The power at this point on the *Π* line is 26.794 volts × 0.023006 amp. = 0.61642 watt. At the corresponding point on the conjugate smooth line, the power is 26.384 volts × 0.023363 amp. = 0.61641 watt.

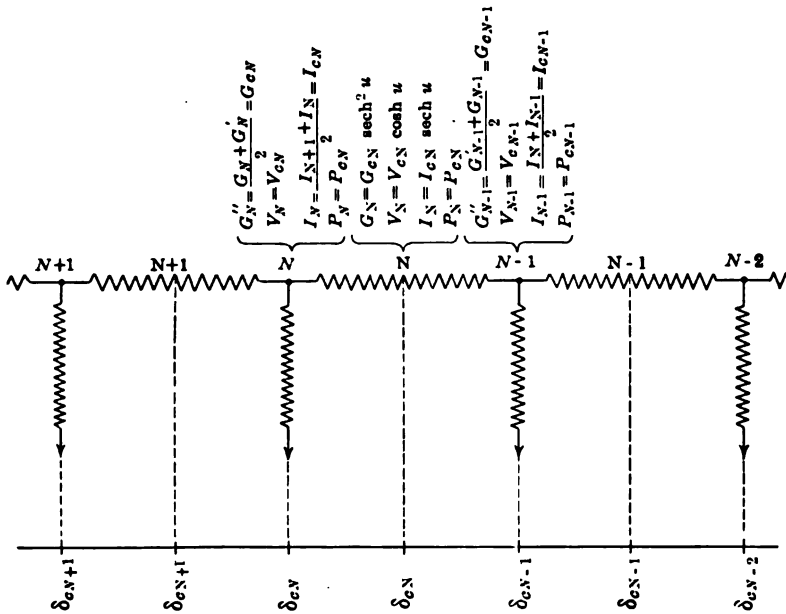


FIG. 46.—Electrical conditions at junctions and midsections of a *Π* line and at corresponding points on the conjugate smooth line.

The relations between the conditions at *Π*-line mid-sections and at corresponding conjugate-line points, are shown in Fig. 46, for reference.

Fall of Potential Compared on *T*, *Π*, and Conjugate Lines Compared.—Fig. 47 represents graphically the fall of potential along the *T* line and *Π* line of Figs. 36 to 38, 42 to 44, as well as along a smooth conjugate line. Strictly speaking, it is not possible to have one and the same smooth line conjugate to both a *T* line and a *Π* line, unless the *r* and *g* in the sections of each are

different, owing to differences in r_0 , but the discrepancy is very small in this case.

It will be seen that taking the "Line Free" graphs, the dotted curve represents a true catenary for the conjugate smooth line. Contacting with this catenary at junction points, are the internal polygon representing the Π -line potential fall, and the external polygon representing the T -line potential fall.

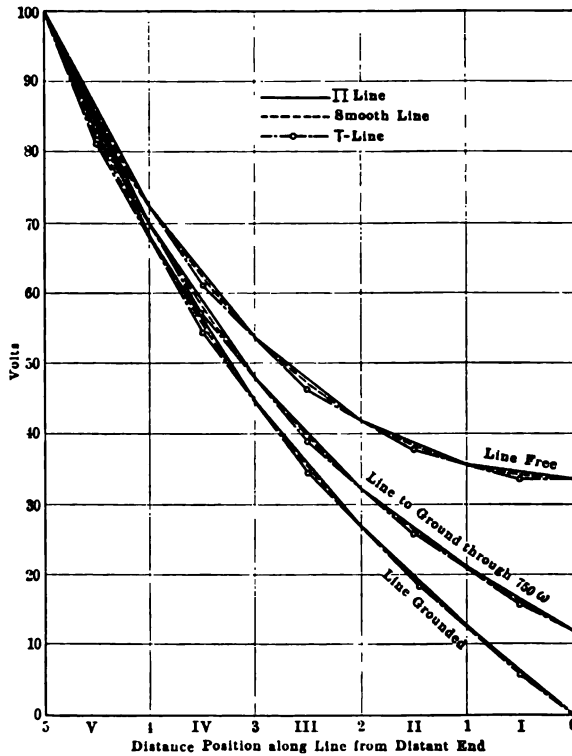


FIG. 47.—Fall of potential on artificial and conjugate smooth line.

These curves indicate that it is possible to arrange two loaded flexible massless strings with suitable masses, in such a manner that both of them shall contact with a common catenary; one of them forming an internal string polygon, and the other an external string polygon.

Fall of Current on T, Π and Conjugate Lines Compared.— Fig. 48 represents graphically the fall of current along the T line of Figs. 36 to 38 and along the conjugate smooth line. The

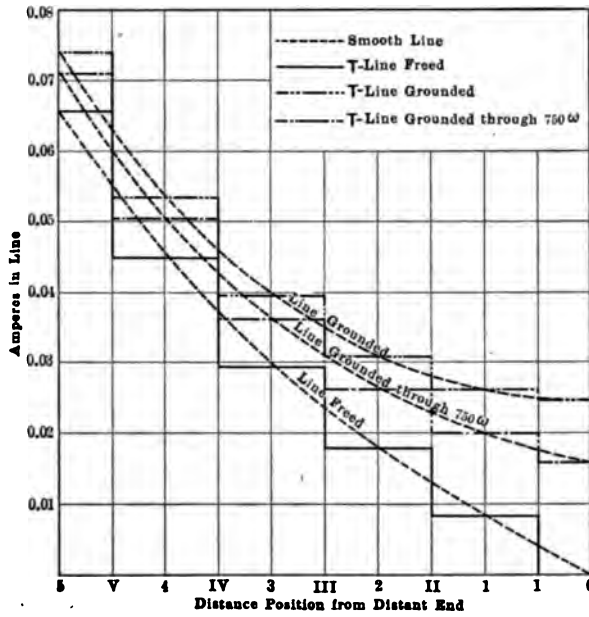


FIG. 48.—Currents in artificial *T* line and in conjugate smooth line.

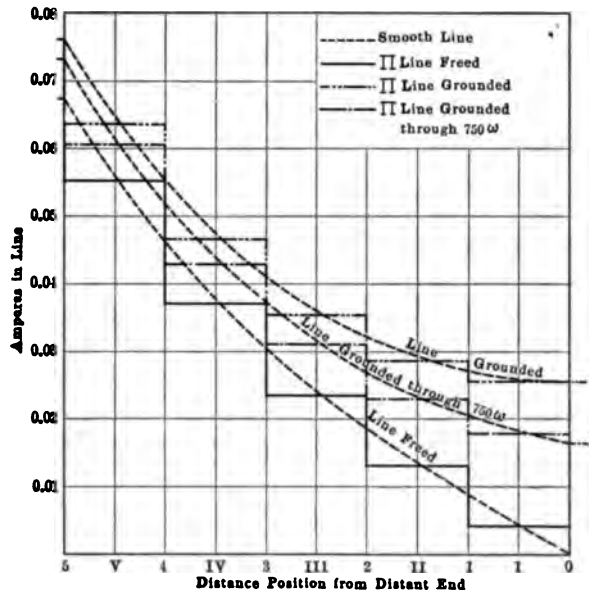


FIG. 49.—Currents in artificial *II* line and in conjugate smooth line.

dotted smooth curves apply to the smooth line in each case. The zigzag T -line current graphs coincide with the smooth curves at section junctions.

In a similar manner, Fig. 49 shows the corresponding Π -line current graphs. Here the mean ordinate at junction points coincides with the corresponding smooth curve.

Artificial Line of Indefinitely Great Number of Very Small Sections.—If a section of lumpy line is large; *i.e.*, contains a relatively large lump of resistance r and a large associated lump of leakance g , the lumpiness correction factor in angle

$$k_v = \frac{\sinh^{-1}\left(\frac{\sqrt{rg}}{2}\right)}{\left(\frac{\sqrt{rg}}{2}\right)} = \frac{\sinh^{-1}v_a}{v_a} \quad \text{numeric } \angle \quad (244)$$

tends to be considerable, and in some a.c. cases may be enormous. The correction factor in surge impedance, either $\cosh v$ or $\operatorname{sech} v$ as the case may be, is also capable of assuming large proportions. As, however, the subdivision of the lumpiness is effected by placing the same total artificial-line resistance and leakance in more numerous sections, both r and g are reduced so that the value of k_v diminishes toward unity. Finally, when the successive sections are all exceedingly small and indefinitely numerous, both r and g tending toward zero, the limit of k_v

$$\left(\frac{\sinh^{-1}v_a}{v_a}\right)_{v_a=0} = 1 \quad \text{numeric} \quad (245)$$

or there ceases to be any correction factor, and the minute apparent angle v_a subtended by a half-section is not to be distinguished from its actual semi-angle v . At the same time the values of $\cosh v$ and $\operatorname{sech} v$, as v approaches zero, tend to the value unity; or the apparent surge impedance by (143) becomes the true surge impedance r_0 . Such a line, however, with indefinitely numerous and indefinitely small lumps of impedance and leakance is, however, a smooth line, which evidently has no lumpiness error.

CHAPTER VII

EQUIVALENT CIRCUITS OF A SMOOTH LINE

In the analysis of the line impedance at any point of a lumpy artificial line, alternating continued fractions naturally present themselves, as was recognized by Mascart in 1883,* and by Herzog and Feldmann in 1903.† The solution of such continued fractions by means of hyperbolic functions in 1908,‡ led in the same year to the conclusions reached in the last chapter, that any T section of artificial line completely replaces, at its terminals, a certain length of conjugate smooth line, and also similarly for a Π section. It followed at once from these propositions,** that conversely, any length of continuous smooth line may be completely replaced at its terminals by a certain T , and also by a certain Π of artificial line. This converse proposition is very important. The T section equivalent to a smooth line is called the "*equivalent T* ," and the corresponding Π section the "*equivalent Π* " of that line. It has been demonstrated algebraically elsewhere†† that the equivalent T and Π of a terminally loaded line, offers both the same sending-end impedance, and the same receiving-end impedance, as the conjugate smooth line. Without repeating the demonstration here, it may be pointed out that the results as to substitutibility of real and artificial-line sections, obtained in the last chapter, indirectly furnish such a demonstration. Moreover, we shall notice some

* MASCART and JOUBERT'S "Treatise of Electricity and Magnetism," Paris, 1883, vol. i, p. 211 (resistance of a conductor when there is loss by the sides).

† J. HERZOG and C. FELDMANN, "Die Berechnung Elektrischer Leitungsnetze," J. Springer, Berlin, April, 1903, vol. i, Chapter V, p. 328.

‡ "The Expression of Constant and of Alternating Continued Fractions in Hyperbolic Functions" by A. E. KENNELLY, *Am. Annals of Mathematics*, Salem Press, vol. ix, No. 2, pp. 85-96, January, 1908.

** "Artificial Lines for Continuous Currents in the Steady State," by A. E. KENNELLY, *Proc. Am. Ac. Arts & Sciences*, vol. xlv, No. 4, pp. 97-130, November, 1908.

†† "The Application of Hyperbolic Functions to Electrical Engineering Problems" by A. E. KENNELLY, London University Press, 1912, Appendix D.

numerical cases of substitution which will supply additional proof arithmetically.

The Equivalent T.—Fig. 50 shows diagrammatically, at AB a smooth line of conductor impedance R ohms \angle , and total leakage G mhos \angle . This line, therefore, possesses an angle of θ

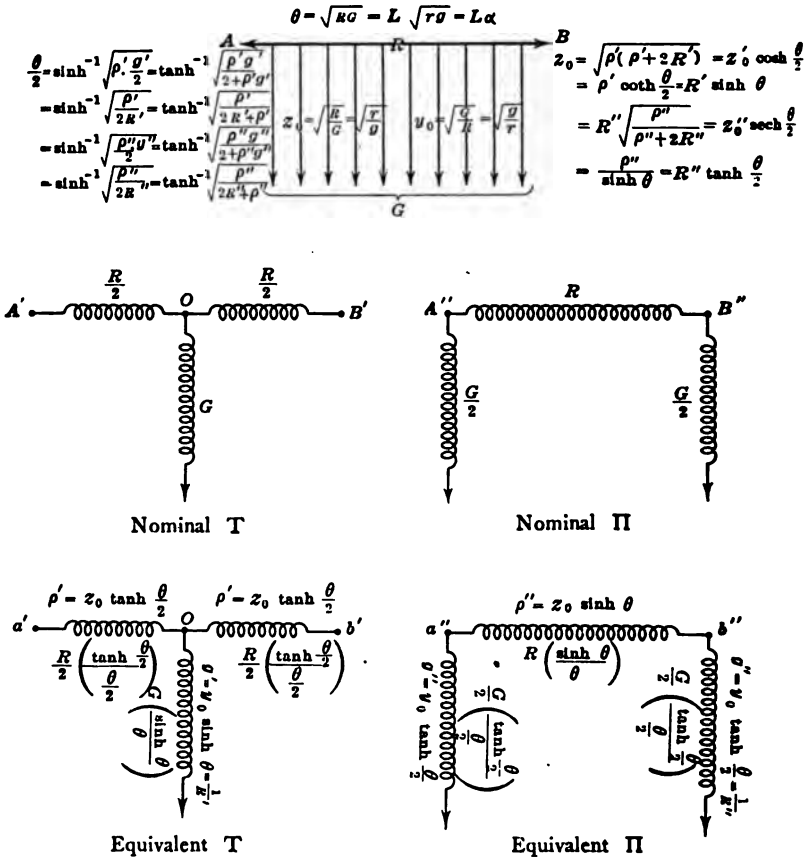


Fig. 50.—Relations between equivalent circuits and their conjugate smooth line.

hyp. \angle , and a surge impedance z_0 ohms \angle , as well as its reciprocal, a surge admittance y_0 mhos \angle . See formulas (18) and (26).

At $A'OB'$, is the "nominal T" of the smooth line AB ; i.e., a T section of impedances having in its elements the nominal values R and G . Thus, the impedance in the line section is R ohms \angle , and the leakage in the single central leak, G mhos \angle .

This nominal T has a lumpiness error, and cannot correctly replace the smooth line. It is only a stepping stone to the "equivalent T ," $a'ob'$, which can correctly replace the smooth line. The correcting factor for the line branches is

$$k_{\rho} = \frac{\tanh \frac{\theta}{2}}{\frac{\theta}{2}} \quad \text{numeric } \angle \quad (246)$$

while the correcting factor for the staff leak is

$$k_{\sigma} = \frac{\sinh \theta}{\theta} \quad \text{numeric } \angle \quad (247)$$

Applying these factors to the respective elements of the nominal T , we find that each branch of the equivalent T has an impedance

$$\rho' = z_0 \tanh \frac{\theta}{2} \quad \text{ohms } \angle \quad (248)$$

while the staff of the equivalent T has an admittance

$$g' = y_0 \sinh \theta \quad \text{mhos } \angle \quad (249)$$

the impedance of the staff $1/g'$ may be denoted by R' .

The Equivalent Π .—The "nominal Π " of the smooth line AB , Fig. 50, is indicated at $A''B''$, the line element having the conductor impedance R , and each leak having half the line leakage G . Lumpiness correction factors must now be applied to these elements in order to produce the "equivalent Π " $a''b''$, which is capable of completely replacing, or of being substituted for, the smooth line AB , in any single-frequency steady state. The correcting factor for the line element is

$$k_{\rho,,} = \frac{\sinh \theta}{\theta} \quad \text{numeric } \angle \quad (250)$$

and the correcting factor for each semi-leak is

$$k_{\sigma,,} = \frac{\tanh \frac{\theta}{2}}{\frac{\theta}{2}} \quad \text{numeric } \angle \quad (251)$$

It is evident that the correcting factors which convert the nominal Π into the equivalent Π of the conjugate smooth line, are the same as those which convert the nominal T into the equivalent T , but in inverse order; so that $k_{\rho,,} = k_{\sigma,,}$ and $k_{\sigma,,} = k_{\rho,,}$.

The corrected elements in the equivalent Π are then found to be

$$\rho'' = z_0 \sinh \theta \quad \text{ohms } \angle \quad (252)$$

and
$$g'' = y_0 \tanh \frac{\theta}{2} \quad \text{mhos } \angle \quad (253)$$

The impedance of each leak $1/g''$ may be denoted by R'' .

Relations between the Equivalent T and Π .—It can be shown that having derived one of these two equivalent circuits of a smooth line, the other can be derived by direct computation.* Thus, if the equivalent T is given, the equivalent Π can be directly computed, and will be found in agreement with the values given in (252) and (253). This is from the known equivalence and general substitutibility of a star and a delta of impedances;† so that one can be replaced by the other in any single-frequency steady electrical system, without disturbing the potentials, currents or powers in the rest of the system.‡

When θ becomes indefinitely small, both the correcting factors $\frac{\sinh \theta}{\theta}$ and $\frac{\tanh (\theta/2)}{(\theta/2)}$ become unity. This means that *when a smooth line is extremely short, its nominal T or Π is also its equivalent T or Π , which is indeed an almost self-evident proposition.*

When θ is large and real, $\frac{\sinh \theta}{\theta}$ becomes large with respect to unity; while $\frac{\tanh (\theta/2)}{(\theta/2)}$ becomes small with respect to unity.

In a.c. cases, with θ complex, both these correcting factors are capable of rapid oscillations in value, as θ changes.

In all e.c. cases, the equivalent T and Π are always physically realizable. That is, their elements are always resistances, which are capable of being designed and constructed. In a.c. cases, however, it frequently happens that either the equivalent T , or the equivalent Π , is physically unrealizable, and sometimes both. That is to say, the values of impedance called for in the

* "The Application of Hyperbolic Functions to Electrical Engineering Problems," by A. E. KENNELLY, London University Press, 1912, Appendix E.

† "The Equivalence of Triangles and Three-pointed Stars in Conducting Networks," by A. E. KENNELLY, *Electrical World and Engineer N. Y.*, vol. xxxiv, No. 12, pp. 413-414, Sept. 16, 1899.

‡ FELDMANN and HERZOG, *Proc. Int. El. Congress, St. Louis, 1904*, vol. ii, section E, pp. 689-709, "The Distribution of Voltage and Current in Closed Conducting Networks."

respective elements may have slopes greater than 90°, and therefore cannot be reproduced in simple series groups of resistors, reactors and condensers. Such cases may be regarded as *arithmetical equivalent circuits*, but not as *physical equivalent circuits*.

Reversion from a T or Π Section to Its Conjugate Smooth Line.—Having given a *T* section or a *Π* section, there must be some conjugate smooth-line equivalent thereto, and it becomes requisite to know the angle θ subtended by the section as well as its surge impedance z_0 or admittance y_0 . This is the problem that presents itself in the use of any given artificial line. It is called the *reversion to the conjugate smooth line*.

Reversion, as the name implies, calls for the reversal of the procedure which determines an equivalent circuit from its conjugate smooth line.

Thus considering the equivalent *T* represented in Fig. 31, we know from (248) that the total line element is defined by the relation

$$r = 2z_0 \tanh \frac{\theta}{2} \quad \text{ohms } \angle \quad (254)$$

and by (249)

$$g = \frac{\sinh \theta}{z_0} = \frac{2 \sinh \frac{\theta}{2} \cosh \frac{\theta}{2}}{z_0} \quad \text{mhos } \angle \quad (255)$$

where θ is the angle, and z_0 the surge impedance of the conjugate smooth line imitated by the section.

Multiplying (254) and (255) we obtain

$$\sinh \frac{\theta}{2} = \sqrt{\frac{r}{2} \cdot \frac{g}{2}} = \frac{\sqrt{rg}}{2} \quad \text{numeric } \angle \quad (256)$$

Dividing (254) by (255) we obtain

$$z_0 = \sqrt{\frac{r}{g}} \times \cosh \frac{\theta}{2} \quad \text{ohms } \angle \quad (257)$$

Again, considering the equivalent *Π* represented in Fig. 32, we know from (252) that the line element is

$$r = z_0 \sinh \theta = 2z_0 \sinh \frac{\theta}{2} \cosh \frac{\theta}{2} \quad \text{ohms } \angle \quad (258)$$

and by (253)

$$\frac{g}{2} = \frac{\tanh \frac{\theta}{2}}{z_0} \quad \text{mhos } \angle \quad (259)$$

Multiplying (258) by (259)

$$\sinh \frac{\theta}{2} = \sqrt{\frac{r}{2} \cdot \frac{g}{2}} = \frac{\sqrt{rg}}{2} \quad \text{numeric } \angle \quad (260)$$

and dividing (258) by (259)

$$z_0 = \sqrt{\frac{r}{g}} \times \frac{1}{\cosh \frac{\theta}{2}} = \sqrt{\frac{r}{g}} \times \operatorname{sech} \frac{\theta}{2} \quad \text{ohms } \angle \quad (261)$$

$$\text{or} \quad y_0 = \sqrt{\frac{g}{r}} \times \cosh \frac{\theta}{2} \quad \text{mhos } \angle \quad (262)$$

The following formulas (263) to (266), for reversion, are also useful.

Reversion from a T to Its Conjugate Smooth Line.—As shown in Fig. 50, and as explained in reference to (170) where $r = 2\rho'$ and $g = g'$

$$\frac{\theta}{2} = v = \sinh^{-1} \sqrt{\rho' \cdot \frac{g'}{2}} = \sinh^{-1} \sqrt{\frac{r}{2} \cdot \frac{g}{2}} = \tanh^{-1} \sqrt{\frac{\rho' g'}{2 + \rho' g'}} \quad \text{hyps. } \angle \quad (263)$$

Also, as explained in reference to (171),

$$\begin{aligned} z_0 &= \sqrt{\rho'(\rho' + 2R')} \\ &= \rho' \coth \frac{\theta}{2} = R' \sinh \theta = \sqrt{\frac{2\rho'}{g'}} \cdot \cosh \frac{\theta}{2} = \sqrt{\frac{r}{g}} \cdot \cosh \frac{\theta}{2} = z'_0 \cdot \cosh \frac{\theta}{2} \quad \text{ohms } \angle \quad (264) \end{aligned}$$

Reversion from a II to Its Conjugate Smooth Line.—As shown in Fig. 50, and as explained in reference to (204), where $r = \rho''$ and $g = 2g''$,

$$\frac{\theta}{2} = v = \sinh^{-1} \sqrt{\rho'' \cdot \frac{g''}{2}} = \sinh^{-1} \sqrt{\frac{r}{2} \cdot \frac{g}{2}} = \tanh^{-1} \sqrt{\frac{\rho'' g''}{2 + \rho'' g''}} \quad \text{hyps. } \angle \quad (265)$$

Also, as explained in reference to (205),

$$\begin{aligned} z_0 &= R'' \sqrt{\frac{\rho''}{\rho'' + 2R''}} \\ &= R'' \tanh \frac{\theta}{2} = \frac{\rho''}{\sinh \theta} = \sqrt{\frac{\rho''}{2g''}} \cdot \operatorname{sech} \frac{\theta}{2} = \sqrt{\frac{r}{g}} \cdot \operatorname{sech} \frac{\theta}{2} = z_0'' \operatorname{sech} \frac{\theta}{2} \quad \text{ohms } \angle \quad (266) \end{aligned}$$

General Relations in Reversion.—It can be shown that just as there is one and only one T and II which can replace a given

smooth line at any one frequency; so, conversely, there is one and only one smooth line which can replace a given T or a given Π . It frequently happens, however, that the conjugate smooth line so determined cannot be physically realized. In other words, the conjugate smooth lines of some T s and Π s are only arithmetically realizable.

To any actual smooth line, operated by direct currents (zero frequency), in the steady state, there is one and only one equivalent T and Π . In the case of a.c. lines, however, θ varies with the impressed frequency, and the correcting factors, $k_p, p_p, k_g, k_g,$ all vary with the frequency. Consequently, an artificial line of T s, or Π s, or both, which is a correct counterpart of some smooth line at a given frequency, ceases to be its correct counterpart when the frequency is changed. In other words, *there is only one frequency at which a given artificial line can correctly represent an actual smooth line.* The amount of error which will attend a change in impressed frequency will depend upon the lumpiness of the line. In general, the fewer the sections, and the greater the corresponding lumpiness in an a.c. artificial line, the greater the errors introduced by changes in impressed frequency. It is for this reason that it is preferable to divide an artificial line into a number of small sections. If it were not for the effect of changes in frequency upon the imitative accuracy of an artificial line, it would be manifestly easier and more convenient to employ a single T or a single Π as the equivalent. It is, however, easy, as we shall see later, so to design an artificial line for the embodiment of a given actual smooth line, that for a given range of impressed frequency, the range of discrepancies in voltage, current, or power, shall be kept within assigned small limits.

Example of Equivalent Circuits.—A convincing numerical example of the substitutibility of an equivalent T or Π for its conjugate smooth line, is furnished by the case of a d.c. line voltageged at both ends.

Fig. 51 represents the case of a line AB , 200 km. long, having a linear resistance $r = 6$, and a linear leakance $g = 1.5 \times 10^{-6}$; so that its total conductor resistance is 1,200 ohms and its total dielectric leakance 0.3×10^{-3} mho; hence its line angle $\theta = 0.6$ hyp., its linear angle $\alpha = 0.003$ hyp. per km., and its surge impedance $r_0 = 2,000$ ohms. The line has a potential of +100 volts applied at A , and a potential of +90 volts applied

at B ; so that the two batteries oppose each other. In such a case, provided that the two impressed terminal potentials are not too far apart, there will be a point of minimum potential somewhere on the line. Let x be the distance of this point in kilometers from A , and θ_1 the corresponding distance in angle. Then, by (77), the potential at X will be:

$$V_x = \frac{V_A}{\cosh \theta_1} = \frac{V_A}{\cosh \alpha x} \quad \text{volts} \quad (267)$$

This will be the same potential as is established over $L - x$ kilometers from B , or

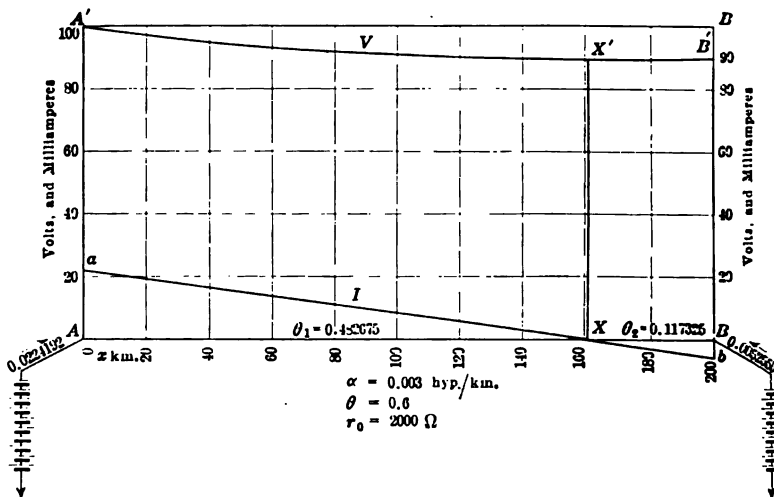


FIG. 51.—Smooth line voltaged at both ends.

$$V_x = \frac{V_B}{\cosh \theta_2} = \frac{V_B}{\cosh \alpha (L - x)} \quad \text{volts} \quad (268)$$

Solving (267) and (268) for x and V_x , we obtain:
 $x = 160.892$ km., $L - x = 39.108$ km., $\theta_1 = 0.482675$ hyp.,
 $\theta_2 = 0.117325$ hyp., and $V_x = 89.384$ volts. The fall of potential is indicated in Fig. 51 by the catenary curve $A'VX'B'$, with its minimum at X' . For electrical purposes, the line may now be regarded as cut at X , because no current can flow at this point. The entering current at A , using (131), is then found to be 0.022 4192 amp., and at B , 0.005 2555 amp. The curve $aIXb$ indicates the strength of current along the line, current flowing toward B being taken as plus.

Incidentally, it may be pointed out that if we know the potential and current at B , the case may be readily worked out by the use of position angles, as described in Chapter IV. Thus with $V_B = 90$, and $I_B = -0.0052555$, the line is virtually grounded

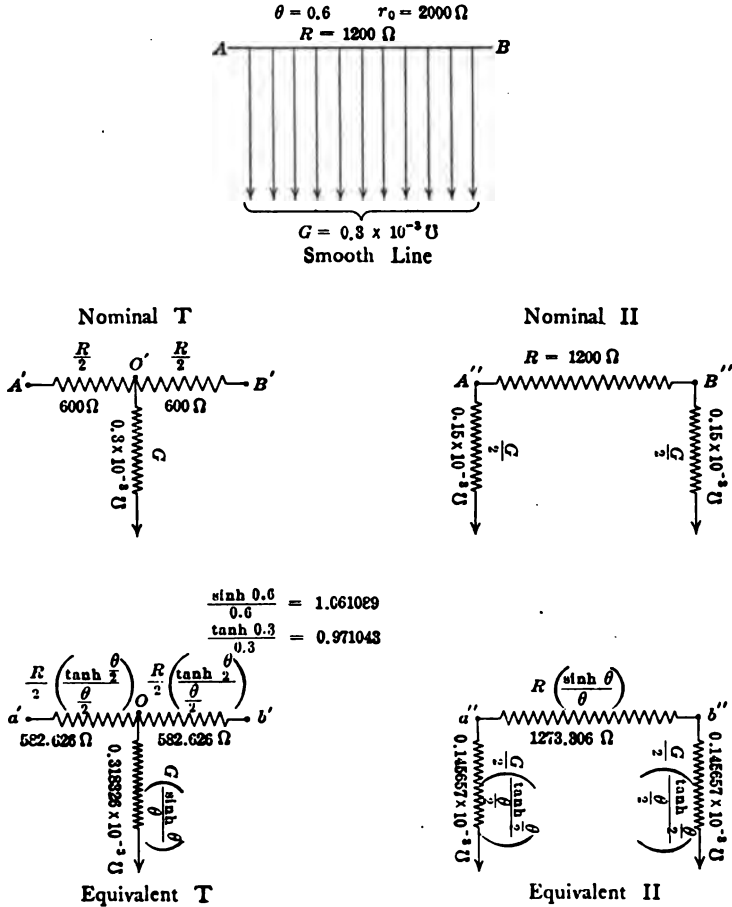


FIG. 52.—Equivalent circuits of a line with $\theta = 0.6$, $r_0 = 2000$ ohms.

at B through a negative resistance $\sigma = \frac{90}{-0.0052555} = -17,125$ ohms. This virtual resistance subtends an angle $\tanh^{-1} \left(\frac{-17,125}{2,000} \right) = \tanh^{-1} (-8.5625) = -0.117325 + j\frac{\pi}{2}$; so that $\delta_x = j\frac{\pi}{2}$, and $\delta_A = 0.482675 + j\frac{\pi}{2}$. The potentials, currents,

impedances, and admittances now follow respectively the sines, cosines, tangents and cotangents of the position angles all along the line, as already described.

Fig. 52 shows at AB a diagram of the smooth line considered. At $A'OB'$ is its nominal T , and at $A''B''$, its nominal Π . The lumpiness correcting factors are seen to be 1.061089 and 0.971043. Using these factors, the equivalent T is indicated at $a'ob'$, and the

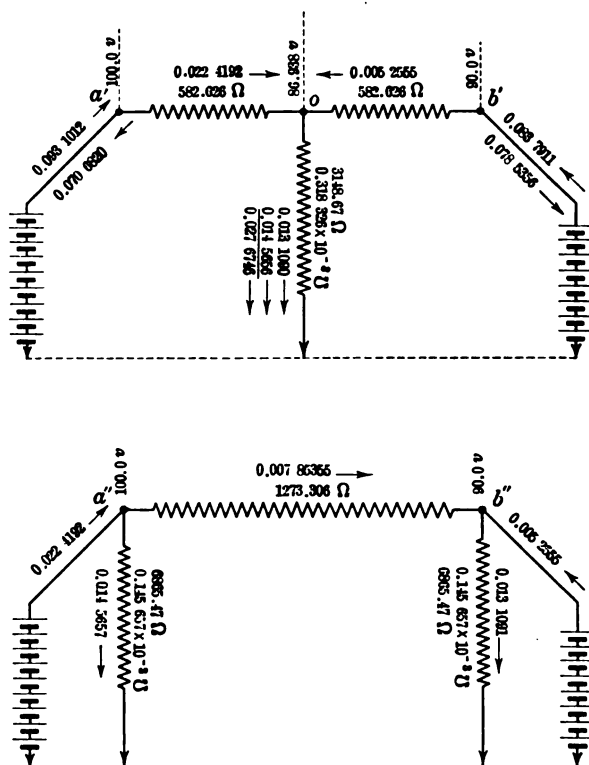


FIG. 53.—Equivalent circuits of smooth line in Fig. 51, voltage at both ends.

equivalent Π at $a''b''$. In the equivalent T , the total line resistance and leakage are 1,165.252 ohms and 0.318326 millimho. In the equivalent Π , the corresponding values are 1,273.306 ohms and 0.291314 millimho.

These equivalent circuits are shown, in Fig. 53, connected to 100 volts at the A end, and 90 volts at the B end. The equivalent T line is at $a'ob'$, in the upper part of the figure, and the

equivalent Π line is at $a''b''$, in the lower part. Considering the equivalent T , if the A battery acted alone, with the B end grounded, the current entering at A would, by Ohm's law computation, be 0.093 1012 amp., splitting at O into 0.078 5356 and 0.014 5656 amp. Similarly, if the B battery acted alone, with the A end grounded, the current entering at B would be 0.083 7911 amp., splitting at O into 0.070 6820 and 0.013 1090 amp. Now applying both batteries as shown, the summation current distribution gives 0.022 4192 amp. preponderating at a' , 0.005 2555 amp. at b' , and 0.027 6746 amp. through the leak to ground. The two entering line currents agree with those indicated in Fig. 51, as obtained by smooth-line formulas.

Turning to the equivalent Π , $a''b''$, it is evident that 100 volts acting, at a'' , through the leak of 0.145 657 millimho, produces a leak current of 14.5657 milliamp. Similarly, 90 volts acting at b'' , through the leak of 0.145 657 millimho, produces a leak current of 13.109 milliamp. The potential difference of 10 volts, between a'' and b'' , acting through 1,273.306 ohms, produces a current in the "architrave" of 7.85355 milliamp. The total entering current at a'' is thus 22.4192 milliamp., and at b'' , 5.2555 milliamp., again in agreement with the values obtained in Fig. 51.

It is thus evident that although the distributions of potentials and currents are very different inside the Π and the T of Fig. 53 and in either from those in the smooth line of Fig. 51, yet at and outside the terminals of these equivalent circuits, all three systems have identical distributions, and any one may be replaced by either of the other two.

We shall see that the same principles apply in any single-frequency a.c. case.

If, therefore, we desire to have an artificial line which shall conform electrically to a given smooth line only at its two ends, we may construct either its equivalent T , or its equivalent Π and the problem is solved, no matter what the terminal conditions may be. If, however, we desire to have the artificial line conform electrically to the smooth line at one internal point, say the middle point of its length, as well as at its terminals, then we may divide the smooth line into halves, and construct an equivalent T or Π for each half. This will make an artificial line of two sections. Proceeding in this way, the more sections we take for the artificial line, the more numerous will be the points of electrical agreement between it and the conjugate smooth line.

Some of the sections of the artificial line may be T s and others Π s; but it is preferable, for symmetry, to adhere to one type only throughout. In the d.c. case, there is very little choice between the two types. In the a.c. case, there may be, as we shall see, a slight advantage in favor of the Π line.

CHAPTER VIII

THE DESIGN, CONSTRUCTION AND TESTS OF CONTINUOUS-CURRENT ARTIFICIAL LINES

Continuous-current artificial lines may be constructed:

1. To furnish an electrical model of some particular telegraph line, with a standard or normal linear leakance.
2. To furnish an electrical model of a low-voltage d.c. railway signal system, where a continuous signalling current is carried over the two parallel rails of a railroad track, so as to respond to the short-circuiting action of an advancing train.
3. To furnish a model for the use of students in an electrical engineering laboratory, to familiarize them with the tests and formulas pertaining to such lines, before proceeding to the less simple and much more extensive field of a.c. line testing.

We shall take up the consideration of a particular example of type (3). In this case it was desired to construct a five-section artificial line,* which could be connected up by the students either as a T line or as a Π line, in order to aid them in forming either of these subtypes.

A rectangular box was constructed of hard wood, well soaked with molten paraffin wax. This box is 57.5 cm. (22.6 in.) long, 17.8 cm. (7 in.) wide, and 10 cm. (4 in.) high. All of the electrical parts and connections are fastened to the cover, which is removable by means of a dozen wood screws. A plan view of the box and its cover appears in Fig. 54.

Three rows of brass strips are seen fastened to the top of the cover, the upper row commencing with $1a$, $1b$, $1c$, and ending with $5a$, $5b$, $5c$. Between the members of each of these five groups are connected resistances AA , each of 250 ohms, of No. 32 B. & S. gage " $Ia-Ia$ " resistance wire, double cotton-covered, anti-inductively wound and impregnated with paraffin wax. These resistances form the line sections. The second, or middle row, contains resistances B , B , each of 4,000 ohms, of the same

* "A Convenient Form of Continuous-current Artificial Line," by A. E. KENNELLY, *Electrical World*, June 14, 1913.

kind of wire. These form the leaks. The third, or bottom row, is a single brass strip *gg*, serving as the common ground connection of the line.

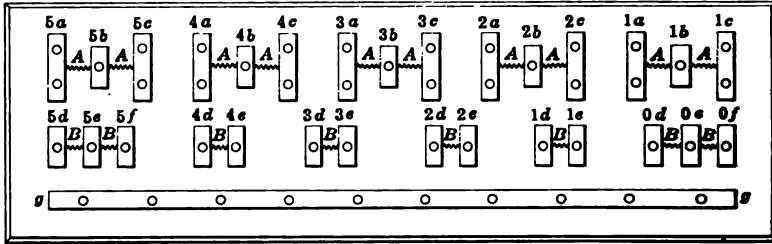


FIG. 54.—Plan view of artificial continuous-current line arranged for one, two, three, four or five sections either of *T*'s or Π 's.

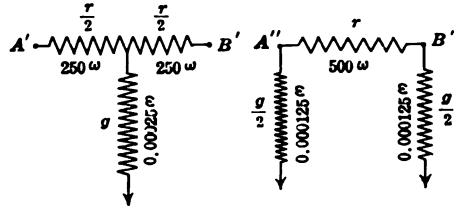


FIG. 55.—Single sections of *T* and Π line.

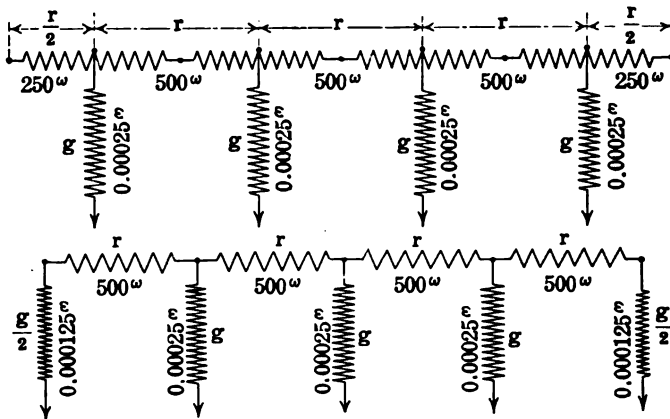


FIG. 56.—Four-section *T* line and four-section Π line.

A single section of *T*-line connection is indicated in Fig. 55, at *A'B'*, and a single section of Π -line connection at *A''B''*. A four-section *T* line, and also a four-section Π line appear in Fig. 56. Pairs of electrically connected brass plugs serve to connect

up the line into as many as five sections of the type desired. In Fig. 57, the box is shown connected as a five-section *T* line.

The electrical behavior of such a five-section *T* or *Π* line is illustrated diagrammatically in Figs. 36, 37, 38, 42, 43 and 44, for the particular cases of grounding, freeing, and loading with 750 ohms

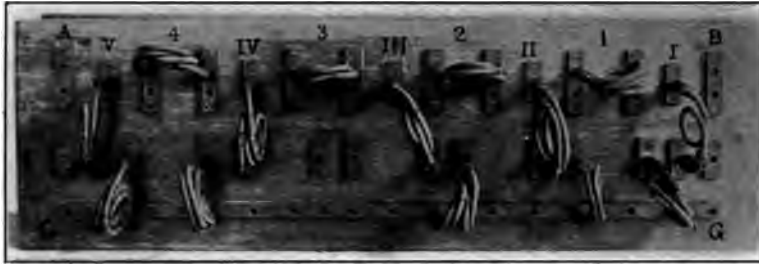


FIG. 57.—Continuous-current artificial-line box connected as a five-section *T* line.

at the distant end. In either case, the section angle is 0.35174 hyp.; but, for reasons already discussed in Chapter VI, the surge impedance of the *T* sections is 1,436.1 ohms, while that of the *Π* sections is 1,392.6 ohms.

Potentiometer Tests of Artificial Line.—The test for fall of

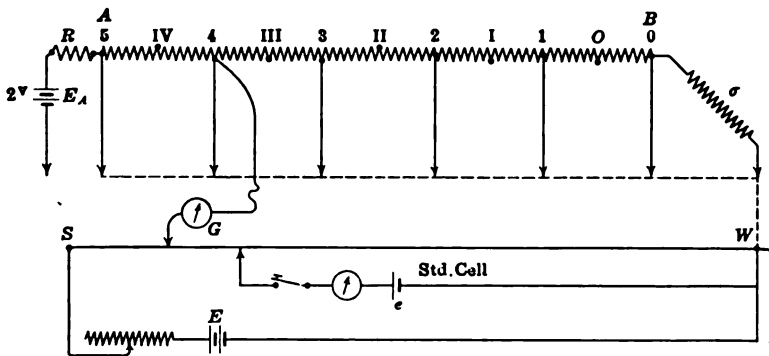


FIG. 58.—Diagram of connections for potentiometer test of c.c. artificial line of *Π* sections.

potential along the junctions and mid-sections of the box, arranged as a five-section *Π* line, loaded at *B* with a resistance of σ ohms, is indicated diagrammatically in Fig. 58. The battery E_A may be a steady storage cell, capable of holding say 2.0 volts at its terminals during the continuance of the test. The resistance

R at A , enables the potential impressed on the end 5 of the line, to be brought within the usual 1.8 volts capable of being read directly on an ordinary potentiometer. The slide wire of this instrument is indicated as SW , the working battery at E , the standard cell at e . As connected, the potential against ground is being measured at junction 4.

The current strengths along the artificial line may be readily measured by observing the potentiometer p.d. on each successive line element 0 1, 1 2, 2 3, 3 4, and 4 5. The entering current at A may likewise be measured by observing the drop of potential in R .

The position angles along the line are determined from the load σ and the line elements, in the manner described in Chapter VI. The potentials and currents at each successive junction and mid-section are then computed by reference to tables of real hyperbolic functions. The observed and computed values are finally recorded, and compared in parallel columns.

If the elements of resistance entering into the line are carefully measured in the first instance, if all of the plug contacts and connections are good, and if the potentiometer measurements are carefully made, it is customary for the student to find the observed and computed values in agreement to the third and sometimes to the fourth significant digit.

There is nothing which gives the student so complete a grasp of the principles and formulas relating to a.c. artificial lines, as preliminary tests on such d.c. artificial lines. It is important to make these d.c. lines stepping stones to a.c. lines; because the technique is easily grasped and followed, and the precision of measurement is all that can be desired. With a.c. lines, the precision attainable is ordinarily lower, the disturbances due to changes in impressed frequency very noticeable, and the computations retarded through the substitution of complex for real numbers, even though the formulas employed remain unchanged.

Wheatstone-bridge Test of Lines.—A useful test on c.c. lines, for θ and r_0 , is conveniently made by means of the Wheatstone bridge (see Fig. 59). This is the measurement of the line resistance at each successive junction, both with the B end freed, and with the B end grounded.

By (169) the resistance at junction N , with B grounded, is

$$R_{\theta N} = r_0 \tanh (N\theta) \quad \text{ohms } \angle \quad (269)$$

With the B end freed, and with $\delta_B = j\frac{\pi}{2}$, the line resistance at junction N is

$$R_{fN} = r_0 \tanh \left(N\theta + j\frac{\pi}{2} \right) = r_0 \coth (N\theta) \text{ ohms } \angle \quad (270)$$

and generally

$$R_{\theta N} = r_0 \tanh (N\theta + \theta') = r_0 \tanh \delta_N \text{ ohms } \angle \quad (271)$$

Multiplying equations (269) and (270) together, we find

$$R_{\theta N} \cdot R_{fN} = r_0^2 \text{ ohms}^2 \angle \quad (272)$$

or

$$r_0 = \sqrt{R_{\theta N} \cdot R_{fN}} \text{ ohms } \angle \quad (273)$$

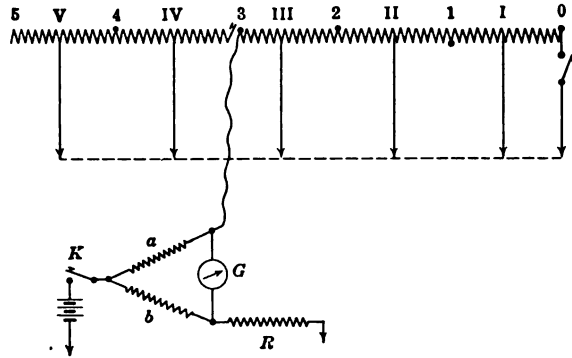


FIG. 59.—Connection diagram for line-resistance test with Wheatstone bridge.

In words, *the product of the impedance free and impedance grounded is constant at any and all section junctions, either of a T or II line. The square root of this product is the surge impedance of the line. In other words, the surge impedance of a line at any testing point is always the geometric mean of R_{θ} and R_f . On a smooth line, any point may be a testing point; but on an artificial line only junctions (or mid-sections, using (231) and (239)).*

Moreover, dividing (269) by (270) we have

$$\tanh (N\theta) = \sqrt{\frac{R_{\theta N}}{R_{fN}}} \text{ numeric } \angle \quad (274)$$

or

$$N\theta = \tanh^{-1} \sqrt{\frac{R_{\theta N}}{R_{fN}}} \text{ hyps. } \angle \quad (275)$$

The angle subtended by the line beyond any junction is the anti-tangent of the root of the ratio of the resistance grounded to the resistance freed.

In other words, *the angle subtended by a line beyond a testing point has as its tangent the geometric mean of R_g , the resistance grounded, and G_f , the conductance freed.*

When these line-resistance tests are made on a T line, it is necessary only to break the line at the junction selected, and to connect the bridge to the end beyond the break. In the case of a Π line, however, it is necessary, in addition, to change the first leak from g to $g/2$ mhos. This may be done by substituting a transferable half-leak for the usual full leak, at the testing terminal.

As an example, consider the T line represented in Figs. 36 and 37. If we cut in at section 3, $R_{gs} = 1,125.7$ ohms, and $R_{fs} = 1,832.2$ ohms. Hence $r_0 = \sqrt{1,125.7 \times 1,832.2} = 1,436.1$ ohms, and $N\theta = \tanh^{-1} \sqrt{\frac{1,125.7}{1,832.2}} = \tanh^{-1} 0.78383 = 1.0552$ hyps.

Since here $N = 3$, $\theta = 0.35173$ hyp. per section.

It is instructive to make measurements of R_g and R_f at each successive junction along the line, and so to derive the values of θ and r_0 .

Distribution of Work of Tests among Observers.—The various tests above described can be made, if necessary, by a single observer, making all his own connections, measurements and records. The work is done more conveniently and expeditiously by a pair of observers, one making the measurements and the other the connections and records, the two occasionally changing duties. Three observers can also advantageously divide the work between them, and a fourth can also be occupied in computing checks as the tests advance.

Disturbances of Potential and Current in the Artificial Line That May Be Produced by the Application of a Leak Load, in Making Potentiometer Measurements.—It has been already pointed out that it is desirable, in making potentiometer measurements of voltage along the line, to keep the impressed potential at the generator end within the direct compass of the potentiometer; so as to avoid having to apply a “reducing box” or “multiplier” to the line, at the testing point. Such a reducing box (see Fig. 60) virtually applies a leak load to the line at the testing point. A small leak of this kind has a surprisingly large effect in lowering the line potential at and near the leak. Fig. 60 represents a four-section T line, loaded at B with a resistance σ , and having the potential at mid-section II measured by potentiometer.

meter. The potential being beyond the direct compass of the instrument, a reducing box X , of say 10,000 ohms, or 0.1 millimho, is applied to the line at this point, and one-tenth, say, of the voltage across the box X to ground, is measured at the potentiometer.

Since it may sometimes be necessary to employ relatively high impressed voltages on the line, and a reducing-box leak of the kind described, we may consider the magnitude of the effect produced, and how to correct for it, if* needful.

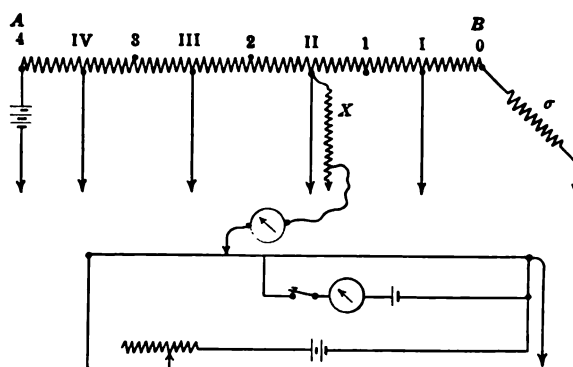


FIG. 60.—Potential test of continuous-current line by potentiometer with aid of a reducing box X .

Fig. 61 shows the effect of applying a leak load of 0.1 millimho (10,000 ohms), to junction 3 of the five-section line already considered in Fig. 38, voltage at A with 100 volts, and loaded at B with 750 ohms. It will be seen that the effect of the leak, such as might be used for potentiometer measurement of potential at 3, is to lower the potential from 48.052 to 45.648 volts, a reduction of 2.404, or approximately 5 per cent. At neighboring test-points, the potential is likewise lowered, although not to the same extent. Another effect of the leak is to introduce a discontinuity in the position angle at 3, from 1.6346 to 1.1503 hyps., the rationale of which will be considered under the subject of composite lines. (Chapter X, page 272.)

The disturbances of potential and current here produced come under the following proposition. *The changes of potential and*

* "Disturbances of Potential and Current Produced in an Active Network by the Application of a Leak Load," by A. E. KENNELLY, *Electrical World*, Dec. 28, 1912.

ARTIFICIAL ELECTRIC LINES

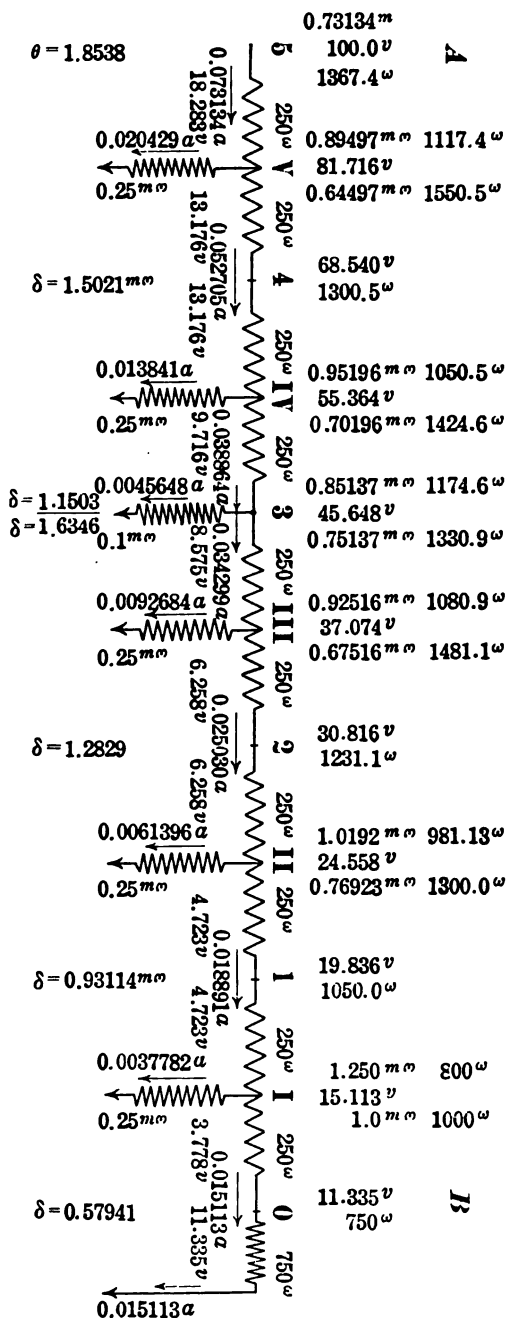


FIG. 61.—Artificial line loaded with a leak of 0.1 millimho at junction 3.

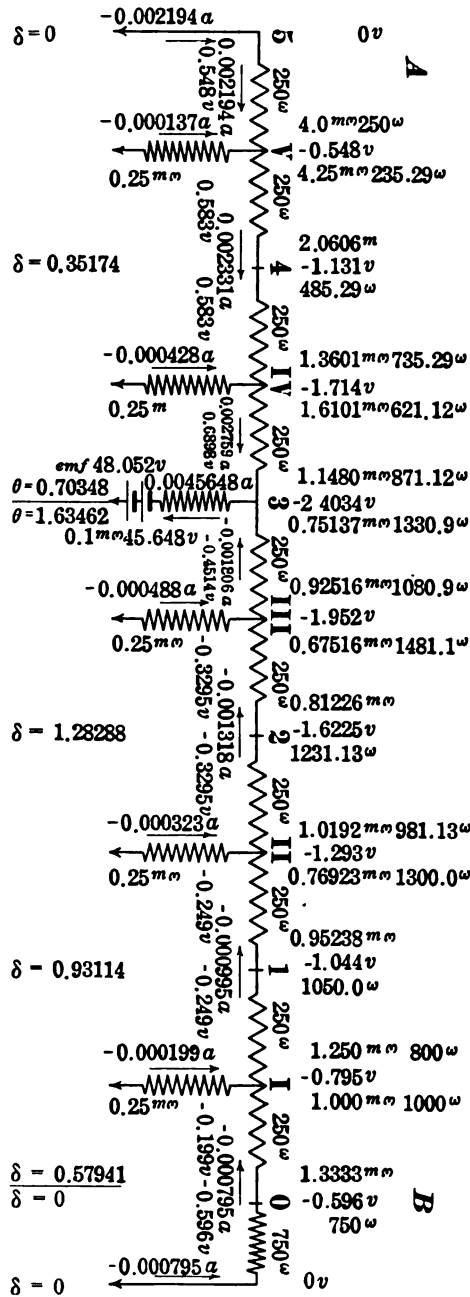


FIG. 62.—Artificial line grounded at A and with the e.m.f. of 48.052 vol inserted outwardly in the leak load at 3.

current produced at a point *P* in a network of conductors, supplied with constant e.m.fs., by the application of a leak at some point *Q*, are equal to the values produced at *P* by the action of the initial e.m.f. at *Q* inserted in the leak at *Q*, all the other e.m.fs. in the system being put to zero.*

Thus, Fig. 62 shows the same artificial line with the impressed

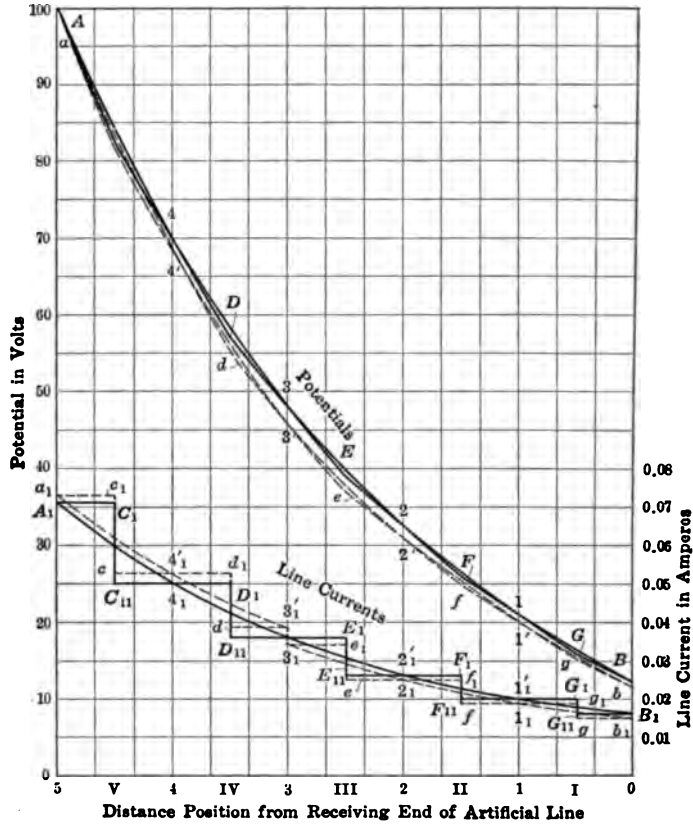


FIG. 63.—Distributions of potential and current over loaded and unloaded artificial line. Solid curves for the unloaded state, broken curves for the loaded state.

e.m.f. removed at *A*, and with the leak applied at 3, this leak containing in it an e.m.f. of 48.052 volts, the potential existing

* It was supposed in 1912 that this proposition might then be new; but it was pointed out by DR. G. A. CAMPBELL, in correspondence, that the proposition is virtually covered by another given in PROF. ANDREW GRAY'S "Absolute Measurements of Electricity and Magnetism," London, 1888, vol. i, pp. 152-161 ("Theory of Networks of Conductors").

there before applying the leak, as in Fig. 38, page 68. The effect of this e.m.f., taken negatively, is to produce a potential at 3 of -2.4034 volts, and correspondingly, in diminishing extent, at more remote testing points. These are precisely the values of the disturbances produced by the leak. The currents in the line Fig. 62, on each side of the leak, are $+2.759$ milliamp. on the upside, and 1.806 milliamp. on the downside, which correspond to the disturbances shown in Fig. 61, by reference to Fig. 38.

Fig. 63 indicates the extent of the disturbances in potential and current at the various testing points along the line, by the application of this $10,000$ -ohm leak.

Correction for Potential Disturbances Due to Leak.—Let V be the potential at the testing point before applying the leak, and v the potential at the same point after applying the leak. Then the “depression factor” of the leak is*

$$d = \frac{v}{V} = \frac{G}{G + g} \quad \text{numeric } \angle \quad (276)$$

where G is the conductance in mhos to ground of the line from the testing point, excluding the leak, and g is the conductance of the leak itself. The factor k which should be applied to the observed potential, to correct for the action of the leak, may be called the *correcting factor of the leak at the point of application* and is:

$$k = \frac{1}{d} = \frac{V}{v} = \frac{G + g}{G} \quad \text{numeric } \angle \quad (277)$$

The conductance G will be the sum of the line conductances to ground, from the testing point, in both directions. If θ_1 is the angle subtended by the A end of the line, at the testing point, when grounded at A , and θ_2 the corresponding angle subtended by the B end of the line, then by (124)

$$G = y_0 (\coth \theta_1 + \coth \theta_2) \quad \text{mhos } \angle \quad (278)$$

In the case considered, $\theta_1 = 0.70348$ and $\theta_2 = 1.63462$; also $y_0 = 0.69633$ millimho; whence $k = 1.05265$. The observed potential at 3, in the presence of the leak, should be multiplied by this factor, in order to arrive at the value of the potential with the leak removed.

Correction for Current Disturbances Due to Leak.—Knowing either the uncorrected potential v , or the corrected potential V ,

* “On the Measurement of the Insulation of Continuous-current Three-wire Systems While at Work,” by E. J. HOUSTON and A. E. KENNELLY, *The Electrical World*, vol. xxviii, July 25, 1896, p. 95 (7).

at the testing point, the extent of the disturbance in current over the adjoining sections can readily be found. If G_1 and G_2 are the conductances to ground on each side, whose sum is G , then

$$i_1 = vg \frac{G_1}{G} \quad \text{and} \quad i_2 = vg \cdot \frac{G_2}{G} \quad \text{amp. } \angle \quad (279)$$

or

$$i_1 = Vg \frac{G_1}{G + g} \quad \text{and} \quad i_2 = Vg \cdot \frac{G_2}{G + g} \quad \text{amp. } \angle \quad (280)$$

are the changes in current due to the application of the leak load. In an artificial line subtending angles θ_1 and θ_2 on each side.

$$i_1 = vg \cdot \frac{\coth \theta_1}{\coth \theta_1 + \coth \theta_2} \quad \text{and} \quad i_2 = vg \cdot \frac{\coth \theta_2}{\coth \theta_1 + \coth \theta_2} \quad \text{amp. } \angle \quad (281)$$

or

$$i_1 = Vg \cdot \frac{y_0 \coth \theta_1}{g + y_0(\coth \theta_1 + \coth \theta_2)} \quad \text{and} \quad i_2 = Vg \cdot \frac{y_0 \coth \theta_2}{g + y_0(\coth \theta_1 + \coth \theta_2)} \quad \text{amp. } \angle \quad (282)$$

The sum of i_1 and i_2 in (281) is obviously

$$i_1 + i_2 = vg \quad \text{amp. } \angle \quad (283)$$

In the case considered, $v = 45.648$, $V = 48.052$, $g = 0.1 \times 10^{-3}$, $G_1 = 1.148 \times 10^{-3}$, $G_2 = 0.7514 \times 10^{-3}$, $G = 1.8994 \times 10^{-3}$, $i_1 = 2.759 \times 10^{-3}$ amp., and $i_2 = 1.806 \times 10^{-3}$ amp.

In general, a new correction factor has to be found for each successive testing point. Hence the desirability of dispensing with a reduction box when using the potentiometer.

Although an artificial line of the character shown in Fig. 54 has the advantage of serving either as a T line or as a Π line at will, yet so much care has to be taken to ensure good contacts at all the plugs, that it is doubtful whether fixed independent T lines and Π lines, with fewer switch contacts, are not preferable.

CHAPTER IX

COMPLEX QUANTITIES AND ALTERNATING-CURRENT QUANTITIES

It is assumed that the student is already acquainted with the elementary principles of the simple a.c. circuit; so that it will be desirable to review only those features of a.c. operation which bear immediately upon the behavior of a.c. artificial lines.

Complex Quantities and Plane Vectors.—"Real quantities" are such as may be represented geometrically by the position of

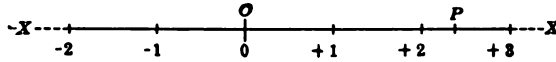


FIG. 64.—Geometrical representation of real numbers by the position of the point P on the straight line $-XOX$.

a movable point P , Fig. 64, with respect to a fixed point or origin O , on an indefinitely extending straight line $-XOX$. Real quantities include positive and negative quantities, integral as well as fractional.

"Complex quantities" are such as may be represented

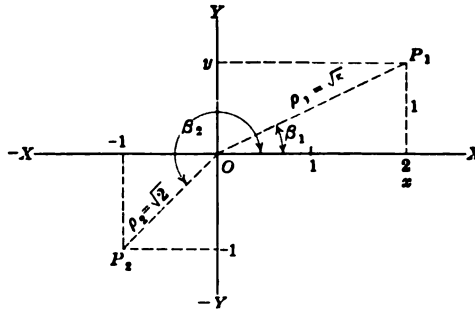


FIG. 65.—Complex numbers represented by the plane vectors OP_1 and OP_2 .

geometrically by the position of a movable point P , in a plane, with respect to a fixed point or origin O in that plane (Fig. 65).

The position of P , with respect to O , can be defined in either of two ways, namely:

1. In rectangular coördinates, sometimes called Cartesian coördinates.
2. In polar coördinates.

In rectangular-coördinate definition, there are two fixed mutually perpendicular axes, $-XOX$ and $-YOY$, in the plane of reference. The former is called the *real axis*, or *axis of reals*; since it corresponds to the axis of real quantities in Fig. 64. The latter ($-YOY$), is called the *imaginary axis*, or *axis of imaginaries*. The qualifying adjective "imaginary," has historical significance only, and does not mean that there is anything indeterminate or fictitious about this axis. The "orthogonal" or perpendicular projections of OP , on the X and Y axes, are respectively the *real component* x , and the *imaginary component* y . The straight line OP connecting the origin O with the mov-

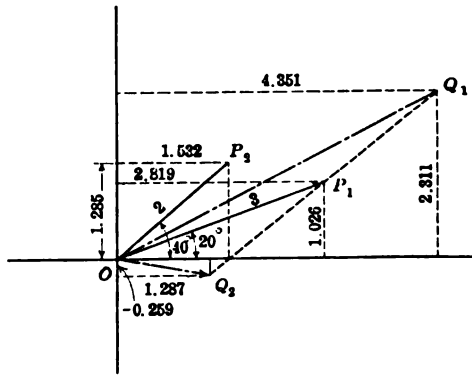


FIG. 66.—Sum and difference of two plane vectors OP_1 and OP_2 .

able point P is not a "vector," in the complete sense of that term as used in mathematics; because, although two complex quantities $OP_1 = 3\angle 20^\circ$ and $OP_2 = 2\angle 40^\circ$, Fig. 66, have as their sum $OP_1 + OP_2 = OQ_1$ and as their difference $OP_1 - OP_2 = OQ_2$, formed according to the same rules as govern true vectors, yet the product $OP_1 \times OP_2$ of these two complex quantities is OQ , Fig. 67, and is equal to the opposite-order product $OP_2 \times OP_1$; whereas two vectors, when multiplied, enjoy a scalar product, as well as a vector product, and the latter depends upon the order of multiplication.

In order to distinguish the straight lines in a plane, which geometrically represent complex quantities, from true vectors, we may call the former *plane vectors*. In what follows, the term "vector" will mean a "plane vector."

Rectangular Plane Vectors.—The magnitudes and signs of the rectangular components x and y completely determine the

position of the vector OP . If x and y are both positive, OP lies in the first quadrant. If x and y are both negative, OP lies in the third quadrant. If x is $-$ and y is $+$, OP lies in the second quadrant. If x is $+$ and y is $-$, OP lies in the fourth quadrant.

To express the vector OP in polar coördinates, we take the same origin O , and axis of reference OX , as the fixed "initial line." From this line, we measure the circular arc XOP , either in radians, degrees, quadrants, or other specified units of circular angle β (Fig. 65). The length of the vector OP is called the "modulus" of the polar coördinate complex quantity; while the circular angle β is called the "argument" of the same. Since the mathematical terms "modulus" and "argument" are not well adapted for practical purposes, we shall follow the terminology suggested by Fleming* and use the term "size" for the modulus, and the term "slope" for the argument of a polar complex quantity. Any plane vector is thus completely specified either by its real and imaginary components, x and y , or by its size ρ and slope β .† The slope may exceed the range $+360^\circ$, or $+2\pi$ radians; but, in most cases, it is simpler and more convenient to keep within these limits. The positive or counter-clockwise direction of rotation in angle is understood, unless the negative sign is prefixed.

A rectangular-coördinate vector or "rectangular vector" may be written:

$$OP = x + jy \quad \text{vector} \quad (284)$$

where $j = \sqrt{-1}$, and indicates that y is measured along the imaginary axis. Proper signs must be given to both x and y .

Polar Plane Vectors.—A polar-coördinate vector, or "polar vector," may be written:

$$OP = \rho\epsilon^{j\beta} \quad \text{vector} \quad (285)$$

where ϵ is the base of Napierian logarithms (2.71828 . . .), and β is in *circular radians*. The factor $\epsilon^{\pm j\beta}$ on being expanded, becomes:

* See "The Wireless Telegraphist's Pocketbook," by PROF. J. A. FLEMING, London, 1915.

† The size of a plane vector quantity z is denoted by $|z|$, and its slope may be denoted by $\angle z$. Thus if $z = 1.5\angle 30^\circ$ say, then $|z| = 1.5$ and $\angle z = 30^\circ$.

$$\begin{aligned}
 \epsilon^{\pm j\beta} &= 1 \pm j\beta - \frac{\beta^2}{2!} \mp j\frac{\beta^3}{3!} + \frac{\beta^4}{4!} \pm j\frac{\beta^5}{5!} - \frac{\beta^6}{6!} + \dots \quad \text{numeric } \angle \quad (286) \\
 &= (1 - \frac{\beta^2}{2!} + \frac{\beta^4}{4!} - \frac{\beta^6}{6!} + \dots) \pm j(\frac{\beta^3}{3!} - \frac{\beta^5}{5!} + \dots) \\
 &= \cos \beta \pm j \sin \beta \quad \text{numeric } \angle \quad (287) \\
 & \quad \text{numeric } \angle \quad (288)
 \end{aligned}$$

This is a “*versor*,” or operator which turns or rotates in one plane the size or modulus ρ from the original direction OX , through $\pm\beta$ radians, as, for example, into the direction OP_1 (Fig. 65).

For ordinary purposes of definition and operation, however, it is sufficient to write (285) in the simpler polar form.

$$OP = \rho \angle \beta \quad \text{vector} \quad (289)$$

which shows that OP has a size of ρ units, and is displaced in phase through a slope of β circ. radians in the positive direction. If β is expressed in degrees, we may write it

$$OP = \rho \angle \beta^\circ \quad \text{vector} \quad (290)$$

If we desire to express a negative phase or angle of rotation, we may write the polar vector

$$OP = \rho \sphericalangle \beta^\circ \text{ or } \rho \angle -\beta^\circ \quad \text{vector} \quad (291)$$

The size ρ may be regarded as essentially positive; but a negative sign applied to it is equivalent to a change of π radians, or 180° , in the slope. That is

$$-\rho \angle \beta^\circ = +\rho \angle (\beta \pm 180^\circ) \quad \text{vector} \quad (292)$$

Interchangeability of Rectangular and Polar Plane Vectors.— It is evident from the elementary trigonometry of Fig. 65, that

$$\rho \angle \beta^\circ = \sqrt{x^2 + y^2} \left| \tan^{-1} \left(\frac{y}{x} \right) \right. \quad \text{numeric } \angle \quad (293)$$

so that a vector whose rectangular coordinates x and y are given, can be converted into a polar vector, whose size is the square root of the sum of the square of the components, and the tangent of whose slope is their ratio y/x .*

* A simple Vector Calculating Rule has been designed by PROF. J. A. FLEMING and manufactured by Messrs. W. F. Stanley & Co., London, for changing the coordinates of a plane vector from rectangular to polar, or reciprocally. See “The Predetermination of the Current and Voltage at the Receiving End of a Telephone or Other Alternating-current Line,” by J. A. FLEMING, *Journ. Inst. Elect. Engr.*, vol. 52, No. 236, pp. 717-723 May, 1914.

We may also write (293) in a form more convenient for computation (see page 151):

$$\begin{aligned} \rho \angle \beta^\circ &= x \sqrt{1 + \left(\frac{y}{x}\right)^2} \left| \tan^{-1} \frac{y}{x} = x \sec \beta^\circ \left| \tan^{-1} \frac{y}{x} \right. \right. \\ &= x \sec \beta^\circ \angle \beta^\circ \qquad \qquad \qquad \text{numeric } \angle \quad (294) \end{aligned}$$

that is, we may find $\tan^{-1}\left(\frac{y}{x}\right) = \beta^\circ$, and then ρ will be $x \sec \beta^\circ$; or

$$\begin{aligned} \rho \angle \beta^\circ &= y \sqrt{1 + \left(\frac{x}{y}\right)^2} \left| \cot^{-1} \frac{x}{y} = y \operatorname{cosec} \beta^\circ \left| \cot^{-1} \frac{x}{y} \right. \right. \\ &= y \operatorname{cosec} \beta^\circ \angle \beta^\circ \qquad \qquad \qquad \text{numeric } \angle \quad (295) \end{aligned}$$

Form (294) is useful for transforming rectangular to polar coördinates, when y is smaller than x , or ρ makes an angle of less than 45° with the $-XOX$ axis; while (295) is preferable when ρ makes a large angle with that axis.

Reciprocally,

$$x + jy = \rho \cos \beta + j\rho \sin \beta \quad \text{numeric } \angle \quad (296)$$

so that the real and imaginary components of a vector are respectively the cosine and sine components of the size.

Addition and Subtraction of Plane Vectors.—To add plane vectors, express them in rectangular coördinates. *The summation vector will then have, as its real component, the algebraic sum of the reals, and, as its imaginary component, the algebraic sum of the imaginaries.*

Thus, the sum of $(5 + j2)$ and $(-3 - j1)$ is $2 + j1$. In Fig. 66, the summation $3\angle 20^\circ + 2\angle 40^\circ = (2.819 + j1.026) + (1.532 + j1.285) = 4.351 + j2.311 = OQ_1$.

Subtraction of a vector is merely its addition according to the preceding rule, after the signs of both of its components have been reversed.

Thus, to subtract $(2 + j7)$ from $(5 - j3)$ add $(-2 - j7)$ to $(5 - j3) = 3 - j10$. In Fig. 66, $3\angle 20^\circ - 2\angle 40^\circ = (2.819 + j1.026) - (1.532 + j1.285) = 1.287 - j0.259 = OQ_2$.

Multiplication of Plane Vectors.—To multiply plane vectors, express them in polar coördinates, or as "polars." *The product will then have, for its size, the product of the sizes, and for its slope, the algebraic sum of the slopes; or*

$$B\angle \beta_2 \times A\angle \beta_1 = A\angle \beta_1 \times B\angle \beta_2 = AB/\beta_1 + \beta_2 \text{ numeric } \angle \quad (297)$$

Thus, $5\angle 30^\circ \times 2\angle 20^\circ = 10\angle 50^\circ$

In Fig. 67, $OP_1 \times OP_3 = 3\angle 20^\circ \times 2\angle 40^\circ = 6\angle 60^\circ = OQ$.

Division of Plane Vectors.—To divide one plane vector by a second, express both as polars, such as $A\angle\beta_1$ and $B\angle\beta_2$. The quotient will then have, for its size, the quotient of the sizes, and for its slope the algebraic difference of the slopes, or

$$A\angle\beta_1 \div B\angle\beta_2 = \frac{A}{B} \angle \beta_1 - \beta_2 \quad \text{numeric } \angle \quad (298)$$

Thus

$$7\angle 60^\circ \div 2\angle 10^\circ = 3.5\angle 70^\circ.$$

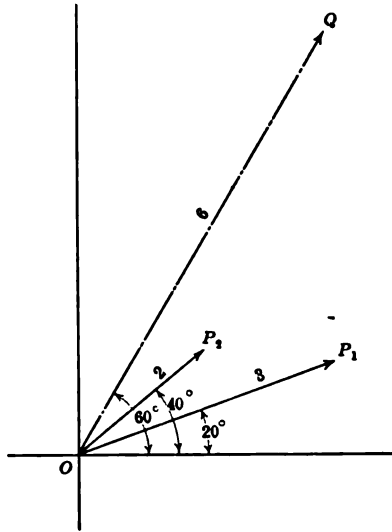


FIG. 67.—Product of two complex quantities represented as plane vectors

Vector multiplication and division may also be effected between rectangulars, although the formulas are not so simple. Thus

$$(x_1 + jy_1)(x_2 + jy_2) = (x_1x_2 - y_1y_2) + j(x_1y_2 + y_2x_1) \quad \text{numeric } \angle \quad (299)$$

The real component of the product contains a difference, and the imaginary component a sum of products in x and y . Again

$$\frac{x_1 + jy_1}{x_2 + jy_2} = \frac{(x_1 + jy_1)(x_2 - jy_2)}{(x_2 + jy_2)(x_2 - jy_2)} = \frac{(x_1x_2 + y_1y_2) + j(x_2y_1 - x_1y_2)}{x_2^2 + y_2^2} \quad \text{numeric } \angle \quad (300)$$

These expressions (299) and (300) are so awkward, by comparison with (297) and (298), that it usually saves time to convert rectangulars to polars in order to effect either multiplication, division, involution or evolution.

Reciprocals of Vectors.—If a plane vector is expressed in polar coördinates, its reciprocal has for its size the reciprocal of the vector's size, and for its slope, the negative of the vector's slope; or

$$\frac{1}{A\angle\beta} = \frac{1}{A} \sphericalangle\beta = \frac{1}{A} \angle - \beta \quad \text{numeric } \angle \quad (301)$$

Thus

$$\frac{1}{5\angle 60^\circ} = 0.2 \sphericalangle 60^\circ.$$

The corresponding result in Cartesian vectors is:

$$\frac{1}{x + jy} = \frac{1}{x + jy} \times \frac{x - jy}{x - jy} = \frac{x - jy}{x^2 + y^2} \quad \text{numeric } \angle \quad (302)$$

Involution and Evolution of Plane Vectors.—*The n th power of a polar plane vector has for its size the n th power of the size, and for its slope n times the slope of the polar; or*

$$(A\angle\beta)^n = A^n \angle n\beta \quad \text{numeric } \angle \quad (303)$$

Thus

$$(5\angle 20^\circ)^3 = 5^3 \angle 60^\circ = 125 \angle 60^\circ.$$

Similarly, the n th root of a polar $A\angle\beta$, has for its size $A^{\frac{1}{n}}$, the n th root of the size, and for its slope β/n , the n th part of the slope.

Thus

$$(64\angle 45^\circ)^{\frac{1}{4}} = 8\angle 22^\circ.5.$$

Fractions of a degree may be expressed in minutes and seconds, but often more conveniently in decimals of a degree, when decimal tables of circular functions are available. The sexagesimal system of angles wastes, in the aggregate, a large amount of the time of engineers.

Complex Hyperbolic Angles.—We have already seen that a "real" hyperbolic angle is associated with a hyperbolic sector, in a manner analogous to the association of a "real" circular angle with a circular sector. We shall next see that an "imaginary hyperbolic angle" is associated with a circular sector. Similarly, an "imaginary circular angle" is associated with a hyperbolic sector. Consequently, there is a close cross-connection between complex hyperbolic and complex circular angles, because each is associated with both a hyperbolic and a circular sector.

Cosine of a Complex Hyperbolic Angle. Geometrical Construction.—In the plane XOY , Fig. 68, with center at the origin O , and with unit radius OA , describe the rectangular hyperbola $HABH'$. Suppose that the complex hyperbolic angle, whose cosine is desired, is $1 + j2$ hyps. Then let AOB be 1 hyp. radian, whose cosine is Ob . With center O , and radius Ob , describe a circle in a "circular" plane, passing through $-XOX$, but mak-

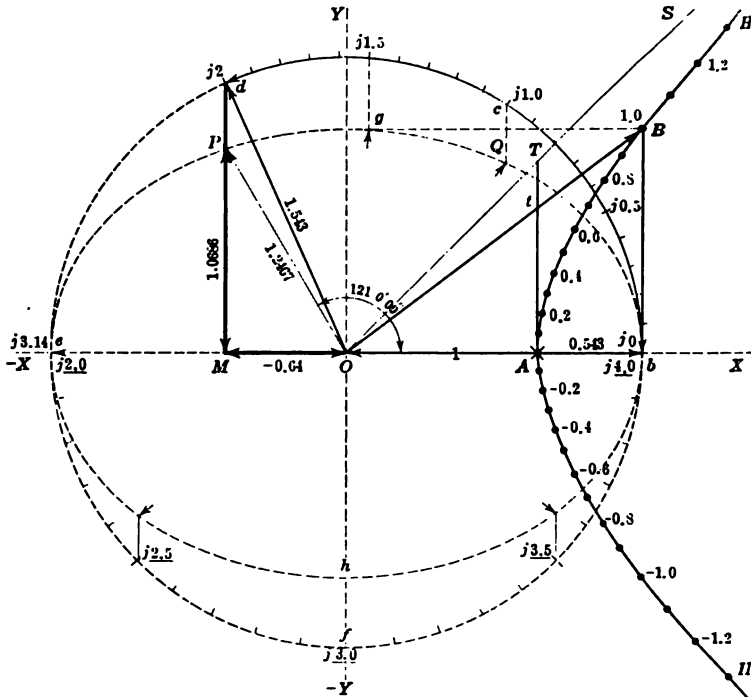


FIG. 68.—Cosine of the hyperbolic angle $1 + j2$.
 $\text{Cosh}(1 + j2) = -0.642148 + j1.06861 = 1.2467 \angle 121^\circ 0' 09''$

ing an angle with the plane XOY such that its cosine is numerically equal to the tangent At of the hyperbolic angle AOB^* . Describe an angle bOd of 2 circular radians, in the plane $bedf$. From d , the end of the circular radius-vector, drop a perpendicular on the plane XOY , intersecting this plane at P . Join OP which

* Incidentally, this angle has been called the "Gudermannian complement" of the hyperbolic angle. See paper by DR. G. F. BECKER, *Phil. Mag.*, October, 1912, "The Gudermannian Complement and Imaginary Geometry."

will then be the required hyperbolic cosine of $1 + j2$, namely, $-0.64215 + j1.06861 = 1.2467 \angle 121^\circ.0'.09''$. Its rectangular components are OM and MP .

It is evident that the cosine of $1 + j0$ would be Ob , that of $1 + j1.0$, OQ , and that of $1 + j1.5$, Og , all in the XOY plane. Moreover, the locus of $\cosh(1 + jy)$ falls on the ellipse $bQgPeh$, whose semi-major axis $Ob = \cosh 1$, and whose semi-minor axis

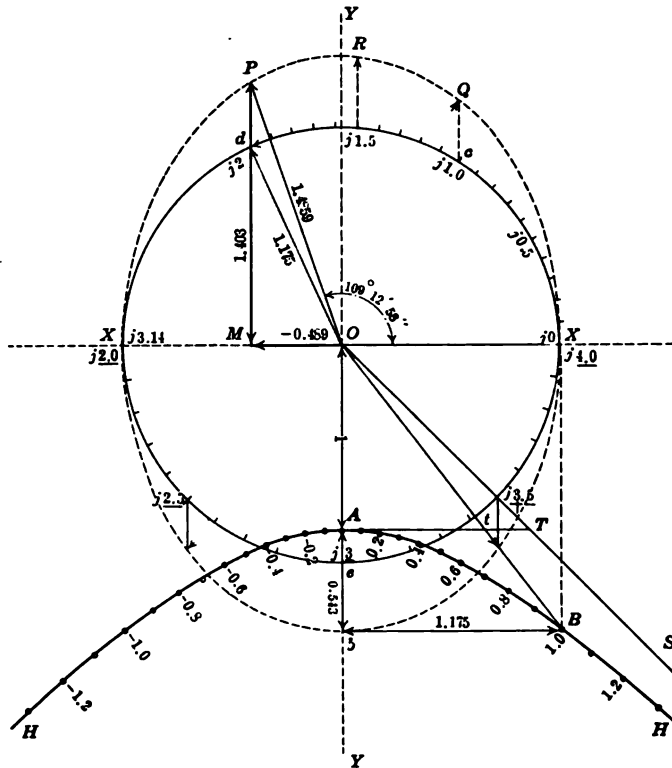


FIG. 69.—Sine of the hyperbolic angle $1 + j2$.
 $\text{Sinh}(1 + j2) = -0.48906 + j1.4031 = 1.4859 \angle 109^\circ.12'.58''$.

$Ob = \sinh 1 = bB$. As y increases from O to 2π , OP runs positively or counter-clockwise once around this ellipse. As y increases from 2π to 4π , OP runs around this ellipse a second time, and so on to infinity.

Sine of a Complex Hyperbolic Angle. Geometrical Construction.—In the plane XOY , Fig. 69, with origin O , and unit radius OA , describe the rectangular hyperbola $HABH'$, whose asymp-

tote is OTS . If the angle whose sine is required is $1 + j2$, draw the radius-vector OB , enclosing a hyperbolic angle AOB of 1 radian. Its sine will be $OX = bB$. Describe 2 circ. radians in the plane XOY , from OX to Od , enclosing the circular angle XOd . Let another plane, which we may call the reference plane, pass through $-XOX$, and make with the plane XOY an angle whose circular sine* is the hyperbolic tangent At . Project the point d perpendicularly out of the plane XOY , until it meets the reference plane in the point P . Then OP in the reference plane will be the required complex sine, having components in that plane OM and MP ; *i.e.*, $-0.48906 + j1.4031 = 1.4859 \angle 109^\circ.12'.58''$. It is evident that the sine of $1 + j1.0$ hyps. would be OQ , and of $1 + j1.5$ hyps. OR , both in the reference plane. Moreover, the locus of $\sinh(1 + jy)$ will be the ellipse $XQRPXb$, whose semi-major axis is $Ob = \cosh 1$, and whose semi-minor axis $OX = bB = \sinh 1$. Thus, *the imaginary component of a hyperbolic angle, whose sine or cosine is required, may be regarded as producing rotation over a corresponding circular sector; while the real component produces rotation over a corresponding hyperbolic sector.*

Cosine of a Complex Hyperbolic Angle. Trigonometrical Expressions.—Referring to (496), Appendix A, the cosine of a complex angle,

$$\cosh(x \pm jy) = \cosh x \cosh jy \pm \sinh x \sinh jy \quad (304)$$

$$= \cosh x \cos y \pm j \sinh x \sin y \quad (305)$$

$$= \cosh x \cos y \pm j \cosh x \sin y \tanh x \quad (306)$$

$$= \frac{1}{2}(\epsilon^x \angle \pm y + \epsilon^{-x} \angle \pm y) \quad (307)$$

$$= \sqrt{\cosh^2 x - \sin^2 y} \angle \pm \tan^{-1}(\tanh x \tan y) \quad (308)$$

$$= \sqrt{\sinh^2 x + \cos^2 y} \angle \pm \tan^{-1}(\tanh x \tan y) \quad (309)$$

$$= \sqrt{\cosh 2x \cdot \cos 2y} \angle \pm \tan^{-1}(\tanh x \tan y) \quad (310)$$

$$\text{where } \cos 2z = \frac{\cos 2y}{\cosh 2x} \quad (311)$$

Each and all of the above formulas (304) to (311) has advantages in particular cases for purposes of computation, while (306) is the formula embodied in the construction of Fig. 68.

Sine of a Complex Hyperbolic Angle. Trigonometrical Expressions.—Referring to (495), Appendix A, the sine of a complex angle,

* Incidentally, this angle is called the Gudermannian of the hyperbolic angle.

$$\sinh (x + jy) = \sinh x \cdot \cosh jy \pm \cosh x \cdot \sinh jy \quad (312)$$

$$= \sinh x \cdot \cos y \pm j \cosh x \cdot \sin y \quad (313)$$

$$= \sinh x \cdot \cos y \pm j \sinh x \cdot \sin y \cdot \coth x \quad (314)$$

$$= \frac{1}{2}(\epsilon^x \angle \pm y - \epsilon^{-x} \sphericalangle \pm y) \quad (315)$$

$$= \sqrt{\sinh^2 x + \sin^2 y} \angle \pm \tan^{-1}(\coth x \cdot \tan y) \quad (316)$$

$$= \sqrt{\cosh^2 x - \cos^2 y} \angle \pm \tan^{-1}(\coth x \cdot \tan y) \quad (317)$$

$$= \sqrt{\cosh 2x \cdot \sin z} \angle \pm \tan^{-1}(\coth x \cdot \tan y) \quad (318)^*$$

where z has the meaning given in (311).

The construction of Fig. 69 is derived from (314); but (312) to (318) are all useful.

Tangent of a Complex Hyperbolic Angle. Trigonometrical Expression.—A geometrical construction for $\tanh (x + jy)$ involving orthogonally intercepting circles, has long been known,† and has been given in detail elsewhere.‡ For practical purposes, however, we may obtain an expression for the tangent, by dividing the cosine into the sine, using any corresponding pairs of formulas between (297) and (311). An additional useful formula is

$$\tanh (x \pm jy) = \frac{\sinh 2x}{\cosh 2x + \cos 2y} \pm j \frac{\sin 2y}{\cosh 2x + \cos 2y} \quad (319)$$

The sines, cosines, and tangents of complex hyperbolic angles have been extensively tabulated and charted** for practical use. These will be frequently referred to in what follows. For accurate arithmetical work, the tables are the more important. For slide-rule computations, where swiftness is desired, with a correspondingly lesser degree of precision, the charts are preferable.

Quadrant Measure for Circular Angles.—It has been pointed out, in connection with Figs. 68 and 69, that the vector value of either $\sinh (x + jy)$ or $\cosh (x + jy)$ is cyclically repetitive, at successive intervals of 2π circ. radians in y . This makes an awkward

* Formulas (310), (311), and (318), are due to Prof. C. L. Bouton.

† CRYSTAL'S "Algebra," Edinburgh, 1889.

‡ "Application of Hyperbolic Functions to Electrical Engineering Problems," Chapter V.

** "Tables of Complex Hyperbolic and Circular Functions," by A. E. KENNELLY, Harvard University Press, 1913.

"Chart Atlas of Complex Hyperbolic and Circular Functions," by A. E. KENNELLY, Harvard University Press, 1913.

interval for tabulation. A much more convenient expedient is to express the imaginary component in quadrants, since 4 quadrants are equivalent to 2π , or 6.283 . . . radians. In Figs. 68 and 69, the lower half of the y circles are indicated in quadrant measure. Thus $\cosh(1 + j2.5) = -1.09 - j0.83$, and $\sinh(1 + j2.5) = -0.83 - j1.09$. This division with decimal subdivisions corresponds precisely to the French system of dividing the circle in grades, or decimals of a quadrant. In order to reduce a complex angle $(x + jy)$ to quadrant measure, the imaginary y must be "quadranted;" i.e., divided by $\pi/2$, or 1.57079 . . . That is

$$x \pm jq = x \pm j \frac{y}{1.57079 \dots} = x \pm j0.63662y \quad \text{hyp. } \angle \quad (320)$$

Thus, $1 + j2$ in radian measure, is $1 + j1.2732$ in quadrant measure. It is advisable to underscore quadranted imaginaries, in order clearly to distinguish them from radians circular measure.

Another advantage pertaining to the use of French quadrant measure, in dealing with the imaginary components of hyperbolic angles, is that when x exceeds 4.0, it is easily shown from (307) and (315), that for most practical purposes,*

$$\sinh(x + jy) \cong \cosh(x + jy) \cong \frac{e^x}{2} \angle y \quad \text{numeric } \angle \quad (321)$$

where the result is expressed as a polar, with its argument in circular measure, which, for practical purposes, has to be reduced to degrees or "grades," according to the tables available. But

$$\sinh(x + jq) \cong \cosh(x + jq) \cong \frac{e^x}{2} \angle q \quad \text{numeric } \angle \quad (322)$$

That is, *the sine or cosine of a hyperbolic angle with a large real component x has a size of half the exponential of x , and a slope equal to the imaginary q , expressed in quadrants, or in grades after shifting the decimal point.*

The tables and charts are largely based on quadrant measure in the imaginary components of the entering hyperbolic angles, and we shall often use quadrant measure in what follows.

Simple Alternating-current Circuits.—A simple a.c. circuit is one which has resistance and reactance (inductive, condensive, or both) and which carries a single frequency; i.e., the e.m.f. and current are sinusoidal without harmonics. In Fig. 70, such a circuit

* The symbol \cong stands for "approximately equals."

is indicated as having an impressed root-mean-square (r.m.s.) e.m.f. of E volts, by voltmeter, impressed upon a non-ferric inductive impedance Z ohms \angle , connected between the mains mm , the current supplied to this reactor being I amp. \angle r.m.s. by ammeter, and the active power P_a watts, by wattmeter. The impressed frequency f in* cycles per second, has an angular velocity,

$$\omega = 2\pi f \quad \text{circ. radians/sec.} \quad (323)$$

In the case represented in Fig. 70, let $f = 63.66$, for which $\omega = 400$ radians per sec. Let the impedance of the coil, as apparent

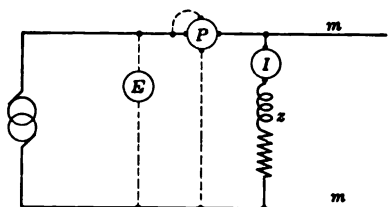


FIG. 70.—Simple alternating-current circuit with the impedance z measured both in size and in slope by volt-ampere-wattmeter readings.

from volt-ampere-wattmeter measurements, be 10 ohms, with a power factor of 80 per cent.; *i.e.*, 8 ohms “active resistance” and 6 ohms “inductive reactance.” The active resistance of a coil is that which it appears to offer from such a.c. measurements. The active resistance of a coil ordinarily exceeds the d.c. resistance, and increases with the frequency. It may include elements due to skin effect (imperfect current distribution over the cross-section of the conductor), eddy-current loss in the conductor, and hysteretic losses in neighboring iron or steel. The inductive reactance of a coil is the positive reactive resistance which it appears to possess by reason of its c.e.m.f. of self-inductance, as modified by skin effect and eddy currents. It is assumed that

$$jX = jL\omega \quad j \text{ ohms} \quad (324)$$

* Signalling frequencies in submarine and land telegraphy range from 1 to 50 or more \sim ($\omega = 6$ to 314). Power and lighting frequencies (low frequencies) ordinarily range from 12 \sim to 60 \sim ($\omega = 75$ to $\omega = 377$). Telephone and telegraph frequencies (audio frequencies or moderate frequencies) ordinarily range from 60 \sim to 10,000 \sim ($\omega = 377$ to $\omega = 62,800$). A standard reference telephonic frequency is $\omega = 5,000$. Radio frequencies (high frequencies) ordinarily range from 10,000 \sim to 1,000,000 \sim , or more. Alternating-current engineering, taken broadly, thus includes the range from $f = 1$ to $f = 10^6$.

expresses the relation between the reactance jX of the coil at impressed angular velocity ω , and the apparent inductance L henrys. In the case considered, $L = 0.015$ henry.

Since the current and the impressed e.m.f. will ordinarily

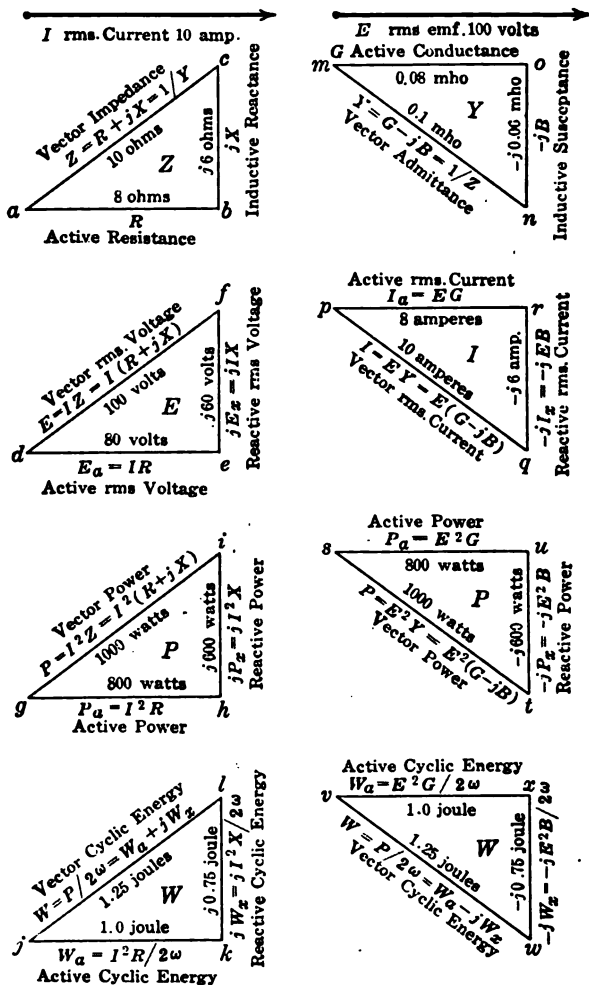


FIG. 71.—Vector diagrams for simple inductive alternating-current circuit.

differ in phase, it is optional to select either of those quantities as having reference phase. That is, we may consider the current I as of standard phase and the impressed e.m.f. E as leading in this case with respect thereto; or, we may consider the e.m.f. as of

standard phase, and the current I as lagging with respect to the same. Each assumption gives rise to a series of four simple stationary vector diagrams, as indicated in Fig. 71. The left-hand column of the *ZEPW* triangles employs the current as of standard phase; while the right-hand column of *YIPW* triangles, employs the e.m.f. as of standard phase.

Vector Impedance.—Commencing with the left-hand column, the impedance triangle abc has for its base, the active resistance R , in this case 8 ohms, and for its hypotenuse, the inductive reactance $+jX$,* in this case $j6$ ohms. If the circuit contained condensive reactance, instead of inductive reactance, this hypotenuse would be in the negative† direction, or would be $-jX$ ohms. We might also describe the impedance in this case as $10\angle 36^\circ.52'.11''$ ohms.

Vector Electromotive Force.—If next we multiply this impedance by $I = |I|\angle 0^\circ = 10\angle 0^\circ$ amp., we obtain the E triangle def , with $IR = 80$ active volts, $jIX = j60$ reactive volts, and $E = IZ = I(R + jX)$ total or vector volts. This is a stationary vector triangle, in which the horizontal or active component is the r.m.s. voltage component consumed actively in overcoming resistance. The vertical or reactive component is the r.m.s. voltage component consumed reactively, in overcoming reactive resistance or reactance; i.e., in neutralizing the c.e.m.f. of self-induction. The total or vector voltage may be described as $100\angle 36^\circ.52'.11''$ volts, to current standard phase.

Vector Power to Current Phase.—If we multiply the E voltage triangle by $I|\angle 0^\circ = 10\angle 0^\circ$ amp., we obtain the power triangle ghi . Here gh is the active power $P_a = I^2R$ watts, both the average and the maximum cyclic rate of transferring energy out of the circuit, in the form either of heat, chemical, or mechanical energy. The imaginary component hi is the reactive power, or the maxi-

* j for $\sqrt{-1}$ was first introduced into electrotechnics by BEDELL and CREHORE, "Alternating Currents," 1893. The application of complex arithmetic and plane vectors to impedance, and the a.c. circuit, was first introduced by the author, "Impedance," *Trans. A. I. E. E.*, vol. x, p. 175, April, 1893. The extension of complex quantities and plane vectors to potentials and currents is due to STEINMETZ, "Complex Quantities and Their Use in Electrical Engineering," *Proc. Int. El. Congress, Chicago*, August, 1893.

† International notation, according to the decision of the International Electrical Commission, at its Turin meeting in 1911, calls for $R + jX$ as the impedance of an inductance coil, here followed. See Standardization Rules of the A. I. E. E.

imum cyclic rate of transferring energy from the mains mm , Fig. 70, into the magnetic flux of the coil, and back again. When the r.m.s. current I in the coil reaches a maximum or crest value I_m amp., either plus or minus, the coil contains magnetic energy $\frac{1}{2}LI_m^2 = LI^2$ joules. At the current zero points, this energy disappears from the coil, returning to the mains and generator system. The maximum cyclic rate of transfer of this energy is equal to this reactive power jP_x watts. This reactive power is sometimes called "wattless power," but this term is both erroneous and misleading. The reactive power jI^2X is just as "wattful" as the active power I^2R . The only difference is that jI^2X is the activity of transferring energy from one part of the circuit to another, while I^2R is the activity of transferring energy from the circuit to its surroundings. It is true that in ordinary industrial practice, reactive power has no effect on customers' watt-hour meters, and therefore is not saleable, but it is illogical to deny the existence of power, merely because it is ordinarily unsaleable.

Similarly, the hypotenuse gi is the total or vector power I^2Z watts. It is commonly described as volt-amperes, to distinguish it from active power. This distinction is a useful one, provided it is realized that a "vector volt-ampere" is also a "vector watt." In this case, the vector power is 1 kw. or 1,000 volt-amp. with an active component of 800 watts, and a reactive component of $j600$ watts.

Vector Cyclic Energy.—If we divide the P triangle by 2ω , or twice the impressed angular velocity, we obtain the stationary vector diagram jkl . Here jk is the active maximum cyclic energy, which is added in successive + and - blocks, in each energy cycle, to the stream of outgoing active energy leaving the circuit. W_a is the cyclic active energy throb, as will be seen later. The reactive component jW_x is the maximum cyclic energy, added in successive + and - blocks to the energy of the magnetic flux linked with the coil. This reactive energy block $W_x = 0.75$ joule. When at its negative maximum, it destroys the energy in the coil ($0.75 - 0.75 = 0$ joule). When at its positive maximum, it produces the full cyclic magnetic energy in the coil ($0.75 + 0.75 = 1.5$ joules). The r.m.s. current I being 10 amp., its maximum cyclic value is $I\sqrt{2} = 14.14$ amp., and the maximum cyclic magnetic energy is

$$W_m = \frac{1}{2}LI_m^2 = LI^2 = 2W_x \quad \text{joules} \quad (325)$$

in this case $\frac{1}{2} \times 0.015 \times (14.14)^2 = 1.5$ joules, as already found. The frequency of this energy cycle is $2f$, or twice the frequency of the impressed current; because $LI_m^2/2$ reaches its maximum at each current wave crest, whether I is plus or minus. Its angular velocity is therefore 2ω radians per second.

Vector Admittance.—Turning now to the second column in Fig. 71, the vector admittance of the branch circuit in Fig. 70 is the reciprocal of the vector impedance Z . In this case $Y =$

$$\frac{1}{10\angle 36^\circ.52'.11''} = 0.1\angle 36^\circ.52'.11'' = 0.08 - j0.06 \text{ mho.}$$

This admittance is represented at *mon*. The real component G , or *mo*, is called the “active conductance.” The imaginary component *on* is $-jB$, the *inductive susceptance*. If the branch circuit under test in Fig. 70 were condensive, instead of being inductive; *i.e.*, if a condenser were either substituted for the reactor, or a condenser of preponderating reactance were inserted in series with the coil, then the susceptance jB would be plus, instead of minus, and would become a *condensive susceptance*. The Y triangle, and its subordinates, may thus be either inverted or erect. Its condition in this respect must always be opposite to that of the Z triangle.

Vector Current.—If taking the impressed r.m.s. e.m.f. E as of standard phase, or as inherently possessing zero slope, we multiply Y by $E = |E|\angle 0^\circ$, we obtain the I triangle pqr . Here pr is the active current $I_a = EG$ amp. The negative perpendicular rq is the reactive current $-jI_x = -jEB$ amp. The active component I_a will be in phase with the impressed e.m.f. E . The reactive component will be in quadrature with E .

Vector Power to Electromotive Force Phase.—If we multiply the r.m.s. current I , or $10\angle 36^\circ.52'.11''$, by the impressed e.m.f. at standard phase $E = 100\angle 0^\circ$ volts, we obtain the vector power diagram stu , or $1,000\angle 36^\circ.52'.11''$ watts. Here E^2G , or 800 watts, is the active power, $-jE^2B$, or $-j600$ watts, the reactive power, and $E^2Y = E^2(G - jB)$, the vector power. It will be observed that the power diagram stu is the same as the power diagram I^2Z , or ghi reversed, the active 800 watts being the same in both; but the reactive components ut and hi being mutually opposite. At first sight, this looks like a contradiction; but, on further examination, the two oppositely directed triangles are consistent. Figs. 72 and 73 show that the crest value of the power always occurs between the maxima of voltage and of current. Conse-

quently, reactive power which is leading with respect to current phase, is lagging with respect to voltage.

Similar considerations apply to the two W triangles kjl and vxz , which are likewise mutually inverted.

Instantaneous Diagram to Current Standard Phase.—Fig. 72 represents diagrammatically one complete cycle of current and voltage in the branch circuit of Fig. 70, under consideration. In order to simplify the diagram, all of the waves, which are actually

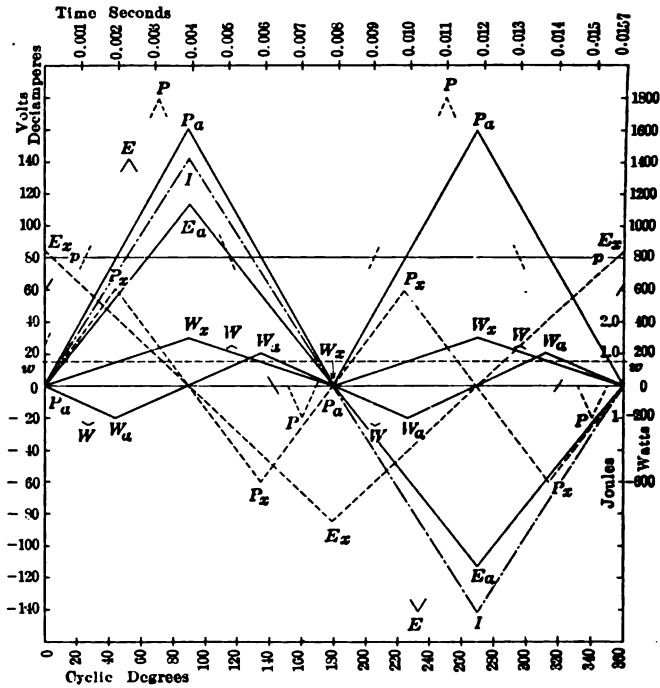


FIG. 72.—Diagram of maximum cyclic current, voltage, power and energy, to current standard phase.

sinusoids, are indicated by simple zigzag or saw-tooth waves. The maxima, minima, and zero points, are correctly presented of such a diagram; but the intersections of the lines do not carry the same significance.*

The current I starts positively at 0° , or with standard phase,

* Corresponding diagrams with full sinusoidal curves are given in the original paper "Vector Power in Alternating-current Circuits," by A. E. KENNELLY, *Trans. A. I. E. E.*, June 27, 1910.

and reaches its crest value 14.14 amp. at 90° . The impressed e.m.f. E , reaches its crest value 141.4 volts, nearly 37° earlier in the cycle. It is analyzed into two components; namely, the active component E_a , 113.1 volts, in phase with I , and a leading reactive component E_z , 84.84 volts, in quadrature with I .

The successive instantaneous products of current and voltage give rise to a P sinusoid of double frequency, executing two complete cycles in one cycle of either current or voltage. This power sinusoid has its crests at +1,800 watts, just midway in time between the crests of I and E . It is therefore a leading power with respect to the current I . The power sinusoid has its axis on the line pp at +800 watts, and its lower maxima at -200 watts. It may therefore be expressed as

$EI \{ \cos \beta + \sin (2\omega t + \beta) \} = P_a + P \sin (2\omega t + \beta)$ watts (326)
 or, in this case, $800 + 1,000 \sin (2\omega t + \beta)$ watts, where $\omega =$ radians per sec. It may be analyzed into an active power component $P_a = 800 - 800 \cos (2\omega t)$ watts corresponding to gh , Fig. 71, and a leading reactive power component P_z in quadrature therewith, $600 \sin (2\omega t)$, corresponding to hi , Fig. 71.

The power P may be considered as the time rate of change of a certain cyclic energy W . This energy, being the integral of (326), will have a double-frequency sinusoid W , 1.25 joules in amplitude, and 37° in energy phase, ahead of its active component W_a of 1.0 joule amplitude. The leading reactive component W_z of 0.75 joule amplitude has its axis $w w$ displaced to 0.75 joule above 00. The three powers P_z , P and P_a , are severally 90° ahead of the three energies W_z , W and W_a . The amplitude 0.75 joule of the reactive energy, in phase with I , causes the crest energy of the current $LI_m^2/2$ to be just 1.5 joules, as has already been pointed out. At the current zeros, the total value of W_z is zero. These energy components correspond to the three vectors of the W triangle jkl , Fig. 71..

Instantaneous Diagram to Voltage Standard Phase.—In Fig. 73, the corresponding series of amplitudes and phase relations is presented to voltage standard phase. E represents the voltage wave of amplitude 141.4, commencing positively at 0° . The current I lags 37° with respect thereto. The power sinusoid P has its crest midway between these, and lags 37° of power phase with respect to E , thus corresponding to st , in Fig. 71. This power may be analyzed into an active component P_a , of 800 watts amplitude, and a lagging reactive component P_z of 600 watts, cor-

responding to u , Fig. 71. To these three cyclic double-frequency powers correspond three cyclic double-frequency energies W_a , W and W_x , of 1.0, 1.25 and 0.75 joules amplitude. The latter is the negative of an energy wave W'_x , of like amplitude, which would represent the energy in a condenser of $+j0.06$ mho conductance, charged to a potential of 141.4 volts. The sinusoid W_x reaches its total crest value of 1.5 joules in phase with I_x . These energy relations correspond to those of the triangle uvr , Fig. 71.

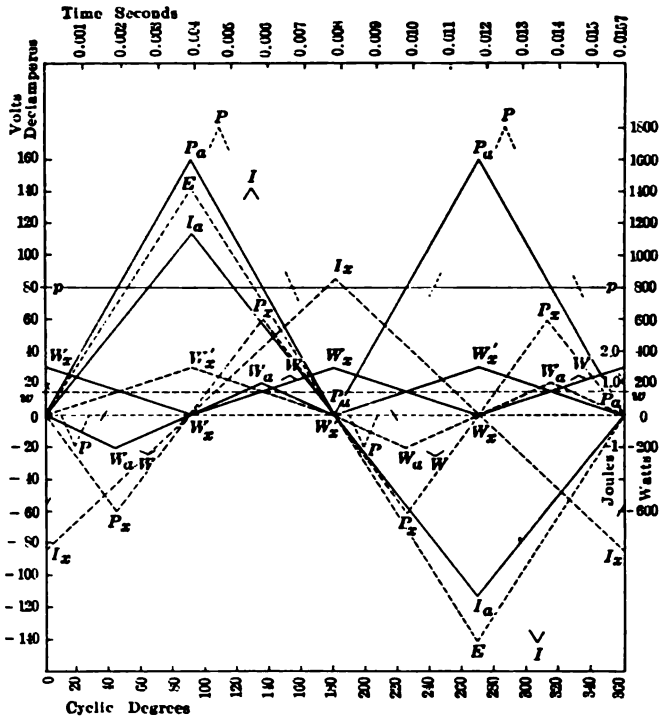


FIG. 73.—Diagram of maximum cyclic voltage, current, power and energy, to voltage standard phase.

Rotative Properties of the E and I Vector Diagrams.—The Z and Y triangles, Fig. 71, are essentially stationary, no benefit being derivable from their rotation. The E and I diagrams, however, def and pqr , although presented as stationary, may be made serviceable as rotary vector diagrams. Thus, let the def triangle be increased $\sqrt{2}$ times in linear dimensions; or let the same triangle have its scale of linear interpretation increased in

this ratio, and be rotated about O , Fig. 74, in the plane of the figure, at the angular velocity ω radians per sec., or 63.66 revolutions per sec. Then the instantaneous projections of the points ef and G , on the axis of reals $-XOX$, will indicate the corresponding instantaneous values of the active, total and reactive electromotive forces.

Similarly, if the I diagram be expanded $\sqrt{2}$ times in linear dimensions, and be rotated about the point O , Fig. 75, in the plane of the paper, at the angular velocity, $\omega = 400$ radians per sec., the instantaneous projections of q , r , and s on the axis of reals $-XOX$, starting from the proper epoch, will mark the corresponding instantaneous values of the total, active and reactive currents.

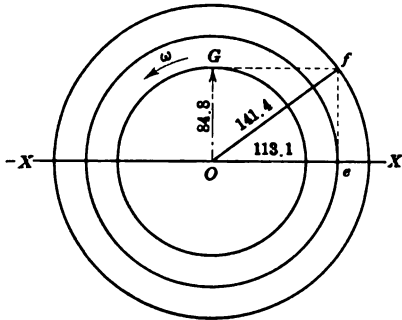


FIG. 74.—Rotation of the E diagram after linear expansion in ratio $\sqrt{2}$, for instantaneous projections.

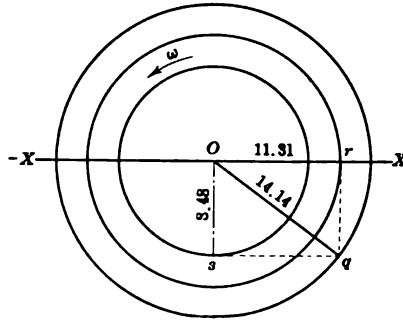


FIG. 75.—Rotation of the I diagram after linear expansion in ratio $\sqrt{2}$, for instantaneous projections.

The stationary E and I diagrams are, therefore, also to be regarded as rotative, if suitably altered in scale of linear dimensions. It also follows that the E and I vectors may be mounted together, at the proper phase displacement, and rotated conjointly as a single diagram, at the common angular velocity ω . Such a rotative diagram, of either voltage or current, has long been used illustratively in a.c. analysis.*

Rotative Properties of the P Vector Diagrams.—If either of the power diagrams in Fig. 71, say ghi , be rotated about the point O , Fig. 76, without any change in scale, at the angular velocity 2ω or, in this case, 127.3 revolutions per sec., and instantaneous projections of h , i and k be taken, on the axis $-XOX$, then these pro-

* J. A. FLEMING, "The Alternating-current Transformer," vol. i, p. 110, London, 1889.

jections will mark the instantaneous values of the active, total and reactive powers. The zero of the reactive power is at O , which also corresponds to the line pp in Figs. 72 and 73; but the point H' corresponds to the power zero OO in those figures.

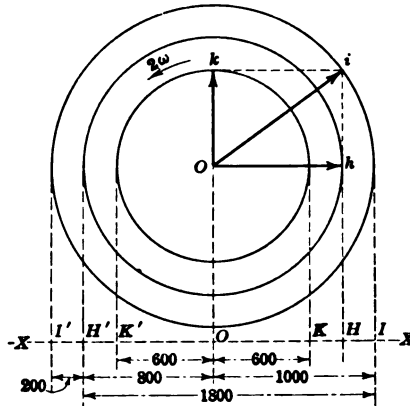


FIG. 76.—Rotative power diagram without change of scale.

Referring to the power triangle ghi , and sut of Fig. 71, it will be evident that the instantaneous power in an a.c. circuit, or branch, oscillates between the sum and difference of the base and hypotenuse of the vector power triangle, (-200 and $+1800$ watts in Fig. 76).

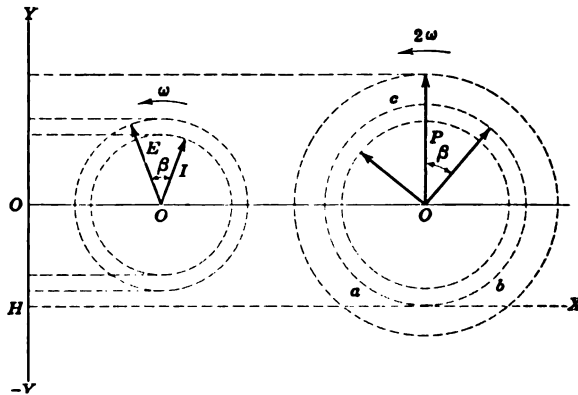


FIG. 77.—Corresponding rotations of the $E I$ and P vectors.

By mounting the I and E vectors on one disk, spinning at ω radians per sec., and the P vectors on another disk, geared with the first in the velocity ratio of 2 to 1, so that the P disk spins at 2ω radians per sec. (Fig. 77), the instantaneous vertical projec-

tions of E , I , P_a , P_s and P , on the vertical axis $-YOY$, will mark off the corresponding instantaneous current, voltage, active, reactive, and total power. The P vector should stand vertical, as shown, when the E and I vectors make equal and opposite angles with the vertical. Powers are read with respect to H as zero, except P_s , which is read with respect to O as zero.

Rotative Properties of the W Vector Diagrams.—By reference to (326), it will be seen that the time integral of the power contains

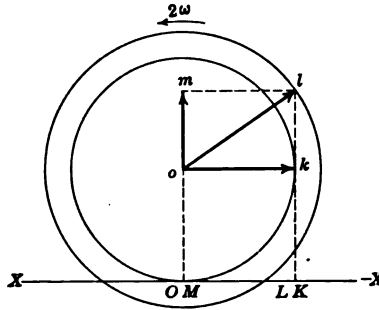


FIG. 78.—Rotation, with rolling, of the W diagram.

a uniformly increasing term $P_a t$, as well as a cyclically oscillating term $\frac{P}{2\omega} \sin(2\omega t + \beta)$. The latter term can be developed by the projection, on a fixed axis, of the energy triangle jkl , or vwx , spinning in the plane of projection, about the points j or v , with the angular velocity 2ω radians per sec. The first term requires a constantly increasing addition to the value of W so developed. The sum of the two terms can, therefore, always be obtained by both rotating and rolling the diagram, developed as a wheel of tread radius W_a and flange radius W , as indicated in Fig. 78. Here the wheel kLM rolls on the rail $+XO-X$, at uniform angular velocity 2ω . The vertical projection of the flange point l , at L on the rail, marks the instantaneous value of the energy delivered to the circuit, for which the energy triangle jkl , Fig. 71, has been prepared.

It will be observed that, as the wheel rotates and rolls, the path of the flange point in the plane of rotation will be a prolate trochoid,* $abcdefg$, containing a closed loop at each revolution. The instantaneous projection at L of the flange point l in this curve

* Greenhill's "Differential and Integral Calculus," 1896, p. 39.

marks off the total energy poured into the circuit from the electric source, up to that instant.

Just as any point on the flange of a railroad-car wheel, running

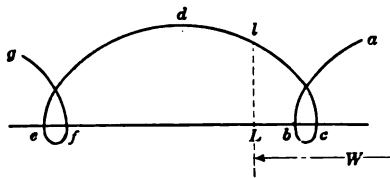


FIG. 79.—Prolate trochoid described by the moving point on the flange of the wheel representing a rotating and rolling energy diagram.

at say 100 km. per hr., over a railroad track, not only comes to rest, but actually retrogresses, or reverses its direction of horizontal translatory motion, once in each wheel revolution; so,

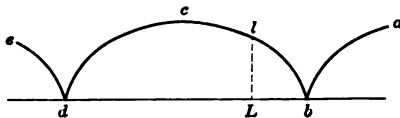


FIG. 80.—Case of reactanceless circuit corresponding to a flangeless wheel, the moving point tracing a cycloid in the plane of rotation.

when the flange point is executing the loops *bc*, *ef*, in Fig. 79, the energy ceases to flow from the source into the circuit, and flows back from the circuit toward the source.

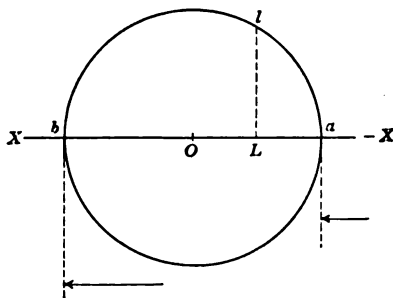


FIG. 81.—Rotation, without rolling, of *W* diagram, in limiting case of resistanceless circuit.

In the particular case of Fig. 80, when the circuit is *non-reactive*, and contains only pure resistance, the flange of the wheel disappears, or the wheel becomes a simple cylinder, and the path of the rotating point *l* becomes a pure cycloid, *abcde*. In this case, the flow of energy momentarily stops at *b* and *d*, but the energy tide does not reverse.

In the opposite case, when the circuit is resistanceless or wholly reactive, the energy vector diagram jkl has zero base, and its hypotenuse coincides with its perpendicular. The triangle shrinks to a mere vertical line, and the tread radius shrinks to the axis O , Fig. 81, leaving the wheel all flange. This "wheel," in

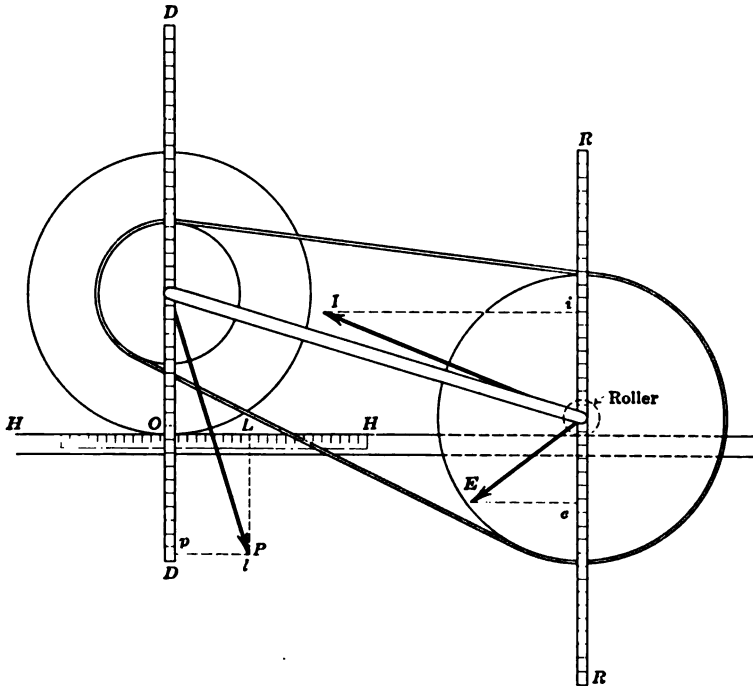


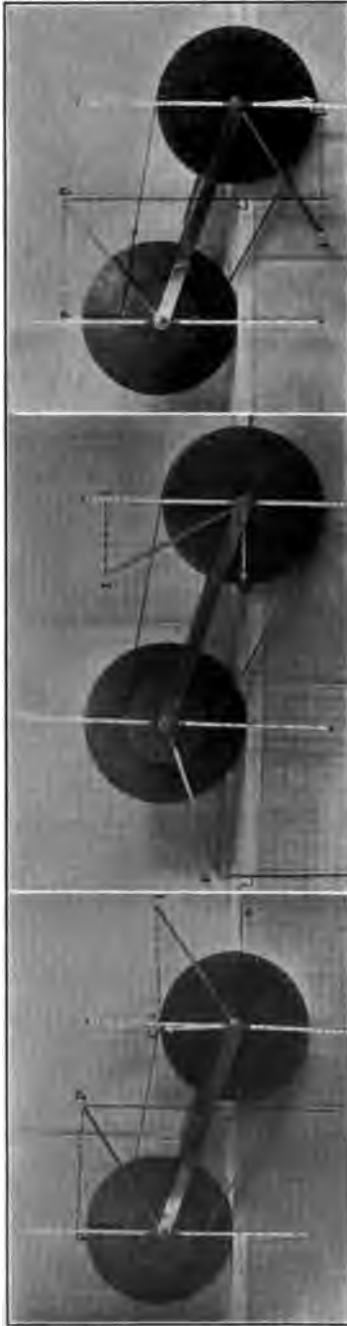
FIG. 82.—Front elevation of model giving simultaneous instantaneous values of $E I P$ and W . The wheel at O is pushed towards the left along the table HH .

rotating, fails to advance by rolling, and the energy oscillates between the limits a and b .

In Fig. 77, if the power disk is allowed to roll upon the tread circle a, b, c over a rail HX , and with it the geared current-voltage disk, the moving system will project on a vertical rod, carried along with it, the instantaneous values of current, voltage, and power; while the vertical projection of the flange point P will trace out, to a suitable linear scale, the energy along the rail. The horizontal speed of the axle O will measure the average power, and also the active watts of the circuit.

Such a model has been constructed for a particular range of

ARTIFICIAL ELECTRIC LINES



$E = 100 \angle 0^\circ$ $\epsilon = 100$ volts $\epsilon = 100 \angle 90^\circ$ $\epsilon = 0$ volts $\epsilon = 100 \angle 180^\circ$
 $I = 200 \angle 0^\circ$ $i = 100$ a.m.p. $I = 200 \angle 30^\circ$ $i = 173.2$ a.m.p. $I = 200 \angle 120^\circ$
 $P = 10$ K.w $W = 0$ K.J $P = 0$ K.w $W = 2.63$ K.J $P = 10$ K.w $W = 2.5$ K.J

FIG. 83.—Pictures of the model in three successive stages of operation. E and I are the instantaneous values of e.m.f. and current revolving vectors; while ϵ and i are their respective instantaneous projections on the vertical rod of the right-hand disk. p is the instantaneous power as projected by the vector head P on the vertical rod of the left-hand disk. W is the instantaneous energy in kilojoules, as projected by the vector head P on the horizontal scale at L . The right-hand disk is supposed to make one revolution per second, corresponding to a frequency of one cycle per second; while the left-hand disk makes two revolutions per second.

current and voltage values.* A front elevation of the model is shown in Fig. 82. Fig. 83 shows pictures of the model in three successive stages of operation for the case of a single-phase circuit having $E_m = 100$ volts, $I_m = 200$ amp. 60° in phase behind E_m , $Z = 0.5\angle 60^\circ$ ohm.

Experimental Development of the Z Vector Diagram.—The vector diagram of e.m.f. *def*, Fig. 71, can be produced experimentally, for a.c. branch circuits having convenient values of impedance and frequency, by developing a rotating current sheet in a metal-

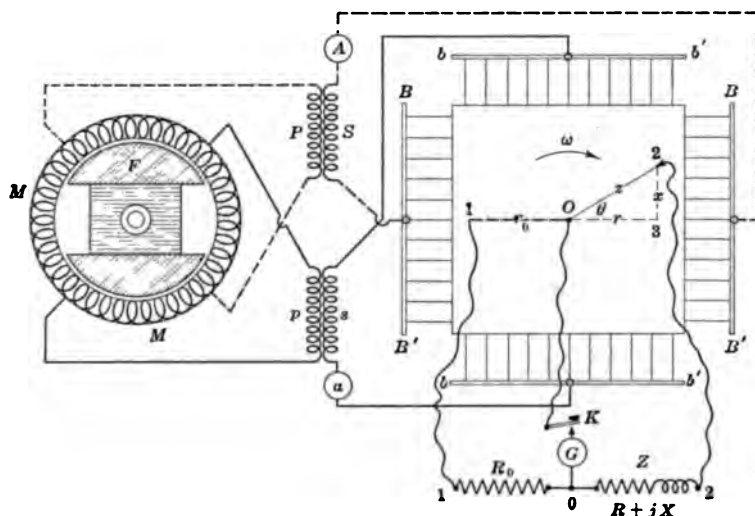


FIG. 84.—Connections of uncompensated vector-diagram apparatus for measuring the impedance Z .

lic plate. The impedance of a simple branch circuit, containing combinations of resistance, inductance, and capacitance in series, can then be measured on the plate in rectangular coordinates, distances along the X axis corresponding to resistance, and distances along the Y axis corresponding to reactance.† The con-

* "A Model for Alternating-current Quantities," by A. E. KENNELLY and H. G. CRANE, *Electrical World*, July 11, 1914.

† "A New and Direct Process of Producing Alternating-current Vector Diagrams Experimentally," by A. E. KENNELLY, H. G. CRANE and J. W. DAVIS, *Electrical World*, March 30, 1911.

"The Rotating Electric-current Field," by A. E. KENNELLY, *Atti del Congresso Internazionale delle Applicazioni Elettriche*, Turin, September, 1911, vol. ii, p. 1180, section III.

"Producing Vector Diagrams Experimentally. Improved Apparatus," by A. E. KENNELLY and H. G. CRANE, *The Electrical World*, April 17, 1915.

nection diagram of the apparatus is given in Fig. 84, and a picture of the compensated plate in Fig. 85.

Although the device above referred to marks off only the Z vector diagram of Fig. 71, through the medium of the corresponding E diagram on the plate, yet the corresponding P and W diagrams may be directly inferred therefrom.

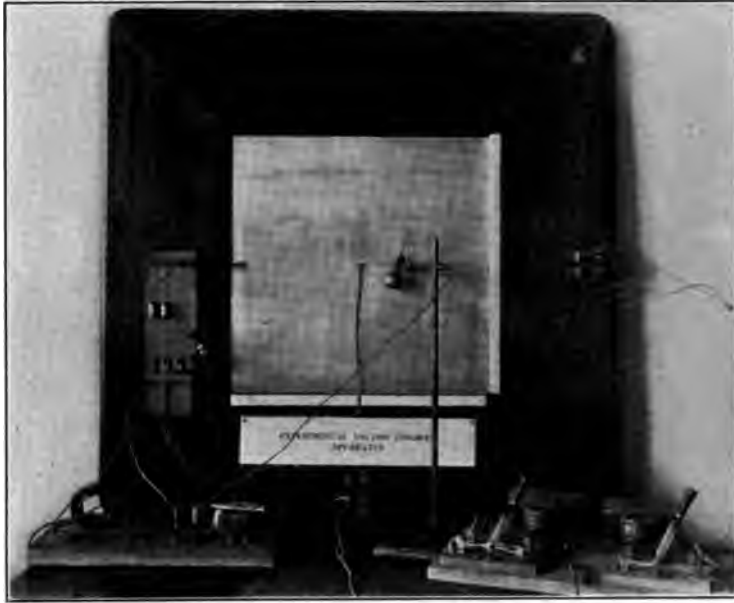


FIG. 85.—Compensated vector-diagram apparatus.

After the student has developed such a vector diagram by experimental exploration over a plate, the series of vectors in Fig. 71, containing the essential properties of an a.c. circuit, become vividly impressed on the mind.

Fictitious Impedance Diagrams.—In cases where the branch circuit of Fig. 70 contains either an active e.m.f. such as that of a synchronous motor, or a combination of condensive and inductive reactances in series, the readings of e.m.f., current and power, will give rise to an impedance Z diagram and its series of subsidiaries, which is arithmetically correct and practically useful, but is physically incorrect as regards impedance elements. Such diagrams, although serviceable, may be described as "*fictitious*."

CHAPTER X

FUNDAMENTAL PROPERTIES OF ALTERNATING-CURRENT REAL LINES

We have already seen that all uniform real c.c. lines, in a steady state of operation, possess or subtend a real hyperbolic angle θ , and have likewise a linear real hyperbolic angle $\alpha = \theta/L = \sqrt{rg}$ hyps. per km. A c.c. artificial line also possesses a real hyperbolic angle θ per section of its length, and, if each section represents a length of L km., a corresponding linear hyperbolic angle θ/L is inferred.

A.c. lines differ from c.c. lines in the effects of inductance and of capacitance. That is, while c.c. lines call only for a consideration of linear resistance r and linear leakance g , a.c. lines call, in addition, for a consideration of linear inductance l , and linear capacitance c . Moreover, the effects of inductance and capacitance vary with the frequency.

Linear Inductance of Real Lines.—The inductance of a very long loop consisting of a pair of parallel uniform round wires, each of radius ρ cm. and set at an interaxial distance D cm., may be defined as the total magnetic flux linked with the loop per unit of current steadily passing around it. The *linear inductance* of such a loop is the total flux, per linear centimeter of the loop, and per unit of current. In c.g.s. magnetic measure, this linear inductance may be expressed in abhenrys per loop centimeter, according to the formula:*

$$l_0 = \mu + 4 \operatorname{logh} \left(\frac{D}{\rho} \right) \quad \frac{\text{abhenrys}}{\text{loop cm.}} \quad (327)$$

where μ is the magnetic permeability of the wire, assumed uniform, which for non-magnetic materials may be taken as unity, and logh signifies hyperbolic or Napierian logarithms, to the base $\epsilon = 2.71828$ The first term signifies the *internal linear loop inductance*, and the second term the *external linear loop inductance*.

Reducing (327) to common logarithms, and to henrys per loop

* CLERK MAXWELL'S "Electricity and Magnetism," vol. ii, p. 293, 1881.

kilometer, we have for non-magnetic wires, in air or other non-magnetic medium,

$$l_{\text{loop}} = \left[1 + 9.2103 \log \left(\frac{D}{\rho} \right) \right] 10^{-4} \frac{\text{henrys}}{\text{loop km.}} \quad (328)$$

The linear inductance of either of the two wires to the mid-plane between them, may be called the *linear wire inductance*. It is half of the linear loop inductance (327) or

$$l = \left[0.5 + 4.6052 \log \left(\frac{D}{\rho} \right) \right] 10^{-4} \frac{\text{henrys}}{\text{wire km.}} \quad (329)$$

It is known* that this non-ferric linear inductance as above defined, by the ratio of the linear flux to the steady current supporting it, is the same for all equal values of D/ρ . In other words, the degree of proximity of the two parallel wires does not have to be considered.

In the case of three parallel and equally spaced wires† forming a three-phase a.c. line system, the linear wire inductance is advantageously used from (329). In such a case, D is the interaxial distance between any pair of the three wires.

As an example, the linear wire inductance of a pair of No. 10 A.W.G. copper wires of diameter 0.2589 cm. interaxially separated by 30.48 cm. (1 ft.) is

$$\begin{aligned} \left(0.5 + 4.6052 \log \frac{30.48}{0.12945} \right) 10^{-4} &= (0.5 + 4.6052 \times 2.3719) 10^{-4} \\ &= (0.5 + 10.923) 10^{-4} = 11.423 \times 10^{-4} = 1.1423 \text{ millihenrys} \\ &\text{per wire km. (1.839 mh. per wire mile.)} \end{aligned}$$

Tables of linear wire inductances for different sizes of wire at various spacings have been worked out by †† various writers.

Linear Capacitance of Real Lines.—It follows from the theorem of the propagation of electric disturbances over a pair of uniform parallel conductors in free space at the speed of light, that for

* A. RUSSELL, "A Treatise on the Theory of Alternating Currents," Cambridge University Press, 1904, vol. i. Chapter, II, pp. 57-60.

† If the wires are unequally spaced, the linear inductances differ, and the linear resistances also virtually differ. The corrections for dissymmetrical spacing, being somewhat remote from the main subject, will not be considered.

†† "The Inductance and Capacity of Suspended Wires," by E. J. HORTON and A. E. KENNELLY, *Electrical World*, July 7, 1894, vol. xxiv, pp. 6-7, also various handbooks, such as "The Standard" or "The American" handbook.

any such pair of conductors, of any cross-sectional shape,* their linear loop capacitance expressed in statfarads per loop centimeter is the reciprocal of their external linear loop inductance expressed in abhenrys per loop centimeter. Consequently, the linear loop capacitance of a pair of round wires in air is

$$c_0 = \frac{1}{4 \log h \left(\frac{D}{\rho} \right)} \quad \begin{array}{l} \text{statfarads} \\ \text{loop cm.} \end{array} \quad (330)$$

Reducing to common logarithms, kilometer lengths, and remembering that 1 statfarad = $\frac{10}{9} \mu\mu f.$ (micromicrofarads) this becomes:

$$c_{,,} = \frac{0.0120635}{\log \left(\frac{D}{\rho} \right)} \times 10^{-6} \quad \begin{array}{l} \text{farads} \\ \text{loop km.} \end{array} \quad (331)$$

If, however, the wires are not separated by a distance of many radii, *i.e.*, if D/ρ is less than 10, say, these formulas (330) and (331) are unreliable and a formula may be substituted, which is correct for all distances, in air, d being the diameter of the wire in cm.

$$c_0 = \frac{1}{4 \cosh^{-1} \left(\frac{D}{d} \right)} \quad \begin{array}{l} \text{statfarads} \\ \text{loop cm.} \end{array} \quad (332)$$

reduced to farads per loop kilometer this is,

$$c_{,,} = \frac{0.027778}{\cosh^{-1} \left(\frac{D}{d} \right)} \times 10^{-6} \quad \begin{array}{l} \text{farads} \\ \text{loop km.} \end{array} \quad (333)$$

Thus the linear loop capacitance of a pair of wires at an interaxial distance of 50 diameters, or 100 radii, is by (331) $0.0120635/2 = 0.006032 \mu f./\text{loop km.}$, and by the strict formula (333), $0.027778/4.6051 = 0.006032$, to four significant digits the same result. At an interaxial distance, however, of 2 diameters or 4 radii, the linear loop capacitance by (331) is $0.0120635/0.60206 = 0.02004$

* *Trans. A. I. E. E.*, June 29, 1909, p. 702, vol. xxviii, part I.

$\mu\text{f./loop km.}$; while by the strict formula (333) it is 0.027778/1.3170 = 0.02109.*

The *linear wire capacitance* is just double the linear loop capacitance, and in the c.g.s. system, is the capacitance per linear cm. of either wire in a uniform insulated loop to the zero-potential mid-plane between them. Hence,

$$c = \frac{0.05556}{\cosh^{-1}\left(\frac{D}{d}\right)} \times 10^{-6} \quad \frac{\text{farads}}{\text{wire km.}} \quad (335)$$

or, for ordinary interaxial distances, very nearly

$$c = \frac{0.024127}{\log\left(\frac{D}{\rho}\right)} \times 10^{-6} \quad \frac{\text{farads}}{\text{wire km.}} \quad (336)$$

The curves of Fig. 85A show the linear wire capacitance of straight round parallel wires in air (uncorrected for insulators, towers or neighboring wires) up to interaxial distances of 25 diameters, in accordance with (335). Fig. 85B shows the cor-

* Seeing that (332) is the correct formula for the linear loop capacitance of a pair of parallel cylinders in air at any distance, the proposition cited connecting linear inductance and capacitance would indicate that (327) should be:

$$l_0 = \mu + 4 \cosh^{-1}\left(\frac{D}{d}\right) \quad \frac{\text{abhenrys}}{\text{loop cm.}} \quad (334)$$

This question has been investigated experimentally. See DR. F. B. SILSBEE on "Inductance of Conductors at Close Spacings," *Electrical World*, July 15, 1916, vol. lxxviii, pp. 125-126. The results indicate that at very high frequencies, formula (334) appears to be correct; but that at low frequencies (327) is correct. The reason seems to be that at low frequencies, the resistivity of the conductor tends to equalize the current density over the cross-section; whereas at high frequencies, the current density is non-uniform and superficial, such as would give effect to (334).

The following references bear upon the linear capacitance formula.

"The Linear Resistance between Parallel Conducting Cylinders in a Medium of Uniform Conductivity," by A. E. KENNELLY, *Proc. Am. Phil. Soc.*, vol. xlviii, April, 1909, pp. 142-165.

"The Electrostatic Capacity between Equal Parallel Wires," by H. PENDER and H. S. OSBORNE, *Electrical World*, vol. lvi, No. 12, pp. 667-670.

"Graphic Representations of the Linear Electrostatic Capacity between Parallel Equal Wires," by A. E. KENNELLY, *Electrical World*, October 27, 1910.

A. RUSSELL, "Alternating Currents," Cambridge University Press, 1904, vol. i, Chapter 2, p. 59.

responding linear wires capacitance up to interaxial distances of 10,000 diameters, in accordance with either (335) or (336).

Thus, in a three-phase aerial line, with the wires separated interaxially by 100 diameters, each wire would have a linear capacitance of $0.0555/\cosh^{-1} 100 = 0.0555/5.298 = 0.01049$ microfarad per wire km.; *i e.*, between each wire and the neutral or zero-potential surface.

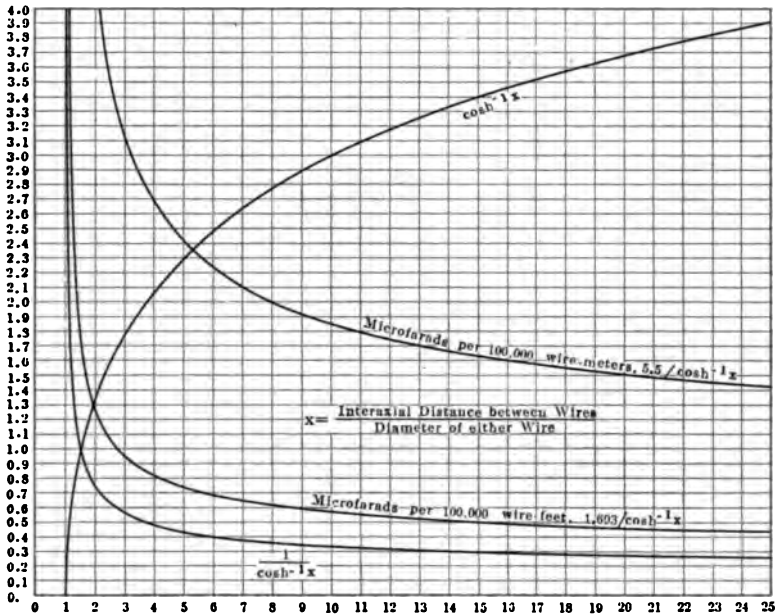


FIG. 85A.—Linear capacitance per 100,000 wire-feet and wire-meters. Graphs of $\cosh^{-1}x$, $1/\cosh^{-1}x$ and linear capacitances of bare, equal, parallel, round wires in air for interaxial distances up to 25 diameters.

In the case of three parallel and equally spaced wires forming a three-phase a.c. line system, the linear wire capacitance is advantageously found from (336). In such a case, D is the interaxial distance between any pair of the three wires.

The *linear wire reactance* $x = l\omega$ of the conductor in ohms per wire kilometer, is the product of l the linear wire inductance, and the impressed angular velocity ω . The linear wire reactance manifestly increases directly with the frequency f . It is just half the *linear loop reactance* l,ω ohms per loop km.

The *linear wire susceptance* $b = c\omega$ of the dielectric, in mhos

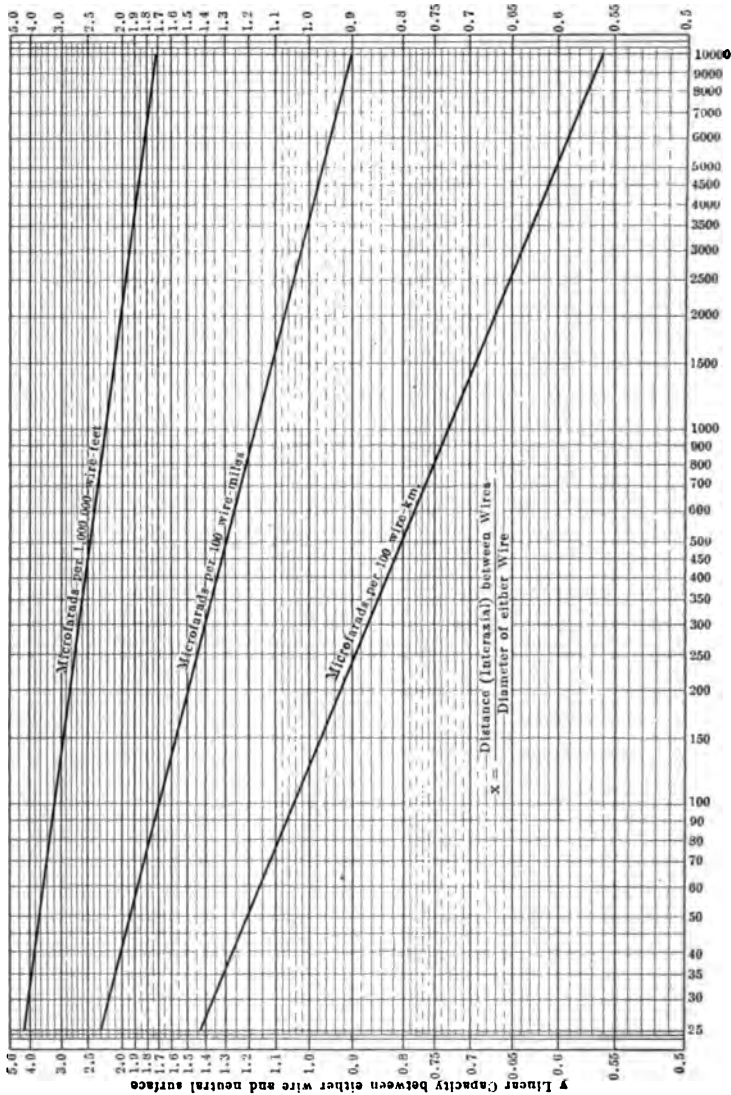


Fig. 85B.—Graphs of linear wire capacitances of bare, equal, parallel, round wires in air for interaxial distances from 25 to 10,000 diameters, in microfarads per 1,000,000 "wire-feet," per 100 "wire-miles" and per 100 "wire-kilometers;" $y = \cosh^{-1} x \mu f.$ per 1,000,000 wire-feet; $y = \cosh^{-1} x \mu f.$ per 100 wire-miles; $y = \cosh^{-1} x \mu f.$ per 100 wire-kilometers.

per wire kilometer, is the product of c the linear wire capacitance, and the impressed angular velocity ω . It also manifestly increases directly with the frequency of operation, and is just double the *linear loop susceptance* $b_{,,}$, mhos per loop km.

The *linear wire impedance* of a real a.c. line is

$$z = r + j l \omega = r + j x \quad \frac{\text{ohms}}{\text{wire km.}} \quad \angle \quad (337)$$

Here r , the real component of the plane vector z , is the linear wire resistance, and, at low frequencies, is the same as though the wire were operated by continuous currents, at the same temperature. At high frequencies, "skin effect," or non-uniform a.c. density, tends to increase r .

Skin-effect Formulas for Round Wires.—In the ordinary case of round wires of radius X cm. and electric conductivity γ abmhos per cm. (the reciprocal of the resistivity ρ in abohm-centimeters), operated at ω radians per sec., a fundamental formula for the internal linear impedance z' of the wire due to "skin effect," *i.e.*, to auto-disturbance of a.c. density over the cross-section, when not too close to neighboring active conductors, is*

$$z' = r \cdot \frac{\alpha_0 X}{2} \cdot \frac{J_0(\alpha_0 X)}{J_1(\alpha_0 X)} \quad \frac{\text{ohms}}{\text{wire km.}} \quad \angle \quad (338)$$

where

$$\alpha_0 = \sqrt{-j 4 \pi \gamma \mu \omega} = \sqrt{4 \pi \gamma \mu \omega} \angle 45^\circ = \sqrt{2 \pi \gamma \mu \omega} - j \sqrt{2 \pi \gamma \mu \omega} = \alpha_2 - j \alpha_2 \quad \text{cm}^{-1} \quad \angle \quad (339)$$

r is the ordinary linear resistance of the wire to continuous currents, in ohms per wire kilometer.

μ is the permeability of the substance of the wire assumed as uniform and as unity for non-magnetic substances.

$J_0(\alpha_0 X)$ is a plane-vector Bessel function of $\alpha_0 X$, of zero order † (numeric \angle).

$J_1(\alpha_0 X)$ is a plane-vector Bessel function of $\alpha_0 X$, of first order (numeric \angle).

The real component of z' is the apparent linear a.c. resistance of the wire, including skin effect, in ohms per wire kilometer.

* "Funktionentafeln mit Formeln und Kurven," by JAHNKE and EMDE, Teubner's, Berlin, 1909, pp. 142-144.

† These vector Bessel functions have been tabulated and charted over a convenient range. See "Experimental Researches on Skin Effect in Conductors," by KENNELLY, LAWS and PIERCE, *Proc. A. I. E. E.*, September, 1915.

The imaginary component of z' is the apparent linear internal reactance of the wire in j ohms per wire kilometer. The external reactance, due to magnetic flux encircling the whole wire, in the air or other external insulating material, is the same as though no skin effect existed, and does not appear in the formula.

At very low frequencies when ω approaches zero, the expression $\frac{\alpha_0 X}{2} \cdot \frac{J_0(\alpha_0 X)}{J_1(\alpha_0 X)}$ approaches $1.0\angle 0^\circ$. At very high frequencies, when α_0 becomes a large inverted semi-imaginary quantity, the limit of $\frac{\alpha_0 X}{2} \cdot \frac{J_0(\alpha_0 X)}{J_1(\alpha_0 X)}$ becomes:

$$\frac{\alpha_0 X}{2} \angle 45^\circ = \frac{\alpha_2 X}{2} + \frac{j\alpha_2 X}{2} = \frac{\alpha_2 X}{\sqrt{2}} \angle 45^\circ \quad \text{numeric } \angle \quad (340)$$

or the internal linear impedance of the wire at very high frequencies is large and semi-imaginary, especially when the radius X of the wire is large.

As an example, a No. 8 A.W.G. copper wire has a radius $X = 0.1632$ cm., a resistivity at 20°C. of $1,724$ abohm-cm. ($\gamma = 0.5801 \times 10^{-9}$), and a linear resistance at 20°C. of 2.061 ohms per wire km., required its internal linear impedance at $820 \sim = 5,152$ radians per sec.

Here $\alpha_0 X = \sqrt{12.566 \times 0.5801 \times 10^{-9} \times 5.152 \times 10^3} \angle 45^\circ \times 0.1632 = 1.0 \angle 45^\circ = 0.707 - j0.707$. Hence by Bessel Tables

$$\begin{aligned} z' &= 2.061 \times \frac{1.0 \angle 45^\circ}{2} \times \frac{1.0155 \angle 14^\circ.217}{0.5014 \angle 37^\circ.837} \\ &= 2.061 (1.01266 \angle 7^\circ.054) = 2.061 (1.0050 + j0.12436) = 2.0713 \\ &+ j0.2563 \frac{\text{ohms}}{\text{wire km.}} \end{aligned}$$

The virtual linear resistance has thus increased 0.5 per cent. by skin effect. The linear inductance is $0.2563/5,152 = 0.4976 \times 10^{-4}$ henry per wire km. = 0.4976 abhenry per wire cm., which is 0.48 per cent. below the normal value of 0.5 (see (329)).

When the value of $\alpha_2 X$ does not exceed unity, as in the above example, the change in internal reactance is so small that it may ordinarily be ignored, and an approximate formula for change of linear resistance, due in its original form to Lord Rayleigh,* may be used, ordinarily only as far as two terms:

$$r' = r \left\{ 1 + \frac{(\alpha_2 X)^4}{48} - \frac{(\alpha_2 X)^8}{2,880} + \dots \right\} \frac{\text{ohms}}{\text{wire km.}} \quad (341)$$

* LORD RAYLEIGH, *Phil. Mag.*, May and December, 1886.

Thus in the case above considered with $\alpha_2 X = 0.707$, this becomes

$$r' = 2.061 \left(1 + \frac{0.25}{48} - \dots \right) = 2.061(1 + 0.0052 - \dots) \quad \text{ohms per wire km.}$$

When $\alpha_2 X$ exceeds 2, the last formula (341) becomes unsuitable, and Russell's formula* may be employed, ordinarily only as far as two terms:

$$r' = r \left(\frac{\alpha_2 X}{2} + \frac{1}{4} + \frac{3}{32 \alpha_2 X} - \dots \right) \quad \frac{\text{ohms}}{\text{wire km.}} \quad (342)$$

Vector Linear Wire Impedance.—In all a.c. problems, the vector linear wire impedance z replaces the real linear wire resistance r of corresponding d.c. problems. Nevertheless, r may be retained in a.c. problems, if it is borne in mind that it has been changed from a real to a complex quantity. The linear wire impedance z of an a.c. loop circuit, is manifestly just half the linear loop impedance $z_{..}$ of the same.

The *linear wire admittance* of a real a.c. line is

$$y = g + jc\omega = g + jb \quad \frac{\text{mhos}}{\text{wire km.}} \quad \angle \quad (343)$$

Here g , the real component of the plane vector y , is the linear wire conductance, and is ordinarily greater than the corresponding leakage conductance of the same line when operated by continuous currents. It is, therefore, necessary to measure g in a.c. cases. The linear wire admittance y of a loop circuit, formed of two uniform parallel wires, is just double the *linear loop admittance* $y_{..}$ of the same circuit, in mhos per loop kilometer.

In all a.c. problems, the vector linear wire admittance y replaces the real linear wire conductance g of corresponding d.c. problems. Nevertheless, g may be retained in a.c. problems, if it is remembered that g has been changed from a real to a complex quantity.

The *linear hyperbolic angle* of a real a.c. line is the vector,

$$\alpha = \sqrt{zy} = \sqrt{(\bar{r} + jx)(g + jb)} = \alpha_1 + j\alpha_2 \quad \frac{\text{hyps.}}{\text{wire km.}} \quad \angle \quad (344)$$

The real and imaginary components and of this vector are:

* A. RUSSELL, *Phil. Mag.*, vol. xvii, p. 524, 1909.

$$\alpha_1 = \sqrt{\frac{1}{2}} \left\{ \sqrt{(r^2 + x^2)(g^2 + b^2) + (gr - bx)} \right. \\ \left. = \sqrt{\frac{1}{2}} \left\{ |\alpha^2| + (gr - bx) \right\} \right. \quad \frac{\text{hyps.}}{\text{wire km.}} \quad (345)$$

$$\alpha_2 = \sqrt{\frac{1}{2}} \left\{ \sqrt{(r^2 + x^2)(g^2 + b^2) - (gr - bx)} \right. \\ \left. = \sqrt{\frac{1}{2}} \left\{ |\alpha^2| - (gr - bx) \right\} \right. \quad \frac{\text{cir. radians}}{\text{wire km.}} \quad (346)$$

where $|\alpha^2|$ means the size of the plane vector α^2 defined by:

$$|\alpha^2| = \sqrt{(r^2 + x^2)(g^2 + b^2)} = |z| \cdot |y| \quad \text{numeric} \quad (347)$$

It is, however, ordinarily more convenient and expeditious to express z and y as polars, and then to find α as a polar; thus:

$$\alpha = \sqrt{|z| \angle \beta_1^\circ |y| \angle \beta_2^\circ} = \sqrt{|zy| \angle \frac{\beta_1^\circ + \beta_2^\circ}{2}} = \sqrt{|zy| \angle \beta^\circ} \\ \frac{\text{hyps.}}{\text{wire km.}} \angle \quad (348)$$

We may take, as an example to be worked out in each way, the case of a loop of "standard" telephone twisted-pair circuit, consisting of two No. 19 A.W.G. copper wires 0.0912 cm. in diameter, paper-insulated and lead-sheathed. The loop-mile constants of this circuit are taken as $r_{,,} = 88$ ohms /l.m., $l_{,,} = 10^{-3}$ h/l.m., $g_{,,} = 5 \times 10^{-6}$ mho/l.m., $c_{,,} = 0.054 \times 10^{-6}$ f/l.m. The corresponding wire kilometer values are $r = 27.34$, $l = 0.3107 \times 10^{-3}$, $g = 6.214 \times 10^{-6}$, $c = 0.6711 \times 10^{-7}$. At the standard telephonic angular velocity $\omega = 5,000$, ($f = 796\sim$), $x = 1.5535$ ohms per wire km., and $b = 335.5 \times 10^{-6}$ mho per wire km. Then by (345):

$$\alpha_1 = \sqrt{\frac{1}{2}} \left\{ \sqrt{(27.34^2 + 1.554^2)(6.214^2 + 335.5^2)10^{-12} +} \right. \\ \left. (6.214 \times 27.34 \times 10^{-6} - 1.5535 \times 335.5 \times 10^{-6}) \right\} \\ = \sqrt{\frac{1}{2}} \left\{ \sqrt{(747.476 + 2.413)(38.61 + 112,560.25)10^{-12} +} \right. \\ \left. (169.891 - 521.288)10^{-6} \right\} \\ = \sqrt{\frac{1}{2}} \left\{ \sqrt{(749.889)(112,598.9 \times 10^{-12}) - 351.397 \times 10^{-6}} \right\} \\ = \sqrt{\frac{1}{2}} \left\{ \sqrt{0.749889 \times 1.125989 \times 10^{-4} - 3.51397 \times 10^{-4}} \right\} \\ = \sqrt{\frac{1}{2}} \left\{ \sqrt{0.844365 \times 10^{-4} - 0.0351397 \times 10^{-2}} \right\} \\ = \sqrt{\frac{1}{2}} \left\{ 0.918893 \times 10^{-2} - 0.035140 \times 10^{-2} \right\} \\ = \sqrt{\frac{1}{2}} \left\{ 0.883753 \times 10^{-2} \right\} = \sqrt{0.441876 \times 10^{-2}} \\ = 0.66474 \times 10^{-1} = 0.066474$$

$$\begin{aligned} \alpha_2 &= \sqrt{\frac{1}{2} \{ (0.918893 \times 10^{-2} + 0.035140 \times 10^{-2}) \}} \\ &= \sqrt{\frac{1}{2} \{ 0.954033 \times 10^{-2} \}} \\ &= \sqrt{0.477017 \times 10^{-2}} = 0.69066 \times 10^{-1} = 0.069066 \\ \text{so that } \alpha &= 0.066474 + j0.069066 \quad \text{hyps. per wire km.} \\ &= 0.066474 + j0.043969 \quad \text{hyps. per wire km.} \end{aligned}$$

Using the polar method by (344) and (348), with (294) and (295)

$$\begin{aligned} \alpha &= \sqrt{(27.34 + j1.5535)(6.214 + j335.5)10^{-6}} \\ &= \sqrt{\left\{ 27.34 \sec \beta_1 \angle \tan^{-1} \frac{1.5535}{27.34} \right\}} \\ &\quad \left\{ 335.5 \operatorname{cosec} \beta_2 \angle \cot^{-1} \frac{6.214}{335.5} \right\} 10^{-6} \end{aligned}$$

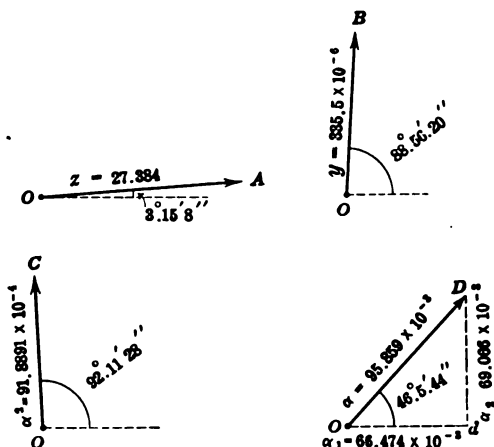


Fig. 86.—Polar development of linear hyperbolic angle.

$$\begin{aligned} &= \sqrt{\{(27.34 \sec 3^\circ.15'.08'') \angle 3^\circ.15'.08''\}} \\ &\quad \{(335.5 \times 10^{-6} \operatorname{cosec} 88^\circ.56'.20'') \angle 88^\circ.56'.20''\}} \\ &= \sqrt{27.384 \angle 3^\circ.15'.08'' \times 335.56 \times 10^{-6} \angle 88^\circ.56'.20''} \\ &= \sqrt{9,188.91 \times 10^{-6} \angle 92^\circ.11'.28''} = 95.859 \times 10^{-3} \angle 46^\circ.5'.44'' \\ &= 0.095859 \angle 46^\circ.5'.44'' \\ &= 0.066474 + j0.069066 \quad \text{hyps. per wire km.} \\ &= 0.066474 + j0.043969 \quad \text{hyps. per wire km.} \end{aligned}$$

The steps of the computation in the latter case are indicated geometrically in Fig. 86.

Alternating-current Attenuation Constant.—We have already seen in Chapter III, that the linear hyperbolic angle α of a c.c.

line measures the attenuation of either potential or current along a line of great length. In the a.c. case, the linear hyperbolic angle has a real component α_1 and an imaginary component α_2 . On an a.c. line of very great length; or of short length, but grounded at the motor end through an impedance equal to the surge impedance z_0 , the steady-state potential being taken as V volts \angle at any point on the line, the potential V_1 at a point 1 km. further along will be, by (21):

$$V_1 = V e^{-\alpha} = V e^{-(\alpha_1 + j\alpha_2)} = V e^{-\alpha_1} \cdot e^{-j\alpha_2} = V e^{-\alpha_1} \angle \alpha_2 \quad \text{volts } \angle \quad (349)$$

That is, the real part of α determines the attenuation in size, and the imaginary part the attenuation in slope, or phase, in unit length of the line. By (21) and (22) the same proposition applies to the normal attenuation of both potential and current.

The phase attenuation α_2 may here be considered as the decay of phase in V , expressed in circular radians per kilometer.

If we consider an a.c. generator applied to the home end of a line, the waves of potential and current flow down the line, each retaining its original phase; *i.e.*, a crest persisting as a crest, and a zero as a zero. But the generator is steadily impressing a new and advancing phase on the line; so that, with respect to the generator, the phases of the waves, as they advance, steadily fall behind that at the generator end. The greater the velocity of wave propagation, the less will be the loss of phase, or phase attenuation α_2 in any single kilometer of line; while, on the contrary, the less rapidly the waves advance, the greater will be the phase attenuation.

Wave Length.—The distance in which the phase attenuation amounts to 360° , or 2π circ. radians, will be one wave length, λ km. For this reason α_2 is sometimes called the “*wave-length constant*.” Consequently,

$$\lambda \alpha_2 = 2\pi \quad \text{radians} \quad (350)$$

$$\lambda = \frac{2\pi}{\alpha_2} = \frac{4}{\alpha_2} \cdot \pi \quad \text{km.} \quad (351)$$

where α_2 is the wave length constant in quadrant measure.

Apparent Velocity of Propagation.—Moreover, the number of waves per sec. emitted by the generator, or passing any point on the line, must be equal to the impressed frequency f in cycles per second; so that the distance through which any wave will advance

in 1 sec. must be $f\lambda$ km., or the *apparent velocity of propagation* v will be

$$\beta = \kappa f \qquad v = f\lambda = \frac{2\pi f}{\alpha_1} = \frac{\omega}{\alpha_1} = \frac{4f}{\alpha_1} \quad \frac{\text{km.}}{\text{sec.}} \quad (352)$$

In the case already considered, the normal attenuation will be approximately 0.06647 per unit, per km., or 6.647 per cent. per km.* The phase attenuation is 0.069066 circ. radian per km.,

or $3^\circ.48'.30''$ per km. The wave length λ is $\frac{6.2832}{0.069066} = 90.974$

km., and v , the apparent velocity of propagation, $\frac{5,000}{0.069066} = 72,395$ km. per sec.

The *actual velocity of propagation* of electric waves over circuit wires in air is accepted as equal to the velocity of light in air, or very closely 300,000 km. per sec. In a dielectric of permittivity κ , and permeability μ , the actual velocity is theoretically reduced in the ratio $1/\sqrt{\kappa\mu}$. The apparent velocity is less than the actual velocity, owing to the effects of attenuation; whereby the advancing waves disappear before reaching their final goal, thus diminishing their apparent speed. In the case of an overhead aerial line, with no losses, *i.e.*, with negligible linear conductor resistance r and dielectric conductance g , the linear hyperbolic angle would be

$$\alpha = \sqrt{j\bar{l}\omega \cdot j\bar{c}\omega} = j\omega \sqrt{cl} = j\alpha_1 \quad \frac{\text{hyp.}}{\text{km.}} \angle \quad (353)$$

or α would be all imaginary. The apparent velocity of propagation would then, by (352), be $v = 1/\sqrt{cl}$. If the wires had negligible internal inductance, and the insulators supporting the wires had negligible capacitance, the value of $1/\sqrt{cl}$ for such an aerial line would be 300,000 km. per sec. Internal inductance, and extra external capacitance tend to lower this slightly. Linear resistance and leakage lower it still more, especially at low frequencies. Solid dielectrics reduce it still further, and loading the line with coils in series, or leaks in shunt, may yet further lower it.

Special Cases of Linear Hyperbolic Angle.—We have already seen that in the particular case of a line with negligibly small r and

* $\epsilon^{-0.06647}$ is actually 0.93569, or 0.06431 per unit loss, and not 0.06647. This discrepancy is due to the fact that α_1 is here so large that the square and higher powers of α_1 are not negligible; see (20).

g , the linear hyperbolic angle α becomes a pure imaginary, with zero attenuation, or for an ideal *lossless line* $\alpha_1 = 0$.

In the case of negligible leakance g , and negligible inductance l , we have $x = 0$ and

$$\alpha = \sqrt{jrc\omega} = \sqrt{jrb} = \sqrt{rb} \angle 45^\circ \quad \begin{array}{l} \text{hyp.} \\ \text{km.} \end{array} \angle \quad (354)$$

and

$$\alpha_1 = \alpha_2 = \frac{|\alpha|}{\sqrt{2}} \quad \begin{array}{l} \text{radians} \\ \text{km.} \end{array} \quad (355)$$

Here α is a "semi-imaginary quantity," i.e., a complex quantity having equal real and imaginary components, or having an argument of 45° . This case corresponds very nearly to cabled lines operated at low frequencies.

In the case when r , x and b are definite, but g is negligibly small, $\beta_1 \cong 90^\circ$ and $\beta^\circ \cong \frac{\beta_1^\circ}{2} + 45^\circ$. This case corresponds very closely to well-insulated overhead aerial lines.

In the case when r , x and g are definite, but b is negligibly small, $\beta_1 \cong 0^\circ$ and $\beta^\circ \cong \frac{\beta_1^\circ}{2}$. This case corresponds very closely to an a.c. signal circuit comprising the two rails of a railroad track.

In the case where $\frac{l}{r} = \frac{c}{g}$; $\beta_1^\circ = \beta_2^\circ = \beta^\circ$, and we have Heaviside's distortionless circuit.*

When the linear inductance is very appreciable, as in ordinary aerial lines, the real attenuation constant α_1 may be approximately expressed as follows, especially at high frequencies,

$$\alpha_1 \cong \frac{r}{\sqrt{c}} \left(1 + \frac{gl}{cr}\right) = \frac{1}{2} \frac{r}{z_{00}} \left(1 + \frac{gl}{cr}\right) = \frac{1}{2} \left(\frac{r}{z_{00}} + gz_{00}\right) = \frac{1}{2} \left(\frac{r}{z_{00}} + \frac{g}{y_{00}}\right) \quad \begin{array}{l} \text{hyp.} \\ \text{km.} \end{array} \quad (356)$$

When the linear leakance g is negligible, this reduces to

$$\alpha_1 \cong \frac{r}{\sqrt{c}} = \frac{1}{2} \frac{r}{z_{00}} \quad \begin{array}{l} \text{hyp.} \\ \text{km.} \end{array} \quad (357)$$

* O. HEAVISIDE, "Reprinted Papers," 1892, vol. ii, p. 307 (*The Electrician*, 1887, 1888).

Linear Hyperbolic Angle as Affected by Unit of Length.—As already pointed out in relation to (19), the value of the linear hyperbolic angle is directly proportional to the unit of length selected. Thus, since 1 naut., or nautical mile, is 1.853 km., the value of α referred to r , l , g and c , in linear nautical measure, would be 85.3 per cent. greater than in linear kilometer measure. Thus, in the case considered,

$$\alpha_{km} = 0.095859 \angle 46^\circ.05'.44'' = 0.66474 + j0.069066 \text{ hyp. per km.}$$

This becomes, proportionately,

$$\alpha_{nt} = 0.1776 \angle 46^\circ.05'.44'' = 0.1232 + j0.1280 \text{ hyp. per naut.}$$

Linear Hyperbolic Angle as Affected by Single-wire or Two-wire Lines.—We have already seen that the value of α is the same whether we form it from loop-kilometer or wire-kilometer linear constants. With respect to wire-linear values, the loop-linear values of conductor impedance (r and jx) will be doubled; while those of dielectric admittance (g and jb) will be halved. It is, therefore, entirely optional whether we enter (344) or (345) with *loop* or *wire-linear constants*, provided we keep entirely to one or the other plan. The values of α and of θ will in either case be the same. Telephone engineers ordinarily use loop-linear values. Telegraph and power-transmission engineers ordinarily use wire-linear values. For simplicity and uniformity, we shall use wire-linear values throughout.

Hyperbolic Angle Subtended by an Alternating-current Line.—Since, by (18), $L\alpha = \theta$, it follows that the hyperbolic angle θ subtended by an a.c. line is:

$$\theta = L\alpha = L(\alpha_1 + j\alpha_2) = L\alpha_1 + jL\alpha_2 = \theta_1 + j\theta_2 \text{ hyps. } \angle \quad (358)$$

This angle consists of a real or hyperbolic component θ_1 , and an imaginary or circular component θ_2 . The former measures the normal attenuation of potential or of current over the line, and the latter the attenuation of phase.

Another expression for θ following (18), is

$$\theta = L \sqrt{z.y} = \sqrt{Z.Y} = \sqrt{(R + jX)(G + jB)} \text{ hyps. } \angle \quad (359)$$

In the case of a “*reactanceless track circuit*,” *i.e.*, a railway-track signal circuit, with negligible rail reactance by comparison with the rail resistance, and with negligible track susceptance by comparison with the track leakance ($X = 0$, $B = 0$), θ is a pure real, or a real hyperbolic angle. This corresponds also to the d.c. case.

In the ideal case of a "lossless line" ($R = 0, G = 0$), θ is a pure imaginary, or corresponds to a circular angle. High-frequency, large, well-insulated aerial lines approximate to this case.

In the case of a "pure cable" ($X = 0, G = 0$), θ is a semi-imaginary quantity at all frequencies.

As an example, we may consider 50 km. of the paper and air insulated twin-wire standard telephone cabled conductor, the linear hyperbolic angle of which we have already seen to be, at $\omega = 5,000$, $\alpha = 0.095859 \angle 46^\circ.05'.44'' = 0.066474 + j0.069066$ hyp. per km. Here $\theta = 50\alpha = 4.79295 \angle 46^\circ.05'.44'' = 3.3237 + j3.4533$ hyps. This means that with normal attenuation, both the potential and the current would attenuate in 50 km. to $\epsilon^{-3.3237} \times \epsilon^{-j3.4533} = 0.0394 \angle 3.4533$ radians $= 0.0394 \angle 197^\circ.51'.34''$. *Normal attenuation is the exponential attenuation which occurs on either an indefinitely long line, or on a line of moderate length, rendered equivalent in behavior to part of an infinite line, by being grounded at the far end through an impedance equal to its surge impedance z_0 .*

Normal Attenuation Factor.—As already explained in connection with (23) and (24), a line of θ hyps. developing normal attenuation, has an attenuation factor, for both potential and current, of

$$\begin{aligned} \epsilon^{-\theta} &= \epsilon^{-\theta_1} \angle \theta_2 \text{ cir. radians} = \epsilon^{-\theta_1} \angle \theta_2 \cdot \frac{180}{\pi} \text{ degrees} \\ &= \epsilon^{-\theta_1} \angle \theta_2 \cdot \frac{2}{\pi} \text{ quadrants numeric } \angle \quad (360) \end{aligned}$$

In cases of *non-normal attenuation*, such as ordinarily present themselves in practice, the attenuation factor is the ratio of a pair of hyperbolic functions.

Distance in Which the Normal Attenuation Factor Attains Specified Values.—If we desire to know the distance $L_{1/n}$ in which the magnitude or vector size either of potential or current will fall to $1/n$ th of its initial value, we have

$$\epsilon^{-\theta_1} = n^{-1} \quad \text{numeric} \quad (361)$$

$$\text{or} \quad \theta_1 = \text{logh } n \quad \text{hyp.} \quad (362)$$

Thus to fall to $1/2$, θ_1 must be $\text{logh } 2 = 0.69315$; so that $L_{1/2} \alpha_1 = 0.69315$, or $L_{1/2} = \frac{0.69315}{\alpha_1}$. Again, to fall to $1/\epsilon$, or to 0.3679,

$\theta_1 = 1$ and

$$L_{1/\epsilon} = \frac{1}{\alpha_1} \quad \text{km.} \quad (363)$$

In the case already considered, where $\alpha_1 = 0.066474$, the potential and current will normally fall to one-epsilon in a distance of $L_{1/\epsilon} = 1/0.066474 = 15.04$ km., and will fall to one-half in a distance of $L_{1/2} = 0.69315/0.066474 = 10.4$ km.

Similarly, if we desire to know the distance in which the phase of either potential or current will normally fall or lag 1 radian with respect to the phase at the line point considered,

$$L_\beta = \frac{1}{\alpha_2} \quad \text{km.} \quad (364)$$

Thus in the case considered, where $\alpha_2 = 0.069066$, the distance of normally attenuating 1 circ. radian in phase would be $1/0.069066 = 14.48$ km. The distance for 1° would be 57.296 times shorter or $14.48/57.296 = 0.2527$ km. The distance for losing 30° would be 7.581 km.

Polar Graph of Normal Attenuation on an Alternating-current Line.—*The polar graph of normal attenuation on any a.c. line is an inward equiangular spiral, in which the circular angle between the tangent and the radius-vector is β° , the slope of α .*

An equiangular spiral may be expressed by the formula*

$$\rho = a^\gamma = ce^{\gamma \cot \beta^\circ} \quad \text{vector size} \quad (365)$$

where ρ is the size and γ the slope of the radius-vector in circular radians. Here a and c are constants, and β° is the circular angle of the spiral.

When the real attenuation component α_1 is small by comparison with the imaginary component α_2 , the circular angle approaches 90° or $\pi/2$ radians. In such a case, the tangent of the "normal attenuation spiral" is nearly perpendicular to the radius-vector, and the spiral departs but little from a pure circle, making many revolutions before collapsing. On the contrary, when α_1 is large with respect to α_2 , as in the case of heavy attenuation, the tangent is nearly coincident with the radius-vector, and the spiral approaches a straight line directed toward the origin.

The normal attenuation spiral for the standard telephone cable, at $\omega = 5,000$, above considered, is shown in Fig. 87, at *ABCDEFGF*. The initial radius-vector $OA = 1$, represents the value of either voltage or current at a given point on the line, say the generator end. The tangent *AT* makes with this radius-vector the circular

* GREENHILL'S "Differential and Integral Calculus," Macmillan & Company, 1896, p. 55.

angle $OAT = \beta^\circ = 46^\circ.5'.44''$, and this property holds for any and all points on the curve. The successive points* B, C, D, E, F, G , have been chosen as marking off successive, equal circular angles at O , in this case 30° .

Such equal angles subtend, in all normal attenuation cases, equal lengths of the line. In this case, 30° corresponds to 7.581 km. Each of these successive radii-vectores OB, OC, OD , etc., is 60.41

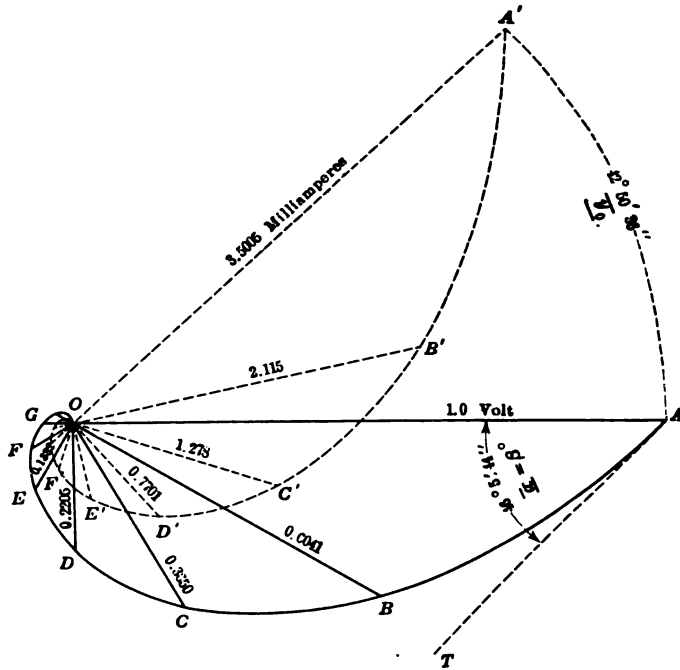


FIG. 87.—Normal attenuation spirals of potential and current.

per cent. of the length of its predecessor, or has attenuated in size 39.59 per cent. in the preceding 30° . The polar equation (365) of this particular spiral is $\rho_e = 1.0e^{-\gamma \cot 46^\circ.5'.44''} = 1.0e^{-0.96247\gamma}$.

It will be observed that at OG , 45.487 km. from A , the potential is oppositely directed to, or 180° in phase from, the initial value OA . In this half-revolution, the remnant is reduced to 0.0486 of the original, and in one complete revolution, or 90.973 km., the remnant would be $(0.0486)^2 = 0.002364$ of the original,

* C. V. DRYSDALE, "The Theory of Alternate-current Transmission in Cables," *The Electrician*, December, 1907 and January, 1908.

an insignificantly small amount. In the case, however, of a well-insulated power-transmission line, β might readily attain 88° , and the normal attenuation of potential or current may be less than 20 per cent. in one complete revolution. In such a case, the direction of the current may be reversed many times, over a long line, without falling to insensible magnitudes. *The higher the frequency, the more numerous and closer these reversals are likely to be along the line, and the more numerous the spiral convolutions in the normal attenuation graph.*

Graphical Relation between Potential and Current Spirals.— If we express the normal attenuation of potential along any actual line by the formula:

$$V_x = V_A e^{-\alpha x} \quad \text{volts } \angle \quad (366)$$

where x is the distance in kilometers from the point where the potential is V_A volts, it follows that

$$\frac{dV_x}{dx} = -\alpha V_A e^{-\alpha x} = -\alpha V \quad \begin{matrix} \text{volts} \\ \text{km.} \end{matrix} \angle \quad (367)$$

or the rate of change of potential is $-\alpha$ times the potential itself. But the normal attenuation graph is an inward equiangular spiral; so that the rate of change of potential along the line is also an equiangular spiral, multiplied by the vector α ; *that is the negative differential of the potential spiral is the same spiral altered in scale by the size of α , and changed in phase by the slope β° of α , in this case $46^\circ.5'.44''$. This differential spiral would start from a line near OF , drawn parallel to AT , and its radii-vectores would lag $133^\circ.54'.16''$ behind those of the potential A, B, C, D, E .*

We know from the fundamental theory discussed in Chapter IV, in relation to (38), that:

$$\frac{dV_x}{dx} = -\alpha V_x = -Iz = -I(r + j l \omega) \quad \begin{matrix} \text{volts} \\ \text{km.} \end{matrix} \angle \quad (368)$$

or

$$I = -\frac{1}{z} \cdot \frac{dV_x}{dx} \quad \text{amp. } \angle \quad (369)$$

This means that if we operate upon the differential spiral by $-1/z$, we shall obtain the graph of the current. Consequently, *the graph of a normally attenuating current is also an equiangular spiral, to an altered scale, and advanced $\beta^\circ - \beta_1^\circ = \underline{\gamma}_2$ beyond the potential spiral.* In this case $A'B'C'D'$, Fig. 87, is the current spiral to a scale of milliamperes, advanced $46^\circ.5'.44'' - 3^\circ.15'.08''$

= $42^{\circ}.50'.36''$ beyond $ABCD$. The initial current at OA' is numerically equal to y_0 , and the current spiral may be regarded as the potential spiral after being operated upon by the plane vector y_0 .

Again, following (43), if we differentiate the potential spiral twice, we obtain the same spiral operated upon by the plane vector α^2 ; *i.e.*, altered in scale by α^2 and advanced in phase by $\alpha^2 = 2\beta^{\circ}$.

In the case of a distortionless circuit, in which z_0 and y_0 are real quantities, or $\beta^{\circ} = 0$, the normal attenuation spirals of V and I have the same direction in the plane of reference, so that one and the same spiral will serve for both with a suitable change in dimensional scale.

Similarity of Sectors in a Normal Attenuation Spiral.—If a normal attenuation spiral of potential or current is subdivided into sectors subtending equal circular angles at the origin, like AOB , BOC , COD , etc., Fig. 87, it is evident from the laws of the equiangular spiral, that these sectors are similar; that is $OA : OB :: OB : OC$, and if we draw chords AB , BC , CD , etc., we shall also have $OA : OB :: AB : BC$. These successive chords, being equally dephased by the sectorial angle, may be also represented in a similar equiangular spiral.

Alternating-current Surge Impedance.—In accordance with (26), which must be now interpreted vectorially, the surge impedance z_0 for a.c. lines is

$$\begin{aligned} z_0 &= \sqrt{\frac{Z}{Y}} = \sqrt{\frac{R+jX}{G+jB}} = \sqrt{\frac{z}{y}} = \sqrt{\frac{r+jx}{g+jb}} \\ &= \sqrt{\frac{|z| \angle \beta_1^{\circ}}{|y| \angle \beta_2^{\circ}}} = \sqrt{\frac{|z|}{|y|} \frac{\beta_1^{\circ} - \beta_2^{\circ}}{2}} \quad \text{ohms } \angle \quad (370) \end{aligned}$$

In the standard telephone cable case already considered, we have

$$\begin{aligned} z_0 &= \sqrt{\frac{27.34 + j1.5535}{(6.214 + j335.5)10^{-6}}} = 10^3 \sqrt{\frac{27.384 \angle 3^{\circ}.15'.08''}{335.56 \angle 88^{\circ}.56'.20''}} \\ &= 285.67 \angle 42^{\circ}.50'.36'' \text{ ohms.} \end{aligned}$$

An indefinitely long line of this type would therefore offer this impedance, for $\omega = 5,000$, at and beyond any point. In this case, because β_2° is so much larger than β_1° , the surge impedance is nearly a semi-imaginary quantity. It behaves like a condenser in series with a resistance. If, on the contrary, $\beta_1^{\circ} > \beta_2^{\circ}$, the slope of

z_0 would be positive, and the surge impedance would be an inductive instead of a condensive impedance.

A long line whose surge impedance is inductive calls for expenditure of $+j$ reactive power, as well as of active power from a traversing electric wave; while a line whose surge impedance is condensive, calls for the expenditure of $-j$ reactive power, as well as of active power, from such waves. A line whose surge impedance is reactanceless, absorbs only active power in transit, without reactive, *i.e.*, stored or transformed, power. Reactively absorbed power involves subsequent release, with corresponding after-effects, or disturbance. Actively absorbed power, *i.e.*, dissipated power, involves no subsequent reaction or disturbance.

It is for this reason that the Heaviside distortionless circuit has at all frequencies a reactanceless z_0 . That is since $x/r = b/g$, $\beta_1^\circ = \beta_2^\circ$ at all frequencies, and $\beta^\circ = 0$.

Loop Surge Impedances.—We have already seen (32), that the surge impedance of a loop line is just double the surge impedance of a wire line. Thus, in the telephone case considered, if we take the linear constants $r_{,,}$, $l_{,,}$, $g_{,,}$ and $c_{,,}$, on the loop-kilometer basis instead of on the wire-kilometer basis, the use of (370) would yield $z_{0,,} = 571.34 \sphericalangle 42^\circ.50'.36''$ ohms instead of $285.67 \sphericalangle 42^\circ.50'.36''$.

At high frequencies, since x and b tend to become large with respect to r and g , the surge impedance tends to the reactanceless value:

$$z_{00} = \sqrt{\frac{l}{c}} = \sqrt{\frac{L}{C}} \quad \text{ohms} \quad (371)$$

Initial Current at Sending End.—When an indefinitely long idle line is suddenly switched upon a single-frequency a.c. generator, there will immediately be an outgoing a.c. wave projected over the line. In general, this consists of two parts, namely: (1) the “*normal wave*,” such as will be delivered to the line in the final steady state; and (2) a “*transient wave*,” which rapidly decays exponentially with time, and, in the course of a few cycles, practically disappears. This transient wave may be called, for convenience, a “*splash*.” The splash will be greatest if the line switch is closed at or near a voltage crest of the generator. It will be least, if closed at or near a zero point of current and voltage. We may assume that by choosing the proper instant for closing the line switch, the splash may be ignored. In that case, if V_A be the vector r.m.s. potential of the generator at standard

phase, the initial outgoing current will be a sinusoidal function of time, whose r.m.s. value will be

$$I_A = \frac{V_A}{z_0} = V_A y_0 \quad \text{amp. } \angle \quad (372)$$

Similarly, at any point along the line, the r.m.s. current will be at the outset, and at all subsequent times, equal to the r.m.s. local potential divided by the surge impedance. This means that the potential and current waves advance steadily along the line with their amplitudes in fixed ratio, and their phases displaced by the angle y_0 .

In the case of a finite line grounded at the far end through z_0 ohms \angle , or shorted in the double-wire case through $z_0' = 2z_0$ ohms \angle , the condition is the same. Ignoring splash, the initial values of outgoing r.m.s. potential and current remain the final values, because the condition is one of normal attenuation, with no reflected waves returning from the distant end. In the case, however, of a finite line grounded at the far end through an impedance other than z_0 , there will be waves reflected from that end, which, running to and fro over the line, will superpose themselves upon the outgoing normal waves. In the final steady state, the outgoing current will settle down to the value (see (129))

$$I_A = \frac{V_A}{z_0 \tanh \delta_A} = V_A \cdot y_0 \coth \delta_A \quad \text{amp. } \angle \quad (373)$$

and at any point P along the line

$$I_P = \frac{V_P}{z_0 \tanh \delta_P} = V_P \cdot y_0 \coth \delta_P \quad \text{amp. } \angle \quad (374)$$

Here the vector factor $\tanh \delta_P$ takes into account all of the superposed reflected waves which enter into the final steady stream,* after theoretically infinite time; but, ordinarily, for practical purposes in the course of a few cycles. *This factor $\tanh \delta_P$ therefore converts the initial line impedance into the final line impedance at P .*

Alternating-current Surge Admittance.—The surge admittance y_0 of a wire line is the reciprocal of the surge impedance. The size of y_0 is therefore the reciprocal of the size of z_0 , and the slope of y_0 is the negative of the slope of z_0 . Thus, in the case consid-

* The process of summation of successive waves is discussed in Chapter VI of "The Application of Hyperbolic Functions to Electrical Engineering Problems" and need not be repeated here.

ered, $y_0 = 1/(285.67 \sphericalangle 42^\circ.50'.36'') = 3.5005 \times 10^{-3} \sphericalangle 42^\circ.50'.36''$ mho.

The surge admittance of a loop line is manifestly one-half that of either of its component wire lines.

The surge admittance at high frequencies evidently tends to the limiting and reactanceless value

$$y_{00} = \sqrt{\frac{c}{l}} = \sqrt{\frac{C}{L}} \quad \text{mhos} \quad (375)$$

General Relations of Potential, Current, Impedance and Admittance with the Position Angle in Alternating-current Circuits.—The fundamental formulas for single-frequency a.c. circuits in the steady state are (99), (111), (123), (124) and (138), already considered in connection with c.c. lines. They are here collected for convenience of comparison.*

$$\frac{V_P}{V_C} = \frac{\sinh \delta_P}{\sinh \delta_C} \quad \text{numeric } \sphericalangle \quad (376)$$

$$\frac{I_P}{I_C} = \frac{\cosh \delta_P}{\cosh \delta_C} \quad \text{numeric } \sphericalangle \quad (377)$$

$$\frac{Z_P}{Z_C} = \frac{\tanh \delta_P}{\tanh \delta_C} \quad \text{numeric } \sphericalangle \quad (378)$$

$$\frac{Y_P}{Y_C} = \frac{\coth \delta_P}{\coth \delta_C} \quad \text{numeric } \sphericalangle \quad (379)$$

$$\frac{P_P}{P_C} = \frac{\sinh 2\delta_P}{\sinh 2\delta_C} \quad \text{numeric } \sphericalangle \quad (380)$$

That is, the potential, current, impedance, admittance and volt-amperes at any point P, bear to the corresponding known quantities at some given point C, a simple ratio of sines, cosines, tangents and cotangents of the position angles of P and C.

* A reader interested in seeing the contrast between these formulas and those which have been developed by competent mathematicians, not using hyperbolic functions, may consult the following references.

O. HEAVISIDE, "Reprinted Electrical Papers," London, 1892, vol. ii, p. 247.

M. LEBLANC, "Formula for Calculating the Electromotive Force at any Point of a Transmission Line for Alternating Current, *Trans. A. I. E. E.*, vol. xix, pp. 759-768, June, 1901.

P. H. THOMAS, "Calculation of the High-tension Line," *Trans. A. I. E. E.*, part I, vol. xxviii, pp. 641-686, June 1909.

CHAPTER XI

FUNDAMENTAL PROPERTIES OF ALTERNATING-CURRENT ARTIFICIAL LINES

A.C. artificial lines are composed of uniform sections, either T 's or Π 's. The series elements of these sections ordinarily contain resistance and reactance, and the shunt elements, or leaks, conductance and susceptance.

There are two fundamental problems which frequently present themselves in discussing the relations between real and artificial a.c. lines. The first is to find the elements of a T or Π section which shall make the section correspond to an assigned length of real line at an assigned frequency. The second is, knowing the impedance and admittance element of an artificial line section, at a given frequency, to find the line angle and surge impedance of the section at that frequency. We shall consider these two problems in the above order.

To Find the Elements of a T or Π Which Shall Form a Section Equivalent to a Given Length of Real Line at a Given Frequency. The procedure is the same as in the d.c. case already considered in Chapters VI and VII, but with the formulas interpreted vectorially. That is, we find the angle θ subtended by the given length of real line, at the assigned frequency, and also its surge impedance z_0 . The conductor impedance of the real section is therefore $Z = \theta z_0$ ohms, and the dielectric admittance is $Y = \theta/z_0 = \theta y_0$. We then map out the nominal T and Π containing these quantities. We next find* the correcting factors $\frac{\sinh \theta}{\theta}$ and $\frac{\tanh (\theta/2)}{\theta/2}$, which, applied to the elements of the nominal sections, gives the corrected elements of the equivalent sections.

As an example, we may consider a length of 7.581 km. (4.71 miles) of the telephone line already employed, at the angular fre-

* Tables of these correcting factors have already been published within certain limits of θ , in the author's "Tables of Complex Hyperbolic and Circular Functions;" but in cases where it is desired to work out these correcting factors, a good plan is to find $\sinh (\theta/2)$ and also $\cosh (\theta/2)$ as polars. Twice their product is then $\sinh \theta$, and their ratio is $\tanh (\theta/2)$. These expressed as polars are then divided by θ and $\theta/2$, respectively.

quency of $\omega = 5,000$. We have already seen that, at this frequency, 7.581 km. subtend a circular angle of 30° , and have a total angle $\theta = 0.726726 \angle 46^\circ.05'.44''$ hyp. $= 0.50394 + j0.52360 = 0.50394 + j0.3$. The surge impedance z_0 is $285.67 \angle 42^\circ.50'.36''$ ohms. The conductor impedance of this length is therefore $0.726726 \angle 46^\circ.05'.44'' \times 285.67 \angle 42^\circ.50'.36'' = 207.602 \angle 3^\circ.15'.8''$ ohms. The dielectric admittance is $0.726726 \angle 46^\circ.5'.44'' / 285.67 \angle 42^\circ.50'.36'' = 2.5439 \times 10^{-3} \angle 88^\circ.56'.20''$ mho. We

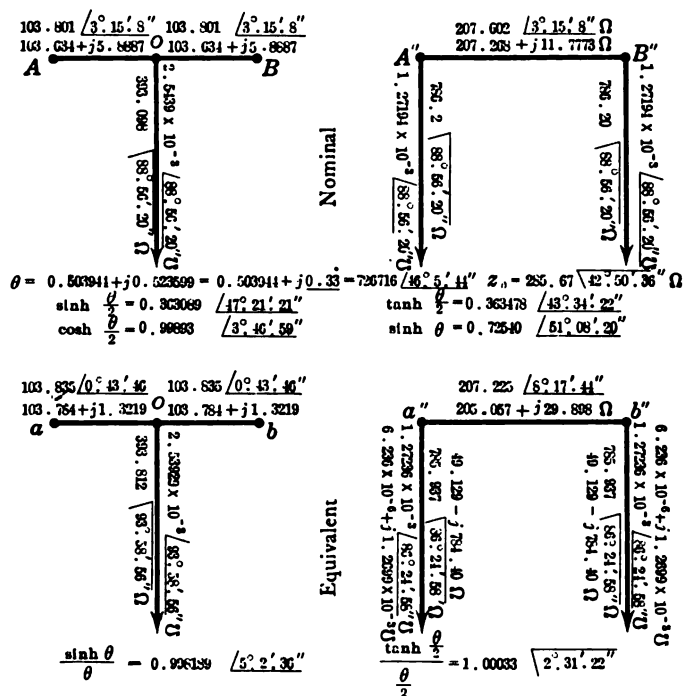


FIG. 88.—Nominal and equivalent T and II artificial-line sections.

draw the nominal T and II containing these values, as shown at AOB, and A''B'', Fig. 88. We now find the correcting factors

$$\sinh (0.726726 \angle 46^\circ.5'.44'') \quad \text{and} \quad \tanh (0.363363 \angle 46^\circ.5'.44'')$$

$$0.726726 \angle 46^\circ.5'.44'' \quad \text{and} \quad 0.363363 \angle 46^\circ.5'.44''$$

to the required degree of precision, from charts, tables, or calculation. They are as shown in Fig. 88, $0.998189 \angle 5^\circ.2'.36''$, and $1.00033 \angle 2^\circ.31'.22''$, respectively. These are the lumpiness corrections. For many practical purposes, these correcting

factors are so near to $1.0\angle 0^\circ$ as to be negligible. In other words, up to the frequency $\omega = 5,000$, the nominal sections of artificial-line T 's or Π 's may be regarded as substantially the same as the equivalent sections up to line lengths of 7.58 km. (4.7 statute miles). The equivalent sections are indicated at aob and $a''b''$. Fig. 88.

I and O Sections of Double-wire Artificial Line.—If we desired two-wire artificial-line sections, we should connect a pair of equivalent T 's, or a pair of equivalent Π 's by their feet, to form what may be called an equivalent I and an equivalent O section,

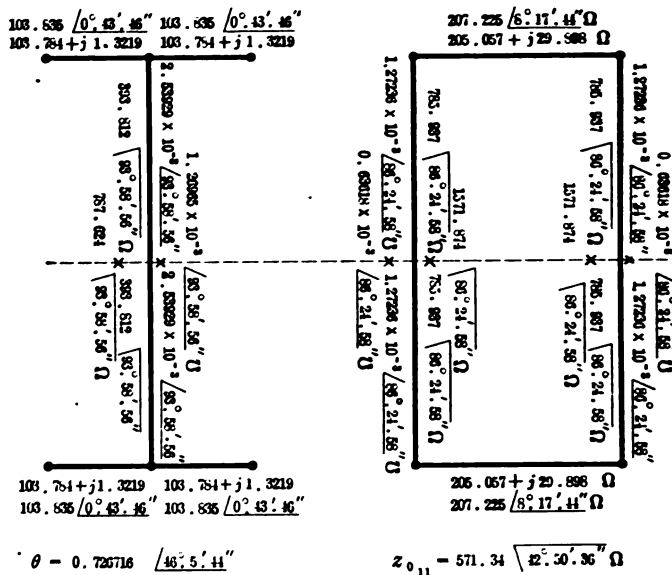


FIG. 89.—Double-wire I and O artificial-line sections.

respectively, as in Fig. 89. The angle subtended by an equivalent I or O is identical with that subtended by the corresponding equivalent T or Π . The surge impedance of the I or O is, as we have already seen, just double the surge impedance of the T or Π respectively.

If we connect in series a number of such equivalent T 's or Π 's, we obtain a corresponding length of artificial T or Π line, as in Fig. 90, which shows the distribution of current and voltage over the first four sections of such a pair of lines. Each line is supposed to have been rendered virtually infinite, by grounding, after any

desired number of sections, through an impedance of $285.67 \angle 42^\circ.50'.36''$ ohms. An impressed a.c. potential of 1.0 r.m.s. volt is applied at A , the generating end, at a frequency of $f = 796\sim$, or $\omega = 5,000$.

Unrealizable Artificial-line Sections.—It will be noticed in Figs. 88 and 89, that there should be no difficulty in constructing and adjusting the elements of the equivalent Π or O . The architrave should have an inductance of $29.898/5,000 = 5.9796 \times 10^{-3}$ henry, with resistance added up to 205.06 ohms, preferably of insulated manganin wire. The Π leaks should have $1,272.36/5,000 = 0.254 \mu f$ capacitance, at the impressed frequency, with an associated leakance of 6.326 micromhos. By taking sufficient pains, these values could be adjusted to within desirable limits of precision. In the case, however, of the equivalent T and I , there would be no way of obtaining, without the aid either of inductive devices or of parallel branches, the required staff elements, by simple series connection of resistance and capacitance, because the slopes of the T leaks exceed 90° . In the case of this length of real line section, and for this assigned frequency, the equivalent T sections would have arithmetical significance only, and would not be physically realizable, in the laboratory, by ordinary simple means. At other frequencies, and with other lengths of real-line section, we might find both T and Π realizable. It sometimes happens that neither the T nor the Π is realizable. In such cases, another length of real-line section should be selected for imitation.

Graphs of Normal Attenuation on Alternating-current Artificial Lines.—If we plot the values of potential and current over the virtually infinite artificial lines of Fig. 90, by comparison with the corresponding values over the conjugate smooth line, as in Fig. 87, we are led to the constructions of Fig. 91, where $ABCD$ is the potential spiral, $A'B'C'D'$ the current spiral, and the constant phase difference between these two spirals is left out of consideration, in order to facilitate inspection. Turning to the potential spiral, Fig. 91, OA being the impressed unit r.m.s. potential at A , to standard phase, then the curve $ABCDEFGF$ represents the fall of potential along the conjugate smooth line, as in Fig. 87. The potential drops in the line elements of the Π line are indicated, both in magnitude and phase, by the interior straight lines, or chords, AB, BC, CD , etc. Similarly, the potential drops in the line elements of the T line are indicated, both in

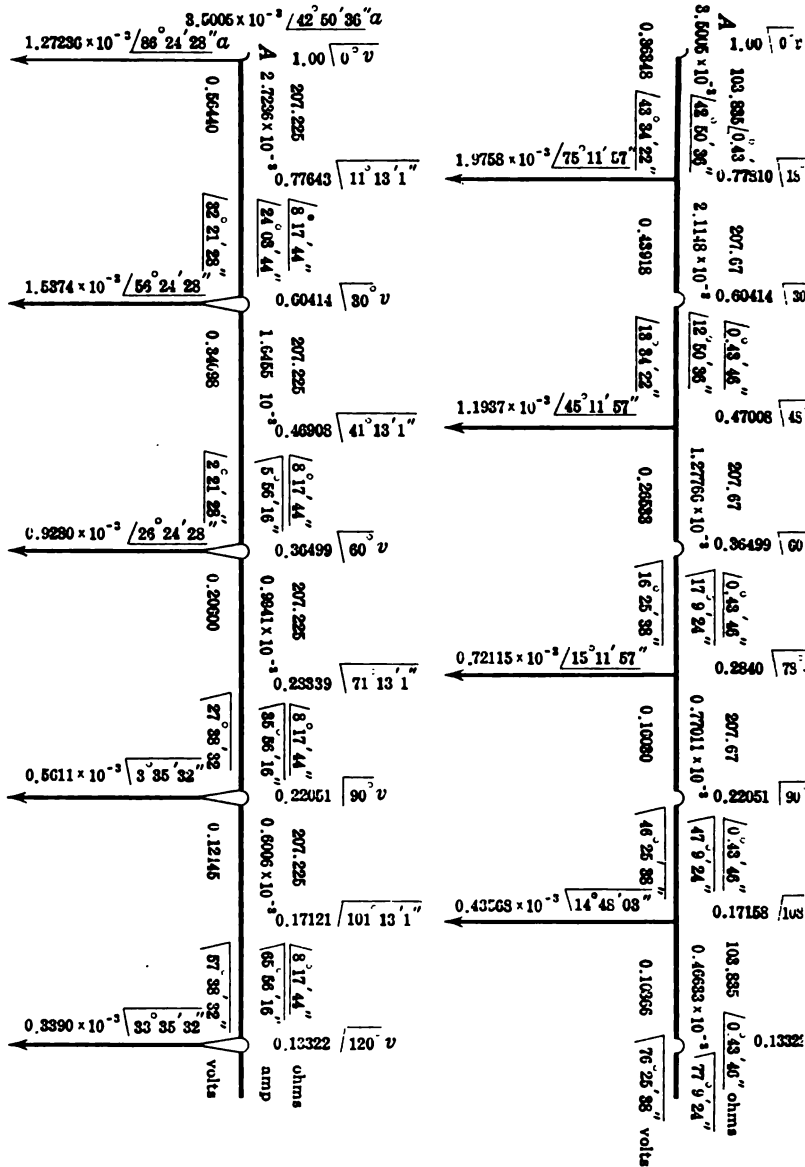


FIG. 90.—Normal attenuation over artificial T and Pi lines.

magnitude and phase, by the exterior straight lines Ak , kBl , lCm , etc. At the junctions the potentials are the same, on both the artificial lines, as well as on the real conjugate line. The T -line normal-attenuation potential thus falls on an external contacting equiangular-spiral polygon, and the Π -line potential falls on an internal contacting polygon, the points of contact representing the terminals and junction points of the sections. To construct these polygons, first draw the equiangular spiral $ABCD$ for the conjugate smooth line or real line. Mark off a mid-section point such as i , where

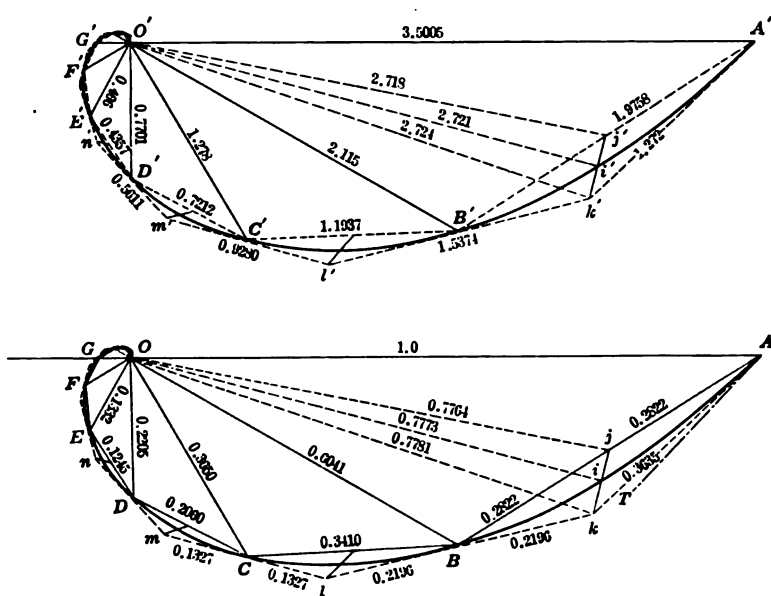


FIG. 91.—Normal attenuation graphs on a real line and on its conjugate artificial T and Π lines.

the radius-vector Oi bisects the circular section angle AOB . Operate on the vector Oi by $\cosh v$; *i.e.*, $\cosh (\theta/2)$, and $\operatorname{sech} v$, or $\operatorname{sech} (\theta/2)$, so as to produce the vectors Oj and Ok respectively. In the case of Fig. 91, $\cosh (\theta/2) = 0.99893 \sphericalangle 3^{\circ}.46'.59''$, and $\operatorname{sech} (\theta/2) = 1.00107 \sphericalangle 3^{\circ}.46'.59''$. The point j will bisect AB . Join Ak and Bk , which will be the vector drops in the arms of the T section, to scale and phase. Moreover, kB will be equal to and in line with lB .

Turning now to the current graph $A'B'C'D'$, Fig. 91, the curve is the normal attenuation spiral of the conjugate smooth line to

initial current standard phase. At junction points $B'C'D'$, the line currents are in coincidence with each other, and with the contacting equiangular spiral. If we operate on the mid-section vector such as Oi' by $\cosh(\theta/2)$ and $\operatorname{sech}(\theta/2)$, as before, we obtain the vectors Oj' and Ok' , the former bisects $A'B'$, and represents the vector arithmetical mean of the line currents $3.5005\angle 0^\circ$ and $2.1148\angle 30^\circ$, in the two branches of the first T section. The latter, Ok' represents the current at the middle of the first Π section, *i.e.*, the current in the architrave of that section. Thus the Π -line normal-attenuation current falls on an external contacting equiangular spiral polygon, and the T -line current falls on an internal contacting polygon, the points of contact representing the terminals and junction points of the lines. The successive sides of these current polygons represent the magnitudes and phases of the leak currents. Each polygonal side may be regarded as equivalent to the vector sum of all the infinitesimal leaks in the subtended smooth section. It will be understood that at any Π -line junction, the true line current requires replacing the single leak at that junction by a pair of parallel half-leaks, and placing the ammeter in the line between them, as in Fig. 41. Otherwise the true line current will be only arithmetically realizable, as the vector arithmetical mean of the two line currents on each side of the junction. Thus, at the end of the first Π -line section, the true line current would be to voltage standard phase

$$\frac{0.56440\angle 32^\circ.21'.28'' + 0.34098\angle 2^\circ.21'.28''}{2} = 2.1148\angle 12^\circ.50'.36''$$

milliamp.

In regard to potential and current, therefore, the T and Π lines are mutually reciprocal. The Π line always follows, for potentials, the inside polygon, and, for currents, the outside polygon. This is true not only in the equiangular spiral graphs, controlling normal attenuations; but also in the hyperbolic-function graphs, which, as we shall see, control in the general case, and of which the equiangular spiral is but a limiting instance.

Deduction of Section Elements from Their Measured Values of θ and z_0 .—Another form in which the preceding problem may present itself, is that where measurements of an artificial line, at a given frequency, in the manner described in the next chapter, and based on formulas (273) and (275), lead to correspondingly deduced values of the section angle θ and surge impedance z_0 . The problem then is to find the elements of the section in

line impedance and leak admittance at that frequency. The procedure is the same as that above outlined. The nominal line impedance of the section is θz_0 ohms, and the nominal leak admittance θy_0 mhos, in either one or two leaks, according as the section is a *T* or a Π section. The nominal *T* or Π is thus formed, and the correcting factors $\frac{\sinh \theta}{\theta}$ and $\frac{\tanh (\theta / 2)}{\theta / 2}$ applied to their elements, to form the equivalent elements. These equivalent values are the respective line impedances and leak admittances, which the section elements possess at the frequency of the measurements.

To Find the Line Angle θ and Surge Impedance z_0 of a *T* or Π Section of Given Elements.—In this problem, we start with either *T* or Π sections, all similar and symmetrical, the line impedance and leak admittance elements of which, at a given frequency, are known. We then have to find the section line angle θ and the surge impedance z_0 .

The procedure corresponds, under a.c. conditions, to that already found, under d.c. conditions, for a *T* section by (170) and (171), or for a Π section by (204) and (206). These formulas are now applied vectorially.

We may take the following illustrative example.

A Π line *AB*, of ten sections, is grounded at *B* through an impedance of $\sigma = 1,216.936 \angle 72^\circ.329 = 369.4 + j1159.5$ ohms, the impressed angular frequency being $\omega = 5,000$ radians per sec. Such a terminal load would be produced by a resistance of 369.4 ohms, containing an inductance of 231.9 millihenrys at this frequency. Each line section has a line impedance of $r = 388.853 \angle 78^\circ.331 = 78.651 + j380.816$ ohms, and a pair of leaks each of admittance $1.82858 \times 10^{-3} \angle 86^\circ.047 = (126.05 + j1824.2) 10^{-6}$ mho, as shown in Fig. 92, the measurements being made at $\omega = 5,000$. Required the line angle and surge impedance of each section. These particular element values are selected, partly because they approximately correspond to an artificial line* on

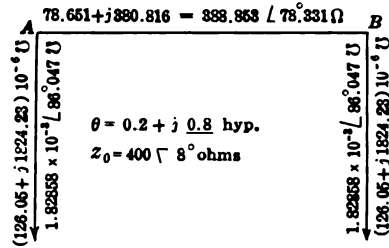


FIG. 92.— Π section of elements from which the section angle θ and surge impedance z_0 are deduced.

* "Test of an Artificial Aerial Telephone Line at a Frequency of 750 Cycles per Second," by A. E. KENNELLY and F. W. LIEBERKNECHT, *Proc. A. I. E. E.*, June, 1913.

which similar tests have been already made and reported, partly because such an artificial line corresponds fairly well to a particular actual aerial telephone line, and partly because the position angles come out in simple round numbers, which may be found in the published tables without interpolation.

Following formula (204) we have

$$\begin{aligned} \sinh v &= \sqrt{\frac{388.853}{2} \angle 78^\circ.331} \times 1.82858 \times 10^{-3} \angle 86^\circ.047 \\ &= \sqrt{0.355524 \angle 164^\circ.378} = 0.59626 \angle 82^\circ.189. \end{aligned}$$

In the published tables and charts (Table X), it is found that this corresponds precisely to $v = 0.1 + j0.4 = 0.1 + j0.62832 = 0.63623 \angle 80^\circ.957$ hyp. In general, it would be necessary to employ interpolation in the charts or tables, with some sacrifice of numerical precision; or else to use formula (517), Appendix B.

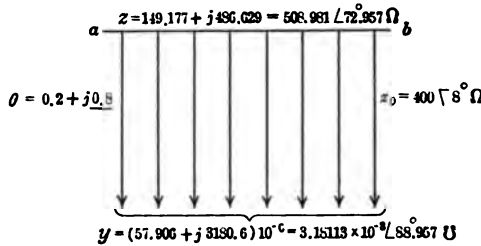


FIG. 93.—Smooth-line section conjugate to assigned II.

In this case, the section angle $\theta = 2v = 0.2 + j0.8 = 0.2 + j1.2566 = 1.27246 \angle 80^\circ.957$ hyps. The angle subtended by the whole line of ten sections would therefore be $2.0 + j8.0$ hyps. The normal attenuation factor of potential or current on such a line would be $\epsilon^{-2} = 0.13533$. The normal phase attenuation would be eight quadrants, or two complete waves of potentials or current developed over the line, or the line would include two wave lengths. At this frequency it would be a *two-wave line*, and the artificial line would have five sections to a wave.

The apparent or uncorrected surge impedance of the line would be, by (159),

$$\begin{aligned} z_0'' &= \sqrt{\frac{388.853 \angle 78^\circ.331}{3.65718 \times 10^{-3} \angle 86^\circ.047}} = \sqrt{10.6327 \times 10^4 \angle 7^\circ.716} \\ &= 326.078 \angle 3^\circ.858 \quad \text{ohms} \end{aligned}$$

and the true or corrected surge impedance by (186) is

$$z_0 = z_0'' / \cosh (0.1 + j 0.4) = \frac{326.078 \angle 3^\circ.858}{0.81520 \angle 4^\circ.142} = 400 \angle 8^\circ \text{ ohms.}$$

The conjugate smooth line would, therefore, have a total angle of $2 + j8 = 2 + j12.566 = 12.725 \angle 80^\circ.957$ hyps., and a surge impedance of $400 \angle 8^\circ$ ohms. If this line had a length of say 800 km., then a length of 80 km. would correspond to one section of the artificial line, and would subtend $0.2 + j0.8 = 0.2 + j1.2566 = 1.27245 \angle 80^\circ.957$ hyps. The conductor impedance of the 80 km. smooth-line section, would be $1.27245 \angle 80^\circ.957 \times 400 \angle 8^\circ = 508.981 \angle 72^\circ.957 = 149.177 + j486.629$ ohms. The linear impedance of the smooth line would be $6.36225 \angle 72^\circ.957 = 1.8647 + j6.08286$ ohms per wire km., corresponding to a linear inductance of 1.2166 millihenrys per wire km. The dielectric

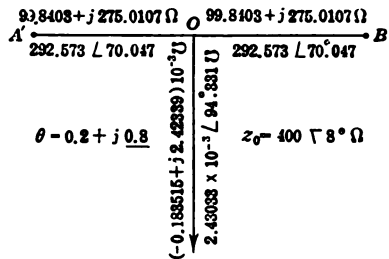


FIG. 94.--*T* section equivalent to assigned II.

admittance of the 80-km. smooth-line section would be $1.27245 \angle 80^\circ.957 / (400 \angle 8^\circ) = 3.18113 \times 10^{-3} \angle 88^\circ.957 = (57.906 + j3180.6)10^{-6}$ mho. The linear dielectric admittance would thus be $(0.72383 + j39.757)10^{-6}$ mho per wire km., corresponding to a linear capacitance of $0.0079515 \mu f.$ per wire km. The smooth section is indicated at *ab*, Fig. 93.

The equivalent *T* of the section is shown in Fig. 94 at *A'OB'*. It will be seen that it happens to be unrealizable because the slope of the leak admittance is $94^\circ.331$, and no simple admittance can have a slope exceeding 90° . However, we may assume, for the purposes of comparison between equivalent II and *T* lines, that this *T* section is not only arithmetically realizable, but is also physically realizable, by some special means, employing, say, the aid of mutual inductance.

TABLE VIII
Distribution of Potential over T Line, II Line and the Conjugate Smooth Line

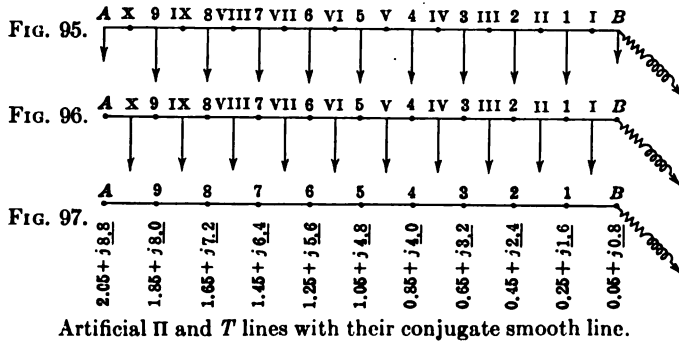
1	2	3	4	5	6	7
Position	$\frac{x}{\text{km.}}$	$\frac{\delta p}{\text{hyp.}}$	$\sinh \delta p$	V_{e^p} r.m.a. volts	II-line r.m.s. volts	T-line r.m.a. volts
A	0	2.05 + j ^{8.8}	3.93620∠72°.551	1.000 ∠0°	0.7234 ∠31°.299	1.08858 ∠39°.583
X	40	1.95 + j ^{8.4}	3.49302∠37°.110	0.88741 ∠35°.441		
9	80	1.85 + j ^{8.0}	3.10129∠0°	0.78789 ∠72°.551		
IX	120	1.75 + j ^{7.6}	2.85165∠322°.339	0.72448 ∠110°.212	0.59060 ∠106°.070	0.88873 ∠114°.354
8	160	1.65 + j ^{7.2}	2.68178∠286°.794	0.68131 ∠145°.757		
VIII	200	1.55 + j ^{6.8}	2.44238∠253°.464	0.62049 ∠179°.087	0.50582 ∠74.945	0.76116 ∠183°.229
7	240	1.45 + j ^{6.4}	2.09821∠219°.047	0.53307 ∠213°.504		
VII	280	1.35 + j ^{6.0}	1.79909∠180°	0.45706 ∠252°.551	0.37260 ∠248.409	0.56068 ∠256°.693
6	320	1.25 + j ^{5.6}	1.70635∠139°.420	0.43350 ∠293°.131		
VI	360	1.15 + j ^{5.2}	1.70971∠104°.880	0.43436 ∠327°.671	0.35408 ∠323°.529	0.53282 ∠331°.813
5	400	1.05 + j ^{4.8}	1.57374∠75°.747	0.39981 ∠356°.804		
V	440	0.95 + j ^{4.4}	1.24674∠44°.483	0.31674 ∠28°.068	0.25820 ∠23°.926	0.38854 ∠32°.210
4	480	0.85 + j ^{4.0}	0.95612∠0°	0.24290 ∠72°.551		
IV	520	0.75 + j ^{3.6}	1.01079∠311°.160	0.25670 ∠121°.391	0.20934 ∠117°.249	0.31501 ∠125°.533
3	560	0.65 + j ^{3.2}	1.17892∠280°.523	0.29951 ∠152°.028		
III	600	0.55 + j ^{2.8}	1.11300∠260°.763	0.28276 ∠171°.788	0.23050 ∠167°.646	0.34686 ∠175°.930
2	640	0.45 + j ^{2.4}	0.74969∠239°.856	0.19047 ∠192°.695		
II	680	0.35 + j ^{2.0}	0.35719∠180°	0.09075 ∠252°.551	0.07398 ∠248°.409	0.11132 ∠256°.693
I	720	0.25 + j ^{1.6}	0.63977∠108°.629	0.16254 ∠323°.922		
I	760	0.15 + j ^{1.2}	0.96290∠92°.769	0.24463 ∠339°.782	0.19042 ∠335°.640	0.30008 ∠343°.924
B	800	0.05 + j ^{0.8}	0.95237∠89°.070	0.24195 ∠343°.481		

Fall of Potential along Artificial and Conjugate Smooth Lines.

—To illustrate the comparative behavior of T , Π , and conjugate smooth lines, we may consider ten-section lines of the three types shown in Figs. 92, 93 and 94, operated at the A end with an impressed potential of 1.0 volt r.m.s., at $\omega = 5,000$, and with a terminal load at B , in each case, of $\sigma = 1,216.936\angle 72^\circ.329$ ohms. The angle subtended by the B terminal load is (89)

$$\theta' = \tanh^{-1}\left(\frac{1,216.936\angle 72^\circ.329}{400\sqrt{8}^\circ}\right) = \tanh^{-1}(3.04234\angle 80^\circ.329) = 0.05 + j0.8 \text{ hyp.}$$

The three types of Π , T , and smooth line are indicated in Figs. 95, 96 and 97 respectively. The position angles of the junctions are also indicated, as pertaining to each of the three lines.



Artificial Π and T lines with their conjugate smooth line.

Remembering that the potentials along any such line are as the sines of the position angles, we obtain the results presented in Table VIII. The first column marks the position along the line, and the second column the distance x in kilometers from the generator end. Column III gives the corresponding position angles, from $0.05 + j0.8$ hyp. at the B end, to $2.05 + j8.8$ hyps. at the A end. The sines of these position angles, as given in the published tables of "Complex Hyperbolic Functions," appear in the fourth column. In the fifth column of potential V_P , starting with the impressed potential of $1.0\angle 0^\circ$ volt r.m.s., at A , the remaining values are simply proportional to the sines of the position angles. The last two columns contain the particulars for the Π and T lines respectively. At junction points, denoted by the arabic numerals, the potentials on all three lines are identical. At mid-sections, the T -line potentials are $\cosh v$ times the corre-

sponding mid-section potentials on the smooth line; while the II-line potentials are $1/\cosh v = \operatorname{sech} v$ times the same. We have already seen that $\cosh v$ is, by tables, $0.81520 \angle 4^\circ.142$, and $\operatorname{sech} v = 1.2267 \angle 4^\circ.142$. These are the multipliers for the last two columns in Table VIII.

The numerical values of V_P recorded in Table VIII, are plotted in Fig. 98. Here OA is the vector $1.0 \angle 0^\circ$ corresponding to the

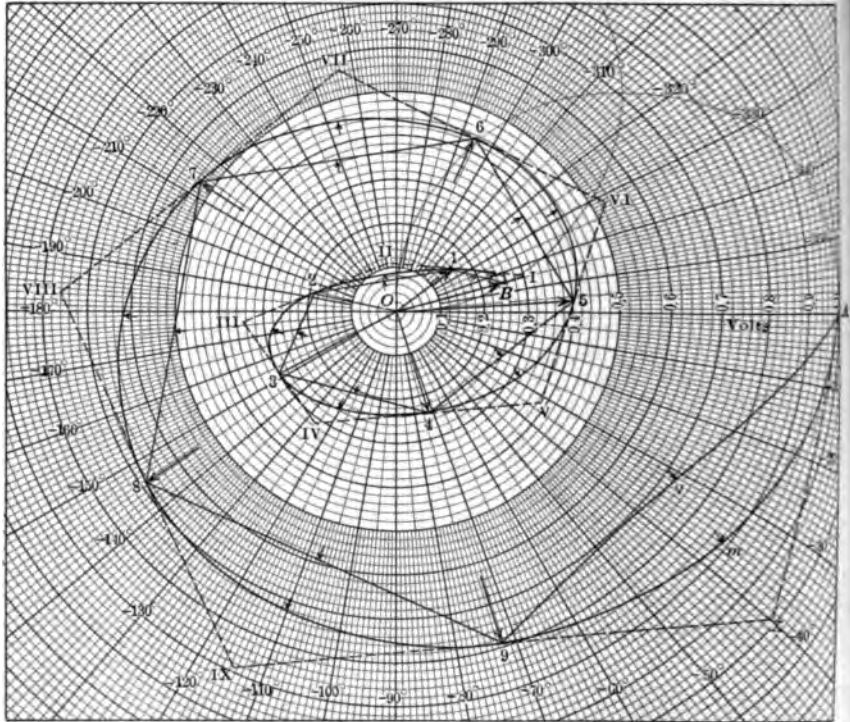


FIG. 98.—Potential distribution over real and artificial lines.

assumed impressed potential. The inwardly directed spiral curve $A, 9, 8, 7, 6$, etc., represents the fall of potential from the generator end at A , to the motor end B , using the values in column 4 of the table, and also intermediate values. The smooth-line potential graph is seen to be a smooth spiral, *i.e.*, a complex hyperbolic sinusoid, making not quite two turns. The voltage attenuation factor of the whole line is shown in Table VIII to be 0.24195 , as against 0.13533 in the normal case, and the lag in

phase amounts to $703^{\circ}.481$, as against 720° in the normal case. The same is true for the conjugate artificial lines. On these, however, the fall of potential takes place in successive straight lines. For the Π line, these straight lines are internal chords to the spiral; while, for the T line, they are external chords, marked in broken lines. Thus, in the first Π section, the potential drop is $A9 = 1.0716\angle 44^{\circ}.542 = 2.7557 \times 10^{-3}\angle 33^{\circ}.789 \times 388.853\angle 78.331$ volts, a voltmeter value greater than the initial impressed e.m.f. The drop in the first half of the first T section, is similarly $AX = 2.43385 \times 10^{-3}\angle 6^{\circ}.883 \times 292.573\angle 70^{\circ}.047 = 0.71208\angle 76^{\circ}.930$. The mid-section point of the smooth line has its potential indicated at $Om = 0.88741\angle 35^{\circ}.441$. If this is multiplied by $\cosh v$, or $0.81520\angle 4^{\circ}.142$, we obtain the mid-point potential $Oq = 0.72341\angle 31^{\circ}.299$, in the middle of the chord $A9$. Again, if we divide Om by $0.81520\angle 4^{\circ}.142$, we obtain $OX = 1.08858\angle 39^{\circ}.583$ volts, the potential at the first T leak.

Proceeding in this way, the lines joining the mid T -section points $X, IX, VIII$, etc., contact with the spiral at their respective centers. At the junction points 9, 8, 7, etc., the internal and external spiral polygons contact with the smooth-line spiral.

General Considerations of Alternating-current Potential Fall.—Although the numerical values tabulated and charted in Table VIII and Fig. 98 pertain to this particular line, operated at the selected frequency, and under the particular assigned motor load, yet the results indicated are typical of fairly long aerial lines operated at any moderate or audio frequency (between $100\sim$ and $10,000\sim$), under any ordinary load. The procedure is the same in all cases, except when the terminal load happens to have an impedance very nearly equal to the line's surge impedance, in which case the voltage spiral approaches, as we have seen, the equiangular spiral of normal attenuation, instead of a sinusoidal spiral of stationary-wave attenuation, corresponding to the general case of superposed waves reflected from the motor end of the line. When the impedance of the motor load differs from the line's surge impedance, the position angle at B may always be found by (89), from tables, charts or computation, whether the size of the motor load impedance is large or small; *i.e.*, whether the line at B is freed, grounded, or in any intermediate state differing from z_0 . The potential at any position angle then follows the \sinh of that angle, and there is no exchange from \sinh

TABLE IX
Distribution of Current over T Line II Line and Conjugate Smooth Line

1	2	3	4	5	6	7
Position	x km.	δp hyds.	$\cosh \delta p$	$I_T p$ milliamp. r. m. a.	T-line milliamp. r. m. a.	II-line milliamp. r. m. a.
A	0	2.05 + j8.8	3.83206 \angle 71° .434	2.43385 \angle 6° .883		
X	40	1.95 + j8.4	3.53698 \angle 34° .904	2.24643 \angle 29° .647	83128 \angle 25° .505	2.7557 \angle 33° .780
9	80	1.85 + j8.0	3.25853 \angle 0°	2.06958 \angle 64° .551		
IX	120	1.75 + j7.6	2.90532 \angle 325° .630	1.84525 \angle 98° .921	1.50424 \angle 94° .779	2.26357 \angle 03° .063
8	160	1.65 + j7.2	2.52644 \angle 289° .280	1.60461 \angle 135° .271		
VIII	200	1.55 + j6.8	2.27074 \angle 250° .426	1.44221 \angle 174° .125	1.17568 \angle 169° .983	1.76916 \angle 178° .267
7	240	1.45 + j6.4	2.17067 \angle 213° .055	1.37865 \angle 211° .496		
VII	280	1.35 + j6.0	2.05833 \angle 180°	1.30730 \angle 244° .551	1.0657 \angle 240° .409	1.60367 \angle 248° .693
6	320	1.25 + j5.6	1.79462 \angle 148° .354	1.13981 \angle 276° .197		
VI	360	1.15 + j5.2	1.45399 \angle 111° .670	0.92347 \angle 312° .881	0.75281 \angle 308° .739	1.13282 \angle 317° .023
5	400	1.05 + j4.8	1.29137 \angle 67° .432	0.82019 \angle 357° .119		
V	440	0.95 + j4.4	1.36505 \angle 28° .257	0.86698 \angle 36° .294	0.70676 \angle 32° .152	1.06353 \angle 40° .436
4	480	0.85 + j4.0	1.38353 \angle 0°	0.87872 \angle 64° .551		
IV	520	0.75 + j3.6	1.15356 \angle 335° .228	0.73276 \angle 89° .323	0.59726 \angle 85° .181	0.89875 \angle 93° .465
3	560	0.65 + j3.2	0.76220 \angle 299° .613	0.48409 \angle 124° .938		
III	600	0.55 + j2.8	0.65555 \angle 237° .010	0.41636 \angle 187° .541	0.33941 \angle 183° .399	0.51075 \angle 191° .683
2	640	0.45 + j2.4	0.93330 \angle 197° .042	0.59277 \angle 227° .509		
II	680	0.35 + j2.0	1.06188 \angle 180°	0.67443 \angle 244° .551	0.54979 \angle 240° .400	0.82732 \angle 248° .693
1	720	0.25 + j1.6	0.84754 \angle 169° .910	0.53830 \angle 254° .041		
I	760	0.15 + j1.2	0.34375 \angle 155° .382	0.21833 \angle 269° .169	0.7798 \angle 265° .027	0.21833 \angle 273° .311
B	800	0.05 + j0.8	0.31304 \angle 8° .741	0.19882 \angle 55° .810		

to cosh, as we have seen may occur in the c.c. case with large motor-load impedances. In this respect, the a.c. interpretation of the algebraic theory is simpler than the c.c. interpretation.

Current Distribution over Artificial and Conjugate Smooth Lines.—The distribution of current over the lines, at the selected frequency and motor load, is shown in Table IX, which is drawn up like Table VIII. Column 4 gives the tabular values of the

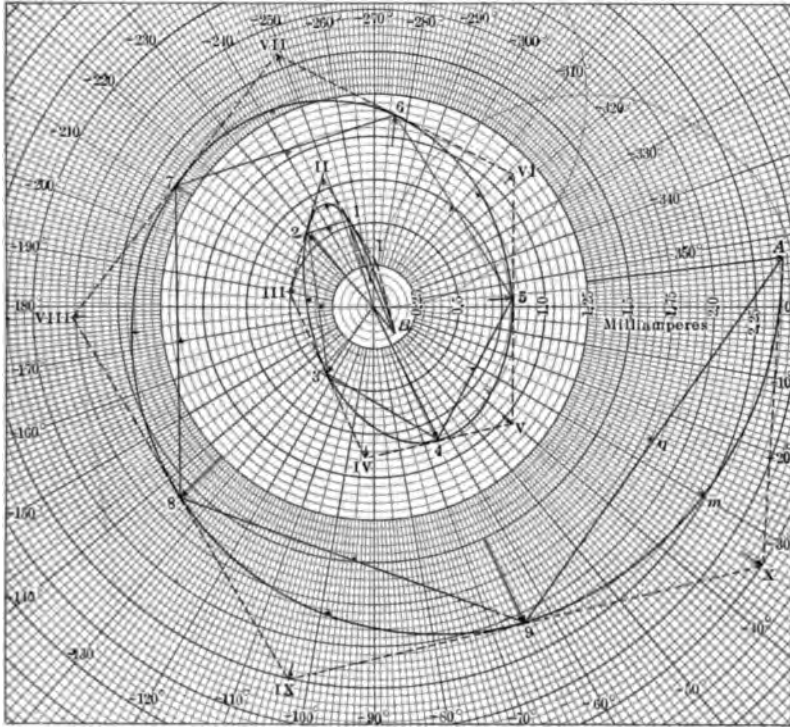


FIG. 99.—Current distribution over real and artificial lines.

cosines of the position angles at junctions and mid-sections. The r.m.s. current entering the line at A is $2.43385 \times 10^{-3} \angle 6^{\circ}.883$ amp. by (126). The line currents at the other positions are then simply proportional to the cosines of the position angles. At junctions, the currents in the artificial lines are identical with the currents in the smooth line; except that in the case of the II line, in order to measure the line current at a junction, it is necessary to substitute a pair of semi-leaks, each of $g/2$ mhos, for the single leak g mhos, and to insert the ammeter in the line between the

two semi-leaks (Fig. 41), as already explained in relation to (201). Otherwise only the Π mid-section currents can be measured.

Column 6 gives the T mid-section currents, by applying $\cosh r$ to the corresponding smooth-line mid-section currents, in the manner set forth with (230); while column 7 gives the Π mid-section currents, according to (242).

The polar graph of the current distribution over the three lines is given in Fig. 99, to voltage standard phase. The entering current is $OA = 2.43385 \angle 6^\circ.883$ milliamp., as in Table IX, or a current leading the impressed voltage at A by $6^\circ.883$. Along the smooth line, the current changes its phase from point to point, along the complex \cosh curve, or inwardly directed hyperbolic cosine spiral $A, 9, 8, 7 \dots B$, making in all, $782^\circ.693$ of rotation or more than two complete revolutions.

The internal spiral polygon $A, 9, 8 \dots B$, belongs to the T line, and the external polygon to the Π line. The vector Om indicates the smooth-line current at the first mid-section X . $Oq = Om \cosh r$, and $OX = Om \operatorname{sech} r$. Consequently, when an ammeter is inserted in this architrave of the Π line, the current observed is Oq .

The chords of the artificial-line spiral polygons necessarily measure the currents in the leaks. Thus $OA - O9 = 9A$, the vector current in the T -line leak X , namely, $1.08858 \angle 39^\circ.583 \times 2.43033 \times 10^{-3} \angle 94^\circ.331 = 2.6456 \times 10^{-3} \angle 54^\circ.748$ amp. Similarly, XA is the vector current in the semi-leak at the entering end of the Π line, $9X$ and IX 9 , the currents in the semi-leaks at Π junction 9 . If there is only one full leak g at this junction, the current in it will be $IX - X$ milliamp.

General Considerations Affecting Alternating-current Graphs of Potential and Current.—It will be observed that the spiral relations of potential and current graphs on T and Π lines are mutually inverted. *The T -line graphs are the internal spiral polygons on the current diagram, but they are the external polygons on the voltage diagram.*

It will also be noticed that the circular angle subtended on these graphs by a section, although identical for any one section on all three types of line, are very different for different sections. Thus in Fig. 99, or Table IX, the last section $B-1$ subtends an arc of nearly 200° ; while the next section, $1-2$, subtends only about 27° . The same remark applies to the potential graph. Consequently, *although in the equiangular spirals of normal attenua-*

tion, equal line sections subtend equal circular arcs, yet in the ordinary case of a hyperbolic sine or cosine spiral of standing-wave attenuation, equal line sections do not, in general, subtend equal circular arcs, especially near the motor end of the line. For this reason, these two-dimensional graphs of potential or current are inadequate to present a correct idea of distances along the line,* and some other device such as a three-dimensional model must be resorted to, if a correct distance representation is called for. Nevertheless, the relatively simple two-dimensional diagrams of Figs. 98 and 99 suffice for many purposes.

Distribution of Impedance over Alternating-current Artificial and Conjugate Smooth Lines.—It is evident from (126) that the line impedance of any real uniform line, in a steady a.c. state, must be a continuous quantity, without sudden changes or discontinuities, in the absence of localized leaks or inserted loads. In the case of lumpy artificial lines, however, the line impedance undergoes a discontinuity, or takes a sudden jump, at each leak.

Table X shows the distribution of line impedance for the particular case already discussed. Column 4 gives the tangents of the position angles, and column 5 the line impedance, respectively proportional to them. In columns 6 and 7 are the corresponding values for the Π and T lines.

It will be observed that the line impedance commences, for all three lines, at A with $410.872\angle 6^{\circ}.883$ ohms. An indefinitely long line of this type would offer $z_0 = 400\angle 8^{\circ}$ ohms. The line impedance ends at B , with $1,216.936\angle 72^{\circ}.329$, for all three types, this being the assigned impedance of the motor load.

In the case of the Π line, of column 6, the impedance falls at the entrance leak from $410.872\angle 6^{\circ}.883$ to $362.885\angle 33^{\circ}.789$ ohms, by (212). At the mid-section X , it is $262.512\angle 2^{\circ}.490$. At the upside of leak 9, it is $285.913\angle 38^{\circ}.762$ ohms, and in the middle of that leak, *i.e.*, at junction g , it is $380.700\angle 8^{\circ}$. Similarly, for the T line in column 7, the entering impedance at A is $410.872\angle 6^{\circ}.883$ ohms. At the upside of the leak X , it is $447.265\angle 46^{\circ}.466$ ohms, and at the downside it is $525.987\angle 24^{\circ}.968$ ohms. Twice the joint impedance of these last two values is $594.437\angle 14^{\circ}.078$

* "Telephonic Transmission Measurements," B. S. COHEN and G. M. SHEPHERD, *Journ. of Proc. Inst. Elec. Engrs.*, London, vol. xxxix, p. 503, 1907.

See also "The Theory of Alternate-current Transmission in Cables," by C. V. DRYSDALE, *The Electrician*, December, 1907 and January, 1908.

TABLE X
Distribution of Impedance over T Line, II Line and the Conjugate Smooth Line

1 Position km.	2 km.	3 ϕ_P hyas.	4 $\tanh \delta_P$	5 Z_{TP} ohms	6 II-line ohms	7 T-line ohms
A	0	$2.05 + j8.8$	$1.02718 \angle 1^\circ.117$	$410.872 \angle 6^\circ.883$	$362.885 \angle 33^\circ.789$ $262.512 \angle 2^\circ.490$ $285.913 \angle 38^\circ.762$	$447.265 \angle 46^\circ.466$ $594.437 \angle 14^\circ.078$ $525.987 \angle 24^\circ.968$
X	40	$1.95 + j8.4$	$0.98757 \angle 2^\circ.206$	$395.028 \angle 5^\circ.794$		
9	80	$1.85 + j8.0$	$0.95175 \angle 0^\circ$	$380.700 \angle 8^\circ$		
IX	120	$1.75 + j7.6$	$0.98153 \angle 3^\circ.291$	$392.612 \angle 11^\circ.291$	$348.074 \angle 30^\circ.512$ $260.907 \angle 3^\circ.007$ $300.991 \angle 42^\circ.694$	$429.408 \angle 49^\circ.803$ $590.801 \angle 19^\circ.575$ $553.838 \angle 20^\circ.917$
8	160	$1.65 + j7.2$	$1.06149 \angle 2^\circ.486$	$424.596 \angle 10^\circ.486$		
VIII	200	$1.55 + j6.8$	$1.07559 \angle 3^\circ.038$	$430.236 \angle 4^\circ.962$	$385.105 \angle 32^\circ.510$ $285.910 \angle 3^\circ.322$ $301.305 \angle 35^\circ.237$	$474.351 \angle 47^\circ.958$ $647.418 \angle 13^\circ.246$ $552.097 \angle 28^\circ.267$
7	240	$1.45 + j6.4$	$0.96665 \angle 5^\circ.993$	$386.660 \angle 2^\circ.007$		
VII	280	$1.35 + j6.0$	$0.87405 \angle 0^\circ$	$349.620 \angle 8^\circ$	$332.398 \angle 35^\circ.189$ $232.337 \angle 0^\circ.284$ $270.325 \angle 44^\circ.438$	$406.682 \angle 45^\circ.197$ $526.107 \angle 16^\circ.284$ $491.899 \angle 19^\circ.504$
6	320	$1.25 + j5.6$	$0.95082 \angle 8^\circ.933$	$380.328 \angle 16^\circ.933$		
VI	360	$1.15 + j5.2$	$1.17587 \angle 6^\circ.790$	$470.348 \angle 14^\circ.790$	$382.676 \angle 23^\circ.892$ $312.565 \angle 6^\circ.506$	$447.461 \angle 55^\circ.616$ $707.778 \angle 23^\circ.074$

5	400	$1.05 + j^4.8$	$1.21866 \angle 8^\circ .315$	$487.464 \angle 0^\circ .315$	$352.936 \angle 39^\circ .781$	$649.632 \angle 25^\circ .306$
V	440	$0.95 + j^4.4$	$0.91333 \angle 16^\circ .226$	$305.332 \angle 8^\circ .226$	$375.931 \angle 43^\circ .632$	$473.719 \angle 35^\circ .091$
4	480	$0.85 + j^4.0$	$0.69107 \angle 0^\circ$	$276.428 \angle 8^\circ$	$242.778 \angle 16^\circ .510$	$549.750 \angle 0^\circ .058$
IV	520	$0.75 + j^3.6$	$0.87623 \angle 24^\circ .068$	$350.492 \angle 32^\circ .068$	$228.395 \angle 32^\circ .115$	$442.164 \angle 32^\circ .341$
3	560	$0.65 + j^3.2$	$1.54680 \angle 19^\circ .090$	$618.720 \angle 27^\circ .090$	$270.269 \angle 20^\circ .914$	$358.483 \angle 60^\circ .982$
III	600	$0.55 + j^2.8$	$1.69780 \angle 23^\circ .753$	$679.120 \angle 15^\circ .753$	$232.917 \angle 23^\circ .784$	$527.419 \angle 40^\circ .352$
2	640	$0.45 + j^2.4$	$0.80327 \angle 42^\circ .815$	$321.308 \angle 34^\circ .815$	$333.248 \angle 58^\circ .563$	$650.710 \angle 0^\circ .595$
II	680	$0.35 + j^2.0$	$0.33638 \angle 0^\circ$	$134.552 \angle 8^\circ$	$586.412 \angle 39^\circ .655$	$716.510 \angle 50^\circ .992$
1	720	$0.25 + j^1.6$	$0.75486 \angle 61^\circ .281$	$301.944 \angle 69^\circ .281$	$451.304 \angle 24^\circ .037$	$1,021.94 \angle 7^\circ .469$
I	760	$0.15 + j^1.2$	$2.80120 \angle 62^\circ .612$	$1,120.480 \angle 70^\circ .612$	$372.907 \angle 1^\circ .012$	$585.153 \angle 51^\circ .579$
B	800	$0.05 + j^0.8$	$3.04234 \angle 80^\circ .329$	$1,216.936 \angle 72^\circ .329$	$230.216 \angle 55^\circ .998$	$187.791 \angle 29^\circ .184$
					$809.415 \angle 0^\circ .284$	$202.473 \angle 16^\circ .284$
					$196.460 \angle 75^\circ .229$	$206.792 \angle 2^\circ .052$
					$606.884 \angle 50^\circ .611$	$557.464 \angle 89^\circ .283$
					$744.605 \angle 62^\circ .318$	$1,686.61 \angle 78^\circ .896$
					$903.415 \angle 70^\circ .170$	$1,509.31 \angle 71^\circ .886$

ohms, which is obtained from $Z_{c,p}$ in column 5 at X, by multiplying with $\operatorname{sech}^2 v$ or $1.50477 \sphericalangle 8^\circ.284$, in accordance with (231).

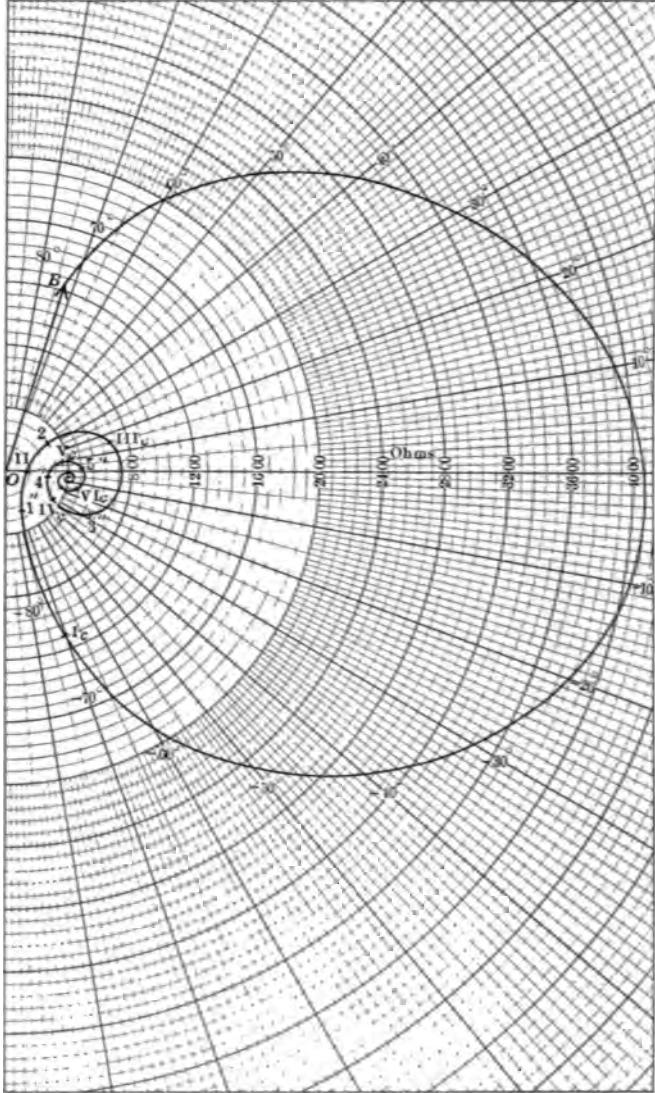


FIG. 100.—Impedance of conjugate smooth line.

The graph of line impedance over the conjugate smooth line is indicated in Fig. 100. Starting with $OB = 1,216.936 \sphericalangle 72^\circ.32\%$

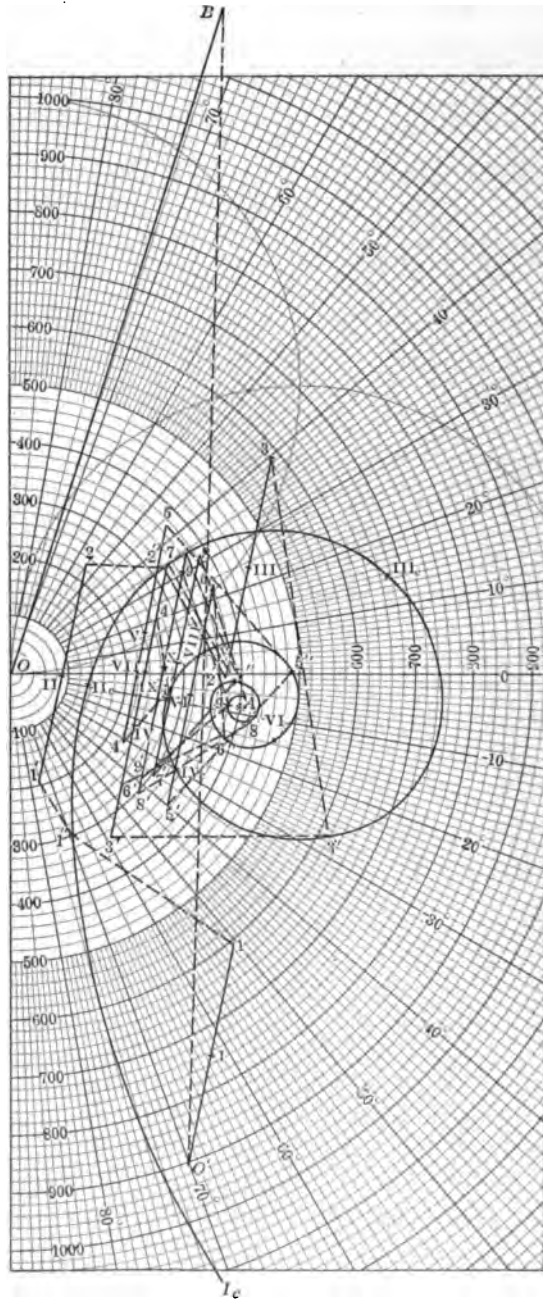


FIG. 102.—Line impedance on Π line and on conjugate smooth line.

ohms at the motor end, the line impedance in the first half section exceeds 4,000 ohms, in a widely extending spiral. There are, in all, about four turns in this inwardly directed hyperbolic tangent spiral, or about twice as many convolutions as in either of the potential or current graphs.

The parts nearer to the origin of Fig. 100 are repeated, in Fig. 101, on an enlarged scale. The T -line impedances are also indicated therein. Each junction point 1, 2, 3, etc., on the spiral, is intersected by a straight line extending $292.573\angle 70^{\circ}.047$ in each direction, or having a length of 585.146 ohms in all. These straight lines are the continuous portions of the T -line impedance graph. Between their ends, there are jumps or discontinuities, due to the sudden effects of the leaks, and indicated by broken connecting lines. Thus the graph jumps from II to II', from III to III', and so on. *The continuous portions of the T -line impedance graphs are thus a bundle of equal and parallel straight lines, whose middle points coincide with corresponding junction points on the smooth-line spiral.*

The corresponding graph for the II line is presented in Fig. 102. Here the continuous portions are a bundle of equal and parallel straight lines, or vectors of $388.853\angle 78^{\circ}.331$ ohms, the mid-points of which are related to the corresponding smooth-line mid-points by the operator, $\cosh^2 v$.

General Considerations Concerning Line Impedance.—The foregoing discussion indicates that the line-impedance graph of a smooth line, in the general case, is a tanh spiral of two convolutions per wave of voltage or current, and confined to the right-hand half of the complex plane, the phase angles being ordinarily limited to $\pm 90^{\circ}$. The line-impedance graphs of artificial lines are discontinuous, and more complicated. At junction points, however, coincidence is complete, assuming that II-line leaks are provided in contiguous pairs.

Since the phase-angle variation of line impedance is approximately twice as rapid as that of potential or current (1.7° per km. in the case considered), the measurements of line impedance at the successive section junctions are particularly liable to be vitiated by accidental changes in impressed frequency.

Distribution of Power over Alternating-current Lines.—The distribution of power over a smooth a.c. line may be computed in two ways. First, the local potential and current may be found, as in Tables VIII and IX. The complex power has then, as its

size, the volt-amperes, *i.e.*, the product of the sizes of the volts and the amperes, and, for its slope, the difference of the slopes of the volts and amperes. Thus, if at position P , the potential is $V_P = V_P \angle \beta_V^\circ$ volts, and to the same reference phase, the current is $I_P = I_P \angle \beta_I^\circ$ amp., the power at P is either:

$$P_P = V_P \cdot I_P \angle (\beta_V^\circ - \beta_I^\circ) \quad \text{watts } \angle \quad (381)$$

$$\text{or} \quad P_P = V_P \cdot I_P \angle (\beta_I^\circ - \beta_V^\circ) \quad \text{watts } \angle \quad (382)$$

according as the power is reckoned to current or potential phase as reference standard (Fig. 71). In the case of the c.c. circuit, the power $P_P = V_P I_P$ watts, where all of the three quantities P , V and I are real. In the case of the a.c. circuit, this equation will hold only if one of the two complex quantities has $\angle 0^\circ$ slope, or is taken as of local standard phase, and the phase of the other is reduced to this local standard. Thus if to the same reference phase, $V = 100 \angle 60^\circ$ r.m.s. volts, and $I = 2 \angle 30^\circ$ r.m.s. amp., the local complex power will be $200 \angle 30^\circ$ watts to local current standard phase, or $200 \angle 30^\circ$ watts to local voltage standard phase.

The second method of computing the distribution of power over the a.c. line is to write down the sinh of twice the position angle opposite each position. The size of the power will then be directly proportional to the size of $\sinh 2\delta_P$, and the slope of the power, to current standard phase, will be the slope of the line impedance at that point.

That is, if V_c and I_c are the vector potential and current at some point C , whose position angle is δ_c ,

$$\frac{V_P \cdot I_P}{V_C \cdot I_C} = \frac{\sinh \delta_P \cdot \cosh \delta_P}{\sinh \delta_C \cdot \cosh \delta_C} = \frac{\sinh (2\delta_P)}{\sinh (2\delta_C)} \quad \text{numeric } \angle \quad (383)$$

$$\text{or} \quad \frac{|P_P|}{|P_C|} = \frac{|\sinh (2\delta_P)|}{|\sinh (2\delta_C)|}$$

or the size of the vector power is as the sinh of twice the position angle. Moreover,

$$P_P = E_P / I_P = z_0 \tanh \delta_P = \underline{Z}_P \quad \text{cir. degrees} \quad (384)$$

or the slope of the power at any point is the slope of the line impedance at that point, to current phase as standard.

Therefore, to local current standard phase,

$$P_P = \frac{|P_C|}{|\sinh 2\delta_C|} \cdot |\sinh 2\delta_P| \cdot \overline{Z}_P \quad \text{watts } \angle \quad (385)$$

TABLE XI
Distribution of Power over Conjugate Smooth Line

1 Position	2 z km.	3 δ_P hypos.	4 $2\delta_P$ hypos.	5 $\sinh 2\delta_P$	6 Z_P	7 P_P milliwatts	8 P_P milliwatts	9 P_P milliwatts
A	0	2.05 + $j8.8$	4.1 + $j17.6$	30.170	$\angle 6^\circ.883$	2.43385 $\angle 6^\circ.883$	2.41631	-j0.29158
X	40	1.95 + $j8.4$	3.9 + $j16.8$	24.709	$\angle 5^\circ.794$	1.99350 $\angle 5^\circ.794$	1.98332	-j0.20115
9	80	1.85 + $j8.0$	3.7 + $j16.0$	20.211	$\angle 8^\circ$	1.63060 $\angle 8^\circ$	1.61473	-j0.22694
IX	120	1.75 + $j7.6$	3.5 + $j15.2$	16.570	$\angle 11^\circ.291$	1.33685 $\angle 11^\circ.291$	1.31097	-j0.26175
8	160	1.65 + $j7.2$	3.3 + $j14.4$	13.551	$\angle 10^\circ.486$	1.09324 $\angle 10^\circ.486$	1.07498	-j0.19897
VIII	200	1.55 + $j6.8$	3.1 + $j13.6$	11.092	$\angle 4^\circ.962$	0.89501 $\angle 4^\circ.962$	0.89165	-j0.07741
7	240	1.45 + $j6.4$	2.9 + $j12.8$	9.1093	$\angle 2^\circ.007$	0.73492 $\angle 2^\circ.008$	0.73447	-j0.02575
VII	280	1.35 + $j6.0$	2.7 + $j12.0$	7.4063	$\angle 8^\circ$	0.59751 $\angle 8^\circ$	0.59170	-j0.08316
6	320	1.25 + $j5.6$	2.5 + $j11.2$	6.1245	$\angle 16^\circ.933$	0.49411 $\angle 16^\circ.934$	0.47268	-j0.14392
VI	360	1.15 + $j5.2$	2.3 + $j10.4$	4.9718	$\angle 14^\circ.790$	0.40112 $\angle 14^\circ.790$	0.38783	-j0.10240
5	400	1.05 + $j4.8$	2.1 + $j9.6$	4.0646	$\angle 0^\circ.315$	0.32792 $\angle 0^\circ.315$	0.32792	+j0.00180
V	440	0.95 + $j4.4$	1.9 + $j8.8$	3.4037	$\angle 8^\circ.226$	0.27461 $\angle 8^\circ.226$	0.27178	+j0.03929
4	480	0.85 + $j4.0$	1.7 + $j8.0$	2.6456	$\angle 8^\circ$	0.21344 $\angle 8^\circ$	0.21136	-j0.02971
IV	520	0.75 + $j3.6$	1.5 + $j7.2$	2.3320	$\angle 32^\circ.088$	0.18810 $\angle 32^\circ.068$	0.15940	-j0.09987
3	560	0.65 + $j3.2$	1.3 + $j6.4$	1.7972	$\angle 27^\circ.090$	0.14499 $\angle 27^\circ.090$	0.12908	-j0.06603
III	600	0.55 + $j2.8$	1.1 + $j5.6$	1.4593	$\angle 15^\circ.753$	0.11773 $\angle 15^\circ.753$	0.11331	+j0.03196
2	640	0.45 + $j2.4$	0.9 + $j4.8$	1.3994	$\angle 34^\circ.815$	0.11291 $\angle 34^\circ.814$	0.09270	+j0.06446
II	680	0.35 + $j2.0$	0.7 + $j4.0$	0.75858	$\angle 8^\circ$	0.06121 $\angle 8^\circ$	0.06061	-j0.00852
I	720	0.25 + $j1.6$	0.5 + $j3.2$	1.08446	$\angle 69^\circ.281$	0.08750 $\angle 69^\circ.281$	0.03096	-j0.08184
I	760	0.15 + $j1.2$	0.3 + $j2.4$	0.66200	$\angle 70^\circ.612$	0.05341 $\angle 70^\circ.613$	0.01773	-j0.05038
B	800	0.05 + $j0.8$	0.1 + $j1.6$	0.59626	$\angle 72^\circ.329$	0.08411 $\angle 72^\circ.329$	0.01460	+j0.04584

The real component of the local vector power P_P is active power, or the rate of energy flow past the point, outward bound from the circuit; while the imaginary component of P_P is reactive power, or the rate of energy flow past the point into storage, or for retention in the circuit.

If we seek for the vector power to potential local standard phase, we must reverse the slope of (385) or

$$P_P = \frac{|P_c|}{|\sinh 2\delta_c|} \cdot |\sinh 2\delta_P| \cdot \overline{Y_P} \text{ watts } \angle \quad (386)$$

where Y_P is the line admittance at and beyond P .

Table XI gives the distribution of vector power over the conjugate smooth line under consideration. Column 4 shows the

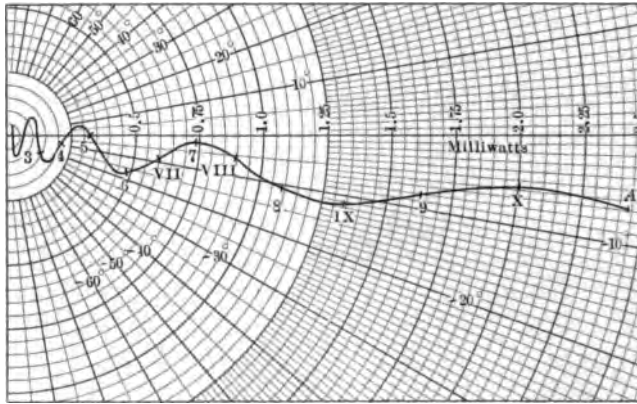


FIG. 103.—Graph of vector power along conjugate smooth line.

doubled position angles, and column 5 the sizes of the corresponding tabular sines. The slope of Z_P , taken from Table X, appears in column 6, as the slope of the power. Column 7 gives the vector power, proportional to the value in column 5, and also equal to the local product of V_P and I_P (Tables VIII and IX), with I_P at local standard phase. The real components, or local active powers, appear in column 8, and the reactive components in column 9. The active power is always positive, and steadily diminishes from the generator toward the motor end. The successive differences are due to the local values of $I_P^2 r$ along the line. The reactive power changes sign several times.

Fig. 103 gives the graph, in polar coordinates, of the vector power along the line. Near the generator end, the power in-

creases rapidly in size, but approaches the limiting value of -8° in slope. The power graph for an indefinitely long uniform a.c. conductor would be a radial straight line. Near the motor end, the fluctuations of power are rapid both in size and slope.

The active and reactive power components of the power are plotted separately in Fig. 104. The active power falls off with distance along an approximately exponential curve. The reactive power fluctuates through about four waves.

The powers at junctions along the artificial line are vectorially identical with those at corresponding junction points on the con-

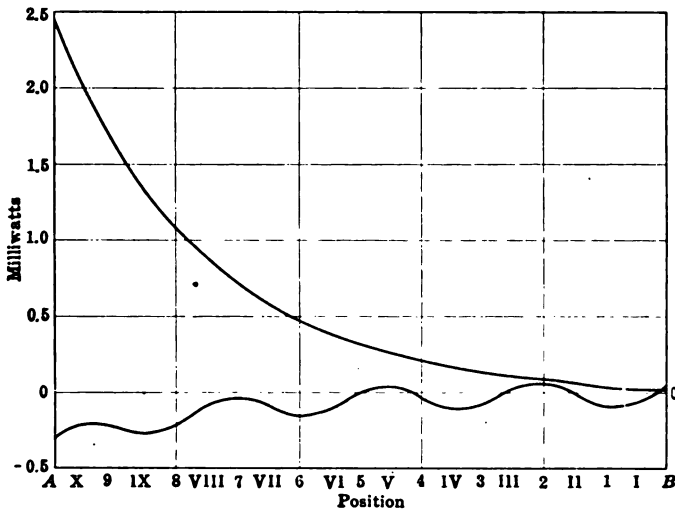


FIG. 104.—Active and reactive components of power along conjugate smooth line.

jugate smooth line. At mid-sections, the volt-amperes or power sizes agree with those at smooth-line mid-sections, but the slopes are different; so that the active and reactive components do not tally, unless corrected.

Thus, if we consider the first II section at the generator end, we find from Tables VIII and IX that

$$V_x = 0.72341 \sphericalangle 31^\circ.299 \text{ volts, and } I_x = 2.7557 \sphericalangle 33^\circ.789 \text{ milliamp.}$$

To local current standard phase, these become

$$V'_x = 0.72341 \sphericalangle 2^\circ.490 \text{ volts, and } I'_x = 2.7557 \sphericalangle 0^\circ \text{ milliamp.}$$

The power at this mid-section point of the II line is then

$$P_x = 0.72341 \times 2.7557 \angle 2^\circ.490 = 1.9935 \angle 2^\circ.490 \text{ milliwatts}$$

But the power at the corresponding point on the smooth line (Table XI) is $P_{c,x} = 1.9935 \angle 5^\circ.794$ milliwatts; so that $P_x = P_{c,x} \angle 8^\circ.284$; or the power at the Π -line mid-section has a slope $8^\circ.284$ greater than that at the corresponding smooth-line mid-section. This condition will be found to apply throughout. The slope of $\cosh^2 v$ is $8^\circ.284$, and at any midsection,

$$P_{c,x} = P_x \angle (P_x - \cosh^2 v) \quad \text{watts } \angle \quad (387)$$

or
$$P_x = P_{c,x} \angle (P_{c,x} + \cosh^2 v) \quad \text{watts } \angle \quad (388)$$

Plural Frequencies or Complex Harmonic Potentials and Currents.—We have hitherto assumed that the impressed a.c. voltages employed possessed one and only one frequency, or were purely sinusoidal; so that, in the absence of iron-cored coils in the circuit, the currents over the line were also of single frequency. We may now consider the effects of plural impressed frequencies; *i.e.*, of the ordinary complex harmonic impressed e.m.f., containing a fundamental frequency associated with multiple frequency harmonics. The n th multiple of the frequency is called the n th harmonic. The fundamental may thus be included as the first harmonic.

In order to deal with the plural-frequency case quantitatively, it is necessary to analyze the impressed potential wave into its harmonic components. As is well known, the complete Fourier analysis of a complex wave may be written

$$\begin{aligned} V_0 + V'_1 \sin \omega t + V'_2 \sin 2\omega t + V'_3 \sin 3\omega t + V'_4 \sin 4\omega t + \dots \\ + V''_1 \cos \omega t + V''_2 \cos 2\omega t + V''_3 \cos 3\omega t + V''_4 \cos 4\omega t + \dots \end{aligned} \quad \text{volts} \quad (389)$$

where V_0 is a continuous potential, such as might be developed by a storage battery, ordinarily absent in an a.c. generator wave, V'_1, V''_1, V'_2, V''_2 , etc., maximum cyclic amplitudes of the various sine and cosine components. The even harmonics are ordinarily negligible in an a.c. generator wave; so that V'_2, V''_2, V'_4, V''_4 , etc., are ordinarily all zeros. If we count time from some moment when the fundamental component passes through zero in the positive direction, $V''_1 = 0$ and the series becomes

$$\begin{aligned} V'_1 \sin \omega t + V'_3 \sin 3\omega t + V'_5 \sin 5\omega t + \dots \\ V''_3 \cos 3\omega t + V''_5 \cos 5\omega t + \dots \end{aligned} \quad \text{volts} \quad (390)$$

Compounding sine and cosine harmonic components into resultant harmonics of displaced phase, this may be expressed as

$$V_{r1} \sin \omega t + V_{r3} \sin (3\omega t + \beta_3^\circ) + V_{r5} \sin (5\omega t + \beta_5^\circ) + \dots \quad \text{volts (391)}$$

where
$$V_{rn} = \sqrt{V'_n{}^2 + V''_n{}^2} \quad \text{volts (392)}$$

and
$$\tan \beta_n^\circ = \frac{V''_n}{V'_n} \quad \text{numeric (393)}$$

Formulas (389) and (390) give the wave analysis in *sine and cosine harmonics*, while (391) gives it in *resultant sine harmonics*.

When considering a plural-frequency a.c. line, we require to know the harmonic analysis of the impressed potential, either in sine and cosine harmonics, or in resultant harmonics. The latter analysis is preferable, as being shorter and containing fewer terms. A decision must be made as to the number of frequencies or upper harmonics which must be taken into account.

Ordinarily, the sizes of the harmonics diminish as their order increases; but there are numerous exceptions to this rule, as when some particular tooth frequency in the a.c. generator establishes a prominent size for that harmonic. Care must therefore be exercised not to exclude any important harmonics. On the other hand, the fewer the harmonics to be dealt with, the better, because the labor involved in correctly solving the problem increases in nearly the same ratio as the number of harmonics retained.

The rule is to work out the position angle, r.m.s. potential, and r.m.s. current distributions, over the artificial or conjugate smooth line, for each harmonic component in turn, as though it existed alone, and then to combine them, at each position, in the well-known way for root mean squares.

Combination of Components of Different Frequencies into a R.m.s. Resultant.—Let the r.m.s. value of each a.c. harmonic component be obtained by dividing its amplitude with $\sqrt{2}$ in the usual way, and let

$$V_n = \frac{V_{rn}}{\sqrt{2}} = \sqrt{\frac{V'_n{}^2 + V''_n{}^2}{2}} \quad \text{r.m.s. volts (394)}$$

be the r.m.s. value of the *n*th harmonic. Then the r.m.s. value of all the harmonics together, over any considerable number of cycles, will be

$$V = \sqrt{V_1^2 + V_2^2 + V_3^2 + \dots} \quad \text{r.m.s. volts (395)}$$

or, as is well known, the joint r.m.s. value of a plurality of r.m.s. values of different frequency, is the square root of the sum of their squares. If a continuous potential V_0 be present, this may be regarded as a r.m.s. harmonic of zero frequency, and be included thus:

$$V = \sqrt{V_0^2 + V_1^2 + V_2^2 + V_3^2 + \dots} \quad \text{r.m.s. volts (396)}$$

Moreover, from (392), it is evident that the squares of the r.m.s. values of the sine and cosine terms of any harmonic may be substituted for the square of their resultant; or that, in this respect, the sine and cosine terms may be treated as though they were components of different frequencies.

The same procedure applies to plural-frequency currents. Find the r.m.s. resultant harmonics. The r.m.s. value of all together will be the square root of the sum of their squares. A continuous current, if present, may be included, as the r.m.s. value of an alternating current of zero frequency.

Graphical Representation of R.m.s. Plural-frequency Combination.—The process represented algebraically in (395) or (396) may be represented graphically by the process of successive perpendicular summation, or "crab addition." An example will suffice to make this clear. A fundamental alternating current of 100 amp. r.m.s., is associated with a continuous current of 50 amp., and with two other alternating currents of other frequencies of 20 and 10 amp. r.m.s., respectively. What will be the joint r.m.s. current? Here by (396),

$$I = \sqrt{100^2 + 50^2 + 20^2 + 10^2} = \sqrt{10,000 + 2,500 + 400 + 100} \\ = \sqrt{13,000} = 114.0175 \text{ amp. r.m.s.}$$

In Fig. 105, OA represents the fundamental r.m.s. current. AB , added perpendicularly to OA , represents the continuous current, or current of 50 r.m.s. amp. at zero frequency. The perpendicular sum of OA and AB is $OB = 111.8034$ amp. Adding similarly the other frequency components BC and CD , the total perpendicular sum is $OD = 114.0175$ amp. The order in which the components are added manifestly does not affect the final result, and it is a matter of insignificance whether the various frequencies coacting are "harmonic," *i.e.*, are integral multiples of a fundamental, or not, so long as they are different.

The complete solution of an a.c. line with complex harmonic potentials and currents thus requires an independent solution of

potential and current for each single frequency in turn, as though the others were non-existent, and then the r.m.s. value at any point on the line is the perpendicular sum of the separate fre-

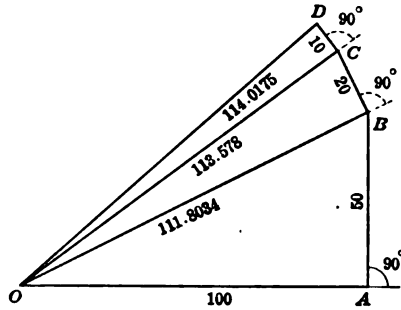


FIG. 105.—Geometrical representation of a joint r.m.s. value of plural-frequency components by perpendicular summation or "crab addition."

quency values. The powers and energies of the different frequencies are independent of each other, and the total transmitted energy is the sum of the energies transmitted at the separate component frequencies.

CHAPTER XII

DESIGN AND CONSTRUCTION OF ARTIFICIAL ALTERNATING-CURRENT LINES

The ordinary a.c. artificial line, designed to represent the behavior of a given actual line at a specified frequency, requires a definite amount of line resistance and inductance per section, and also a definite amount of leakance and capacitance per section. This calls for reactors, with or without external resistance, in the line, and condensers, with or without external resistance, in the leaks. In certain cases, however, such as artificial twisted-pair telephone cables, or artificial submarine telegraph cables, the inductance required in the line circuit is so small that it can be neglected.

The preliminary calculation designs, conducted in the manner already indicated, will show how much line impedance and shunt admittance is required per section, and the numerical values of the elements needed for the equivalent T or Π .

Relative Merits of T and Π Sections.—As to the choice between T and Π sections, assuming that they are both readily realizable, T sections have the advantage that the ammeters, or equivalent current-measuring devices, can be inserted at section junctions, without disturbing adjacent leaks. Moreover, series loading coils at junctions can much more easily be inserted experimentally in T lines than in Π lines. On the other hand, the terminal sections of a T line call for half reactors. It is often inconvenient to supply terminal reactors of half the usual section reactance, or to find the correct mid-points of the section reactances. It is ordinarily preferable to make all the line reactors similar, and equal, without mid-point taps. Two section reactors may be used in parallel to form each terminal semi-reactance, but this is wasteful of material. It is easier in such cases to employ Π sections, with full reactors throughout, and semi-leaks at the terminals. Each of these two types of artificial line has, therefore, its particular advantages and disadvantages, and the selection between them will depend on the merits of each case.

Line Reactors.—The line reactors should be as simple to construct as possible. They should be capable of being adjusted into close mutual agreement. They should be so mounted that the mutual inductance between adjacent reactors should be negligible. They should be easily insulated from ground, and should be impregnated with a waterproof insulating compound so as to maintain good internal insulation. Finally, they should be solidly constructed so that their electrical constants may remain unaltered with time.

A question, which naturally arises early in the design, is whether the reactors should be *ferric* or *non-ferric*; *i.e.*, whether they should have, or should not have, subdivided iron cores. The advantage of iron cores is that they enable the needed amount of reactance to be obtained with cheaper, smaller, more compact and less mutually reactive toroids, than if wooden or air cores are used; so that the whole artificial line can be compressed into a relatively small compass. On the other hand, the disadvantage of iron cores is that the electrical constants of their coils vary appreciably, not only with the frequency, but also with the strength of exciting alternating current, at one and the same frequency.

If, therefore, an artificial line with reactors is needed for first approximation purposes only, and especially if it is required to be semi-portable, laminated steel cores should be used, preferably in toroid coils. If, however, the line is needed for quantitative purposes, and especially for careful study in the laboratory, non-ferric reactors should be selected. Up to the present time, artificial lines used industrially, for practical checks, commonly use ferric reactors, and artificial lines in the testing laboratories of technical colleges ordinarily employ non-ferric reactors.

Non-ferric reactors for artificial lines have been constructed in three forms, namely: (1) toroids with wooden ring cores; (2) square wooden frames intended roughly to simulate closed circular solenoids; and (3) toroidal coils of wire wound on forms and assembled in air, so as to approximate closed circular solenoids.

The first type is described by Mr. G. M. B. Shepherd.* “They are wooden-core toroids of nearly the same dimensions as the loading coils commonly used for underground cables.” There

* “An Artificial Equivalent of an Open-wire Line for Telephonic Experiments,” by G. M. B. SHEPHERD, *The Post Office Electrical Engineers' Journal*, vol. vii, part 3, October, 1914.

are two windings on opposite halves of the ring, the middle point of each being brought out and connected to the capacity as shown in Fig. 106. This figure shows a two-wire artificial line in I sections, each representing 8 miles (12.9 km.) of overhead telephone copper pair conductor, except two sections of 4 miles each (6.45 km.). The loop resistance is 72 ohms per section, the loop inductance is 0.0296 henry per section, the loop capacitance 0.08 μ f. per section, and the loop leakance adjustable in three steps between 8 and 80 micromhos per section. There are altogether 26 sections, representing in all 200 miles (322 km.) of aerial loop pair. This line is made up in two wooden-frame cases, each about 37 in. by 7 in. by 10 in. high (94 cm. by 17.8 cm. by 25.4 cm. high).

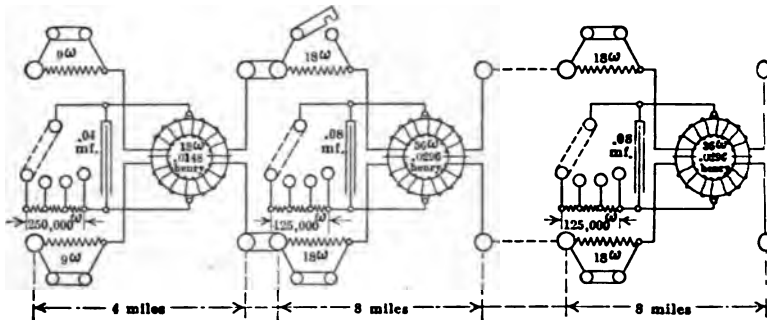


FIG. 106.—Artificial telephone line in I sections, with adjustable section resistances and leakances.

The second type is described* in the *Electrical World* of Feb. 17 1912. It consists of a four-section square wooden frame, such as is indicated in Fig. 107. Each coil is separately wound in the lathe, with double cotton-covered copper wire, and then thoroughly impregnated with paraffin wax. The ends of each coil are soldered to small brass terminal plates, and the direction of winding is such as to imitate that of a closed circular solenoid. The wooden cores are assembled into square frame reactors by a single brass screw bolt *S*, at each corner. Such a frame reactor possesses an appreciable amount of external magnetic leakage; so that it is desirable to screw them down to the supporting shelf

* "An Artificial Power-transmission Line," by A. E. KENNELLY and H. TABORSSI, *Electrical World*, Feb. 17, 1912. See also "Measurements of Voltage and Current over a Long Artificial Power-transmission Line at 25 and 60 Cycles per Second," by A. E. KENNELLY and F. W. LIEBERKNECHT, *Trans. A. I. E. E.*, June, 1912.

alternately in perpendicular planes as is suggested in Figs. 108 and 109. The particular frame reactor of Fig. 107 weighs, unwound, 2.8 kg. (6.2 lb.). The insulated wire on the frame weighs 5.6 kg. (12.4 lb.). Each of the four component coils is wound with 1,190 turns of d.c.c. No. 19 A.W.G. wire, of bare diameter 0.915 mm. (0.036 in.), and of mean covered diameter 1.14 mm.

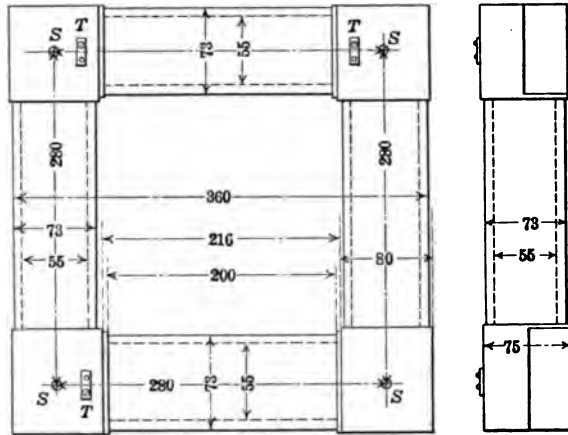
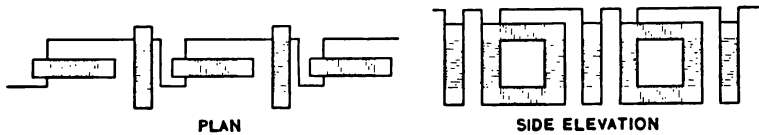


FIG. 107.—Outline sketch of one coil. Dimensions in millimeters.

(0.045 in.) occupying approximately seven layers of 170 turns each. The total inductance of each frame reactor averages 90 millihenrys. The total resistance of each frame reactor at 20°C. averages 24.1 ohms.

In the particular II line into which these frame reactors enter, there are 30 reactors in all. Each section approximately repre-



FIGS. 108 AND 109.—Plan and side elevation of the grouping of reactors on shelf.

sents 80 km. (49.7 miles) of No. 000 A.W.G. aluminum stranded three-phase conductor of overstrand diameter 1.195 cm. (0.47 in.), suspended parallel in air, at equal interaxial distances of 230 cm. (90.5 in.). The total length of the artificial line is therefore 2,400 km. (nearly 1,500 miles) if connected single-phase, as in Fig. 110, or 800 km. (nearly 500 miles) if connected three-phase,

as in Figs. 111 and 112. The line is mounted on three shelves, as shown in Fig. 113. For many purposes, a much shorter artificial line would suffice.

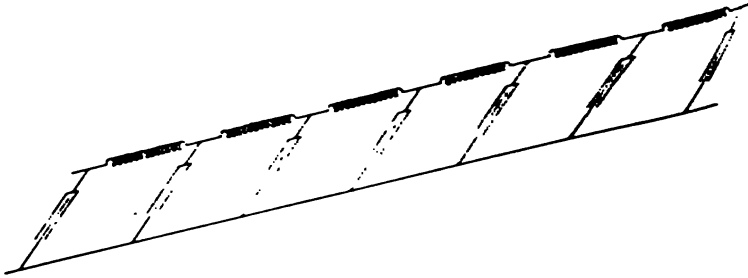


FIG. 110.—Connection of sections when operated as a single-phase line.

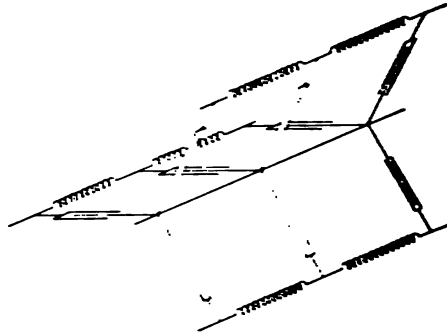


FIG. 111.—Connection of sections when operated as a three-phase line.

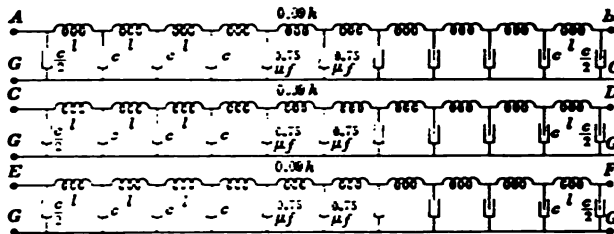


FIG. 112.—Diagram of connections of artificial line.

The condensers are of leadfoil and impregnated paper, of the type employed in telephony. Each section condenser averages $0.75 \mu f$. The six terminal condensers of Fig. 112 are each of $0.375 \mu f$. Each condenser is placed in a separate tin box, 20 cm. by 5.6 cm. by 14.2 cm. high (7.9 by 2.2 by 5.6 in.), which is then

filled up with paraffin wax. They are tested initially to withstand 500 volts a.c. They have a small dielectric leakance at a low frequency, which, if fairly uniform, measured, and taken into account, is no practical disadvantage.

The total weight of insulated copper wire in the entire 30-frame line is 168 kg. (370 lb.), and the total capacitance 22.5 μf .

The constants of the conjugate smooth line at low frequencies, not exceeding 60~, are given in the accompanying table.*



FIG. 113.—Picture of artificial line in cabinet.

TABLE XII

Nominal Linear Constants of Artificial 85 sq. mm. (168,000 circ. mils) Aluminum Line, taking each Section as representing 80 km. (49.7 miles) of conductor

	Per wire km.	Per wire mile
Linear resistance r ohms at 0°C.....	0.278	0.445
Linear resistance r ohms at 20°C.....	0.301	0.485
Linear inductance l henrys.....	1.13×10^{-3}	1.82×10^{-3}
Linear capacitance c farads.....	9.38×10^{-9}	15.1×10^{-9}
Linear leakance g mhos.....	0.12×10^{-6}	0.19×10^{-6}
Linear hyperbolic angle hyps. at 60~..	$0.00135\angle 71^{\circ}.5$	$0.00218\angle 71^{\circ}.5$

* Tests of one of the reactors, removed from the line, at different impressed frequencies, have shown that its effective resistance at 28°C. was 25.3 ohms at zero frequency, 26.8 ohms at 1,000~, 31.5 ohms at 2,000~ and 35.5 ohms at 2,500~.

The angle θ subtended by each section at 60~ is $0.108\angle 71^{\circ}.5$ hyp. The angle ν subtended by each half-section at 60~ is $0.054\angle 71^{\circ}.5$ hyp. The lumpiness correction factor, at 60~, is $1.0007\angle 0^{\circ}.03$; so that there is practically no correction for lumpi-

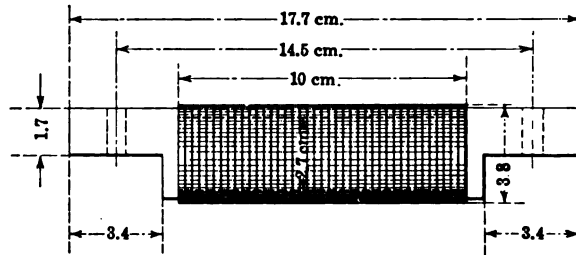


FIG. 114.—Single coil and wooden core of square-frame reactor.

ness at this frequency. The total angle subtended by the whole single-phase line of 30 sections, at 60~, is $3.24\angle 71^{\circ}.5$ hyps.

This type of artificial power-transmission line has been found convenient for experimental investigations at low frequencies.

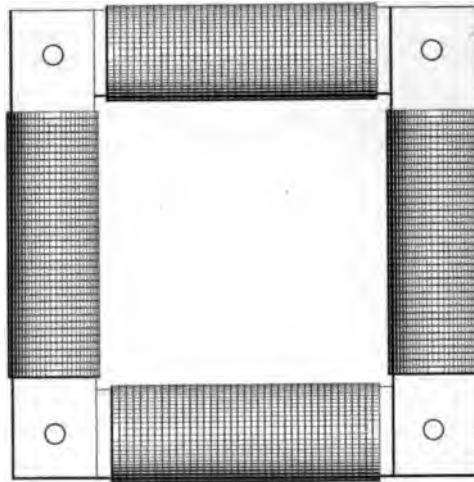


FIG. 115.—Reactor frame.

It has been found practicable to insert a small manganin wire resistor in circuit with each reactor when it is desired to have the line approximately imitate a telephone overhead copper line say 3.65 mm. (0.144 in.) in diameter. The line is then, however, not well adapted for use with telephonic frequencies, because of

the large lumpiness correction factor, and for telephonic measurements, a similar line has been constructed with smaller and more numerous frame reactors and sections.

The dimensions of the frame in this higher-frequency line are indicated in Figs. 114 and 115. The winding consists of No. 24 A.W.G., d.c.c. copper wire, diameter bare 0.51 mm. (0.020 in.), covered 0.76 mm. (0.03 in.). Each of the four limbs composing the frame carries 975 turns, in approximately $7\frac{3}{4}$ layers of 125 turns per layer. The mean diameter of the winding is 32.5 mm. (1.27 in.), and the length of wire on each limb is 100 m. (328 ft.). The total length per frame is thus 400 m. (1,310 ft.), with a total frame resistance of 33.0 ohms at 20°C., and a total frame inductance of 0.031 henry. The weight of wire on each frame is approximately 0.735 kg. (1.62 lb.).

There are 80 frame reactors and sections in the line, making the total weight of wire 58.8 kg. (130 lb.). The total line resistance of the 80 reactors is 2,640 ohms at 20°C., and their total inductance 2.48 henrys. They are connected as a Π line. The reactors are arranged alternately in mutually perpendicular upright planes, as in Figs. 108 and 109. The line occupies two shelves of a pair of cabinets which, in combination, are 6.75 m. (22 ft. 2 in.) long, 45.7 cm. wide (18 in.) and 88 cm. (34.5 in.) high. These cabinets are provided in front with sliding glazed doors. They are shown on the upper right-hand side in Fig. 118.

The condensers are selected telephone condensers of leadfoil and paper, tested up to 500 volts, a.c., r.m.s. The average capacitance of each condenser is 0.325 $\mu f.$, making the aggregate capacitance of the 80 sections, 26 $\mu f.$ Each section is intended to represent 30 km. (18.7 miles) of heavy long-distance aerial telephone wire.

TABLE XIII

Nominal Linear Constants of Artificial Line for 15.67 sq. mm. (30,000 circ. mils) copper aerial conductor at interaxial distance of 30 cm. from its parallel return conductor, each section being taken as representing 30 km. (18.7 miles) of wire

	Per wire km.	Per wire mile
Linear resistance r ohms at 0°C.....	1.013	1.63
Linear resistance r ohms at 20°C.....	1.1	1.77
Linear inductance l henrys.....	1.03×10^{-3}	1.66×10^{-3}
Linear capacitance c farads.....	10.8×10^{-9}	17.4×10^{-9}
Linear leakance g mhos.....	1.2×10^{-8}	1.93×10^{-8}

The conjugate smooth line is 2,400 km. (1,490 miles) of aerial copper conductor, one of a pair of parallel copper wires 0.447 cm. in diameter (0.176 in.) at an interaxial distance of 30 cm. (11.8 in.). The cross-section of such a wire would be 15.67 sq. mm. (0.0243 sq. in. or 30,900 circ. mils) between the sizes of Nos. 5 and 6 A.W.G.

The data concerning the conjugate smooth line, at low frequencies appears in the preceding table.

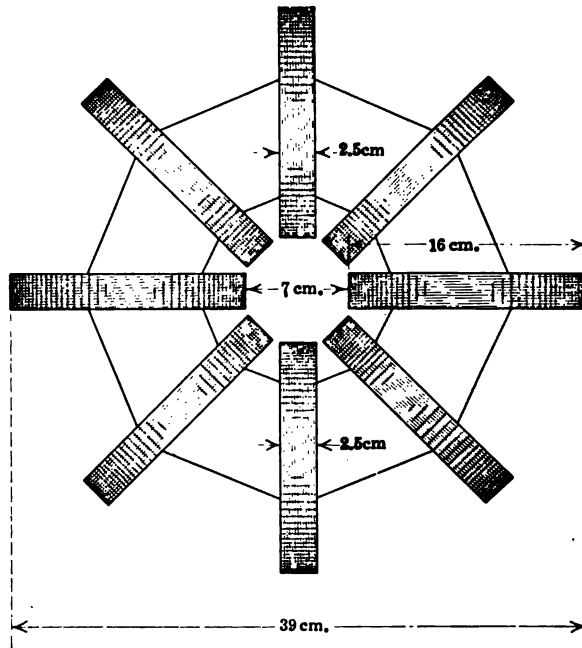


FIG. 116.—Non-ferric reactor for artificial power transmission line. Plan view. Wooden wedge-shaped spacing pieces between coils.

The third type of non-ferric reactor is described by R. D. Huxley,* and by Prof. C. E. Magnusson.† In each case, there are wooden-cored or air-cored coils of insulated wire mounted on a base, in such a manner as to approximate the structure and behavior of a closed circular solenoid, or toroid.

* R. D. HUXLEY, "Design for Artificial Transmission Line," *Electrical World*, May 2, 1914, p. 980.

† C. E. MAGNUSSON, J. GOODERHAM and R. RADER, "A 200-mile Artificial Transmission Line," *Electrical World*, June 22, 1915. See also "An Artificial Transmission Line with Adjustable Line Constants," by C. E. MAGNUSSEON, and S. R. BURBANK, *Trans. A. I. E. E.*, September, 1916.

In the Pender and Huxley design, there are eight coils in an octagonal reactor group, as shown in plan by Fig. 116. Each coil is wound in the lathe on a wooden form. The axial length is 2.5 cm., the internal winding diameter 5.75 cm., the external winding diameter about 16.0 cm. or the winding depth 5.13 cm.

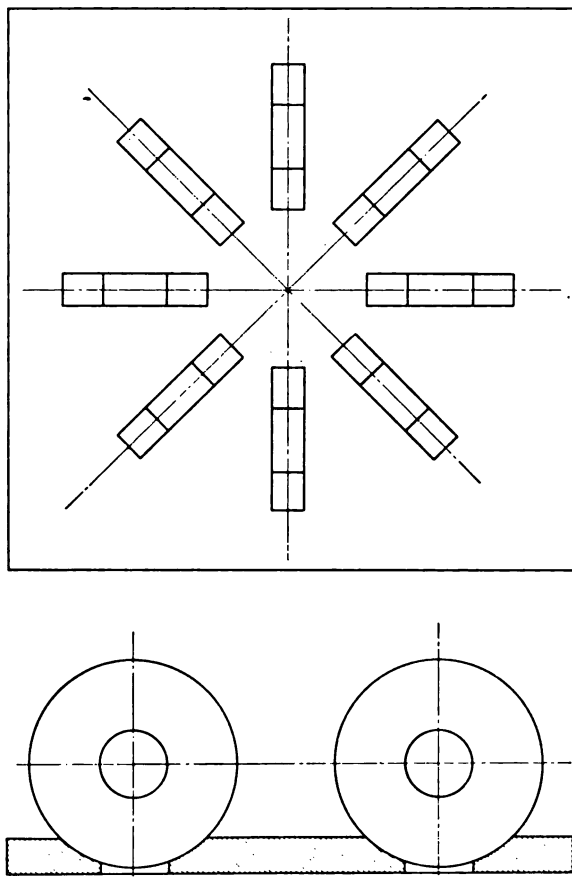


FIG. 117.—Supporting base of reactor and mode of assembling coils.

in 23 layers of about 10 turns each, or 230 turns in all, per coil of No. 12 A.W.G. double cotton-covered copper wire 0.0808 in. (2.05 mm.) bare, 0.092 in. (2.35 mm.) covered diameter. The weight of wire in each reactor group of eight coils is approximately 43 lb. (19.5 kg.). The d.c. resistance of each reactor

group at 20°C. averages 3.39 ohms. Its average inductance at low frequencies is 0.056 henry.

As each coil was completed, it was transferred from the lathe to an oven, where it was dried for several hours. It was then thoroughly impregnated in a bath of molten beeswax and rosin.

The coils, painted with paraffin wax, are mounted by setting them in channel holes cut out in a wooden base, as indicated in Fig. 117, and the connections between coils are soldered together.

The capacitance per section is 0.485 μ f. in paper condensers of the telephone type, sealed in tinned iron cases and individually



FIG. 118.—Picture of cabinets containing artificial lines.

designed to withstand 2,000 volts. At 60~, the condenser phase-angle defect was less than 15 minutes of arc. These condensers were specially selected for uniformity.

Each section of the artificial line represents approximately 30 miles (48.25 km.) of aerial power-transmission copper conductor of 500,000 circ. mils (253 sq. mm.) cross-section, spaced at equal interaxial distances of 9 ft. (275 cm.). The entire line of 26 Π sections thus represents 780 miles (1,250 km.) of single-phase conductor. The total weight of insulated wire is about 1,100 lb. (500 kg.). The sections are mounted in racks five shelves deep in two cabinets, each capable of holding 15 sections. Each cabi-

net measures approximately 185 cm. by 61 cm. by 167.5 cm. high, with a floor space of 1.1 sq. m. The appearance of the line is shown in Fig. 118, on the left-hand side of the picture.

The linear constants of the conjugate smooth line at low frequencies are given in the following table.

TABLE XIV

Nominal Linear Constants of 250 sq. mm. (500,000 circ. mils) copper artificial power-transmission Line taking each section as representing 30 miles (48.3 km.)

	Per wire km.	Per wire mile
Linear resistance r ohms at 20°C.....	0.0702	0.113
Linear inductance l henrys.....	1.16×10^{-3}	1.87×10^{-3}
Linear capacitance c farads.....	1.004×10^{-8}	1.617×10^{-8}
Linear leakage g mhos.....	0.013×10^{-6}	0.021×10^{-6}
Linear hyperbolic angle α hyps. at 189.4~.....	0.0407 $\angle 88^\circ.2$	0.0655 $\angle 88^\circ.2$

No lumpiness correction factor has to be applied on this line, in practice, below 200~. The section angle at 189.4~ is 0.1964 $\angle 88^\circ.2$ hyp. (see page 289). At 189.4~, the lumpiness correcting factor is 1.002 $\angle 0^\circ.01$.

This line is relatively heavy to construct, but is very well adapted to manifest a.c. and transient phenomena, owing to its relatively very low linear resistance, and its small section angle.

The University of Washington design of non-ferric section reactor employs four hollow coils arranged in a square, as shown in Fig. 119, on a wooden supporting back. These four fixed coils are so connected, with one of them subdivided, that different values of inductance can be included between the pairs of terminals selected. Moreover, one of the coils can be rotated adjustably in azimuth, to change the mutual inductance. The section inductance can thus be varied between 0.01 and 0.021 henry. The section line resistance can also be varied within certain limits by means of the loop of resistance wire. An extra section resistance of 50 ohms can be inserted in each section when telephone wires are imitated.

The coils are wound with d.c. No. 14 A. W. Gage, 0.072 in. (1.83 mm.) bare, 0.081 in. (2.06 mm.) covered diameter. Their axial length is given as 5.47 cm., internal diameter 4.8 cm., external diameter 6.3 cm., 76.3 m. of wire in 216 turns—eight layers

of 27 turns each. The average reactor resistance is 2.59 ohms at 25°C. The section capacitance is adjustable between 0.092 and 0.92 μf .

Each *T* section is designed to imitate 10 miles (16.1 km.) of aerial line of almost any practical size of copper wire up to No. 0000 A.W.G., diameter, 0.46 in. (11.6 mm.) or 211,600 circ. mils (107 sq. mm.), at interaxial spacings up to 10 ft. (3.05 m.).

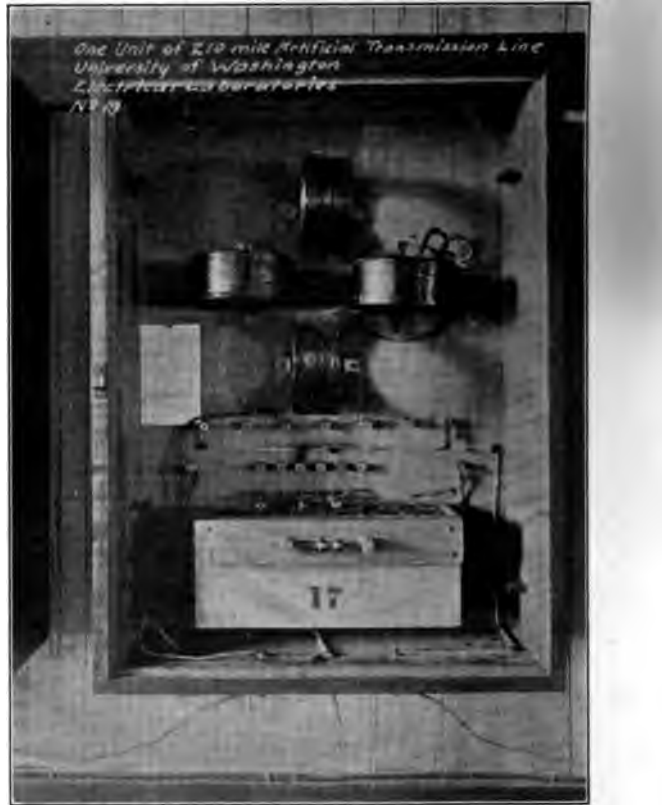


FIG. 119.—Section of University of Washington *T* line.

There are 20 sections in the artificial *T* line as described, aggregating a length of 200 miles (322 km.) of aerial line.

The construction described offers the advantage of enabling different sizes and types of overhead line to be tested on different occasions. Such advantage is accompanied by a corresponding need for increased care in ascertaining that all the section ad-

ments are similar, and that all the screw terminal contacts are in good electrical condition.

The short equivalent length of the section in this line enables a relatively high audio frequency to be used on it, or assists in the study of transient phenomena.



FIG. 120.—Assembled artificial line.

A picture of the line of 20 sections, as given in the *Electric-World* article appears in Fig. 120.

General Remarks Concerning Artificial-line Connections.—In establishing the connections of an artificial line, it is important to have as few and firm electric contacts as possible, and to pro-

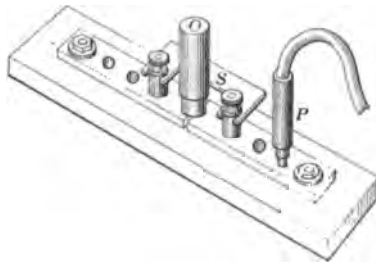


FIG. 121.—Convenient form of plug contact piece.

vide a convenient means for testing the continuity and uniformity of the sections. A particular form of plug contact piece having the advantages for connecting consecutive sections, is shown in Fig. 121. The condenser is connected to the brass split plug, capable of being tightly inserted in the piece and of being

speedily removed. By throwing off all the condenser plugs, a Wheatstone-bridge test of the line circuit, or of any part thereof, can be speedily made. The open-circuiting plug *O*, permanently short-circuited by the removable brass strip *S*, enables the line to be opened conveniently at that point, or permits the insertion of a small resistance in the line, for measuring line current by potentiometer.

One of the most important requirements of any artificial line is obviously uniformity among the sections. It is usually more important that they should be all alike, even if they are somewhat off standard, than that some should approach the standard electric conditions very closely while others depart appreciably therefrom. It is very disconcerting to observers and computers to find certain sections too far off the average. If electrical discrepancies exist, it is usually better to place them near the motor end of the line, and to have the highest available degree of uniformity in the generator-end sections, where the fall of potential and current is greatest.

It is found advantageous to insulate elaborately all parts of the line circuit, and to ground carefully the ground side. For some purposes it is insufficient to employ the ground side as a mere return conductor, and actual grounding to water pipes is to be preferred as a general practice.

T and Π Artificial Lines of Double Surge Impedance.—We have seen that *T* and Π artificial lines are single-wire lines with ground or zero-potential return. Consequently, when an actual two-wire line circuit is imitated by a *T* or Π artificial line, the latter should be operated with half the e.m.f. applicable to the two-wire line at the generator end, and with half the impedance load at the motor end, as is indicated in Figs. 15 and 16. In some practical cases, there may be difficulty in testing the artificial line with half the voltage and half the load that should be applied to a double-wire model, *i.e.*, an artificial line of *I* or *O* sections (Fig. 89). This objection may be overcome in a *T* or Π line by employing sections of *double surge impedance*.

In Fig. 122, a single-section *I* artificial line is indicated at *AB*, with 20 volts applied across the two sides at *A*, and a 2,000-ohm load across the two sides at *B*. This line nominally represents a single mile (1.6 km.) of standard telephone twisted-pair cable, having a capacitance of 0.08 mf. and a total conductor resistance of 88 ohms, half in each conductor. At $\omega = 5,000$,

the angle subtended by this I line is $0.0839\angle 45^\circ$ hyp., uncorrected for lumpiness, and the uncorrected surge impedance is $z_{0'} = 1,048.8\angle 45^\circ$ ohms at this frequency.

The nominal T section corresponding to this line is shown at $A'B'$. It has 44 ohms conductor resistance and 0.16 mf. capacitance to ground return. It should be operated with 10 volts at A' and with 1,000 ohms at B' , in order to develop the same dis-

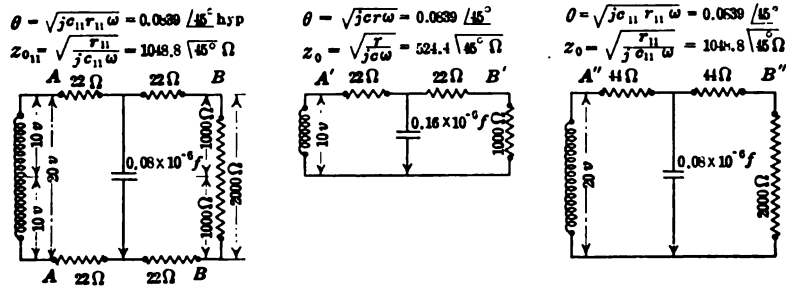


FIG. 122.— I section and T section, with a T of double surge impedance.

tribution of position angles, potential and current as the I line at AB . The nominal angle subtended by the T section $A'B'$ is the same as that of the I section ($0.0839\angle 45^\circ$ hyps.); but its surge impedance is only half that of the I section.

If, however, the T section be given the same total conductor resistance as the I section (88 ohms) as at $A''B''$, Fig. 122, with

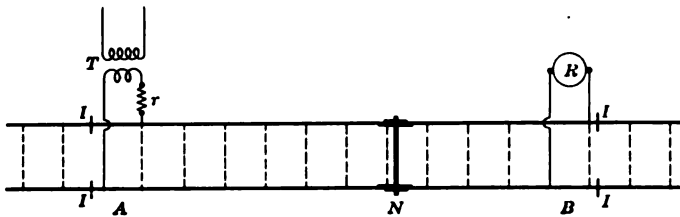


FIG. 123.—Elementary-connection diagram of a railway-track signal system.

the same capacitance as the I section, we obtain a T of the same section angle as before; but with *double surge impedance*. This T section may now be operated with full voltage at A'' and full impedance at B'' , in order to develop the same distribution of position angles, potentials and currents as the I section. The correcting factors for lumpiness will also be the same for all three types of equivalent circuit. Moreover, the equivalent II can be

similarly produced for double surge impedance by keeping the same leaks as in the *O* section, but putting all of the conductor impedance into one line, and using the other as a ground return.

From an examination of the foregoing conditions, we are led to infer that *in any two-wire artificial-line section, either of the I or O variety, no change is made, either in its angle or in its surge impedance, by changing the proportions of conductor impedance between the two sides.* As an extreme case, all of the line impedance can be collected in one side (as at *A''B''*, Fig. 122), in which case the section becomes a *T* or *II* section of double surge impedance.

Alternating-current Track-signaling Circuits.—Many steam railroads employ automatic block-signal systems, in which the bonded track rails form the operating conductors. A very simple set of connections in such a system is indicated in Fig. 123. An a.c. transformer *T*, at position *A*, supplies say 8 volts, at 25~, to the rails of the track *AB*, through the current-limiting resistance, *r*. The rails are electrically disconnected at the insulating points *II, II*. A track relay *R*, at the distant end *B* of the section, is arranged to be operated by the alternating current from *A*, unless a train *N*, at any position between *A* and *B*, establishes a short-circuit between the rails. As soon as the train clears the section, the relay *R* will become reenergized.

The two rails of the track, if properly and uniformly bonded at joints, form the two conductors of a two-wire circuit, with an impressed e.m.f. at *A*, and a permanent load at *B*. The leakage across the track due to moisture in the ties and ballast, will tend to develop a uniformly distributed leakance, the linear value of which will depend upon the chemical and mechanical conditions of the track, and also on the weather. It is reported, as the result of many electrical observations on a variety of lengths and locations of track, that this linear leakance, at any one locality and time, is substantially uniform and uniformly distributed; so that this distributed leakance obeys Ohm's law sufficiently nearly to admit of being treated as uniform, in the engineering application of the hyperbolic theory.

The linear impedance of the track rails will depend upon their size and shape, the conductivity and permeability* of the steel at

* "Experimental Researches on the Skin Effect in Steel Rails," by A. E. KENNELLY, F. H. ACHARD and A. S. DANA, *Journal of the Franklin Institute*, August, 1916, pp. 135-189.

the working temperature, on the impressed frequency, the current strength, and on the nature of the bonding. Tables of linear impedance* for different sizes of rails and different kinds of bonding have been prepared by Railway Signal Engineers. Its size is estimated to vary between 0.3 and 1.5 ohms per track km. (0.1 and 0.5 ohm per track 1,000 ft.), and its slope between 12° and 66° . The linear leakance may also vary between 0.15 and 1.2 mhos per track km. (0.05 and 0.4 mho per track 1,000 ft.), according to the nature of the ballast, and the wetness of the same. This linear leakance is relatively so large that the capacity susceptance is ordinarily negligible.

In preparing an artificial line to represent a signal circuit of given length and track conditions, the linear resistance would be taken from tables, for the rail size and character of bonding, as well as for the impressed frequency of the signaling current. The linear leakance would naturally be selected at a reasonable maximum value† likely to be met with under the worst prevailing weather conditions. If the signaling apparatus worked with an ample margin of safety in the laboratory on such an artificial line, it might be expected to work satisfactorily over the corresponding actual track circuit under all normal operating conditions, all defective rail bonds having been removed.

A particular 1-km. section of track is indicated at AB in Fig. 124. Here the linear impedance is taken as $z_{\prime\prime} = 1.18\angle 22^\circ.2$ ohms per track km. ($0.36\angle 22^\circ.2$ ohm per track 1,000 ft.) and $y_{\prime\prime} = 0.563\angle 0^\circ$ mho per track km. ($0.172\angle 0^\circ$ mho per track 1,000 ft.). These conditions lead to $\theta = 0.815\angle 11^\circ.1$ hyp. per km. and $z_{o,\prime\prime} = 0.725\angle 11^\circ.1$ ohm, or $y_{o,\prime\prime} = 1.380\angle 11^\circ.1$ mhos.

The correcting factors for the equivalent circuits of this length of track are indicated in Fig. 124. The larger is $1.106\angle 2^\circ.3$. For shorter lengths of track, these correcting factors would be nearer to unity. For lengths of 0.25 km. or less, the nominal T 's and Π 's would be substantially equivalent T 's and Π 's.

The equivalent I section for 1 km. is indicated at $A'B'$. Each line wire has $0.562\angle 21^\circ.1$ ohm, and the central leak has $1.608\angle 2^\circ.3$

* "Alternating-current Signaling," by HAROLD MCCREARY, Union Switch and Signal Co., Swissvale, Pa., 1915, p. 440.

† "Electric Interlocking," by the Engineering Staff of the General Railway Signal Co., Rochester, N. Y., 1915.

† *Technological Papers of the Bureau of Standards*, No. 75, "Data on Electric Railway Track Leakage," by G. H. AHLBORN, August, 1916.

ohms. The equivalent T is found on either side of the neutral line NN' .

The equivalent O section is shown at $A''B''$. It has $0.653\angle 24^\circ.5$ ohm on each side, and $3.81\angle 1^\circ.1$ ohms in each leak. On each side of the neutral line $N''N'''$ is an equivalent Π .

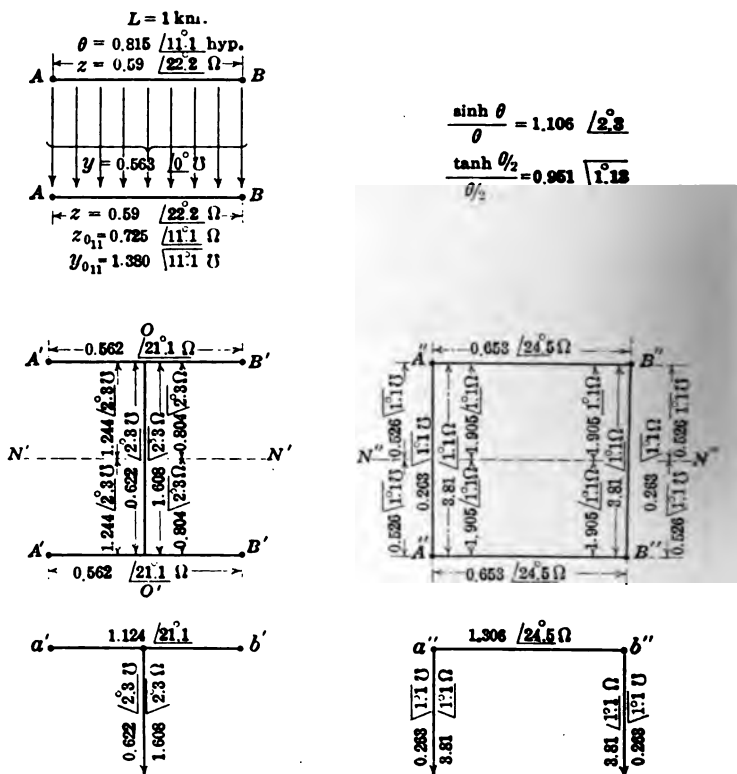


FIG. 124.—Diagrams of a particular 1-km. track section and its equivalent circuits.

At $a'b'$ is the equivalent T with double surge resistance, and at $a''b''$ is the corresponding equivalent Π with double surge resistance.

By making up a set of such similar equivalent sections for various lengths of track, say three of 1 km., two of 0.5 km., two of 0.25 km., and two of 0.125 km., it would be readily possible to connect up an artificial track line of any desired length from 0.125 km. up to 4.75 km. On this artificial line, any specific

piece of apparatus such as a track relay might be tested under conditions resembling those occurring in actual operation.*

Fig. 125 shows an artificial track circuit for connecting various lengths of line with suitable e.m.f. and auxiliary devices, on a pair of switchboards, as used by the General Railway Signal Co.

Artificial Telephone Lines.—Fig. 126 shows a convenient and portable form of artificial twisted-pair standard telephone cable as constructed by the Western Electric Co. for comparative tests, either electrical or auditory, on actual operating telephone cir-

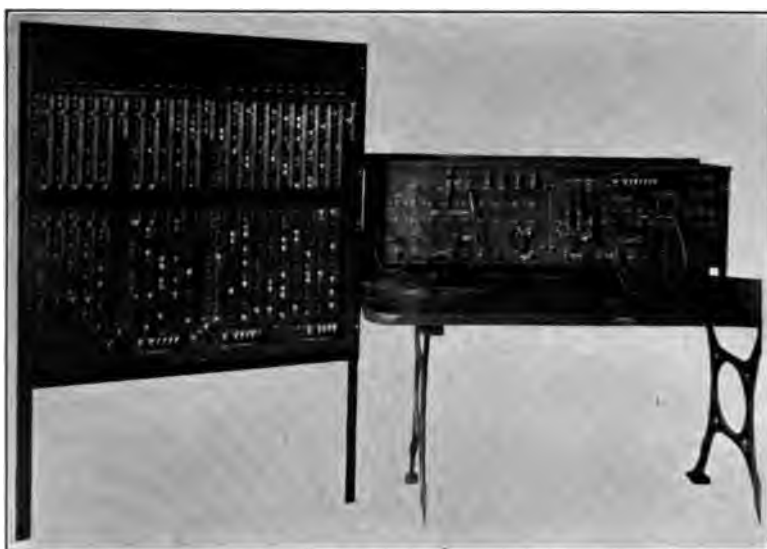


FIG. 125.—Artificial track circuit used by the General Railway Signal Co.

cuits. The approximate inside dimensions of the box are 35.5 cm. by 19 cm. by 14 cm. deep (14 in. by 7.5 in. by 5.5 in. deep). The electrical connections are indicated in Fig. 127. The box contains 32 miles (51.5 km.) of artificial cable in 7 sections of 16, 8, 4, 2, 1, and 1 miles. Each 1-mile section has 88 ohms conductor resistance and 0.08 μf . intercapacitance, as at *AB*, Fig. 122. These sections are connected each to a quadruple group of binding posts along the central line. A pair of throw-over double-blade switches are also connected to each section, in such a man-

* L. V. LEWIS, *The Signal Engineer*, July, 1911. "Analytic Method of Solving Track Circuit Problems," by C. F. ESTWICK, *Journal of the Railway Signal Association*, May, 1916, 21st year, No. 2, pp. 348-362.

ner that when *AA* and *BB* are made the main terminals of the line, each pair of switches brings in a section when thrown in-



FIG. 126.—32-mile artificial twisted-pair standard telephone cable.



FIG. 126A.—Western Electric Company's artificial aerial telephone line
ward, and cuts it out of circuit when thrown outward. As connected in Fig. 127, there is one section of 2 miles (3.2 km.) left inserted in the line. By selecting the proper combination o

switches, any integral number of miles of standard cable between 1 and 32 inclusive can be connected in circuit.

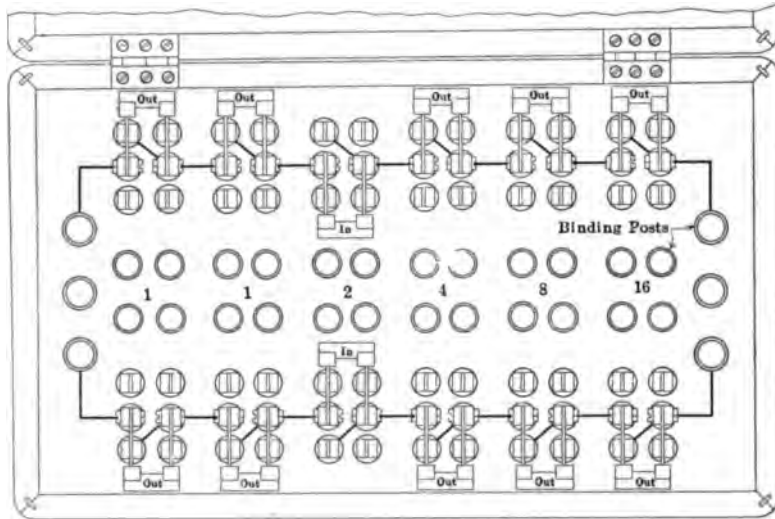


FIG. 127.—Connection-diagram of Western Electric artificial telephone line.

A larger Western Electric Co.'s artificial telephone line box is illustrated in Fig. 126A. It contains 1 sections of artificial No.



FIG. 128.—Box of artificial line for submarine telegraph cable, containing distributed resistance and capacitance.

12 N.B.S. gage, diameter 0.104 in. (2.64 mm.) aerial open two-wire line of the following constants, $r_{..} = 10.4$ ohms/loop mile (6.46 ohms/loop km.), $l_{..} = 3.67$ millihenrys/loop mile (2.28

millihenrys/loop km.), and $c_s = 8.35 \text{ m}\mu\text{f./loop mile (5.19 m}\mu\text{f./loop km.)}$.* The plan of connection by switches is the same as in the box of Fig. 126. By means of these switches, any length between 10 miles (16 km.) and 600 miles (966 km.) of two-wire line may be inserted by 10-mile steps.

Artificial Submarine Cables.—A box of smooth artificial line containing resistance and associated distributed capacitance for a particular type of submarine cable is represented in Fig. 128. The box contains the equivalent of about 60 nauts. of ordinary cable (112 km.). The distributive association of resistance and capacitance in such a box has already been described in Chapter I.

* $\text{m}\mu\text{f}$ is a symbol for millimicrofarad or 10^{-9} farad.

CHAPTER XIII

TESTS OF ALTERNATING-CURRENT ARTIFICIAL LINES

Steady-state tests of artificial lines are ordinarily of three kinds, namely: (1) Tests of plane-vector impedance or admittance; (2) tests of plane-vector potential; (3) tests of plane-vector current. These tests may need to be made at any point along the line, and especially at any section junction.

Impedance Tests.—Impedance or admittance tests are ordinarily one of two types: (1) Bridge tests by some null method;

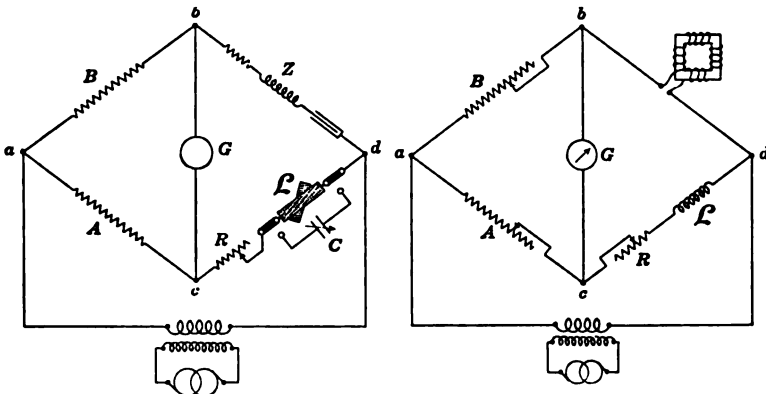


FIG. 129.

FIG. 130.

FIG. 129.—Rayleigh bridge.

FIG. 130.—Modified Rayleigh bridge for measurement of one of a series of nearly uniform impedances in terms of a fixed inductance standard.

and (2) equality of potential-difference tests, by electrostatic voltmeter.

Bridge Balances.—In order to measure the vector impedance or admittance of an a.c. line, it is necessary to obtain a bridge balance with both resistance and reactance. One method of such measurement employs the Rayleigh bridge, which has an adjustably variable inductance L in that arm of the quadrilateral (Fig. 129) which equilibrates the line to be measured. When the line is condensively reactive, an adjustable capacitance C may be used instead of an adjustable inductance. The balance is noted either

on a vibration galvanometer, tuned to the measured frequency of the testing alternating e.m.f., or on a pair of head telephones substituted for the galvanometer. In case a variable inductance standard is not available, a fixed standard inductance may be employed of the same order of magnitude as that to be measured. In that case (Fig. 130), the ratio arms A and B must be so ad-

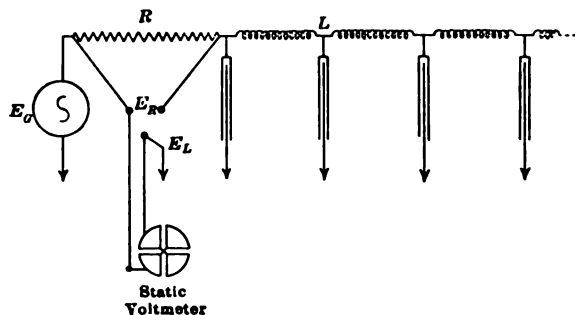


FIG. 131.—Connections for sending-end impedance measurement.

justed for balance with the aid of a rheostat R , that their ratio corresponds both to the resistances and inductances of the arms bd and cd . This dual ratio is sometimes tedious to attain.

Tests of Equality of Potential Difference.—Fig. 131 indicates a method of measuring line impedance when a bridge balance or equivalent null method is unavailable, and when a suitable electrostatic voltmeter is at hand.

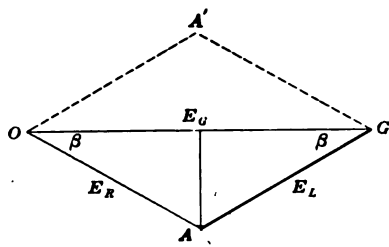


FIG. 132.—Graphic method of determining the line impedance.

The a.c. testing source E_G of carefully measured and controlled frequency, is impressed upon the artificial line to be tested, through the non-inductive adjustable resistance R . The electrostatic voltmeter is connected alternately to read the voltage drop in the resistance R , and in the line to

ground. The resistance R must then be adjusted, by successive trials, until these two readings are equal. This means that the size of the line impedance is equal to the numerical value of the resistance R , in ohms. By repeating the observations many times, this adjustment can be made with considerable precision. After equality has been obtained, the two voltmeter readings are

recorded, and the reading from the generator to ground is noted. This reading, the voltmeter connections for which are indicated in Fig. 131, corresponds to the total drop in line L and resistance R together.

From the calibration curve of the voltmeter, the three voltage drops or potential differences E_G , E_L , and E_R , are found. The former represents the size of the total p.d. The other two have been made equal by adjustment, and represent the sizes of the line p.d. and resistance p.d. In Fig. 132, let OG be drawn to scale to represent E_G , and likewise OA and GA , to represent E_R and E_L . Then, since the same a.c. produces all three p.d.s., the diagram may be regarded as an impedance diagram to a suitable scale, as well as a voltage diagram. The impedance scale must be such that if the length of OA be taken numerically equal to

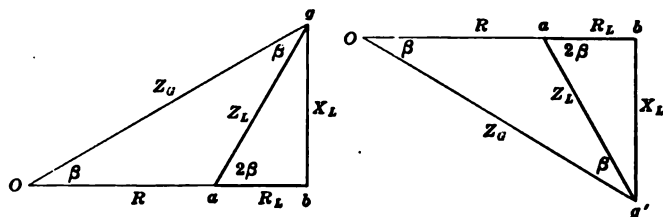


FIG. 133.—Indeterminate alternative vector diagrams obtainable from line-impedance measurements conducted as in Fig. 131.

the adjusted resistance R at equality, E_L will represent the impedance offered by the line, both in size and slope.

The line impedance, whose size is R , will now have a slope of $2\beta^\circ$, where β° is the angle AOG .

In practice, it is not necessary to draw the diagram, because evidently

$$\cos \beta^\circ = \frac{E_G}{2E_R} \quad \text{numeric} \quad (397)$$

Knowing E_G and E_R , β° may be immediately obtained from tables of circular functions.

Strictly speaking, the method is open to ambiguity in interpretation; because the line impedance may be either $R \angle \beta^\circ$, or $R \sphericalangle \beta^\circ$, as is shown by Fig. 133. The uncertainty may be overcome, either by preliminary rough computation, as to whether the line is inductive or condensive; or else a definite increment of reactance, such as a suitable reactor or condenser, should be added to the testing end of the line, and the test repeated. Knowing

the sign and approximate magnitude of the reactance increment, the interpretation of the sign of the slope β° should thus be reduced to certainty.

The precision of the test in regard to the slope β° is usually distinctly less than in regard to the size R , because of the effect a small error in voltmeter reading or in the voltmeter calibration may have in (397).

Potential Tests.—There are two types of tests for measuring the potential along the line, namely: (1) a.c. potentiometer tests; and (2) electrostatic voltmeter tests.

The Drysdale-Tinsley c.c. and a.c. potentiometer measures both the size and the slope of the a.c. potential applied to its test terminals. A view of the instrument is presented in Fig.



FIG. 134.—Drysdale-Tinsley a.c. and e.c. potentiometer.

134, and a simplified diagram of the principal connections appears in Fig. 135. In the latter, the a.c. mains MM , $M'M'$, supply both the testing transformer T_1 , for energizing the artificial line AB , and the split-phase rotary-field transformer T_2 , for delivering any desired phase of e.m.f. in the secondary circuit to the slide wire of the potentiometer. The phase-splitting is accomplished by means of the adjustable rheostat r , and condenser C . The values of resistance and capacitance, at r and C , necessary for splitting the phase, vary with the impressed frequency, and have to be adjusted by trial, at the frequency of the test, until the e.m.f. in the secondary circuit of T_2 has the same size at all positions of the secondary coil, which is capable of being moved around the circle by means of the handle L (Fig. 134).

The potentiometer is first calibrated for continuous currents,

by throwing the change-over switch *H* to the points *p**q*. This permits the working e.m.f. *E* of 8 volts to flow through the slide wire *WW*, dynamometer milliammeter *D*, and the controlling rheostat *R*. When the standard Weston cell *S* has established zero balance at 1.018 volts on the slide wire, with the aid of the c.c. galvanometer *g*, the milliammeter *D* should indicate precisely 50 milliamp. on its scale. With this adjustment, the instrument can be used to measure c.c. potentials, up to 1.8 volts, in the usual way.

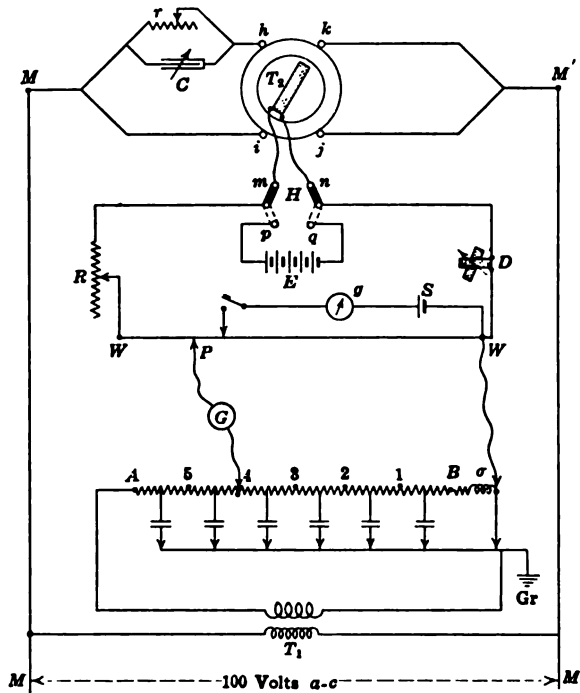


FIG. 135.—Simplified connections of a.c.-c.c. potentiometer.

If the change-over switch *H* is then thrown over to the points *m**n*, an a.c. potential difference of 8.0 volts, and adjustably controllable phase, is supplied to the slide wire, from transformer *T₂*, through dynamometer milliammeter *D*, and rheostat *R*. The latter must be so adjusted as to bring the pointer of *D* exactly back to 50 milliamp.

The slide wire will then carry just the right current to indicate correctly in r.m.s. volts. If now we connect any a.c. potential

difference less than 1.8 volts, such as that between junction 4 and ground, to the slide wire, through a tuned vibration galvanometer G , the latter can show zero current only when the size and slope of the slide-wire potential and junction-4 potential are respectively equal. The zero-current indication of G must, therefore, be reached by successive adjustment of the size and slope of slide-wire potential. The size can manifestly be adjusted by sliding the contact pointer P along the wire WW , and by the usual drop rheostats dd . The slope can be independently adjusted, by rotating the secondary winding of the rotary-field transformer T_2 , under the control of handle L . The tuned vibration galvanometer G will show zero current when both the slide reading and the phase reading are conjointly in proper adjustment. Reduction to zero reading must, therefore, be effected in alternate steps on the slide and on the phase shifter. The potential differences are thus read of the type $E\angle\beta^\circ$, or $E\searrow\beta^\circ$, the phase being taken with respect to that of the impressed 100 volts single-phase e.m.f. at the split-phaser, within the range 0 – 1.8 volts in E , and $\pm 180^\circ$ in β° .

The precision of the instrument,* with some practice, is considerable, although not up to that obtainable when it is used for d.c. measurements, because the calibration of the slide wire is determined by the full-scale deflection of the milliammeter A , instead of by a null method.

A convenient form of vibration galvanometer for use with the instrument, when the frequency is between about 20~ and 100~ is shown in Figs. 136 and 137. Alternating current in the coil C impresses a cofrequent vibromotive torque on the suspended magnet ns . The galvanometer is easily tuned, by sliding a magnetic shunt S over the poles of the controlling permanent magnet M , under the control of the projecting screw shaft Sc . The e.c. resistance of the coil C is ordinarily 40 ohms, and the sensibility of the instrument, at 50~, is about 4 mm. per microamp. at 1 m.

The potentiometer itself may be employed up to a testing frequency of 1,000~ or over, if a correspondingly tuned vibration galvanometer is used.

* C. V. DRYSDALE, "The Use of the Potentiometer on Alternating-current Circuits," *Phil. Mag.*, vol. xvii, p. 402, March, 1909; also *Proc. Phys. Soc.*, London, vol. xxi, p. 561, 1909; also *The Electrician*, London, vol. lxxiii, p. 8, April 16, 1909; also J. A. FLEMING's "Propagation of Electric Currents in Telephone and Telegraph Conductors," 1911, London, p. 216.

In order to make the apparatus available, the impressed a.c. frequency must be held nearly constant; not only on account of potential variations along the line, caused by variations in fre-

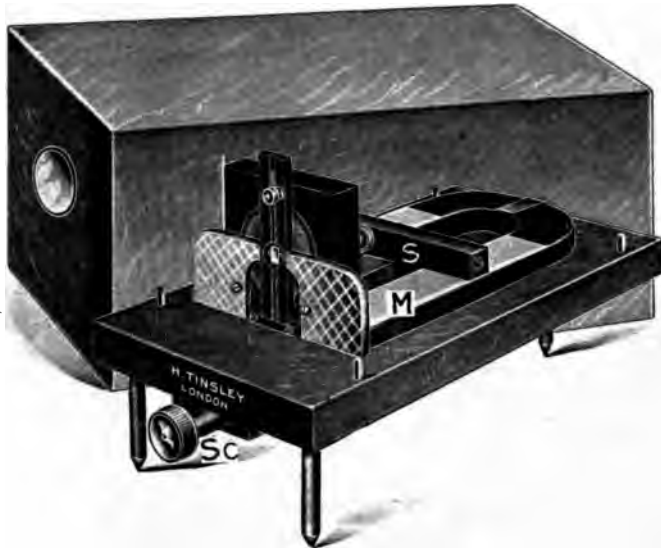


FIG. 136.—Vibration galvanometer.

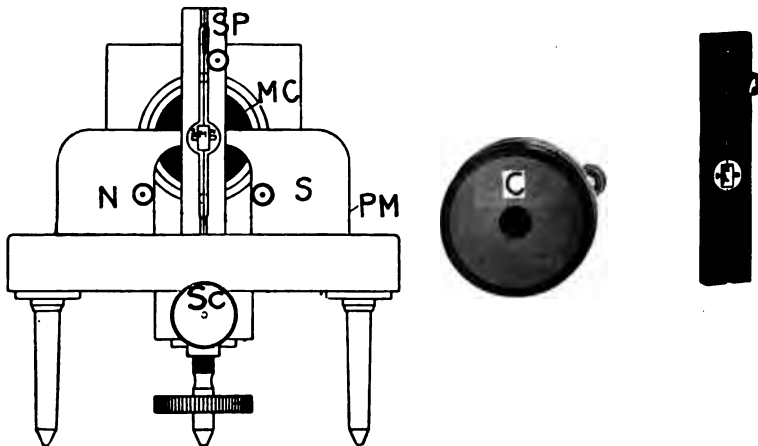


FIG. 137.—Front elevation and details of vibration galvanometer.

quency, but also because the auxiliary split-phasing and galvanometer tuning become distressingly upset when the impressed frequency changes. If, however, the frequency cannot be held

sufficiently uniform to make the apparatus serviceable, the observed values of impedance, potential and current, along the line, are not likely to be closely dependable under any method of measurement.

Line Potentials by Electrostatic Voltmeter.—If an a.c. voltmeter is used to determine the potentials at line junctions or mid-sections, it is very desirable to use an electrostatic voltmeter, in order to avoid the reduction of potential brought about by the

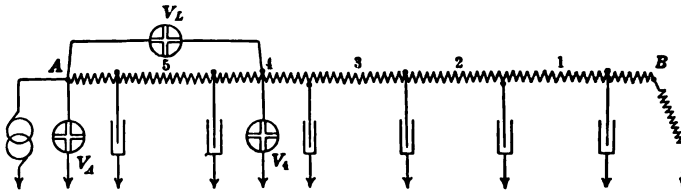


FIG. 138.—Connection diagram for plane-vector potential test along a.c. artificial line.

admittance of the instrument. In practice, a good arrangement is to employ one electrostatic voltmeter over the range between 2 and 20 volts, another over the range between 20 and 100 volts, and a third for higher voltages. The calibrations should be carefully checked, from time to time, on storage-battery voltages.

Since an electrostatic voltmeter, used in the ordinary way, measures the size but not the slope of the a.c. voltage to which

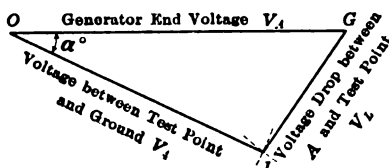


FIG. 139.—Triangle of three observed voltages for determining their phase relations.

it is applied, additional measurements are needed in order to evaluate the slope.

Fig. 138 shows a method for carrying out this plan. If the potential V_4 has to be measured between junction 4 and ground, the potential V_A , at the generator end is also measured, as well as V_L the voltage drop between A and 4. In practice, V_A is measured once for all, and held constant by means of an auxiliary a.c. voltmeter, which need not be electrostatic. A single testing electrostatic voltmeter is used to measure V_L and V_4 , alternately in succession. The three values V_A , V_L and V_4 determine a voltage triangle, from which the phase or slope of V_4 can be determined, in the manner indicated in Fig. 139, where OG is the generator voltage V_A at A, GJ the voltage drop

TABLE XV
Distribution of Voltage and Current over the Line at 60.7 Cycles per Second, Distant End Free

Junction	Distance from receiving end		Angular distance from receiving end, hyps.	Potential at each junction, volts						Current in each mid-section, amperes			
	Km.	Miles		Observed by potentiometer		Observed by static voltmeter		Computed		Observed by potentiometer		Computed	
				Magni-tude	Phase	Magni-tude	Phase	Magni-tude	Phase	Magni-tude	Phase	Magni-tude	Phase
0	1,040	646.1	1.405/69°.7	100.0	∇0°		100.0	∇0°	0.506	/41°.9	0.506	/41°.9	
1	960	596.0	1.297 "	102.8	∇11°.8	101.8	102.4	∇11°.2	0.475	/38°.0	0.472	/38°.2	
2	880	547.0	1.189 "	108.5	∇21°.9	108.1	107.0	∇21°.7					
3	800	497.0	1.135 "	115.3	∇30°.6	115.5	114.6	∇30°.5	0.446	/36°.2	0.446	/36°.3	
4	720	447.0	1.081 "	123.7	∇37°.5	124.0	121.1	∇36°.1	0.414	/34°.2	0.416	/34°.7	
5	640	398.0	0.973 "	132.5	∇43°.2	132.8	132.2	∇43°.1	0.377	/33°.0	0.383	/33°.3	
			0.919 "										
6	560	348.0	0.865 "	140.7	∇47°.7	141.2	141.5	∇47°.7	0.344	/31°.1	0.345	/32°.0	
			0.811 "										
7	480	298.0	0.757 "	149.2	∇51°.2	148.3	149.8	∇51°.4	0.305	/30°.0	0.305	/31°.0	
			0.703 "										
8	400	249.0	0.649 "	155.7	∇53°.9	155.7	157.7	∇54°.3	0.262	/28°.5	0.266	/30°.1	
			0.594 "										
9	320	199.0	0.540 "	161.5	∇57°.0	161.8	164.1	∇56°.5	0.214	/28°.1	0.210	/29°.2	
			0.486 "										
10	240	149.0	0.432 "	166.0	∇58°.7	167.0	169.4	∇58°.2	0.170	/25°.4	0.166	/28°.7	
			0.375 "										
11	160	99.4	0.324 "	169.7	∇60°.0	170.7	173.4	∇59°.3	0.124	/25°.0	0.124	/28°.3	
			0.270 "										
			0.216 "										
12	80	49.7	0.162 "	172.6	∇60°.9	172.0	175.8	∇60°.0	0.077	/21°.7	0.074	/28°.0	
			0.108 "										
13	0	0	0.054 "	173.8	∇61°.0	173.3	176.6	∇60°.2	0.023	/20°.5	0.023	/27°.9	
			0										
I	II	III	IV	V	VI	VII	VIII	IX					

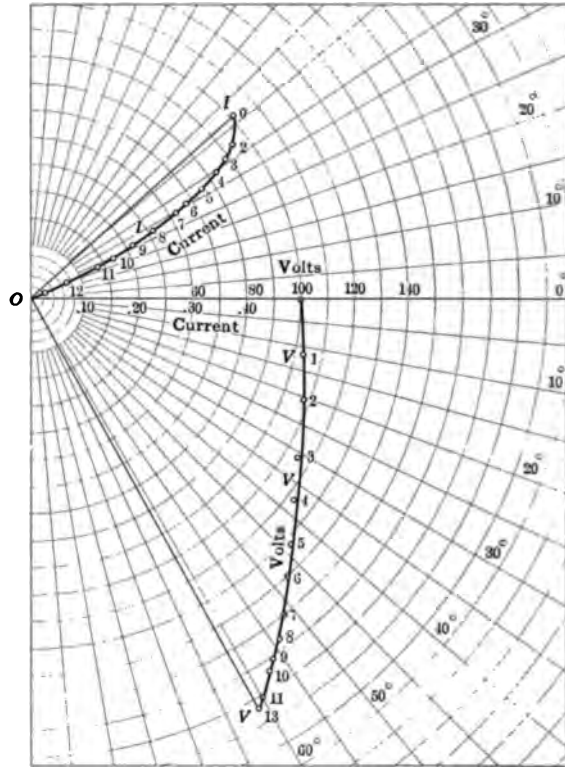


FIG. 140.—Curves showing phase relations of voltage and current for point on the open line.

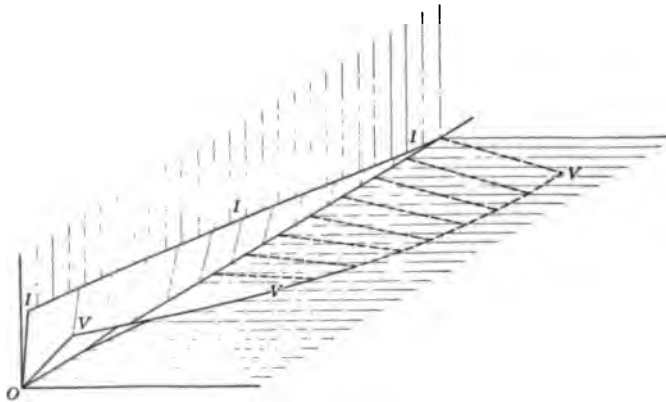


FIG. 141.—Line free at distant end—60 cycles per second.

on the line, and OJ the voltage V_4 at the test point. The size of this voltage in Fig. 139 would be OJ , and its slope $\sphericalangle\alpha^\circ$, taking OG as at standard phase. The triangle is easily produced graphically, using the points O and G as successive centers, with intersecting arcs at J . The circular angle α° is then measured with a protractor. There is a possible ambiguity as to the side of OG on which the triangle should lie, which means that the slope

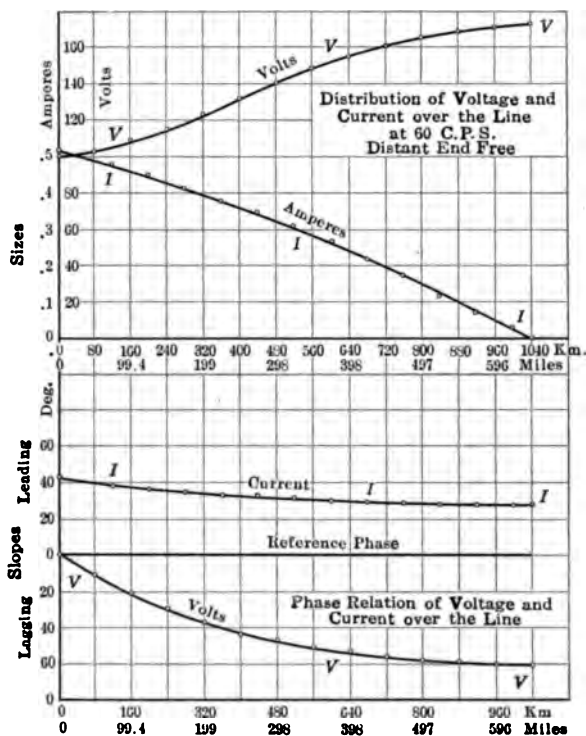


FIG. 142.—Voltage, current and phase relations along line at 60 cycles per second and no-load. Rectangular coördinates.

α° might be either $\sphericalangle\alpha^\circ$ or $\sphericalangle\alpha^\circ$; but ordinarily, there is no difficulty in deciding this either by the aid of a rough calculation, or by means of a special test with an added known reactance.

The triangulation is repeated at each junction on the same sheet of polar coördinate paper, keeping the generator end voltage V_A constant, say at $100\angle 0^\circ$ volts. Fig. 140 gives an example of this procedure in the particular case of a 13-section line of the type defined in Table XII and representing 1,040 km.

of aerial power-transmission conductor operated at 60.7~, with the distant end free, and with 100 volts r.m.s. impressed at the generator end. The successive vertices of the triangles obtained from electrostatic voltmeter measurements fall on the points 1, 2, 3, . . . 13, which, connected by the line *VVV*, show the graph of potential along the artificial line, and also, by inference, on the conjugate smooth line at this frequency. The open-end voltage is $173.8\sqrt{61}^\circ$. The observations are recorded both by voltmeter and potentiometer for this case in Table XV.* Two other methods of presenting the results of these observations to the eye are given in Figs. 141 and 142.

Relative Advantages of Potentiometer and Voltmeter Methods.

—The electrostatic voltmeter method of measuring line potentials has the advantage that its technique is simple and requires but little preparation. Impressed potentials of 100 volts r.m.s. are ordinarily applicable with it. Disadvantages are that its precision is seldom very high, because it is a deflection method, and moreover, if there are harmonics in the wave of impressed voltage, these enter into the measurements by perpendicular summation, as already described, and vitiate the results for the fundamental frequency as obtained by computation. The potentiometer method, on the other hand, is capable of much greater precision, and the tuned vibration galvanometer responds almost entirely to the fundamental sinusoid, but it involves a more elaborate technique. For class-laboratory work, therefore, the easier voltmeter method is to be preferred, unless the generated voltage wave available is very impure. For research purposes, the potentiometer is superior. In potentiometer measurements, it may be advisable to limit the impressed voltage at the generator end to 1.8 volts, so as to dispense with multipliers and their attendant errors.

Relations between the Impressed Voltage, the Current and Power.—In Fig. 143, we have an artificial line whose line impedances and leak admittances may be assumed properly to correspond with those of a certain imitated conjugate smooth line. The motor-end load *Z*, also has the same apparent impedance as the load which the actual line has to carry, as determined by the vector ratio of receiving-end volts to amperes. We

* "Measurements of Voltage and Current over a Long Artificial Power-transmission Line at 25 and 60 Cycles per Second," by A. E. KENNELLY and F. W. LIEBERKNECHT, *Proc. A. I. E. E.*, June 25, 1912.

have to consider how the current and power in the artificial-line impedance model compare with those on the actual line as the impressed voltage is varied.

It will be evident, on examination, that if the voltage impressed on the artificial line in the laboratory is $1/n$ th of that impressed on the actual line at the same frequency, the artificial-line currents will be $1/n$ th those at corresponding points on the actual conjugate smooth line, and the artificial line powers will be $1/n^2$ those on the actual line. Thus if the star voltage on a three-phase transmission line is say 10,000 volts r.m.s. to neutral, and its conjugate artificial-line impedance model is operated at 10 volts r.m.s. to ground, or $1/1,000$ th of the actual working pressure, then each milliampere of observed current at junctions will correspond to an ampere on the actual line, and each micro-watt of power on the artificial line will represent 1 watt on the actual line. The results obtained in the laboratory are, therefore,

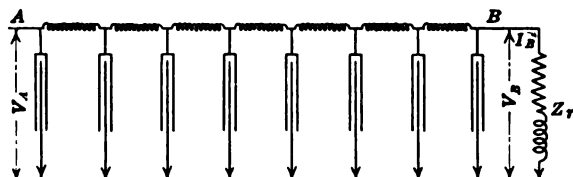


FIG. 143.—Impedance model of a single-phase, single-wire line and its receiving-end load.

readily interpretable in ordinary magnitudes, if we maintain the correct motor-end load impedance.

The effects of synchronous-motor or "rotary-condenser" compensation at any point on the line, say at the receiving end, on the voltage regulation, can be investigated experimentally by connecting the proper equivalent reactance to the line at that point, and studying the corresponding distributions of potential and current.

Current Tests.—There are three types of tests for alternating current along an artificial line; viz., potentiometer tests, fall of potential tests, and ammeter tests.

Potentiometer Tests for Vector Current.—In this method, a small non-inductive resistance of manganin strip, say 0.1 ohm, is inserted in the line at the test junction, and the vector voltage drop in this measured at its terminals by a.c. potentiometer. This method succeeds well at low frequencies, and the error

introduced by the insertion of 0.1 ohm at any junction is ordinarily unimportant. This is a useful "research method." An appropriate set of contact plug connections is indicated in Fig. 144.

Sectional Fall of Potential Tests.—When an electrostatic voltmeter capable of measuring from 2 to 20 volts is used, the voltage drop upon a reactor in the line, adjacent to the test point, can be observed. Knowing the vector impedance of the reactor, and the slope of the vector drop from triangulation, as above described, the vector current strength in the reactor can be immediately deduced by Ohm's law. This is a useful "laboratory-class method."

Ammeter Tests.—Occasionally, the line currents may be observed directly by the insertion of a suitable a.c. ammeter at the

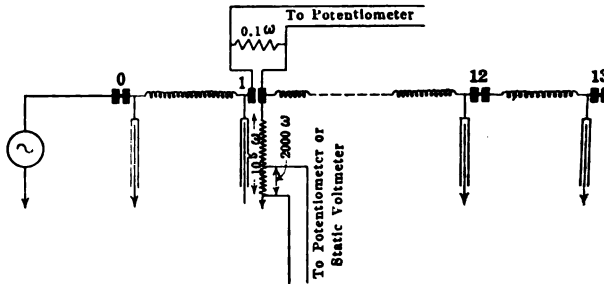


FIG. 144.—Connections used in a series of measurements of potential and current along the line.

test junction. Ordinarily, however, the impedance of the ammeter is sufficiently great to introduce an appreciable error into the line distributions.

Distribution of Test Operations among Observers.—It is possible for a single observer, if he has ample time at his disposal, to make, unaided, all the observations of potential and current along an artificial line, if all the apparatus and controlling devices are conveniently arranged. It is much easier, however, for two observers to carry on the work between them. As many as six observers may coöperatively take part in the observations, with mutual advantage, especially if the electrostatic voltmeter methods are used.

There are a number of tests which can be effectively carried out by students of electric transmission on an artificial line with different line lengths, impressed frequencies, loads, load

power factors and positions of load. As a rule, such tests on a.c. artificial lines should be preceded by preliminary tests on c.c. artificial lines. Such a.c. experiments properly checked, and supported by computation, give the student an unassailable comprehension of essential steady-state a.c. line phenomena.

Barretter Tests.—The Fessenden hot-wire barretter has been employed in measuring apparatus for determining the distribution of potential and current over an artificial telephone twisted-pair line.* The barretter consists of a little filamentary loop of platinum a few millimeters long, and a few microns in diameter, etched electrochemically out of a piece of platinum-cored silver Wollaston wire, and warmed by the passage of the feeble alternating current to be measured. The rise in temperature is detected by change in the resistance of the filament in a local c.c. circuit.

The technique of these barretter instruments is somewhat difficult, and the barretters themselves are apt to burn out by accidental current overloads. Improvements in a.c. potentiometer testing methods, employing the inherent sensitiveness of the vibration galvanometer, have brought the latter methods to the front rank, and they are likely to be still further improved. In special cases, however, the barretter method has undoubted advantages.

Measurements of Individual Inductances.—Although the measurement of the inductance of a line-section reactor belongs to the general domain of laboratory electrical measurement rather than to the particular province of artificial lines, yet it may be of service to offer a brief outline of the tests which have been found to be conveniently adapted to the measurement of artificial-line section elements. For more detailed and comprehensive information, the reader may refer to text-books on electrical measurements.

In addition to the Rayleigh-bridge method already described in connection with Figs. 129 and 130, there are at least two

* "High-frequency Telephone Circuit Tests," by A. E. KENNELLY, *Proc. Int. El. Congress St. Louis*, sec. G, vol. iii, pp. 414-437, 1904.

"On the Production of Small Variable-frequency Alternating Currents Suitable for Telephonic and Other Measurements," by B. S. COHEN, *Phil. Mag.*, September, 1908, and *Proc. Phys. Soc.*, London, vol. xxi, 1909, p. 283.

"Description et Utilisation de la Méthode pour la Mesure des Constants de Ligne au Moyen du Barretter," BELA GATI, *La Lumière Elec.*, October, 1908.

other bridge methods which have been found useful in the measurement of line-section reactor inductances, namely:

1. The Anderson bridge.
2. The Campbell bridge.

It is always desirable to employ at least two methods in the measurement of the section inductances, especially when the reactors are non-ferric, and a fairly high degree of precision is aimed at. In the tests by different methods, different rheostats, instruments and parts should be employed, as far as possible. If the results arrived at, with different apparatus, in these differ-

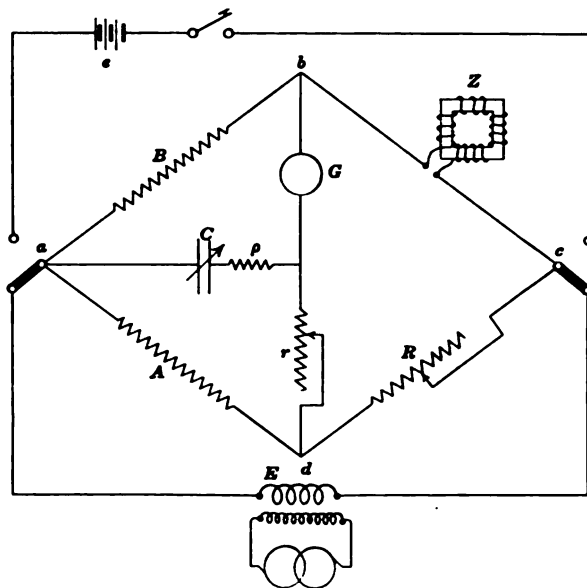


FIG. 145.—Anderson bridge for measuring impedance.

ent ways, are in close agreement, their mean values become correspondingly reliable.

The Anderson bridge is indicated in Fig. 145. The reactor Z is first balanced to continuous currents by the resistance R and an ordinary c.c. galvanometer G . Leaving A , B , R and Z unchanged, the a.c. source E is substituted for the c.c. source e , and either a telephone or a vibration galvanometer for the c.c. galvanometer. An a.c. balance is then obtained by adjusting the condenser C , with the aid perhaps of adjustment in the bridge-wire resistance r . The final capacitance of the condenser C is supposed to be known. The inductance L of the reactor is then

$$L = \frac{CB}{1 + \rho^2 C^2 \omega^2} \left(r + \frac{Rr}{A} + R \right) \text{ henrys (398)}$$

Here ρ is the effective internal resistance in ohms of the capacitance C at the testing angular frequency ω radians per sec. If the capacitance C is pure, $\rho = 0$, and the formula reduces to the well-known form

$$L = CB \left(r + \frac{Rr}{A} + R \right) \text{ henrys (399)}$$

This method is very serviceable when a suitably adjustable condenser is available.*

The Campbell Mutual-inductance Bridge.—Another convenient device for measuring the inductance of line reactors with

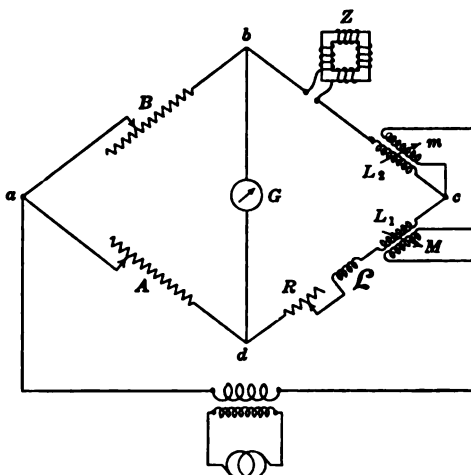


FIG. 146 — Campbell bridge for measuring impedance.

precision is the Campbell mutual-inductance bridge, the connections for which are indicated in Fig. 146. The bridge arms A and B are adjustable anti-inductive rheostats. The zero-current indicating instrument G is preferably a vibration galvanometer tuned to the frequency of the a.c. testing source. The inductometer Mm consists of a pair of like coils L_1L_2 , with adjustable and measurable mutual inductance on the secondary windings M and m . Assuming that the bridge arms A and B

* "A Handbook for the Electrical Laboratory and Testing Room," by J. A. FLEMING, vol. ii, p. 192.

"The Propagation of Electric Currents in Telephone and Telegraph Conductors," by J. A. FLEMING, 1911, p. 208.

are equal, it is necessary for a zero balance in G that the resistances of the arms bc and cd should be made equal, by adjusting the resistance R , and also that the inductance of the reactor Z should be balanced with the aid of the mutual inductances M and m . The unknown inductance L_x will then be*

$$L_x = \mathcal{L} + 2(M + m) \quad \text{henrys (400)}$$

where \mathcal{L} is the auxiliary fixed inductance inserted in the arm cd in cases where the mutual-inductance range $(M + m)$ is less than half the inductance L_x to be measured.



FIG. 147.—Campbell variable mutual inductance.

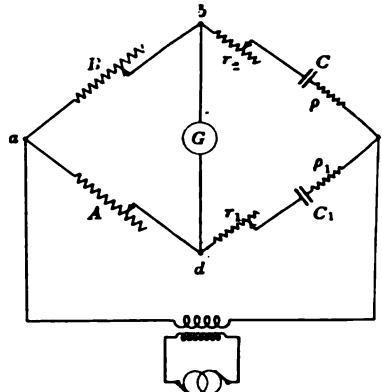


FIG. 148.—Connections for condenser test.

The Campbell variable mutual inductance containing the coils L_1L_2M and m is illustrated in Fig. 147. The primary coils L_1L_2 , (Fig. 146) of about 6 ohms each, are connected to the binding posts on the right-hand side. The secondary coils, of about 7 ohms' in all, are connected to the terminals on the left-hand side. The graduated dial indicates to microhenries.

Measurements of Section Capacitances.—Since mica condensers in sufficient number to satisfy an ordinary artificial line are expensive and difficult to obtain, condensers of rolled impregnated paper are customarily employed. Such condensers vary appreciably in capacitance and leakage at different frequencies,

* "On the Use of Variable Mutual Inductances," by A. CAMPBELL, *Phil. Mag.*, January, 1908, pp. 155-171; also *Proc. Phys. Soc. London*, vol. xxi.

"The Use of Mutual Inductometers," by A. CAMPBELL, *Phil. Mag.*, April, 1910, pp. 497-507; also *Proc. Phys. Soc. London*, vol. xxii.

ordinarily diminishing in capacitance and increasing in leakance, as the frequency and temperature rise; so that it is desirable to measure these quantities at the frequency and temperature which are to be employed in the tests.

Two convenient methods are available for measuring the capacitance and leakance of a condenser,* namely:

1. The series-resistance method.
2. The Anderson-bridge method.

The Series-resistance Method.—The two condensers to be compared are connected in a bridge as shown in Fig. 148. The two ratio arms of anti-inductive resistance A and B —preferably equal—are adjusted for zero balance on the vibration galvanometer G , which is tuned to the testing frequency. The condenser of C farads under test has a certain equivalent internal series resistance ρ ohms, and the adjustable condenser is C_1 whose internal resistance is ρ_1 . By adjusting C_1 and either r_1 or r_2 , balance is obtained. Then

$$C = C_1 \cdot \frac{A}{B} \quad \text{farads} \quad (401)$$

and

$$\rho = \frac{B}{A} (r_1 + \rho_1) - r_2 \quad \text{ohms} \quad (402)$$

The last formula expresses ρ in terms of the observed resistances r_1, r_2 and the internal resistance ρ_1 of the adjustable condenser. If ρ_1 is not known, some standard mica condenser of small known ρ may be balanced as a substitute for C , so that from it ρ_1 may be determined. The phase angle defect of the condenser C or the complement of its impedance angle will be

$$\phi = \tan^{-1}(\rho C \omega) \quad \text{degrees} \quad (403)$$

The leakance G , in parallel to the condenser, equivalent to the resistance ρ in series with it, is very nearly

$$G = \rho C^2 \omega^2 \quad \text{mhos} \quad (404)$$

Anderson-bridge Method.—The Anderson bridge, already illustrated in Fig. 145, instead of being used to measure an un-

* "Simultaneous Measurements of the Capacity and Power Factor of Condensers," by F. W. GROVER, *Bulletin of the Bureau of Standards*, vol. iii, pp. 371-431, 1907.

"The Capacity and Phase Difference of Paraffined Paper Condensers as Functions of Temperature and Frequency," by F. W. GROVER. *Bulletin of the Bureau of Standards*, vol. vii, No. 4, pp. 495-578, 1911.

known inductance in terms of resistances and a known capacitance, may be used inversely to measure an unknown capacitance in terms of the resistance and a known inductance. A suitable standard condenser of known capacitance and internal resistance is first balanced and the unknown condenser then substituted. From the two balances, both C and ρ can be evaluated.

Frequency Measurements.—Artificial-line tests conducted at power-distribution frequencies call for no recommendations as to the measurement of impressed frequency beyond watchfulness and care. The ordinary laboratory frequency meters, properly checked and calibrated, are satisfactory. A good means of checking the frequency of a vibrating-reed frequency meter is to examine it, in a good light, through the vibrating slits of a stroboscopic tuning fork.*

At telephonic frequencies, however, special methods are needed for measuring frequency with the necessary degree of precision. One means is an improved stop-watch electromagnetic revolution counter.†

A second means is a stroboscopic tuning fork applied to a target mounted on the shaft of the alternator supplying the testing current. In practice it is found convenient to place the testing apparatus within view of, but at a suitable distance from, the alternator. The observer at the apparatus can then control the speed and delivered frequency of the alternator by a hand rheostat, while he watches the stroboscopic image of the illuminated rotating target on the alternator, at a distance of say 15 meters, through a small telescope which has a stroboscopic fork mounted in front of its eyepiece.

A third means is the acoustic tonometer, or series of small tun-

* "The Measurement of Rotary Speeds of Dynamo Machines by the Stroboscopic Fork," by A. E. KENNELLY and S. E. WHITING, *Trans. A. I. E. E.*, July, 1908, vol. xxvii, pp. 727-742.

"Stroboscopic Measurements of Alternating-current Frequency with Electric Lamps," by A. E. KENNELLY, *Electrical World*, Dec. 26, 1908. "Separation of the No-load Stray Losses in a Continuous-current Machine by Stroboscopic Running-down Methods," by D. ROBERTSON, *Journ. Inst. Elect. Engrs.*, vol. liii, February, 1915, pp. 308-322.

"The Stroboscope in Speed Measurements and Other Engineering Tests," by D. ROBERTSON, *Trans. Inst. Engin. and Ship Builders*, vol. vi, 1912-13, pp. 37-82. *Mech. Eng.*, vol. xxxi, 1913, pp. 512-515, 539-543.

† "Experimental Researches on Skin Effect in Conductors," by A. E. KENNELLY, F. A. LAWS and P. H. PIERCE, *Trans. A. I. E. E.*, September, 1915, p. 1757.

ing forks, such as are found in acoustic laboratories. The testing alternating current is supplied through a suitable impedance to an ordinary telephone receiver, and the observer finds by trial the tuning fork giving the pitch nearest to that of the telephonically emitted tone. When the a.c. frequency is steady, as, for example, when it is delivered from a carefully operated Vreeland oscillator, the difference in pitch between the a.c. telephonic tone and the tuning-fork tone can be found by counting acoustic beats during a measured time interval, such as half a minute.

Frequency Limitations of Artificial Lines.—It will be evident from an inspection of Figs. 98 and 99 with their polygonal section voltages and currents, that as the frequency impressed upon an artificial line is increased, the number of sections per wave is diminished, and the lumpiness correction factors tend to increase. There is ordinarily no difficulty in operating an artificial line up to the frequency which provides on the average three sections per wave, although the correction factor is then sensitive to small frequency changes. Operation ordinarily becomes impracticable at or below two sections per wave.

CHAPTER XIV

COMPOSITE LINES

A composite line is a line composed of a plurality of single lines in series, each possessing its own linear electric constants. In practice, composite lines are more frequently met than single lines, especially when long circuits are used. Thus, a telephone circuit may include an underground-cable twisted pair, from the subscribers' set to his local exchange, then a different size of underground-cable pair to the outskirts of the city, then one or more different sizes of overhead copper-pair lines, and finally underground lines to the called subscriber's set. No steady-state working theory of a.c. lines can therefore be satisfactory, which fails to deal with composite lines in a reasonably simple way.

We may first consider the d.c. theory of composite lines employing real hyperbolic functions, and then apply it to a.c. cases, by vector interpretation of the formulas; *i.e.*, by extending them from one dimension to two dimensions.

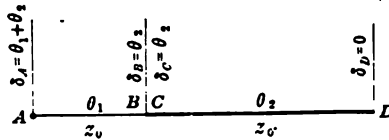


FIG. 149.—Two-section composite line of constant surge resistance.

Case of Two Sections Having Different Linear Constants but the Same Surge Impedance.—If two single lines AB , CD , Fig. 149, are joined at BC , and these lines happen to possess the same value of surge impedance z_0 , then the composite line AD has very simple properties.

Suppose the composite line AD to be grounded at D and voltage at A . Let θ_1 be the angle subtended (18) by AB , and θ_2 that subtended by CD . Then, if we assign position angles to the system, commencing at D where $\delta_D = 0$, we find the position angle at C is $\delta_C = \theta_2$. The line impedance at C is also

$$Z_C = z_0 \tanh \delta_C = z_0 \tanh \theta_2 \quad \text{ohms } \angle \quad (405)$$

The section CD may now be regarded in its entirety as a single

motor-end load applied to the section *AB*. Then by (89), $\sigma = Z_c$ and

$$\tanh \theta' = \frac{\sigma}{z_0} = \frac{z_0 \tanh \theta_2}{z_0} = \tanh \theta_2 \quad \text{numeric } \angle \quad (406)$$

whence $\theta' = \theta_2$. Consequently, at a junction between single lines possessing identical vector surge impedances, the position angles on each side of the junction are equal. The reason for this is that each and every individual electric wave which passes a junction, either way, undergoes no disruption, unless the surge impedances of the sections differ. The wave passes over from one section to the other as though the junction did not exist.

The position angle at *A*, Fig. 149, will now be $\delta_A = \theta_1 + \theta_2$ hyps. \angle , and the distributions of potential, current and impedance will be continuously proportional, respectively, to the sinh, cosh and tanh of the position angle, as on an ordinary single line.

Similar conditions will present themselves if we ground the composite line *AD* of Fig. 149, at *A*, and voltage it at *D*. The position angles will distribute themselves over the system without any discontinuity at the junction *BC*. Again, if one terminal of the composite line, having unchanged surge impedance, is grounded through a terminal load, subtending a terminal angle θ' , the position angles will increase continuously to $\delta_A = \delta_D = \theta_1 + \theta_2 + \theta'$ hyps. \angle at the other end.

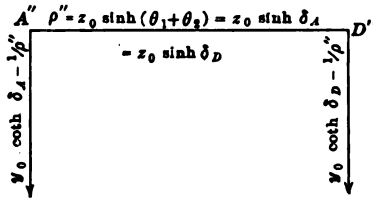


FIG. 150.—Equivalent II of two-section composite line with constant surge impedance.

Equivalent II of Composite Line with Constant Surge Impedance.—The equivalent II of the composite line of Fig. 149, with constant z_0 is shown in Fig. 150. The architrave ρ'' has an impedance $z_0 \sinh \delta_A = z_0 \sinh \delta_D$, the position angles, δ_A and δ_D being each reckoned from the opposite grounded end. The admittance of the *A* leak is

$$g''_A = Y_A - 1/\rho'' = y_0 \coth \delta_A - 1/\rho'' = y_0 \coth \delta_A - \nu \quad \text{mhos } \angle \quad (407)$$

Similarly, the D leak admittance is

$$g''_D = Y_D - 1/\rho'' = y_0 \coth \delta_D - 1/\rho'' = y_0 \coth \delta_D - \nu \quad \text{mhos } \angle \quad (408)$$

where the architrave admittance is

$$\nu = 1/\rho'' \quad \text{mhos } \angle \quad (409)$$

These two leaks are equal. At either end, the rule is: Ground the composite line at the distant end. *The home-end leak will*

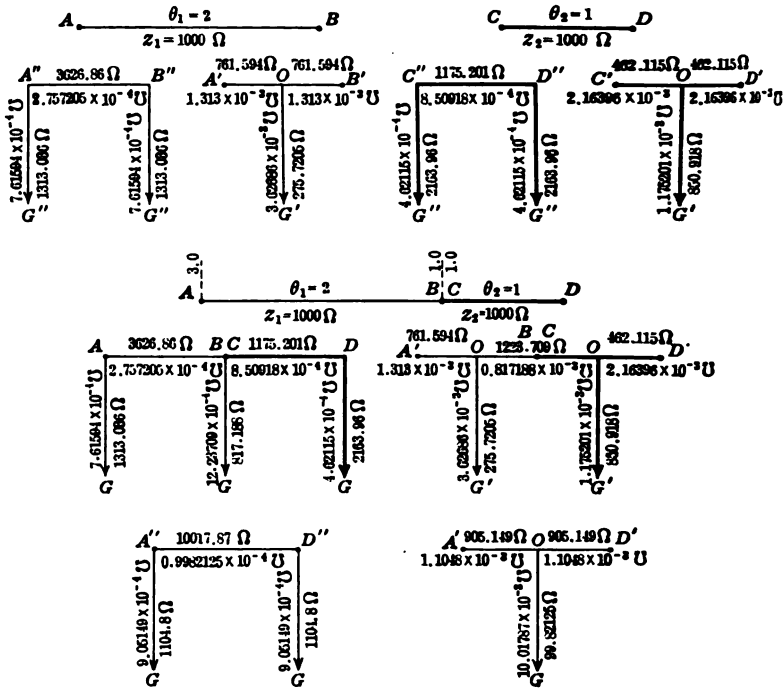


FIG. 151.—Two-section composite-line merger and hyperbolic equivalent circuits.

then be equal to the line admittance at the home end, minus the architrave admittance ν .

In Fig. 151, we have a particular case of a composite line with elements of equal surge impedance. The line AB has an angle $\theta_1 = 2.0$ hyps., and $z_1 = 1,000$ ohms. The line CD has $\theta_2 = 1.0$, and $z_2 = 1,000$ ohms. Beneath each line is placed its equivalent Π and equivalent T . The two lines are connected at the junction BC . The merger Π and T are indicated underneath the composite line AD . The "merger Π ," $A''D''$, is such as can be obtained

by direct computation from (406) to (409), Fig. 150. The merger $T, A'D'$, can also be computed by hyperbolic formulas,* but we shall, for simplicity, here confine ourselves to a consideration of *merger equivalent* Π 's, and *hyperbolic equivalent* Π 's.

Merger Π 's and Hyperbolic Π 's.—In all cases of composite lines, it is possible to replace each single section by its equivalent Π , to connect these Π 's end to end, and to resolve them, by successive steps, into a single resultant or merger equivalent Π . Thus, in Fig. 151, the central star $ABCDG$, of the double Π immediately under and to the left of the composite line AD , can be replaced, through known formulas, by its equivalent delta, and so lead to the merger equivalent $\Pi, A''D''$. This process is very laborious, and liable to arithmetical error. The process of obtaining the same equivalent Π of the composite line by line position angles is much simpler. This process leads to what may be called the "hyperbolic Π ." In the example offered throughout this chapter, the final Π has in each case been obtained by both the merger and hyperbolic methods, as mutual checks; but only the hyperbolic method is recommended in practice.

Transmission and Reflection Coefficients for Individual Waves.—If a composite line is composed of two single lines having different surge impedances z_1 and z_2 , Fig. 152, then a voltage wave; *i.e.*, an electric-flux wave, advancing from z_1 to z_2 , will be disrupted at the transition, in the manner originally analyzed by Heaviside.† The transmission coefficient, m_v , or coefficient of voltage transmission is

$$m_v = \frac{z_2}{\left(\frac{z_1 + z_2}{2}\right)} = \frac{2z_2}{z_1 + z_2} \quad \text{numeric } \angle \quad (410)$$

and the reflection coefficient $-(1 - m_v)$ is

$$m_v - 1 = \frac{z_2 - z_1}{z_1 + z_2} \quad \text{numeric } \angle \quad (411)$$

On the other hand, a current wave; *i.e.*, a magnetic-flux wave, advancing from z_1 to z_2 , will be disrupted, with a transmission coefficient m_c

$$m_c = \frac{z_1}{\left(\frac{z_1 + z_2}{2}\right)} = \frac{2z_1}{z_1 + z_2} \quad \text{numeric } \angle \quad (412)$$

* "The Equivalent Circuits of Composite Lines in the Steady State," by A. E. KENNELLY, *Proc. Am. Ac. Arts & Sciences*, November, 1909.

† "Reprinted Electrical Papers," by O. HEAVISIDE, London, 1892, vol. 1.

and a reflection coefficient $-(1 - m_c)$

$$m_c - 1 = \frac{z_1 - z_2}{z_1 + z_2} \quad \text{numeric } \angle \quad (413)$$

Thus, a wave of voltage $100\angle 0^\circ$ volts passing from a section of surge impedance $z_1 = 100\angle 0^\circ$ ohms to another of surge impedance $z_2 = 300\angle 0^\circ$ ohms, develops a transmission coefficient by (410) of $m_v = 1.5\angle 0^\circ$, or rises to $150\angle 0^\circ$ volts, after passing the junction. The reflected wave has a coefficient $0.5\angle 0^\circ$, or a value of $+50\angle 0^\circ$ volts. This reflected wave retreats along z_1 , and

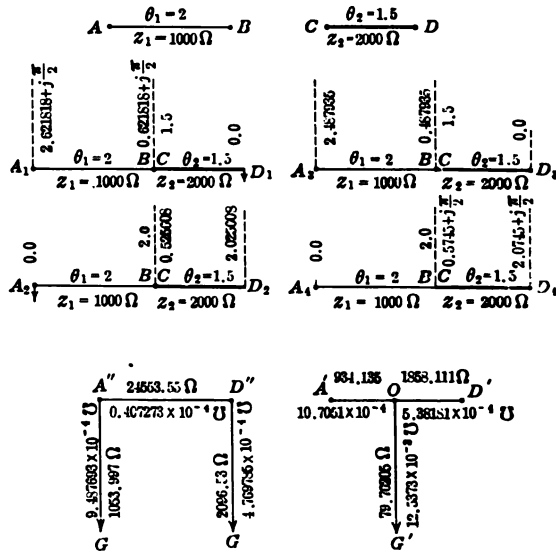


FIG. 152.—Two-section composite line with equivalent II and T.

raises the voltage on that side of the junction to $150\angle 0^\circ$ volts. There is thus no discontinuity of voltage at the junction, after the incoming wave has split. The incoming current on z_1 was $100\angle 0^\circ / 100\angle 0^\circ = 1.0\angle 0^\circ$ amp. On reaching the junction, it splits, the transmitted current, by (412), being $0.5\angle 0^\circ$ amp., and the reflected current, by (413), $-0.5\angle 0^\circ$ amp. Before the transition, there was $100\angle 0^\circ$ volts and $1.0\angle 0^\circ$ amp. on z_1 . After the transfer there is $150\angle 0^\circ$ volts and $0.5\angle 0^\circ$ amp. on both. The effect of the transition is, therefore, to raise the voltage and to lower the current in the system, so far as this particular set of waves is concerned.

The effect of the terminal impedances, as well as of composite-

line junctions, is to split up the initial waves of potential and current into subtrains, which move thereafter to and fro along the circuit, undergoing further splitting and also steady attenuation. The final state in the line is the vector sum of all these split, reflected and attenuated waves, see Figs. 178 and 179. In general, the arithmetical process of finding the resultant steady-state summation is very long and tedious; but the hyperbolic-function method of assigning potential and currents is relatively very easy and swift, offering, as it does, a short cut to the final result, without the necessity of adding the numerous successive vector increments that present themselves in the preliminary unsteady or formative state.

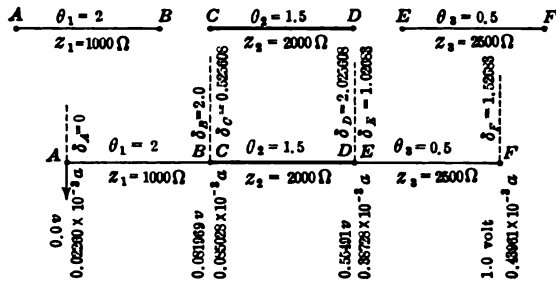


FIG. 153.—Three-section composite line grounded at A.

General Case of Composite Lines with Differing Surge Impedances.—In Fig. 153, three line sections are presented with the following constants:

For AB, $\theta_1 = 2.0$, $z_1 = 1,000$.

For CD, $\theta_2 = 1.5$, $z_2 = 2,000$.

For EF, $\theta_3 = 0.5$, $z_3 = 2,500$.

We proceed to determine the distribution of position angles, potential and current over the composite line AF, when grounded at A and voltaged at F.

Position-angle Distribution.—Starting from the grounded motor end at A, the position angle $\delta_A = 0$. At B, the position angle is evidently $\delta_B = \theta_1$. The line impedance of BA at B is $z_1 \tanh \theta_1 = 1,000 \tanh 2.0 = 1,000 \times 0.96403 = 964.03$ ohms, and this may be regarded as a terminal load σ at C, applied to the section DC. The position angle at C just across the junction from B is therefore, by (89),

$$\tanh \delta_C = \frac{Z_{\sigma B}}{z_2} = \frac{z_1 \tanh \theta_1}{z_2} = \frac{964.03}{2,000} = 0.482015,$$

from which $\delta_c = 0.525608$ hyp. The junction BC thus introduces a discontinuity into the position angle. On the B side of the junction, this angle is 2.0. On the C side, it is 0.525608.

From C to D , the position angle increases in the regular way, and at D it has reached the value 2.025608 hyps. The line impedance at D is thus $Z_{gD} = z_2 \tanh \delta_D = 2,000 \tanh 2.025608 = 2,000 \times 0.96579 = 1,931.58$ ohms. This may again be regarded as a terminal load to the section FE . The angle subtended by this load will be

$$\tanh \delta_E = \frac{Z_{gD}}{z_3} = \frac{z_2}{z_3} \tanh \delta_D = \frac{1,931.58}{2,500} = 0.772632,$$

from which $\delta_E = 1.02683$ hyps. This position angle is marked off on the upside of the DE junction.

From E to F , the position angle increases regularly to 1.52683 hyps. at F .

Potential Distribution.—Considering now a potential steadily applied at F , the potential at any point along any section of the composite line will be simply proportional to the sine of the position angle. At the junctions there is discontinuity of position angle, but no discontinuity of potential. If, therefore, the potential at any point of the composite line is given, the potentials at the ends of that section are readily found, and these give known potentials at the terminals of the next adjacent sections, which likewise can be worked up for potential distribution, and so on, throughout all the sections.

Thus, having given that the impressed potential at F is 1.0 volt, the potential V_E is

$$1.0 \times \frac{\sinh 1.02683}{\sinh 1.52683} = 0.55491 \text{ volt.}$$

This must also be the potential V_D at the beginning of the DC section. Consequently, the potential V_C is

$$0.55491 \times \frac{\sinh 0.525608}{\sinh 2.025608} = 0.081969 \text{ volt.}$$

This must also be the potential V_B at the beginning of the BA section; while $V_A = 0$, since the line is assumed to be grounded at A .

Line-admittance Distribution.—The line admittance in each section will be, by (127), proportionate to the cotangent of the position angle; so that

$$Y_{oB} = y_1 \coth \delta_B = 10^{-3} \times \coth 2.0 = 1.0373 \times 10^{-3} \text{ mho;}$$

$$Y_{oD} = y_2 \coth \delta_D = 0.5 \times 10^{-3} \times \coth 2.025608 = 0.51771 \times 10^{-3} \text{ mho;}$$

$$Y_{oF} = y_3 \coth \delta_F = 0.4 \times 10^{-3} \times \coth 1.52683 = 0.43961 \times 10^{-3} \text{ mho.}$$

The entering current I_F at F is therefore 0.43961×10^{-3} amp.

Line-current Distribution.—The line current in each section may either be determined by the formula (128), or by taking the cosines of position angles and using formula (111). Thus

$$I_B = 0.43961 \times 10^{-3} \times \frac{\cosh 1.02683}{\cosh 1.52683} = 0.38728 \times 10^{-3} \text{ amp.}$$

This must also be the current I_D , just beyond the DE junction.

Again,

$$I_C = 0.38728 \times 10^{-3} \times \frac{\cosh 0.525608}{\cosh 2.025608} = 0.085028 \times 10^{-3} \text{ amp.}$$

This must also be the current I_B just beyond the BC junction.

Finally,

$$I_A = 0.085028 \times 10^{-3} \times \frac{\cosh 0}{\cosh 2.0} = 0.022600 \times 10^{-3} \text{ amp.}$$

Power Distribution.—The power distribution over the composite line may be obtained either from the product of the local volts and amperes, or, in each section successively, by taking its size proportional to the sine of twice the position angle, and its slope from the line impedance, as previously described.

General Case of Composite Line with Terminal Load.—If the line, instead of being grounded directly at A , had been grounded through a motor-end load of assigned actual or virtual impedance, the procedure would be the same, except that instead of starting with a position angle of zero at A , there would be a definite starting position angle $\delta_A = \tanh^{-1} (\sigma/z_1)$ hyps.

Reversed Distribution of Position Angles.—If instead of grounding the composite line at A , Fig. 153, and voltaging it at F , we ground it at F , and voltage it at A , the distribution of position angles will be different from that already found, but will be determinable by the same process. The distribution is shown

in Fig. 154, for the three-section composite line above considered. Starting from F grounded, where $\delta_F = 0$, $\delta_E = 0.5$ hyp. At the other side of the junction DE , however, the line angle is

$$\delta_D = \tanh^{-1} \left(\frac{z_3}{z_2} \tanh \delta_E \right) = \tanh^{-1} (1.25 \tanh 0.5) \\ = \tanh^{-1} 0.57765 = 0.65892.$$

The position angle then regularly increases to 2.15892 hyps. at C . Again,

$$\delta_B = \tanh^{-1} \left(\frac{z_2}{z_1} \tanh \delta_C \right) = \tanh^{-1} (2.0 \tanh 2.15892) \\ = \tanh^{-1} (2 \times 0.97369) = \tanh^{-1} (1.94738)$$

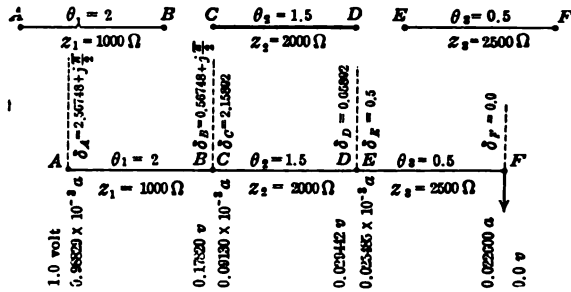


FIG. 154.—Three-section composite line grounded at F .

The antitangent of a quantity greater than unity must contain an imaginary quadrant or $j \frac{\pi}{2}$ (see Fig. 23); so that

$$\delta_B = \coth^{-1}(1.94738) + j \frac{\pi}{2} = 0.56748 + j \frac{\pi}{2} = 0.56748 + j1.0 \text{ hyp.}$$

The position angle now increases regularly to $2.56748 + j \frac{\pi}{2}$ at A .

The effect of the imaginary quadrant in the position angles on the AB section will be virtually to transmute sines into cosines, cosines into sines, and tangents into cotangents in using the standard formulas. This complication presents itself only in c.c. cases. It does not intrude in a.c. cases.

Repeating the development of potential and current distributions, we find that the current I_F to ground at F is 0.022600×10^{-3} amp., which is the same as I_A in Fig. 153. This is a general law which may be expressed as follows.*

* Am. Ac. Arts & Sciences, *loc. cit.*, 1909.

Any composite line of any number of sections, with or without loads of any kind, operated in the steady state either by a direct current or by a single-frequency alternating current, has the same receiving-end impedance from each end; so that if say 1 volt is applied to each end in turn, the current strength received to ground at the other end will be the same.

It is assumed in the above proposition that all the elements of the composite-line system are subject to Ohm's law in complex arithmetic; *i.e.*, that there are no faults, or bad contacts, subject to erratic variation.

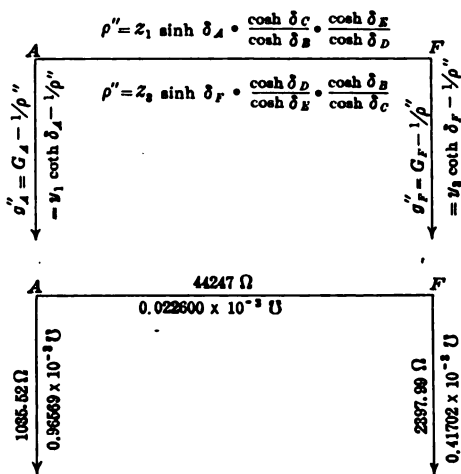


FIG. 155.—Equivalent II of three-section composite line.

Formation of the Hyperbolic Equivalent II of Composite Line.—In order to form the hyperbolic II of the composite line represented in Figs. 153 and 154, we first find the value of the architrave impedance and then, in turn, the value of each terminal leak admittance.

The steps in the process are indicated in Fig. 155. The architrave impedance by (252), if there were only a single section *AB* in Fig. 154, grounded at *B*, and voltaged from *A*, would be

$$\rho'' = z_1 \sinh \delta_A \quad \text{ohms } \angle \quad (414)$$

At each transition down line from the voltaged end, take the ratio of the cosine of the downside terminal position angle to the cosine of the upside terminal position angle. As there are two transitions in Fig. 154, namely at *B-C* and *D-E*, the com-

posite architrave impedance working from the voltaged end A^* is

$$\rho'' = z_1 \sinh \delta_A \cdot \frac{\cosh \delta_C}{\cosh \delta_B} \cdot \frac{\cosh \delta_E}{\cosh \delta_D} \text{ ohms } \angle \quad (415)$$

If we worked from the F voltaged end, with A grounded, we should have for a single section EF (Fig. 153).

$$\rho'' = z_2 \sinh \delta_F \text{ ohms } \angle \quad (417)$$

Applying cosine ratios at transitions in position angles we obtain

$$\rho'' = z_2 \sinh \delta_F \cdot \frac{\cosh \delta_D}{\cosh \delta_B} \cdot \frac{\cosh \delta_E}{\cosh \delta_C} \text{ ohms } \angle \quad (418)$$

The same process would be continued for any number of transitions, one cosine ratio being applied for each in turn. The value of ρ'' working from either end will be the same; *i.e.*, ρ'' is identical in (415) and (418).

Hence to find the architrave impedance of a composite line: Ground one end, and determine the distribution of position angles at transitions. The architrave ρ'' has then the value which would present itself if the last single line were the only line, but multiplied by the ratio of the cosines of the down to the up terminal position angles, at each transition in turn.

The process is well adapted to either slide-rule or logarithmic computation, when a number of transitions occur. A composite line containing n single lines will embody $n - 1$ transitions and $n - 1$ cosine ratios.

Thus, in the case above represented in Fig. 153, using (418),

$$\begin{aligned} \rho'' &= 2,500 \times \sinh 1.52683 \times \frac{\cosh 2.025608}{\cosh 1.02683} \times \frac{\cosh 2.0}{\cosh 0.525608} \\ &= 2,500 \times 2.1932 \times \frac{3.8563}{1.5752} \times \frac{3.7622}{1.1414} = 44,247 \text{ ohms.} \end{aligned}$$

* "It may be noted that this formula (415) for evaluating the architrave impedance from the position angles is not the only one available. An alternative formula is

$$\rho'' = z_1 \sinh \theta_1 \cdot \frac{\sinh \delta_D}{\sinh \delta_C} \cdot \frac{\sinh \delta_F}{\sinh \delta_E} \text{ ohms } \angle \quad (416)$$

This is called the "second method" in the original paper, *Proc. Am. Ac. Arts & Sciences*, November, 1909. The first method only will be developed here.

Again, in the case of Fig. 154, using (415),

$$\begin{aligned} \rho'' &= 1,000 \times \sinh \left(2.56748 + j \frac{\pi}{2} \right) \times \frac{\cosh 2.15892}{\cosh \left(0.57648 + j \frac{\pi}{2} \right)} \\ &\quad \times \frac{\cosh 0.5}{\cosh 0.65892} \\ &= 1,000 \times j \cosh 2.56748 \times \frac{\cosh 2.15892}{j \sinh 0.57648} \times \frac{\cosh 0.5}{\cosh 0.65892} \\ &= 1,000 \times 6.5549 \times \frac{4.3886}{0.59843} \times \frac{1.1276}{1.2251} = 44,247 \text{ ohms.} \end{aligned}$$

Leak Admittances of Equivalent Π .—The admittance of the leak g''_A of the hyperbolic Π is equal to the line admittance at A , minus the architrave admittance. By (127) the line admittance at A to ground at F is G_{gA} in the c.c. case or Y_{gA} in an a.c. case. Using the latter for generality,

$$\begin{aligned} Y_{gA} &= y_1 \coth \delta_A \\ &= 10^{-3} \times \coth \left(2.56748 + j \frac{\pi}{2} \right) = 10^{-3} \times \tanh 2.56748 \\ &= 0.98829 \times 10^{-3} \text{ mho.} \end{aligned}$$

The architrave admittance will be $\nu = 1/\rho'' = 1/44,247 = 0.02260 \times 10^{-3}$; so that

$$\begin{aligned} g''_A &= Y_{gA} - \nu = y_1 \coth \delta_A - \nu \quad \text{mhos } \angle \quad (419) \\ &= (0.98829 - 0.02260)10^{-3} = 0.96569 \times 10^{-3} \text{ mho.} \end{aligned}$$

Similarly, the admittance of the leak g''_F is equal to the line admittance at F minus the architrave admittance. The line admittance at F to ground at A (Fig. 153), is G_{gF} (or Y_{gF} in the general case)

$$\begin{aligned} Y_{gF} &= y_3 \coth \delta_F \quad \text{mhos } \angle \quad (420) \\ &= 0.4 \times 10^{-3} \coth 1.52683 = 0.4 \times 10^{-3} \times 1.09905 \\ &= 0.43962 \times 10^{-3} \text{ mho;} \end{aligned}$$

so that

$$\begin{aligned} g''_F &= y_3 \coth \delta_F - \nu \quad \text{mhos } \angle \quad (421) \\ &= (0.43962 - 0.02260)10^{-3} = 0.41702 \times 10^{-3} \text{ mho.} \end{aligned}$$

The leak admittance at either terminal of the equivalent Π of a composite line is therefore the line admittance of that terminal, reduced by the architrave admittance.

General Considerations Concerning the Equivalent Π of a Composite Line.—Since the line admittance will, in general, have different values at the two terminals of a composite line, *it follows that the terminal leaks of the equivalent Π of a composite line have, in general, different values; or a composite line has a dissymmetrical equivalent Π .* Similarly, a composite line has, in general, a dissymmetrical equivalent T .

The architrave impedance of a composite-line equivalent Π is the receiving-end impedance to ground; because if one terminal is grounded and the other voltaged by V , the current to ground must be V/ρ'' amp.

If, therefore, a motor-end load, of impedance σ ohms \angle , be applied successively to each terminal of a composite line, and the other terminal is at the same time voltaged to the same potential V , the current received through the load will, in general, be different in the two cases, unless $\sigma = 0$. This is for the reason that the value of the shunt applied to σ by the leak at that terminal will be different in the two cases.

In order to find the architrave and the leak at one terminal of a composite line, it is only necessary to work out the distribution of position angles over the system in the direction toward the required leak. If, however, both leaks are required, so as to complete the equivalent Π , then it becomes necessary to work out the position-angle distributions in both directions over the system.

Terminal Cantilevers.—Cantilever is the name proposed for the architrave and one leak* of an equivalent Π . The architrave and the leak at the voltaged end, such as can be computed from one series of position angles toward that end, as in Fig. 156, may be called the "*A* cantilever" of the composite line. The corresponding oppositely developed architrave and leak as in Fig. 157 may be called the "*F* cantilever" of the same line. Although both cantilevers have to be worked out, in order to complete the equivalent Π of a composite line, yet, in particular cases, it may be necessary to work out only one of them. For example, if the composite line is to be voltaged at *A* and grounded at *F*, it is of no immediate practical interest to determine the *F* leak of the

*The term "Gamma" (Γ) has been suggested to denote one leak and the architrave of an equivalent Π ; but this term is not easily applied for the opposite case (1). The term "cantilever" may be considered as applying to either case.

equivalent Π ; because, by assumption, that leak is to remain short-circuited. It is, therefore, only necessary in that case, to work out the A cantilever, and to ground the distant end of the architrave. When, however, the complete equivalent Π , and

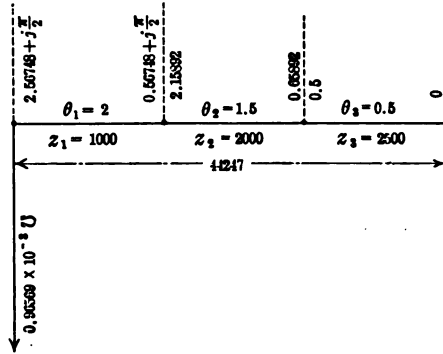


FIG. 156.—A-cantilever of three-section composite line.

both cantilevers, are computed, there is the advantage of the check that the architrave impedance ρ'' should be the same in both.

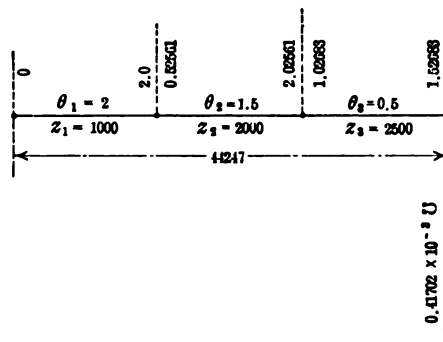


FIG. 157.—F-cantilever of three-section composite line.

Artificial-line Elements in a Composite Line.—If any single line in a composite-line system be replaced by its proper conjugate artificial lumpy line, having any number of T or Π sections, the steady-state distribution of potentials and currents in the rest of the system will remain unchanged. Consequently, any composite-line system may be completely replaced by the corresponding system of conjugate artificial lines, with or without corresponding loads at their ends.

Loads.—Loads in a line may be either *regular* or *casual*. Regular loads are such as are applied at regular intervals, in order, for instance, to improve the current delivery on telephone cables. Casual loads are of an irregular or incidental character, such as might occur at transitions, or at the terminals of a composite line. In the former case, they would be *intermediate casual loads*, and in the latter case *terminal casual loads*. We shall discuss regular loads in Chapter XVI, so that only casual loads will be considered here.

Loads may also be divided into two classes, namely: *impedance*

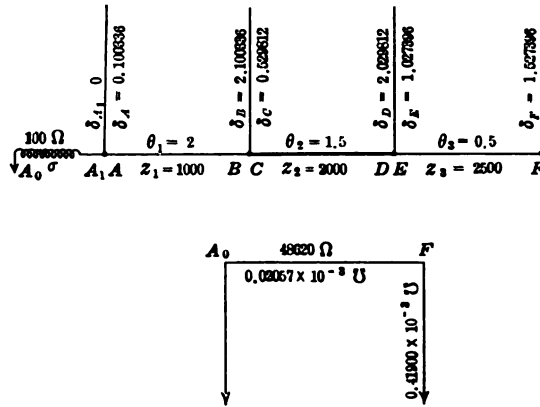


FIG. 158.—Three-section composite line with terminal resistance load at *A*.

loads, or those inserted in the line, such as resistors or reactors; and *leak loads*, applied in derivation to the line.

Terminal Impedance Loads (Motor-end or Down-end).—Terminal impedance loads commonly present themselves in practice. They are necessarily the rule rather than the exception. Fig. 158 shows the same three-section composite line as in Fig. 153, but with a terminal load of 100 ohms at *A*. With the line voltaged at *F*, and grounded at *A*, this is a motor-end load.

No position angle can exist within a simple impedance load. On the upside of the *A* terminal, however, $\delta_A = \tanh^{-1} (100/1,000) = \tanh^{-1} (0.1) = 0.100336$ hyp. The successive transitions in position angle are indicated at *B*, *C*, *D* and *F*. At *F*, the position angle is $\delta_F = 1.527396$ hyps., and this is the angle subtended at *F* by the loaded composite line. The admittance at *F* is, therefore, $Y_{\sigma F} = 0.4 \times 10^{-3} \coth 1.527396 = 0.43957 \times 10^{-3}$ mho. The architrave impedance is, by (418),

$$\begin{aligned}
 \sigma'' &= z_3 \sinh \delta_F \cdot \frac{\cosh \delta_D}{\cosh \delta_B} \cdot \frac{\cosh \delta_B}{\cosh \delta_C} \cdot \frac{\cosh \delta_{A1}}{\cosh \delta_A} \quad \text{ohms } \angle \quad (422) \\
 &= 2,500 \times \sinh 1.5274 \times \frac{\cosh 2.0298}{\cosh 1.0274} \times \frac{\cosh 2.10034}{\cosh 0.52981} \\
 &\qquad \qquad \qquad \times \frac{\cosh 0}{\cosh 0.10034} \\
 &= 2,500 \times 2.19454 \times \frac{3.87196}{1.57587} \times \frac{4.14569}{1.14366} \times \frac{1}{1.00503} \\
 &\qquad \qquad \qquad = 46,819.7 \text{ ohms.}
 \end{aligned}$$

It may be observed that when the system AF of Fig. 153 is reduced to a single line, by eliminating discontinuities at $B-C$ and $D-E$, formula (422), becomes equivalent to formula (134). The architrave admittance is thus $\nu = 1/48,620 = 0.020568 \times 10^{-3}$ mho. Subtracting this from the line admittance at F , we obtain the F leak of the equivalent Π ; i.e. $(0.43957 - 0.02057)10^{-3} = 0.41900 \times 10^{-3}$ mho. This completes the F cantilever, so that for 1.0 volt applied at F , the current entering the line is 0.43957 milliamp., of which 0.41900 may be regarded as going to ground directly through the F leak, and 0.02057 milliamp. through the load at A to ground.

It is important to notice that when the motor-end load is included in the architrave, as in the case just considered, there is ordinarily no need of knowing the value of the leak g''_A in the equivalent Π at the motor end, because it becomes short-circuited by the ground connection beyond the load. The generator-end cantilever is all that is necessary for determining the electrical conditions at the terminals of the composite-line system.

Change in Equivalent Π to Include a Motor-end or Down-end Terminal Load.—Another way at arriving at the change in the F cantilever when a terminal load is added at A , which does not require a recomputation of position angles over the line, is indicated in Fig. 159. In the upper part of the figure, a load of σ ohms \angle , or $\mu = 1/\sigma$ mhos \angle , is added to the line at the A terminal. If we employed the equivalent T of the system, it would be necessary only to add σ ohms to the A arm of the T , and the proper modification in the equivalent system would be made. But since the equivalent Π is more generally useful, we proceed to find the Π which may replace the T of Fig. 159, A_0AFg_1 . This substitute Π is shown in the lower part of the figure, with sloping

pillars. The architrave ρ'' is greater than the original architrave ρ , by the load σ and the term $\rho\sigma g_1$. The leak at A_0 is the original

leak g_1 mhos multiplied by the ratio $\frac{\mu}{\mu + \nu + g_1}$; or in this case
 $10 + 0.0226 + 0.96569 = \frac{10}{10.9883}$, which reduces the A_0 leak to 0.87884×10^{-3} mho. The architrave is

$$\begin{aligned} \rho'' &= \rho + \sigma + \rho\sigma g_1 && \text{ohms } \angle \quad (423) \\ &= 44,247 + 100 + 4.4247 \times 10^6 \times 0.96569 \times 10^{-3} \\ &= 44,347 + 4,273 = 48,620 \text{ ohms.} \end{aligned}$$

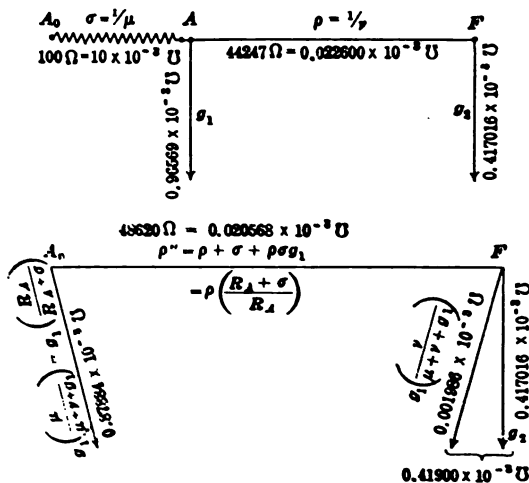


FIG. 159. —Modification of a composite-line equivalent Π so as to include a terminal impedance load.

The additional leak at F is

$$g: \left(\frac{\nu}{\mu + \nu + g_1} \right) \quad \text{mhos } \angle \quad (424)$$

in this case,

$$0.96569 \times 10^{-3} \times \frac{0.02260}{10.9883} = 0.001986 \times 10^{-3},$$

which added to the existing leak at g_2 makes the new F leak 0.41900×10^{-3} mho. With the system grounded at A_0 , the A_0 leak is ordinarily of no importance.

Terminal Load at the Generator End or Up End.—If the terminal load r ohms \angle is applied at the generator end, then as in

Fig. 154, we ground the system at F , and distribute position angles toward A . No change occurs in this distribution, but the line impedance $Z_{\sigma A_0}$ is increased by σ (Fig. 160) with a corresponding change in the line admittance $Y_{\sigma A_0}$.

The line impedance $Z_{\sigma A}$ at A , as in Fig. 154, is 1,011.9 ohms, with the F end grounded. The cantilever at A , before applying

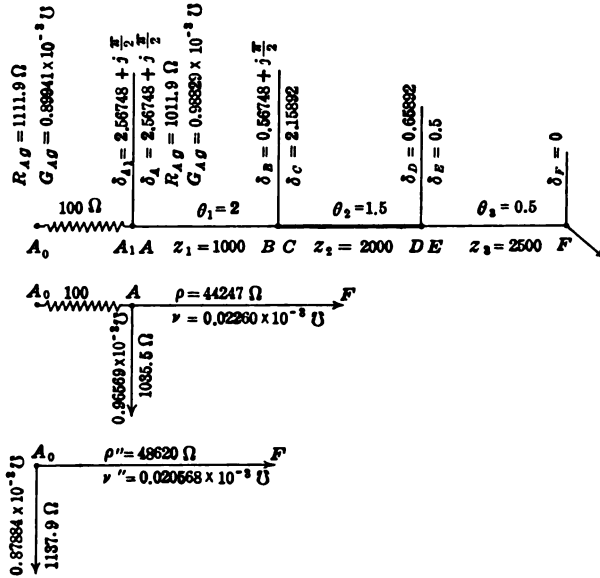


FIG. 160.—Composite line loaded at the generator end with a terminal impedance, and the corresponding A_0 cantilever.

the load, has an architrave impedance AF of 44,247 ohms and a leak of 0.96569 millimho = 1,035.5 ohms. The new line impedance at A will be $1,011.9 + 100 = 1,111.9$ ohms. The effect of the load with its change of terminal from A to A_0 is to increase both architrave and leak impedances in the ratio of the new line impedance to the old; or $\frac{1,111.9}{1,011.9} = 1.0988$. That is,

$$\rho'' = \rho \left(\frac{Z_{\sigma A} + \sigma}{Z_{\sigma A}} \right) \quad \text{ohms } \angle \quad (425)$$

and
$$g''_1 = \frac{1}{g_1} \left(\frac{Z_{\sigma A} + \sigma}{Z_{\sigma A}} \right) \quad \text{ohms } \angle \quad (426)$$

or
$$g''_1 = g_1 \left(\frac{Z_{\sigma A}}{Z_{\sigma A} + \sigma} \right) \quad \text{mhos } \angle \quad (427)$$

Thus the A_0 cantilever, Fig. 143, has an architrave impedance of

$$\rho'' = 44,247 \times 1.0988 = 48,620 \text{ ohms,}$$

and $g''_1 = 0.96569 \times \frac{1}{1.0988} = 0.87884 \text{ millimho,}$

or $\frac{1}{g''_1} = \frac{10^3}{0.96569} \times 1.0988 = 1,035.5 \times 1.0988 = 1,137.9 \text{ ohms.}$

This is a general principle expressible in the following terms.

Effect of a Terminal Load on the Cantilever at That Terminal.—

The addition of a terminal impedance load to any composite line alters the impedance of the architrave, and of that terminal's leak, in the ratio of the increase in line impedance, when the distant end is grounded. This proposition holds whether the composite-line system had or had not other loads before the addition of the terminal load. The proposition also holds whether the terminal to which the load is added is a generator end or a motor end; but it is serviceable only when the position-angle distribution has been worked out with the unloaded terminal as a motor terminal to ground in order to determine the value of $Z_{\theta A} = z_A \tanh \delta$, ohms \angle .

If, therefore, we apply 1 volt at A_0 , Fig. 160, the total current taken by the composite-line system will be $(0.87884 + 0.02057)10^{-3} = 0.89941 \times 10^{-3}$ amp., of which 0.87884×10^{-3} amp. pass through the virtual terminal A_0 leak to ground, while 0.02057×10^{-3} amp. will pass out at F , the distant grounded end of the system. If the potentials and currents along the line are required, they will follow respectively the sines and cosines of the position angles, except that from A_0 to A , there are no position angles and the line current in the terminal load is constant with a simple Ohm's law potential drop.

By similar reasoning, if an impedance is removed from a terminal, the impedance of the architrave and of the same terminal's leak in the composite-line equivalent Π will be altered in the ratio of the terminal-line impedance before and after the change, the distant terminal being to ground.

If instead of the A_0 cantilever, the full equivalent Π of A_0F is required, the change in the F leak can be determined by (424); or by 421, after distributing position angles from A_0 grounded up to F .

In the case of a single uniform line θ , z_{θ} , we know that $Z_{\theta A} = z_{\theta} \tanh \theta$ will have the same value from each end in turn. Con-

sequently, the addition of a terminal load σ will have the same effect on the architrave at whichever end it is applied. Before loading, the architrave will be $\rho = z_0 \sinh \theta$, and after loading, by (425), see (135).

$$\rho'' = z_0 \sinh \theta \left(\frac{z_0 \tanh \theta + \sigma}{z_0 \tanh \theta} \right) = z_0 \sinh \theta + \sigma \cosh \theta \quad \text{ohms } \angle \quad (428)$$

But in the general case, the line impedance Z_0 of a composite line will be different at the two terminals A and F ; so that the effect on the architrave of a given terminal load σ will be different when it is applied to each terminal in succession. In the case of the three-section composite line of Figs. 153 and 154, applying $\sigma = 100$ ohms at A , makes the A_0F architrave 48,620 ohms, as above; whereas applying $\sigma = 100$ ohms at F , makes the AF_0 architrave 46,192 ohms.

Virtual Angle of a Generator-end Terminal Impedance.—

We have already seen in (89) and elsewhere, that a simple motor-end or down-end terminal load σ , although devoid of hyperbolic angle in itself, yet possesses a virtual angle θ' when added to a line of definite surge impedance. In the same way, a generator-end or up-end terminal load σ possesses a virtual angle θ'' , when added to a line of surge impedance z_1 , which may form the first section of a composite-line system.

Let the architrave impedance of the composite-line equivalent Π be

$$\rho = Mz_1 \sinh \delta_A \quad \text{ohms } \angle \quad (429)$$

where M is a multiplier consisting of cosine ratios, as in (415). Then, the architrave impedance of the equivalent Π , after the addition of the load at A , Fig. 161, will be, by (425),

$$\rho'' = Mz_1 \sinh \delta_A \left(\frac{z_1 \tanh \delta_A + \sigma}{z_1 \tanh \delta_A} \right) \quad \text{ohms } \angle \quad (430)$$

Let
$$\frac{\sigma}{z_1} = \tanh \theta'' \quad \text{numeric } \angle \quad (431)$$

where θ'' is the virtual angle of the sending-end load when applied to the line of surge impedance z_1 ; then

$$\rho'' = Mz_1 \sinh \delta_A \left(\frac{\tanh \delta_A + \tanh \theta''}{\tanh \delta_A} \right) \quad \text{ohms } \angle \quad (432)$$

$$= Mz_1 (\sinh \delta_A + \tanh \theta'' \cosh \delta_A) \quad \text{ohms } \angle \quad (433)$$

and, applying (506),

$$= Mz_1 \frac{\sinh(\delta_A + \theta'')}{\cosh \theta''} \quad \text{ohms } \angle \quad (434)$$

These conditions are illustrated in Fig. 161 for the case already considered. Here $\theta'' = \tanh^{-1} (100/1,000) = 0.100336$ hyp. Formula (434) is well adapted for logarithmic or slide-rule work in an a.c. case.

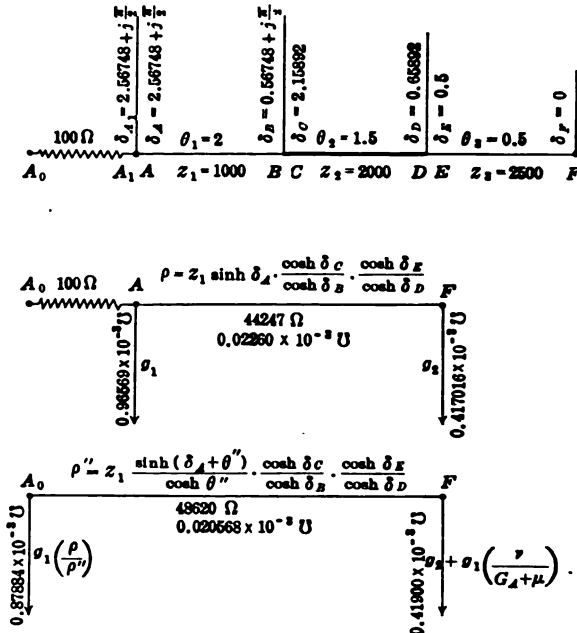


FIG. 161.—Composite line of three sections loaded at the A terminal.

Impedance Loads at Each Terminal of a Composite Line.—

Applying an impedance load to each terminal of a composite line, we may ground one terminal and lay out the position-angle distribution up to the other. We may then use (434) in order to determine the cantilever from the up terminal. This cantilever will give the currents at both terminals of the system when the impressed potential is given, and from these, the potentials at the terminals of the composite line are readily found.

An example is given in Fig. 162, using the three-section composite line already referred to. The line is grounded at F₀, through a terminal load of $\sigma = 100$ ohms. The position angle

at A is then 1.52740 hyps. The A cantilever has an architrave impedance of 48,620 ohms and an A leak of 0.41900 millimho. Impedance, $z_s = 200$ ohms at the sending end, is then added to the A terminal. This load has a virtual angle of $\tanh^{-1}(200/2,500) = 0.08017$ hyp. The cantilever at A_0 has then an architrave impedance of 52,890 ohms, and an A_0 leak of 0.38515 millimho.

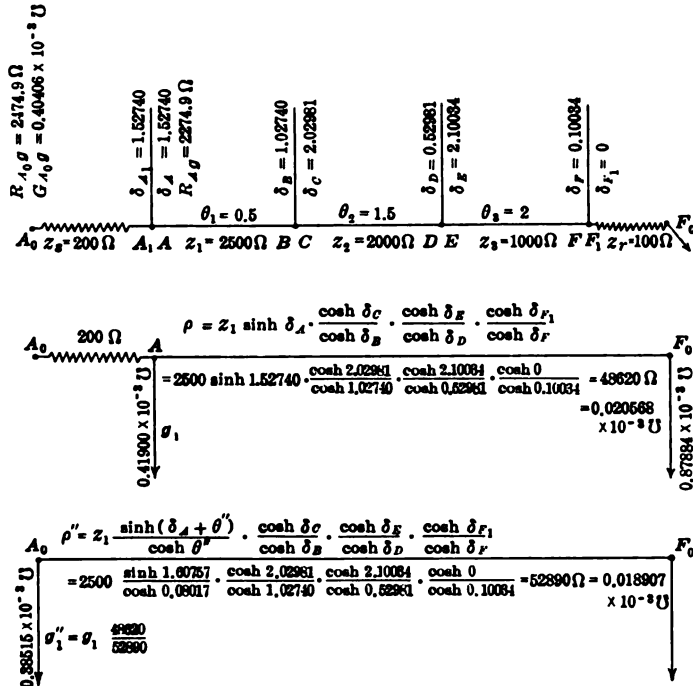


FIG. 162.—Composite line loaded at both ends and its A -end cantilever.

Alternating-current Example of Composite Line.—The following example may illustrate the application of the foregoing principles to an a.c. case. In Fig. 163, we have a diagrammatic representation of a three-section composite telephone line. At A is the generator, of angular frequency 5,000 radians per sec. ($f = 796\sim$), impressed on a 5-km. section of a standard twisted-pair telephone cable from A to B . Then from C to D there is a 250-km. overhead section of double-wire telephone line, and finally from E to F another 5-km. of underground wire like that between A and B . At F is a terminal load, such as a receiving set between the wires of the circuit. The impedance of this load, at

impressed frequency, is taken as $1,500\angle 70^\circ$ ohms per loop; *i.e.*, $750\angle 70^\circ$ ohms per wire. It is required to find the distributions of position angle, potential and current over the composite line, assuming $2.0\angle 0^\circ$ volts applied across the lines at *A*; *i.e.*, $1.0\angle 0^\circ$ volt per wire.

The linear constants of the three single lines are recorded in Table XVI. The angle subtended by each underground line is $0.3324 + j0.2199 = 0.4793\angle 46^\circ.096$ hyp., and that subtended by the overhead line $1.171 + j2.785$ hyp. = $1.171 + j4.375 = 4.53\angle 75^\circ.017$ hyp.

In Fig. 164, we have at the top, the three sections. Their respective single equivalent Π 's are given below these. The under-

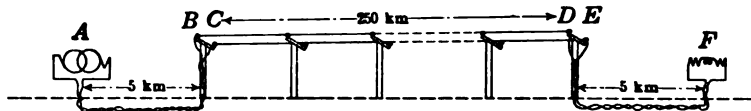


Fig. 163.—Composite telephone circuit of central overhead section and terminal cable sections.

ground-section Π 's are clearly realizable in the laboratory. The overhead-section Π is not, however, realizable by ordinary simple impedances. At $A'' B'' E'' F''$, the three Π 's are joined end to end, and adjoining leaks are merged by vector addition. The central Π , at $B'' E''$, is then replaced by its equivalent T at $B''' E'''$. As the next step, the T at $A''' F'''$, which happens to be symmetrical in this case, is replaced by its equivalent Π , $a'f'$, with sloping pillars. Finally, the terminal leaks are merged by vector addition, and we obtain the merger Π of the system, at $afgg$. The architrave has an impedance of $1,113\angle 103^\circ.4$ ohms, an unrealizable value with ordinary simple impedance elements in series. Each leak has $2.35\angle 16^\circ.933$ millimho. The merger Π of a three-section line calls for two $\Pi - T$ or $T - \Pi$ transformations, and a merger Π of an n -section line calls, in general, for $n - 1$ such transformations, besides incidental auxiliary computations. It is a tedious, and error-provoking process.

It is evident from this merger Π , that if the composite line were directly grounded at *F*, and voltaged with $1.0\angle 0^\circ$ at *A*, the received current at *F* would be $0.8984\angle 103^\circ.4$ milliamp. Although apparently leading the impressed e.m.f. by $103^\circ.4$, the received current would actually lag $360^\circ - 103^\circ.4 = 256^\circ.6$ behind it.

TABLE XVI
Linear Constants of the Sections of Composite Line in Fig. 163.

	Section A-B	Section C-D	Section E-F
Section length, km.....	5.0	250.0	5.0
Linear resistance, r , ohms per loop km.....	54.68	6.586	54.68
Linear inductance, L , henrys per loop km.....	0.6213×10^{-3}	2.284×10^{-3}	0.6213×10^{-3}
Linear capacitance, c , farads per loop km.....	0.3355×10^{-7}	0.4982×10^{-8}	0.3355×10^{-7}
Linear leakage, g , mhos per loop km.....	3.107×10^{-6}	0	3.107×10^{-6}
Hyperbolic angle θ , at $\omega = 5,000$, hyps.....	$0.3324 + j0.2199$	$1.171 + j2.785$	$0.3324 + j0.2199$
Linear hyperbolic angle α , at $\omega = 5,000$, hyps. km.....	$0.06647 + j0.04398$	$0.004684 + j0.01114$	$0.06647 + j0.04398$
Surge impedance per wire, at $\omega = 5,000$, ohms.....	$285.7 \angle 42^\circ .843$	$363.7 \angle 14^\circ .983$	$285.7 \angle 42^\circ .843$

The hyperbolic Π is worked out in full in Fig. 148, with the aid of the "Chart Atlas of Complex Hyperbolic Functions." The first step is to lay off the position angles, each of which takes

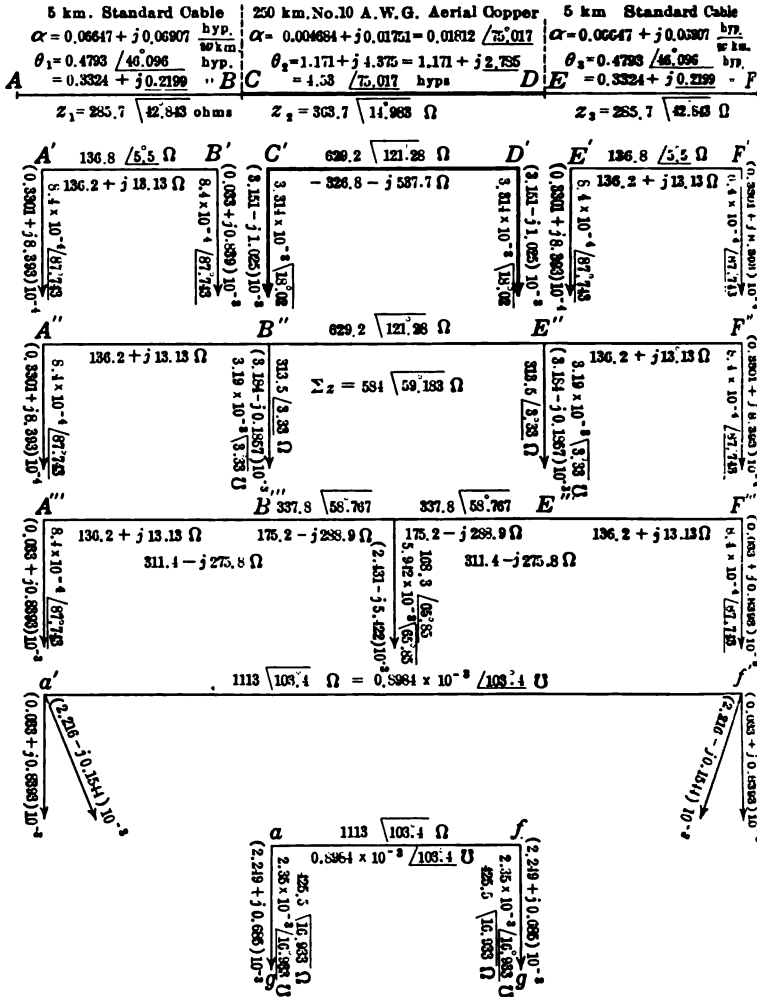


Fig. 164.—Successive steps in determining the merger Π of the three-section composite line.

one line on the page, and two references to the chart. Thus, in finding δ_D , we require to find $\tanh \delta_E = \tanh (0.3324 + j0.2199)$. The charts do not, as a rule, admit of being used to this degree of precision, but we can readily find from Chart

$IX_A, \tanh(0.33 + j0.22) = 0.471 \angle 41^\circ.5$, the last digit of the size being doubtful. We then have to find from the same chart $\tanh^{-1}(0.3703 \angle 13^\circ.64)$, by entering on the rectilinear background for $0.370 \angle 13^\circ.6$, and interpolating on the curvilinear system, $0.36 + j0.065$ hyp.

$5 \text{ km. Standard Cable}$ $\alpha = 0.00647 + j0.06907$ $\theta_1 = 0.4793 \angle 46^\circ.096$ $= 0.3324 + j0.2199 \text{ hyp.}$	$250 \text{ km. No.10 A.W.G. Aerial Copper}$ $\alpha = 0.004684 + j0.01751 = 0.01812 \angle 75^\circ.017$ $\theta_2 = 1.171 + j4.376 = 1.171 + j2.786$ $= 4.53 \angle 75^\circ.017 \text{ hyps.}$	$5 \text{ km. Standard Cable}$ $\alpha = 0.00647 + j0.06907$ $\theta_3 = 0.4793 \angle 46^\circ.096$ $= 0.3324 + j0.2199 \text{ hyps.}$
$A \quad z_1 = 286.7 \angle 42^\circ.843 \Omega$	$B \quad C \quad z_2 = 363.7 \angle 14^\circ.963 \Omega$	$D \quad E \quad z_3 = 286.7 \angle 42^\circ.843 \Omega$

$$\delta_D = \tanh^{-1} \left(\frac{z_3}{z_2} \tanh \delta_E \right) = \tanh^{-1} \left(\frac{286.7 \angle 42^\circ.843}{363.7 \angle 14^\circ.963} \times 0.4713 \angle 41^\circ.5 \right) = \tanh^{-1} (0.3703 \angle 43^\circ.64)$$

$$\delta_D = 0.36 + j0.065$$

$$\theta_2 = 1.171 + j2.786$$

$$\delta_C = 1.531 + j2.850$$

$$\delta_B = \tanh^{-1} \left(\frac{z_1}{z_2} \tanh \delta_C \right) = \tanh^{-1} \left(\frac{286.7 \angle 42^\circ.843}{363.7 \angle 14^\circ.963} \times 1.094 \angle 2^\circ.43 \right) = \tanh^{-1} (1.393 \angle 30^\circ.29)$$

$$\delta_B = 0.575 + j0.685$$

$$\theta_1 = 0.332 + j0.220$$

$$\delta_A = 0.907 + j0.905$$

$$\rho_{11} = z_1 \sinh \delta_A \cdot \frac{\cosh \delta_C}{\cosh \delta_B} \cdot \frac{\cosh \delta_E}{\cosh \delta_D}$$

$$= 286.7 \sinh(0.907 + j0.905) \cdot \frac{\cosh(1.531 + j2.850)}{\cosh(0.575 + j0.685)} \cdot \frac{\cosh(0.3324 + j0.220)}{\cosh(0.36 + j0.065)}$$

$$= 286.7 \angle 42^\circ.843 \times 1.434 \angle 89^\circ.9 \times \frac{2.268 \angle 256^\circ.3}{0.760 \angle 43^\circ.9} \times \frac{1.00 \angle 6^\circ.5}{1.062 \angle 2^\circ.4} = 1119 \angle 103.1 \Omega$$

$$Y_{A0} = y_1 / \tanh \delta_A = 3.500 \times 10^{-3} \angle 42^\circ.843 / 1.368 \angle 5^\circ.6 = 2.559 \times 10^{-3} \angle 37^\circ.243 = (2.037 + j1.549) \times 10^{-3} \text{ U}$$

$$1/\rho_{11} = 0.8937 \times 10^{-3} \angle 103.1 = (-0.208 + j0.870) \times 10^{-3} \text{ U}$$

$$Y_{A0} = (2.240 + j0.679) \times 10^{-3} \text{ U}$$

$$= 2.341 \times 10^{-3} \angle 16^\circ.87 \text{ U}$$

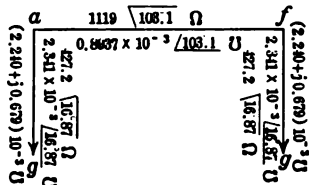


FIG. 165.—Full computation of hyperbolic II for the three-section composite line.

After establishing the position angles, we know that in any one section, the potentials are as their sines, and the currents as their cosines, there being no discontinuity at junctions. We start at A, where the potential is given, and where the current is, by (128), $I_A = y_1 \coth \delta_A = 2.559 \angle 37^\circ.243$ milliamp.

The architrave ρ'' of the hyperbolic Π , by (415), appears beneath δ_A in Fig. 165. In the formula, there are five successive references to chart X-XI. The result is $1,119 \angle 103^\circ.1$, as against $1,113 \angle 103^\circ.4$ by the merger method. The discrepancy is attributable to the limits of graphic interpolation precision in the charts. By numerical interpolation in the corresponding tables, a closer approximation would be obtainable, at a greater expenditure of time.

At the bottom of the arithmetic is the computation for the a

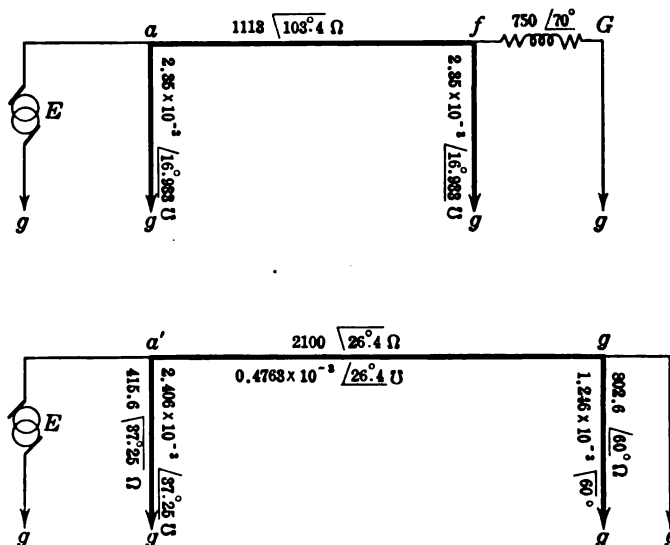
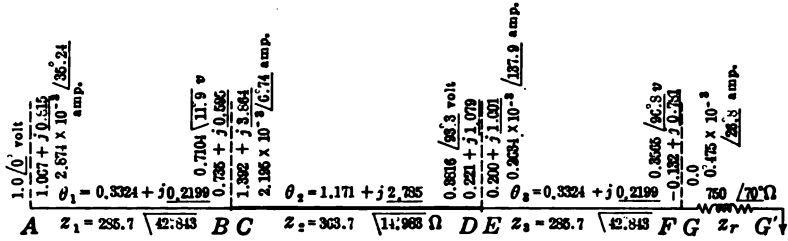


FIG. 166.—Complete computation of the A cantilever of the three-section composite line including the terminal load at G .

leak; namely $2.341 \times 10^{-3} \angle 16^\circ.87$ mho. Ordinarily, the f leak could not be found without a new distribution of position angles from A to F' ; but, in this case, by symmetry, the f and a leaks are identical.

In Fig. 166, we have the merger Π extended to include the receiving instrument between f and G . The new Π , which is dissymmetrical, has an architrave impedance $a'g$ of $2,100 \angle 26^\circ.4$ ohms. One volt applied at a' would, therefore, deliver a current through the receiving instrument of $0.4763 \angle 26^\circ.4$ milliamp. Fig. 167 gives the corresponding A cantilever by the hyperbolic-function method. The position angles have been recast from G to A . The final result gives an architrave impedance $a'g'$ of



$$\delta_F = \tanh^{-1}\left(\frac{z_F}{z_3}\right) = \tanh^{-1}\left(\frac{750 \angle 70^\circ}{363.7 \angle 42.843^\circ}\right) = \tanh^{-1}(2.026 \angle 112.843^\circ) = \tanh^{-1}(-1.019 + j2.420)$$

$$\delta_F = -0.132 + j0.781$$

$$\theta_3 = 0.332 + j0.220$$

$$\delta_E = 0.200 + j1.001$$

$$\delta_D = \tanh^{-1}\left(\frac{z_2}{z_3} \tanh \delta_E\right) = \tanh^{-1}\left\{\frac{285.7 \angle 42.843^\circ}{363.7 \angle 42.843^\circ} \tanh(0.200 + j1.001)\right\} = \tanh^{-1}(3.98 \angle 26.31^\circ)$$

$$\delta_D = 0.221 + j1.079$$

$$\theta_2 = 1.171 + j2.785$$

$$\delta_C = 1.392 + j3.964$$

$$\delta_B = \tanh^{-1}\left(\frac{z_2}{z_1} \tanh \delta_C\right) = \tanh^{-1}\left\{\frac{363.7 \angle 42.843^\circ}{285.7 \angle 42.843^\circ} \tanh(1.392 + j3.964)\right\} = \tanh^{-1}(1.137 \angle 24.98^\circ)$$

$$\delta_B = 0.735 + j0.585$$

$$\theta_1 = 0.332 + j0.220$$

$$\delta_A = 1.067 + j0.815$$

$$\begin{aligned} \rho_{11} &= Z_1 \sinh \delta_A \frac{\cosh \delta_C}{\cosh \delta_B} \cdot \frac{\cosh \delta_B}{\cosh \delta_D} \cdot \frac{\cosh \delta_D}{\cosh \delta_F} \cdot \frac{\cosh \delta_D}{\cosh \delta_F} \\ &= 285.7 \angle 42.843^\circ \sinh(1.067 + j0.815) \frac{\cosh(1.392 + j3.964)}{\cosh(0.735 + j0.585)} \frac{\cosh(0.200 + j1.001)}{\cosh(0.221 + j1.079)} \cdot \frac{\cosh 0}{\cosh(-0.132 + j0.781)} \\ &= 285.7 \angle 42.843^\circ \cdot 1.002 \angle 76.9^\circ \cdot \frac{2.125 \angle 11^\circ}{1.002 \angle 40.3^\circ} \cdot \frac{0.201 \angle 90.18^\circ}{0.255 \angle 126.16^\circ} \cdot \frac{1.0 \angle 0^\circ}{0.363 \angle 26.3^\circ} = 2108 \angle 26.5^\circ \Omega \end{aligned}$$

$$\begin{aligned} Y_{AG} &= y_1 \left[\tanh \delta_A = 3.500 \times 10^{-3} \angle 42.843^\circ / 1.218 \angle 71.6^\circ = 2.874 \times 10^{-3} \angle 35.243^\circ = (2.347 + j1.638) \times 10^{-3} \text{ } \Omega \right] \\ 1/\rho_{11} &= 0.4744 \times 10^{-3} \angle -26.5^\circ = (0.425 + j0.212) \times 10^{-3} \text{ } \Omega \\ Y_{AG} &= (1.922 + j1.446) \times 10^{-3} \text{ } \Omega \\ &= 2.406 \times 10^{-3} \angle 37.0^\circ \end{aligned}$$

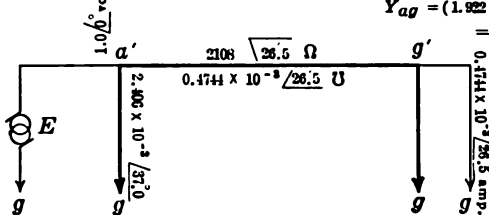


FIG. 167.—Merger II of composite line including terminal load at G.

2,108∠26°.5 ohms, and an a' leak admittance of 2.406∠37° millimhos. One volt at A would, therefore, send 0.4744∠26°.5 milliamp. through the receiving instrument, which means that 2.0 volts across the circuit in Fig. 163 would send this same current through the 1,500∠70°-ohm instrument at F . The potentials and currents at transitions are also indicated in the upper part of Fig. 167. The discrepancy of 0.4 per cent. between the hyperbolic and merger architraves is again attributable to the limits of graphic interpolation in the use of charts.

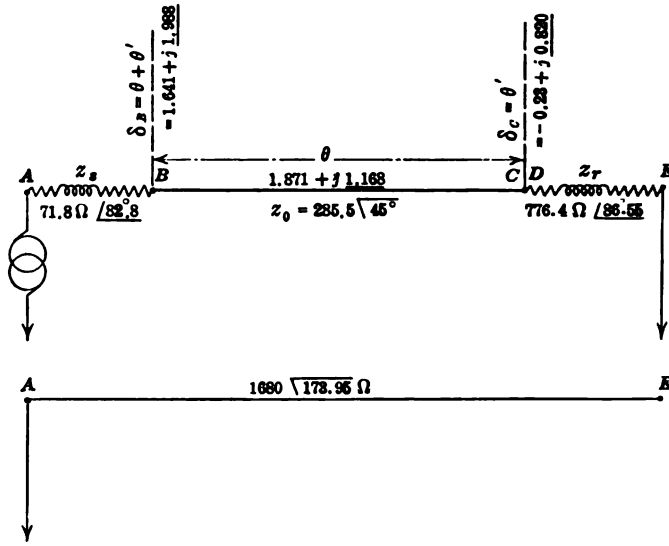


FIG. 168.—Line loaded at each end and the A cantilever.

Alternating-current Case of Impedance Loads at Each Terminal.—As an instance of terminal loads at each end of a line, the case of Fig. 168 may be taken. Here the single line subtends an angle of $\theta = 1.871 + j1.835 = 1.871 + j1.168$ hyps., and has a surge impedance of 285.5∠45° ohms. The motor-end load DE has an impedance $Z_r = 776.4\angle 86^\circ.55$; so that it subtends a virtual angle of $\theta' = \tanh^{-1} \left(\frac{776.4\angle 86^\circ.55}{285.5\angle 45^\circ} \right) = \tanh^{-1} (2.719\angle 131^\circ.55) = -0.23 + j0.820$ hyp. by Chart XII. Similarly, the the virtual angle of the generator-end impedance is $\tanh^{-1} \left(\frac{71.8\angle 82^\circ.8}{285.5\angle 45^\circ} \right) = \tanh^{-1} (0.2515\angle 127^\circ.8) = -0.149 + j0.128$ hyp.

also by chart. The *A* cantilever of this system has therefore by (434) an architrave impedance of

$$\begin{aligned} \rho'' &= 285.5 \angle 45^\circ \times \frac{\sinh(1.492 + j2.116)}{\cosh(-0.149 + j0.120)} \times \frac{\cosh 0}{\cosh(-0.23 + j0.820)} \\ &= 285.5 \angle 45^\circ \times \frac{2.118 \angle 168^\circ.5}{0.363 \angle 37^\circ.8} \times \frac{1.0 \angle 0^\circ}{0.9912 \angle 1^\circ.75} = \\ & \qquad \qquad \qquad 1,680 \angle 173^\circ.95 \text{ ohms.} \end{aligned}$$

A potential of 1.0∠0° volt impressed at *A*, Fig. 168, would thus send a current of 0.0595∠173°.95 milliamp. through the terminal impedance at *DE*.

Intermediate Impedance Loads in a Composite Line.—A case of an intermediate impedance load is represented in Fig. 169. A resistance of 100 ohms is introduced between the *AB* and *CD* sections of Fig. 153. At *A*₁*F*₁, the position angles are distributed from *F* grounded, toward *A*. At *C*, the position angle is δ_{*C*} = 2.15892, as in Fig. 154, and *Z*_{*gC*} = *z*₂ tanh δ_{*C*} = 2,000 tanh 2.15892 = 1,947.385 ohms. At *B* this line impedance is increased to *Z*_{*gB*} = 2,047.385 and the new position angle at *B* is

$$\begin{aligned} \delta_B &= \tanh^{-1} \left(\frac{Z_{gB}}{z_1} \right) \quad \text{hyps. } \angle \quad (435) \\ &= \tanh^{-1} \left(\frac{2,047.385}{1,000} \right) = \tanh^{-1} 2.047385 = 0.534 + j \frac{\pi}{2} = \\ & \qquad \qquad \qquad 0.534 + j1. \end{aligned}$$

The position angle then advances regularly to δ_{*A*} = 2.534 + *j* $\frac{\pi}{2}$.

The distribution of potentials and currents now commences from some point where either the potential or the current is given. The potentials from this point follow the sines and the currents the cosines of the position angles to the nearest transitions. At transitions, there is no change in line current, and also no change in potential, except at *BC*, where there is an Ohm's law vector drop from *B* to *C*.

The *A* cantilever has its architrave determined by (415). That is,

$$\begin{aligned} \rho &= 1,000 \sinh \left(2.534 + j \frac{\pi}{2} \right) \cdot \frac{\cosh 2.15892}{\cosh \left(0.534 + j \frac{\pi}{2} \right)} \cdot \frac{\cosh 0.5}{\cosh 0.65892} = \\ & \qquad \qquad \qquad 45,766.5 \text{ ohms,} \end{aligned}$$

and *ν* = 1/ρ = 0.02185 × 10⁻³ mho.

The line admittance at A is $Y_{oA} = y_1 \coth \delta_A = 10^{-3} \times \coth (2.534 + j1) = 10^{-3} \times \tanh 2.534 = 0.98749 \times 10^{-3}$ mho. Subtracting ν from Y_{oA} , we have the A leak admittance $g_1 = 0.96564 \times 10^{-3}$ mho. One volt applied at A would thus deliver 0.98749 milliamp. to the system, and 0.02185 milliamp. to ground at F .

If the complete equivalent Π of the system is desired, we must

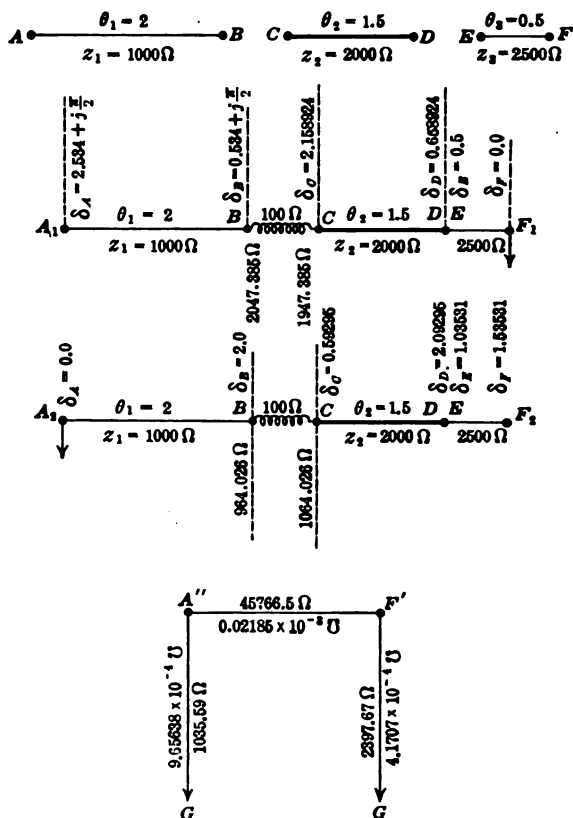


FIG. 169.—Three-section composite line with series intermediate load.

ground A at A_2 , and develop the position angles toward F_2 , Fig. 169. At B , the angle is $\delta_B = 2.0$ and $Z_{oB} = z_1 \tanh \delta_B = 1,000 \tanh 2 = 964.026$ ohms, as shown. At C , this is increased to 1,064.026. The position angle $\delta_C = \tanh^{-1} \left(\frac{Z_{oC}}{z_2} \right) = \tanh^{-1} \left(\frac{1,064.026}{2,000} \right) = \tanh^{-1} 0.532013 = 0.59295$ hyp. From this point

on to F , the position angles advance in the manner already described. Potentials now follow sines and currents cosines, starting from some point where either the potential or the current is known. No discontinuities are made at transitions, except at $B-C$, where an Ohm's law vector drop occurs.

The F cantilever now follows, by (418),

$$\rho = 2,500 \sinh 1.53531 \times \frac{\cosh 2.09295}{\cosh 1.03531} \times \frac{\cosh 2.0}{\cosh 0.59295} = 45,766.5 \text{ ohms,}$$

and $\nu = 1/\rho = 0.02185 \times 10^{-3}$ mho. This provides a check on the computation, since ρ'' must have the same value from either terminal of the system. The line admittance $Y_{oF} = 0.4 \times 10^{-3} \coth 1.53531 = 0.4 \times 10^{-3} \times 1.0973 = 0.43892 \times 10^{-3}$ mho. The F leak is thus 0.41707×10^{-3} mho.

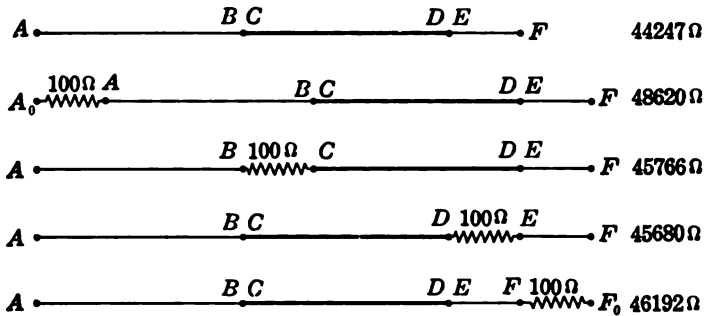


FIG. 170.—Effect of position of a series load in a composite line upon the architrave resistance.

The above process indicates that when the position angles have been adjusted, to make allowance for an intermediate impedance load, the architrave of the equivalent Π is obtained by the same formula (415) or (418), as though no intermediate load had been introduced.

The effect of a given impedance load on the architrave impedance of the system will, in general, differ at different positions of insertion. For the particular case of the three sections here discussed, Fig. 170 shows the effects of introducing a resistance of 100 ohms at different points. It will be seen that the system architrave impedance varies from 45,680 to 48,620 ohms.

In a.c. cases, such differences may be surprisingly large.

Terminal Leak Loads.—It is obvious that if a leak be applied at one terminal of a composite-line system, it will have no effect

on the system if that terminal is grounded, and the distribution of position angles toward the opposite terminal will be the same as before the leak was applied. If a terminal impedance to ground is added after applying the leak to the terminal, the leak will serve to modify the value of the terminal impedance by shunting it.

If the leak be applied at the up terminal, or generator terminal, then a given voltage applied to that terminal will produce the same distribution of potential and current over the line as before the load was applied, except that a current to ground will flow through the leak by Ohm's law.

Similarly, if terminal leaks are applied simultaneously at both ends of the line, the changes produced in the system will be of a simple and self-evident character. The equivalent Π of the system will be unchanged in architrave; but the terminal leaks will be respectively increased by the values of the terminal leak loads.

Intermediate Leak Loads.—A casual intermediate leak in a composite line may always be assumed to be applied at a junction between sections; because, if it should actually occur within a single section, that section may be regarded as divided into two single lines, with a junction at the leak.

An example of an intermediate leak load is offered in Fig. 171. Here a leak of 0.5 millimho is applied at junction DE . If the F_1 terminal be grounded, position angles may be distributed toward A . At E , $\delta_E = 0.5$, $Z_{gE} = z_3 \tanh \delta_E = 2,500 \tanh 0.5 = 1,155.29$ ohms. Converting this into an admittance $Y_{gD} = y_3 \coth \delta_E = 0.86558 \times 10^{-3}$ mho. To this line admittance we add the admittance of the leak 0.5×10^{-3} , making $Y_{gE} = 1.36558 \times 10^{-3}$. Consequently, the impedance load at D on the section CD is $Z_{gE} = 1/Y_{gE} = 732.289$ ohms. The position angle at D is thus

$$\delta_D = \tanh^{-1} \left(\frac{Z_{gE}}{z_2} \right) = \tanh^{-1} \left(\frac{732.289}{2,000} \right) = \tanh^{-1} 0.361145 = 0.38396 \text{ hyp.}$$

The remaining position angles to A_1 are worked out in the usual way. The potentials and currents are then distributed in the manner previously described, without discontinuities at transitions; except that, at D , the line current suddenly drops by the amount supplied through the leak.

If we seek the A cantilever, the architrave impedance is

$$\rho = z_1 \sinh \delta_A \cdot \frac{\cosh \delta_C}{\cosh \delta_B} \cdot \frac{\cosh \delta_E}{\cosh \delta_D} \cdot \frac{Z_{oE}}{Z_{oD}} \quad \text{ohms } \angle \quad (436)$$

$$= z_1 \sinh \delta_A \cdot \frac{\cosh \delta_C}{\cosh \delta_B} \cdot \frac{\cosh \delta_E}{\cosh \delta_D} \cdot \frac{Y_{oD}}{Y_{oE}} \quad \text{ohms } \angle \quad (437)$$

$$= 1,000 \sinh \left(2.58135 + j \frac{\pi}{2} \right) \times \frac{\cosh 1.88396}{\cosh \left(0.58135 + j \frac{\pi}{2} \right)} \times \frac{\cosh 0.5}{\cosh 0.38396} \times \frac{1,155.29}{732.29} = 60,240 \text{ ohms.}$$

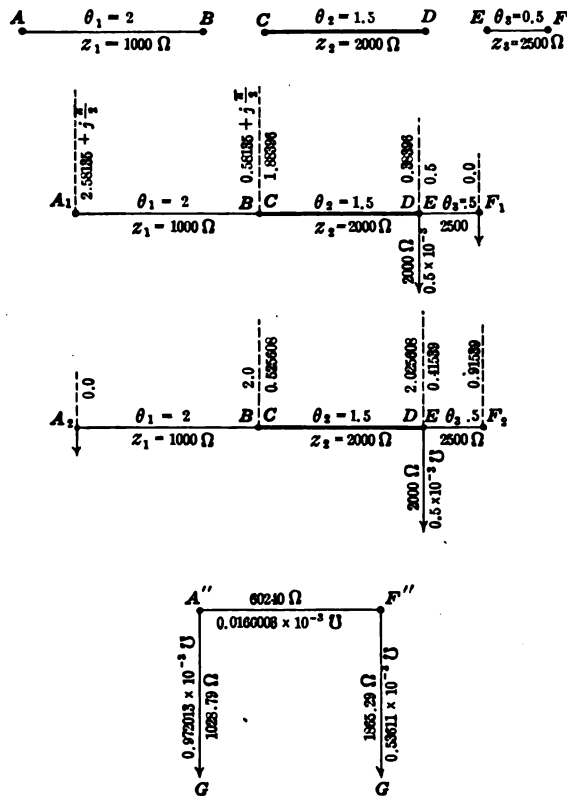


FIG. 171.—Three-section composite line with leak load.

The *A* leak is found in the ordinary way (419).

It will be observed that in addition to the usual cosine ratios appearing in the formula for the architrave, we have to introduce an additional ratio of either line impedances, or line admittances, on each side of the leak load.

To complete the equivalent Π , we ground at A , develop position angles toward F , and take the leak into account in the same way as above. The architrave impedance is then

$$\rho = z_3 \sinh \delta_F \cdot \frac{\cosh \delta_D}{\cosh \delta_E} \cdot \frac{\cosh \delta_B}{\cosh \delta_C} \cdot \frac{Z_{oD}}{Z_{oE}} \text{ ohms } \angle \quad (438)$$

$$= 60,240 \text{ ohms, as before.}$$

The F leak is then worked out regularly.

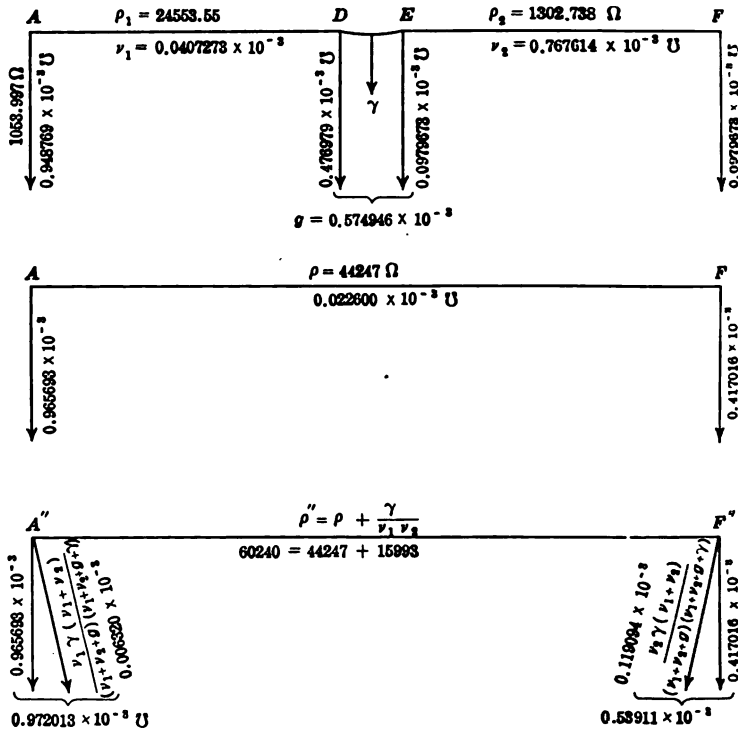


FIG. 172.—Development of equivalent Π of composite line having a leak load γ at the junction DE .

It will be observed on comparing equivalent π 's in Figs. 155 and 171, that the effect of the intermediate leak has been to increase the architrave impedance, and also each pillar leak. It may in fact be easily shown that if, as in Fig. 172, a composite line AF is divided into two sections AD, EF , each with its equivalent Π as shown, then the merging of these two sections with their combined leak g at DE , gives rise to the equivalent Π , AF with architrave ρ . The effect of an added leak at DE of γ

mhos is to increase the architrave by an amount $\frac{\gamma}{v_1 v_2}$ ohms, and to distribute increments to the terminal leaks in direct proportion to the architrave admittances v_1 and v_2 . In this case $\gamma = 0.5 \times 10^{-3}$ $v_1 = 0.0407273 \times 10^{-3}$ and $v_2 = 0.767614 \times 10^{-3}$. The increment in ρ is thus $\frac{0.5 \times 10^{-3}}{0.31263 \times 10^{-7}} = 15,993$ ohms. Also $v_2/v_1 = 18.84$, and this is the ratio of the increments due to the leak load, namely $\frac{0.119094}{0.006320} = 18.84$.

Bifurcating Composite Lines.—Considering the composite line in Fig. 171, with its leak load at *D*, it is evident that this

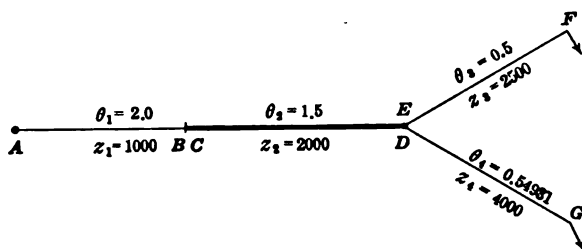


FIG. 173.—Bifurcated composite line.

corresponds to a case of a composite line bifurcating at *D*, as in Fig. 173. The branch *DG* is grounded at *G*. Its surge resistance may be, say, 4,000 ohms, in which case its line angle must be 0.54931 hyp. Its line admittance at *D* will be $0.25 \times 10^{-3} \coth 0.54931 = 0.5 \times 10^{-3}$ mho. Consequently, a bifurcation in a composite line may be dealt with, either by regarding the two branches *DF* and *DG* as constituting jointly a terminal load at *D*, and distributing the position angles over the system on that basis; or, one branch, such as *DG*, may be regarded as a casual leak, at the junction *DE* of the composite line *AF*.

There is thus no difficulty theoretically in dealing with any system of composite lines, consisting of a generator end, a main section leading therefrom, and any number of bifurcations or successive ramifications proceeding from this or from its branches. Each branch is assigned a definite terminal load, which is zero if that branch is grounded, and infinity if it is freed. Volt-ampere-wattmeter measurements, in the general

case, fix the values of the terminal loads. The line admittance or impedance of each branch is then determinable at the point where it joins the supply main. Any tree system of mains, therefore, possesses its natural distribution of position angles, and comes under the domain of our hyperbolic theory.

Tabulation of Changes in Architrave Formula with Casual Loads.—The following table, which may be useful for reference, contains a summary of the changes made in architrave impedance by the casual loads already considered.

TABLE XVII

Nature of load	Change introduced by load into the formula (415) for ρ	New formula
Terminal impedance:		
At down end <i>A</i>	$\cosh 0 / \cosh \delta_A$	(422)
At up end <i>A</i>	$Z_{\rho A 0} / Z_{\rho A} = (Z_{\rho A} + \sigma) / Z_{\rho A}$	(425)
At up end <i>A</i>	also $\sinh (\delta_A + \theta') / \cosh \theta'$	(434)
Intermediate impedance.....	None	
Terminal leak:		
At down end.....	None	
At up end.....	None	
Intermediate leak at <i>D-E</i>	$\frac{Z_{\rho H}}{Z_{\rho D}} = \frac{Y_{\rho D}}{Y_{\rho H}}$	(436) and (437)

Plurality of Loads in a Composite Line.—It appears that the corrections introduced into the architrave impedance ρ , for casual loads, are mutually independent. That is to say, when several casual loads occur simultaneously, in a composite system, whether they are of the same kind, or of different kinds, they each call for their independent individual corrections.

An example of a three-section composite line, with three casual loads in Fig. 174. Here the same three sections *AB*, *CD*, *EF* as before, have an intermediate impedance load of 100 ohms at *BC*, a terminal impedance load of 200 ohms at *GH*, and a leak load at *FG*. This leak is virtually an intermediate leak.

Referring to Table XVII, we see that no change in the architrave formula is introduced by the *BC* load, and the leak at *FG* introduces one extra impedance ratio. When the *H* end is

down and grounded, the terminal impedance GH , introduces one extra cosine ratio. When the H end is up, the same terminal impedance introduces one extra resistance ratio Z_{GH}/Z_{GD} .

Thus grounding at H_1 , the architrave impedance is

$$\rho = z_1 \sinh \delta_A \cdot \frac{\cosh \delta_C}{\cosh \delta_B} \cdot \frac{\cosh \delta_E}{\cosh \delta_D} \cdot \frac{\cosh 0}{\cosh \delta_F} \cdot \frac{Z_{GD}}{Z_{GF}} \quad \text{ohms } \angle \quad (439)$$

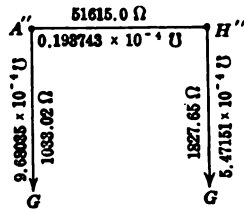
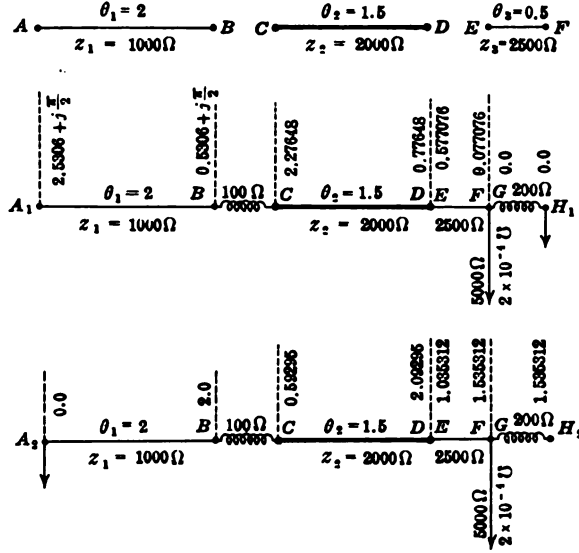


FIG. 174.—Three-section composite line with one leak load, one intermediate series load and one terminal series load.

$$\begin{aligned} &= 1,000 \sinh \left(2.5306 + j\frac{\pi}{2} \right) \times \frac{\cosh 2.27648}{\cosh \left(0.5306 + j\frac{\pi}{2} \right)} \\ &\quad \times \frac{\cosh 0.577076}{\cosh 0.77648} \times \frac{\cosh 0}{\cosh 0.077076} \times \frac{200}{192.31} \\ &= 1,000 \times j6.32032 \times \frac{4.92248}{j0.55585} \times \frac{1.17118}{1.31691} \times \frac{1}{1.00297} \times \frac{200}{192.31} \\ &= 51,615 \text{ ohms.} \end{aligned}$$

Again, grounding at A_2 , the architrave impedance is

$$\begin{aligned}
 &= \frac{Z_{\sigma H}}{Z_{\sigma F}} \cdot z_3 \sinh \delta_F \cdot \frac{\cosh \delta_D}{\cosh \delta_B} \cdot \frac{\cosh \delta_B}{\cosh \delta_C} \cdot \frac{Z_{\sigma F}}{Z_{\sigma G}} \quad \text{ohms } \angle \quad (44) \\
 &= \frac{1,765.14}{2,278.32} \times 2,500 \times \sinh 1.53531 \times \frac{\cosh 2.09295}{\cosh 1.03531} \\
 &\qquad\qquad\qquad \times \frac{\cosh 2.0}{\cosh 0.59295} \times \frac{2,278.32}{1,565.14} \\
 &= 0.7760 \times 2,500 \times 2.21368 \times \frac{4.11606}{1.58555} \times \frac{3.76220}{1.18101} \times \frac{2,278.32}{1,565.14} \\
 &\qquad\qquad\qquad = 51,615 \text{ ohms.}
 \end{aligned}$$

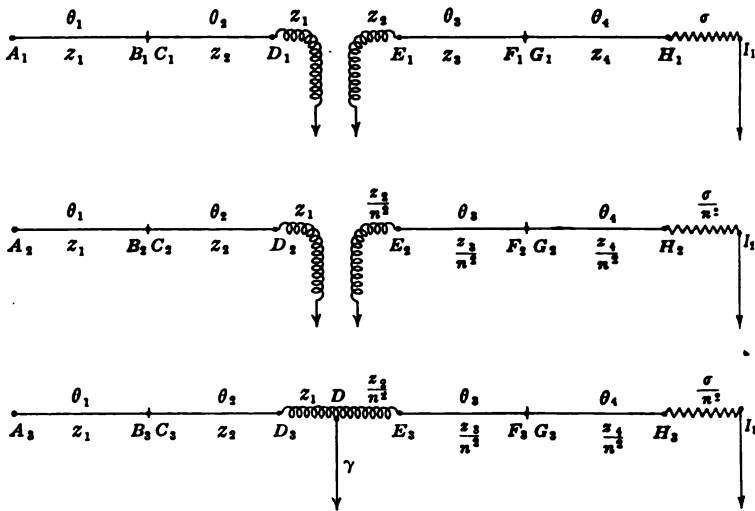


FIG. 175.—Treatment of inductively connected composite lines.

Case of an Alternating-current Transformer Inserted in Composite Line.—In Fig. 175, we have a composite line AB, CD connected inductively through a transformer with another composite line EF, GH grounded at H , through a terminal load σ ohms. The four single lines have the respective angles and surge impedances $\theta_1, \theta_2, \theta_3, \theta_4$ and z_1, z_2, z_3, z_4 . The transformer may be assumed to have a voltage ratio of n , in the sense that after deducting the primary IZ drop, 1 volt of internally induced primary c.e.m.f. will be associated with n volts in the secondary winding. Both the primary and secondary windings have impedances comprising the effective resistance r , and the effective self-reactance jx ohms. The self-reactance is that reactance which is due to magnetic flux not linked with the other winding.

From this standpoint, a transformer contains a pure resistanceless mutual reactance and a pair of external impedances, one in each circuit.

We may next assume that the transformer is changed to a level transformer, with ratio 1, and with equal numbers of mutual turns in primary and secondary winding. The levelling may be imagined as effected to either primary or secondary voltage. We may assume, as in Fig. 175, that the primary winding remains unchanged, but the secondary winding is levelled to it. All impedances in the secondary system must now be divided by n^2 , and all admittances multiplied by n^2 . This condition is indicated at E_2, F_2, G_2, H_2 . The two level-voltage composite systems may now be joined conductively at F , at a leak γ , which has such admittance as will carry the observed exciting current of the transformer when a corresponding exciting voltage is applied at D . The composite system $A_2 - I_2$ is now a four-section composite line, with a terminal impedance of σ/n^2 ohms \angle at HI , an intermediate impedance D_2E_2 , and a leak γ in the same. The section angles θ_3, θ_4 , have not been altered by the ideal process described.

After the position angles have been assigned to the modified through composite line A_2I_2 , the potentials and currents may be worked out in the usual way. The resulting potentials are then multiplied by n , between D_1 and I_1 , to derive the actual potentials with the actual unlevel transformer, and the resulting currents are likewise divided by n , between D_1 and I_1 . The vector powers on the imaginary level system will agree with the vector powers at corresponding points of the actual system.*

If more than one transformer link occurs in the system, the procedure is the same. There will then be three or more voltage levels, any one of which may be selected as reference level, and the others reduced thereto, by the proper transformation ratios. Thus, if there is a step-up transformer at one end of a section, and a similar step-down transformer at the other, then either the high-voltage or low-voltage level may be accepted as the refer-

* The Application of Hyperbolic Functions to Electrical Engineering Problems," p. 157.

C. P. STEINMETZ, "Theory and Calculation of Alternating-current Phenomena," New York, 1897.

A. E. KENNELLY, "On the Predetermination of the Regulation of Alternating-current Transformers," *Electrical World*, N. Y., vol. xxxiv, p. 343, Sept. 2, 1899.

ence level, in constructing the conductive system. Ordinarily, the low-voltage level is the more convenient. The levelling process introduces no change into the angles which the various sections subtend. It changes only the surge impedances along with all the impedances and admittances of the same circuit. If there were negligible impedance and negligible losses in the transformers, their effect would be confined arithmetically to changing the surge impedances of the sections affected.

Composite-line Tests in the Laboratory.—The following case is taken from experimental tests, at 60~, of a two-section composite line consisting of a telephonic resistance-condensance line, like that indicated in Figs. 122 and 127, joined to part of the line specified* in Table XIII. The connections are indicated in Fig. 176. At the impressed frequency of 60.5~, the artificial telephone line *AB* subtended $0.654 + j0.4068$ hyp., with a surge impedance of $1,365\sqrt{44}^{\circ}.02$ ohms; while the artificial power line *CD* subtended $0.127 + j1.008$ hyp., with a surge impedance of $347.6\sqrt{3}^{\circ}.92$ ohms. The equivalent Π of each section and the equivalent Π of the composite line *AD* are also shown in Fig. 176. The composite line equivalent Π has an architrave of $535\angle 107^{\circ}.5$ ohms, and two dissymmetrical leaks, one of them having a size more than three times that of the other, the slopes also being very different. The composite line was loaded at *D* with $1,000\angle 0^{\circ}$ ohms.

The results of the Drysdale potentiometer tests, reduced to $100\angle 0^{\circ}$ volts at *A*, appear in Fig. 177. The curves indicate the values of potential and current over the conjugate smooth line, while the circles represent the observations at selected junctions along the composite artificial line. It will be seen that the voltage falls along a nearly straight line over the artificial telephone line, from $100\angle 0^{\circ}$ at *A*, to $11.07\sqrt{14}^{\circ}.76$ at *B*. It then rises to $23.21\sqrt{103}^{\circ}.44$ at *D*.

Fig. 178, is a schematic representation of reflected voltage waves over the composite line, assuming that an outgoing wave of $100\angle 0^{\circ}$ volts is suddenly launched from *A* without any accompanying splash or oscillatory disturbance. The coefficients used are given in Table XVIII, based on (360), (410), (411), (412), and (413).

* These tests are recorded in theses at the Massachusetts Institute of Technology by MESSRS. C. W. WHITALL, and F. W. MCKOWN, June, 1916.

Thus, the first outgoing wave from *A*, in Fig. 178, arrives at *B* in the condition $52.00\angle 36^\circ.61$ (line 5, column 1, Table XVIII), or $41.74 - j31.01$ volts. At junction *BC* this wave splits, the transmitted portion is $21.96\angle 4^\circ.33$, and the reflected portion $35.43\angle 124^\circ.06$. This reflected portion returns to *A* under

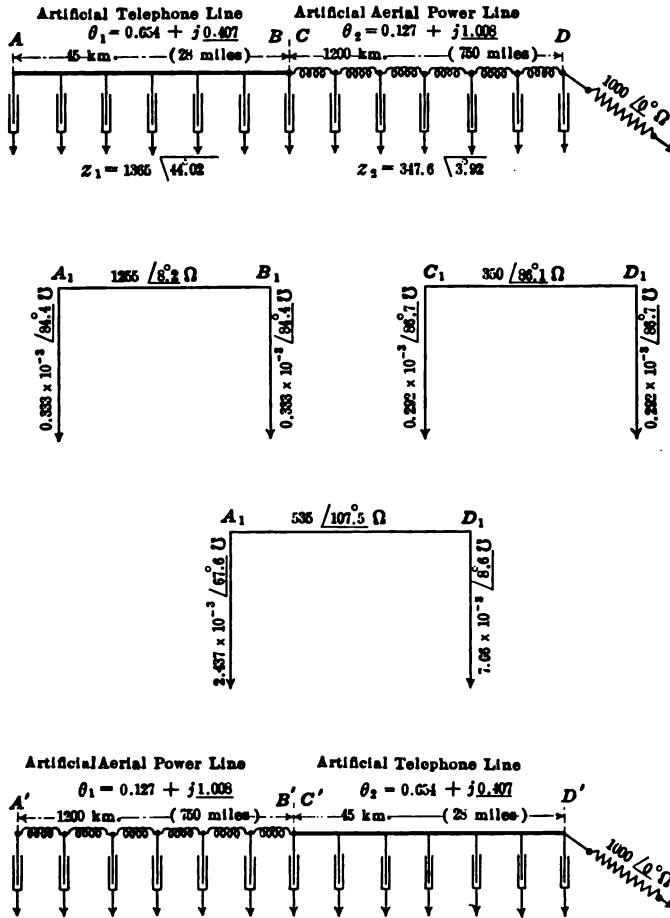


FIG. 176.—Connections of composite artificial line in laboratory test.

attenuation, then to *B*, again is partially reflected back to *A*, and so on, for four *ABBA* return trips, before it is exhausted to below 0.1 volt in size, after which it is ignored in the schedule.

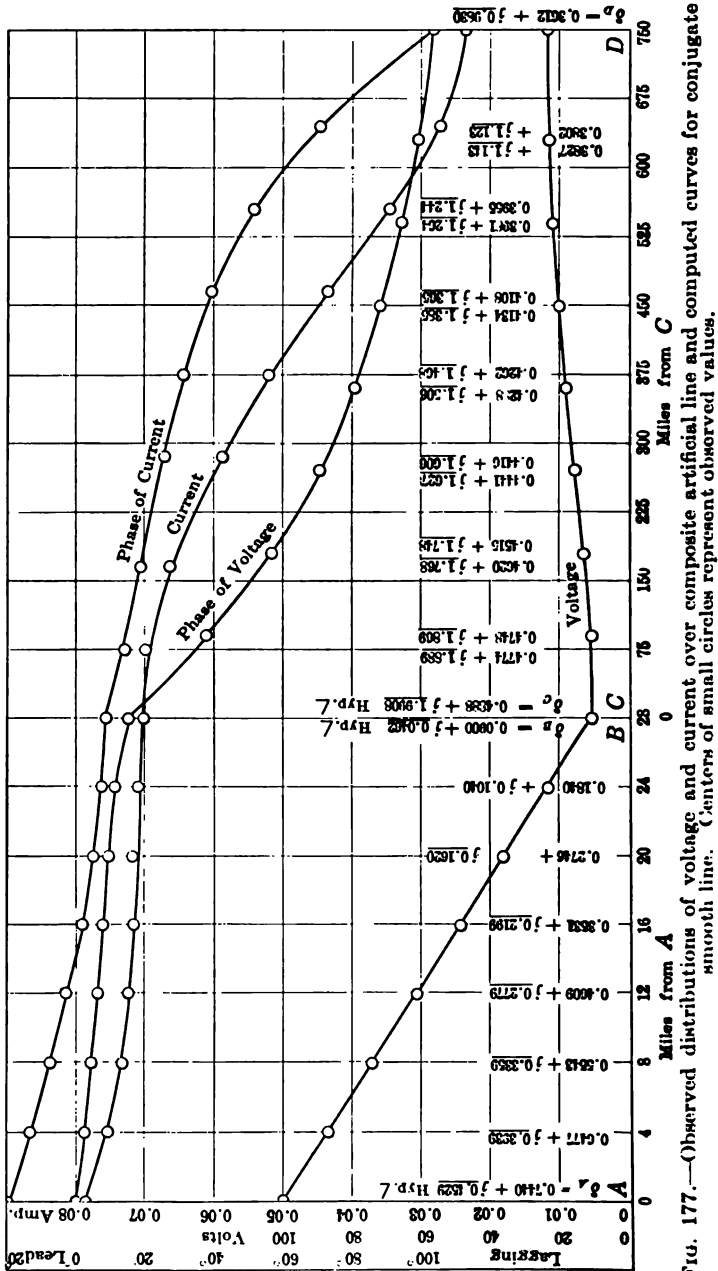
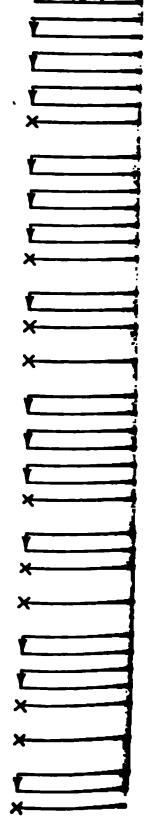


Fig. 177.—(O)bserved distributions of voltage and current over composite artificial line and computed curves for conjugate smooth line. (Centers of small circles represent observed values.)

A

100 + 70



x Sums { 100 + 70

By Hypothesis

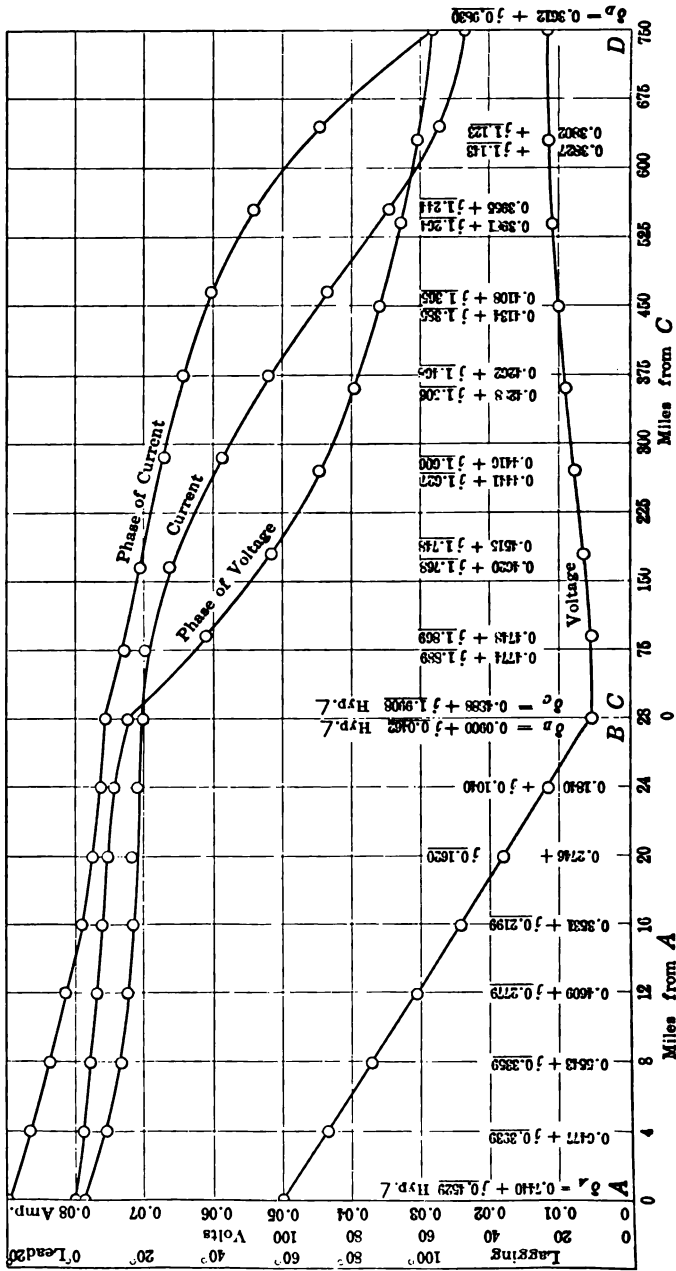


Fig. 177.—Observed distributions of voltage and current over composite artificial line and computed curves for conjugate smooth line. Centers of small circles represent observed values.

Fig. 178 recognizes 40 successive vector increments at *B*, 32 such increments at *C*, and 29 at *D*. The vector sums of these various series appear at the foot of each column. The vector sum at *B* is 11.33∠13°.73 volts, and at *C* 11.17∠16°.37. These sums differ because of the neglect of wave tailings below 0.1 volt in size. If the summations were extended, without mistakes, to a sufficiently great number of terms and wave increments, they would agree with each other, and with the steady-state hyperbolic function value 11.07∠14°.76 volts, as shown below on the lowest line.

Fig. 179 is a similar schedule of current waves, and of their descendants by rupture at junctions. Here 29 increments are included at *A*, 38 at *B*, 50 at *C* and 49 at *D*, before extinction to below 0.1 milliamp. The vector sums are compared with the steady-state hyperbolic values on the two lowest lines of the schedule.

It is clear from Figs. 178 and 179 that if we had to depend on vector summation of reflected and transmitted waves for arriving at final steady states, as in these schedules, the work would frequently be prohibitively laborious. The hyperbolic-function method, on the other hand, by virtually summing up to infinity all these series of vector increments, is a most effective labor-saving device.

Time Interval of a Line.—The apparent velocity of transmission over an artificial line of hyperbolic angle $\theta_1 + j\theta_2$ and representing *L* km. (or miles) of actual conjugate-line length varies somewhat with the frequency, and is by (352),

$$v = \frac{\omega}{\alpha_2} = \frac{L\omega}{\theta_2} \quad \begin{array}{l} \text{km.} \\ \text{sec.} \end{array} \quad (441)$$

and the number of transits per second made by a wave at this velocity in either direction over the line is

$$n = \frac{\omega}{\theta_2} \quad \text{numeric} \quad (442)$$

while the time consumed in any transit in either direction is

$$T = \frac{1}{n} = \frac{\theta_2}{\omega} \quad \text{sec.} \quad (443)$$

This may be called the *time interval* of an a.c. real or artificial line, for the impressed angular frequency ω .

A
E
E
E
E

E

E
E

E

E
E
E

E

:

E
E

E

E
E

E

...



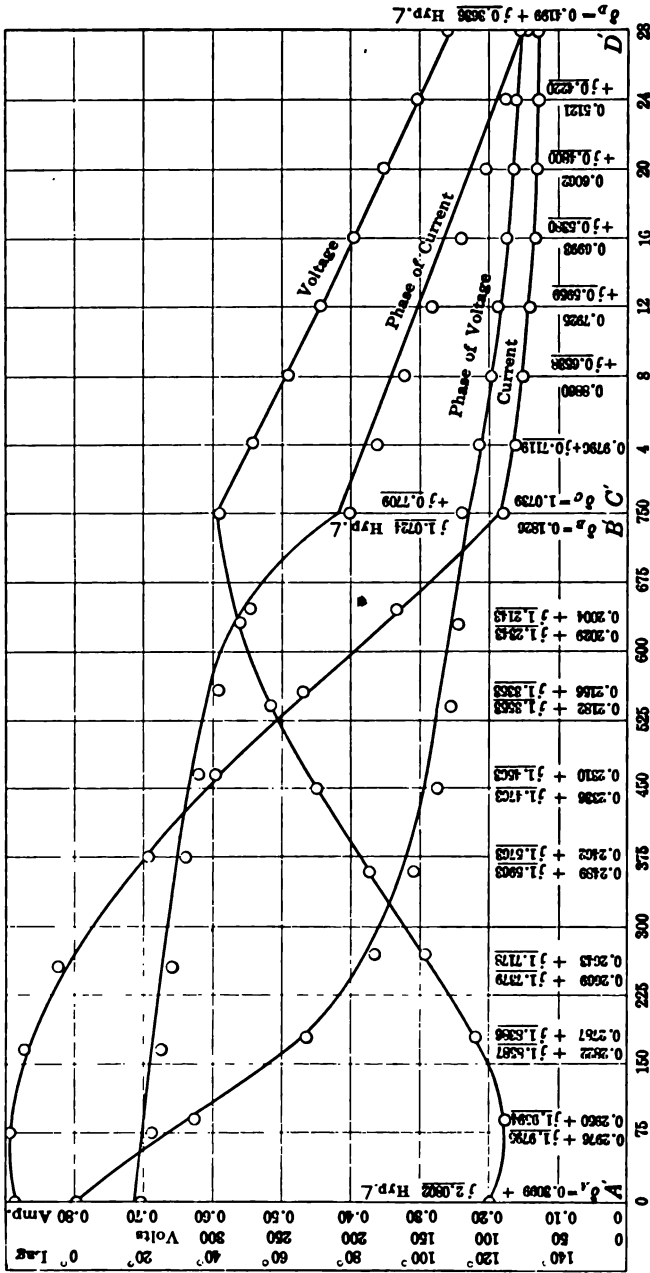


FIG. 180.—Observed distributions of voltage and current over composite line reversed and computed curves for conjugate smooth line. Centers of small circles represent observed values.

In the last three formulas, ω is expressed in radians per second, and θ_2 in circular radians; but if θ_2 is expressed in circular quadrants, ω may be correspondingly expressed in quadrants per second, where

$$\omega_q = 4f \quad \frac{\text{quadrants}}{\text{sec.}} \quad (444)$$

Thus, the artificial power line CD , 1,200 km. long, subtending an angle of $0.1273 + j1.008$ hyps., and the impressed frequency being $60.5 \sim$, the quadrantal angular velocity would be $\omega_q = 242$. Hence $n = 242/1.008 = 240$ single transits per second, $T = 1.008/242 = 0.00416$ second, and $v = 1200 \times 240 = 288000$ km./sec.

It is, therefore, evident that all of the vector increments scheduled in Figs. 178 and 179 are delivered in less than $\frac{1}{4}$ sec. after closing the switch at the generator end A of this composite line. The smaller the losses in the sections, and the higher the attenuation coefficient size $\epsilon^{-\theta_1}$, the more numerous these successive increments must be, in order to reach exhaustion below assigned limits of voltage and current. On the other hand, either on an infinite line, or on a finite line with very great attenuation, the first wave will be the only one to consider in determining the steady state.

Fig. 180 shows the results of the tests on the composite line when the power line was connected to the generator and the telephone line loaded with $1,000\angle 0^\circ$, ohms as at $A'D'$, in Fig. 176. Here the voltage rises from $100\angle 0^\circ$ volts at A' , to $294\angle 112^\circ.9$ volts at B' , and then falls nearly on a straight line to $129.9\angle 128^\circ.6$ volts at D . As in Fig. 177, the curves follow the computed values over the conjugate smooth line and the circles mark the observed values on the artificial line.

Estimating Composite-line Attenuation in Miles.—It has been the custom among telephone engineers to state and compare degrees of attenuation in the sizes of their transmitted telephonic alternating currents in "miles of standard twisted-pair cable." This procedure, while very useful as a first step to engineering accuracy, is quantitatively inferior to the use of architrave or receiving-end impedance. A telephone line, single or composite, becomes commercially unserviceable when its architrave impedance, including that of the receiving terminal apparatus, exceeds certain values at certain frequencies. It is not yet, however,

accurately known what the minimum number of defining frequencies is, or what the limiting impedances are at those frequencies. The "mile" is by comparison with the "architrave ohm" a mere makeshift. In the first place, its effect is not in simple arithmetical progression, but in geometrical progression. Although the same percentage is lost by normal attenuation in each mile, the actual loss is greater in the first mile than in a more distant mile, which gives an element of perplexity to estimates based on length. Again, the "reflection losses" at the junctions of a composite line, when stated in equivalent miles of standard cable, ignore the cumulative effects of such transitions. It would be hopelessly complicated to classify and tabulate with precision, all the necessary corrections in such reflection losses; whereas the architrave impedance of the equivalent Π or cantilever is capable of giving the correct value at once.

CHAPTER XV

QUARTER-WAVE AND HALF-WAVE LINES

If an a.c. line has quarter-wave length to a given frequency, it follows that its hyperbolic angle is then expressible in the form

$$\theta_{\lambda} = \theta_1 + j\frac{\pi}{2} = \theta_1 + j\underline{1} \quad \text{hyp. } \angle \quad (445)$$

When such a line is freed at the motor end, we know that the ratio of the generator-end to motor-end voltage, at the same frequency, is, by (101) or (113),

$$\frac{V_A}{V_B} = \cosh \theta_{\lambda} = \cosh \left(\theta_1 + j\frac{\pi}{2} \right) = j \sinh \theta_1 \quad \text{numeric } \angle \quad (446)$$

On a line of small transmission losses and low attenuation, the real quantity θ_1 may be much less than unity, in which case $\sinh \theta_1 \cong \theta_1$, and the A/B voltage ratio on the quarter-wave line is very nearly

$$\frac{V_A}{V_B} \cong j\theta_1 \quad \text{numeric } \angle \quad (447)$$

or the voltage at A is to that at B in the quadrature ratio of θ_1 . Such a line develops what is commonly called a large Ferranti effect at no load.

Similarly, if this quarter-wave line is shorted or grounded at the far end, we have, by (111),

$$\frac{I_A}{I_B} = \frac{\cosh \theta_{\lambda}}{\cosh 0} = \frac{\cosh \left(\theta_1 + j\frac{\pi}{2} \right)}{1} = j \sinh \theta_1 \quad \text{numeric } \angle \quad (448)$$

which is the same ratio as in (446), or the ratio of currents at generator and motor ends (grounded) are approximately in the quadrature ratio of θ_1 .

An approximate particular case is presented in Fig. 142, where a line of $1.405\angle 69^\circ.7 = 0.487 + j1.318 = 0.487 + j0.839$ hyp. This line had only 83.9 per cent. of a quadrant or quarter-wave length, but its observed free-end voltage ratio was about 1.75; or $V_A/V_B = 0.57$, and $\sinh 0.487 = 0.506$.

Similarly a quarter-wave line whose angle was $0.1 + j1$ would have an A/B voltage ratio of approximately 0.1 or B/A voltage ratio of 10. In power transmission at fundamental frequencies of 60~ or less, lines are hardly ever sufficiently long to reach quarter-wave length; so that this large resonant quarter-wave rise of potential on open circuit was computed* before it was even observed on artificial lines in the laboratory.

An experimental test of this resonant rise was made† on the laboratory artificial line of Table XIV with the connections shown in Fig. 181. The line had a length of 240 miles (386 km.) corresponding to 500,000 circ. mils or 250 sq. mm. cross-section,

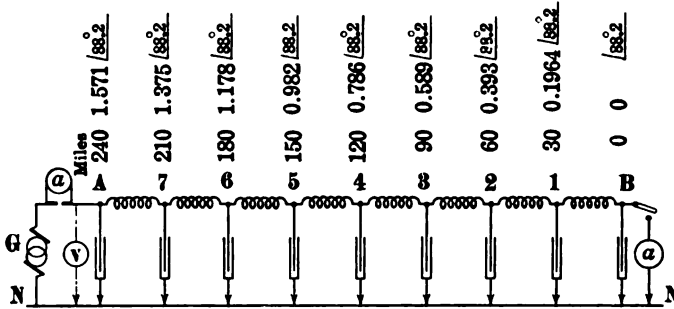


FIG. 181.—Connections for quarter-wave line tests.

in eight sections of 30 miles (48.3 km.) each. In order to make this a quarter-wave line, the impressed frequency was raised to 189~. The data concerning the line at this frequency are given in Table XIX. The angle subtended by the line was then found to be $1.5712 \angle 88.2 = 0.0493 + j1.5706 = 0.0493 + j1$ hyp. According to (447), the ratio of home to far free-end potential should be 0.0493, with a resonant-rise ratio of $1/0.0493 = 20.28$. This was in fact observed within the limits of experimental error. The dots in Fig. 182 indicate observations and the curve connects the computed corresponding values. Table XIX gives

* "Resonance in Alternating-current Lines," by E. J. HOUSTON and A. E. KENNELLY, *Trans. A. I. E. E.*, April, 1895.

† "The Influence of Frequency on the Equivalent Circuits of Alternating-current Transmission Lines," by A. E. KENNELLY, *Electrical World*, Jan. 21, 1909.

"The Application of Hyperbolic Functions to Electrical Engineering Problems," Chapter VII.

† "Resonance Tests of a Long Transmission Line," by A. E. KENNELLY and HAROLD PENDER, *Electrical World*, Aug. 8, 1914.

the observations at junctions and their position angles. In this case, therefore, 1,000 volts applied at the generator end between any pair of the three conjugate smooth-line conductors, at 189~ (386 km.) distant. A corresponding current ratio was also measured with the line grounded at the distant end, in accordance with (448).

TABLE XIX.—VOLTAGES AT SECTION JUNCTIONS OF QUARTER-WAVE ARTIFICIAL LINE FREED AT FAR END

Position	Position angle δ_p hyps. with B grounded	Cosh δ_p by chart	Potential V_p	
			Computed, volts	Observed, volts
B	0	1.000 \angle 0° .0	1,044 \sphericalangle 90° .0	1,033
1	0.1964 \sphericalangle 88° .2	0.98 \angle 0° .10	1,023 \sphericalangle 89° .9	1,015
2	0.393 \sphericalangle 88° .2	0.924 \angle 0° .25	965 \sphericalangle 89° .75	960
3	0.589 \sphericalangle 88° .2	0.832 \angle 0° .75	869 \sphericalangle 89° .25	860
4	0.786 \sphericalangle 88° .2	0.708 \angle 1° .3	739 \sphericalangle 88° .7	735
5	0.982 \sphericalangle 88° .2	0.555 \angle 2° .7	579 \sphericalangle 87° .3	559
6	1.178 \sphericalangle 88° .2	0.383 \angle 5° .3	400 \sphericalangle 84° .5	397
7	1.375 \sphericalangle 88° .2	0.200 \angle 11° .5	209 \sphericalangle 78° .5	211
A	1.571 \sphericalangle 88° .2	0.0493 \sphericalangle 90° .0	51.5 \sphericalangle 0° .0	51.5 \sphericalangle 0°

In power-transmission practice, there is at present no reason for fearing the results of any such large resonant rise of potential, partly because of the great length of line necessary, at 25~ or even at 60~, to approximate quarter-wave conditions, and partly because expedients are available for keeping down the motor-end voltage at light load, should it rise seriously. This may be done by means of a synchronous-motor reactance at the far end, or of inductive reactances applied at points along the line. It may be expected, however, that harmonic frequencies in the impressed voltage wave, on a relatively short line, may happen to excite quarter-wave resonance, and so produce, by perpendicular summation, a relatively large rise at the distant free end. Thus, a 5 per cent. harmonic, multiplied twenty-fold by accidental quarter-wave resonance, would produce a 100 per cent. harmonic component at the distant open end, which, by (395), would give rise to 41.4 per cent. increase in local r.m.s. voltage, neglecting any normal rise in voltage due to the fundamental frequency alone.

Three-quarter, five-quarter and odd-quarter wave lines, in general, give rise to resonant free-end voltages of the same general character as those on quarter-wave lines, but ordinarily much less marked in size.

Half-wave Lines.—On the other hand, half-wave, whole-wave and even-quarter wave lines generally, are characterized by

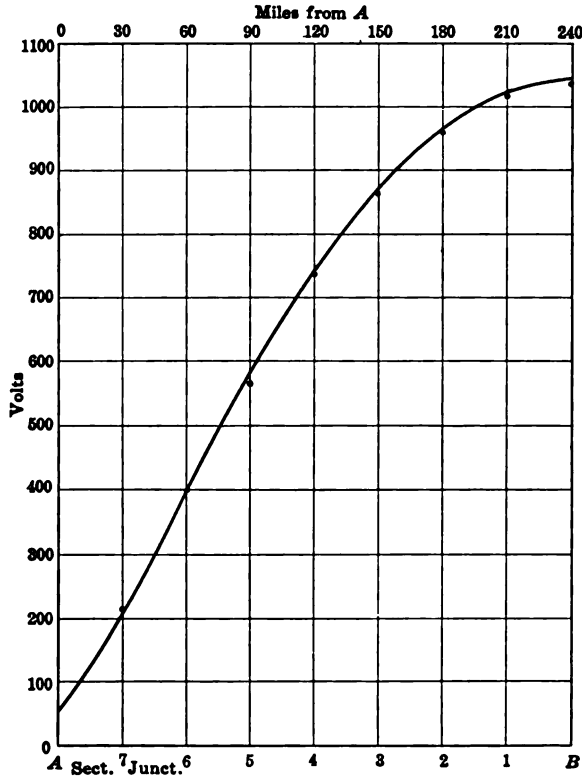


FIG. 182.—Theoretical curve of voltage along conjugate smooth line and observed values at artificial-line junctions.

comparative uniformity between the potentials at their terminals.* A half-wave line has an angle $\theta_{\frac{1}{2}}$

$$\theta_{\frac{1}{2}} = \theta_1 + j\pi = \theta_1 + j2 \quad \text{hyps. } \angle \quad (449)$$

and when freed at B , the A/B potential ratio is, by (111),

* "An Artificial Transmission Line with Adjustable Line Constants," by C. E. MAGNUSSEN and S. R. BURBANK, *Proc. A. I. E. E.*, Sept. 5, 1916.

$$\frac{V_A}{V_B} = \frac{\sinh(\theta_{1/2} + j\frac{\pi}{2})}{\sinh j\frac{\pi}{2}} = \cosh \theta_{1/2} = -\cosh \theta_1 \quad \text{numeric} \quad (450)$$

When θ_1 is less than 0.2,

$$\cosh \theta_1 \cong 1 + \theta_1 \quad \text{numeric} \quad (451)$$

so that for half-wave lines of very small attenuation,

$$\frac{V_A}{V_B} \cong -(1 + \theta_1) = (1 + \theta_1) \angle 180^\circ \quad \text{numeric} \angle \quad (452)$$

or V_A is greater in size than V_B ,

Similarly, if a half-wave line is grounded or shorted at the motor end B , the currents at A and B have, by (111), the ratio

$$\frac{I_A}{I_B} = \frac{\cosh \theta_{1/2}}{\cosh 0} = \frac{\cosh(\theta_1 + j\pi)}{1} = -\cosh \theta_1 = \cosh \theta_1 \angle 180^\circ \quad \text{numeric} \quad (453)$$

or in the case of small real attenuation with $\cosh \theta_1 \cong 1 + \theta_1$, the currents at the two ends of the line will have opposite phases but nearly the same strength.*

General Remarks Concerning Voltage and Current Ratios on Single Lines.—It follows from (99) and (109) that if a single uniform line of any length or number of waves, is freed at the motor end, and the A/B voltage ratio under a given impressed frequency is denoted by the complex number N , then when the same line is shorted or grounded directly at the motor end, the A/B current ratio under the same frequency must also be N ; because, while the A/B voltage ratio is a sine ratio, yet because the open end virtually adds an imaginary quadrant to the position angles throughout, this ratio becomes virtually a cosine ratio, similar to the A/B current ratio.

As an example to illustrate the above relations, we may consider the case of the smooth line referred to in Chapter XI, having a linear hyperbolic angle of $\alpha = 0.0025 + j0.01$ and a surge impedance of $z_0 = 400 \angle 8^\circ$ ohms. This 800-km. line, when freed at the motor end B and voltage at the generator end

* "The Propagation of Electric Energy by Standing and Traveling Waves, Experimental Test of an Artificial Transmission Line," by JOHN F. H. DOUGLAS, *Electrical World*, Aug. 10, 1912.

with $1.0\angle 0^\circ$ volts, develops the distribution of position angles, potentials and currents shown in Table XX and indicated to polar coordinates in Fig. 183. Referring to the table, the first column indicates positions along the line, with their corresponding distances from *A* in the second column. The third column gives the position angles of those positions. Column IV gives

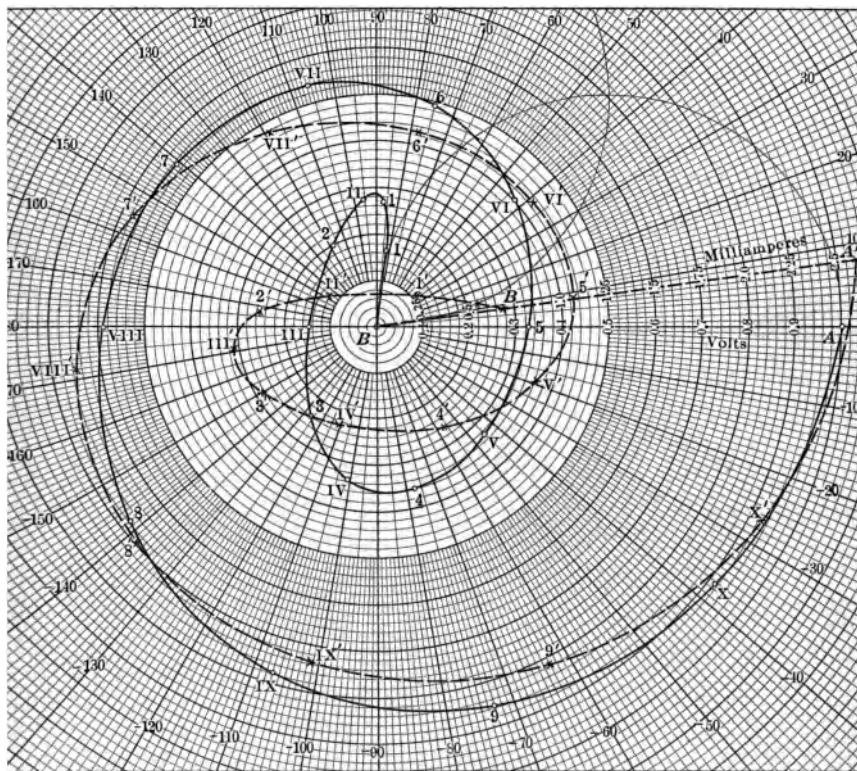


Fig. 183.—Graphs of potential and current along line of $\theta = 2 + j8$ and $z_0 = 400\angle 8^\circ$ grounded at *B*.

the sines of the position angles, from pages 90 to 105 of the "Tables of Complex Hyperbolic Functions." The potentials in column V are in direct proportion to the sines of column IV, starting with $V_A = 1.0\angle 0^\circ$. Column VI gives the cosines of the position angles from pages 106 to 121 of the book of tables. The currents in column VII are directly proportional to the cosines in column VI, starting with $I_A = V_A / (z_0 \tanh \delta_A)$ amp.

Because all the position angles have round numbers, their sines and cosines can be taken directly from the tables, to five decimal places, by direct inspection. In more general cases, either numerical interpolation would be required for any high degree of precision; or the chart atlas could be used for swift graphical interpolation of lesser precision.*

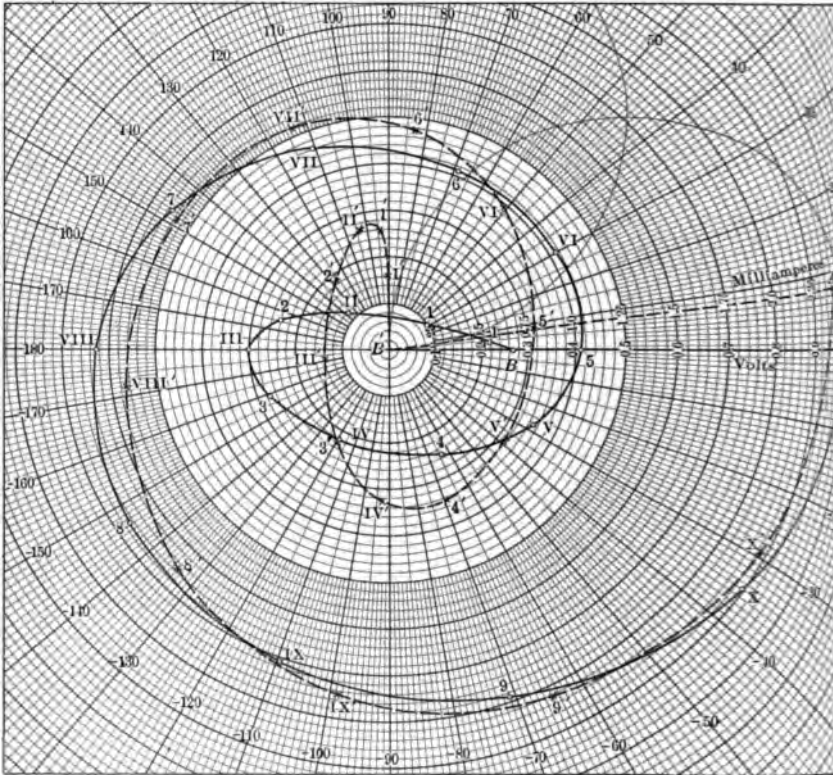


FIG. 184.—Graphs of potential and current along line of $\theta = 2 + j8$ and $z_0 = 400^\circ$ when freed at B .

In Fig. 183, the heavy line is the potential graph; while the broken line is the current graph. The current leads the potential

* It may be noted that when, as in the case considered, the potential or current distribution extends over a considerable range of circular angle or phase displacement, the points along the line at which the position angles are quadrantal, or have an integral number of quadrants in the imaginary, can always be found, and at these points the sines or cosines are always obtainable, from tables of real hyperbolic functions, to at least five places of decimals.

over considerable portions of the line. Both the potential and current curves describe two complete revolutions in phase; but the difference of phase between them is not constant.

In Table XXI and Fig. 184, the same line is considered as freed at the *B* end, and voltage at *A* with $1.0\angle 0^\circ$ volts. The table is prepared in the same manner as its predecessor No. XX. The position angles of Table XXI exceed the corresponding position angles of Table XX by one imaginary quadrant, since the free end adds $j\frac{\pi}{2}$, or $j\underline{1}$, to all the position angles. It will be seen on comparing the two tables, that the sizes of the sines in

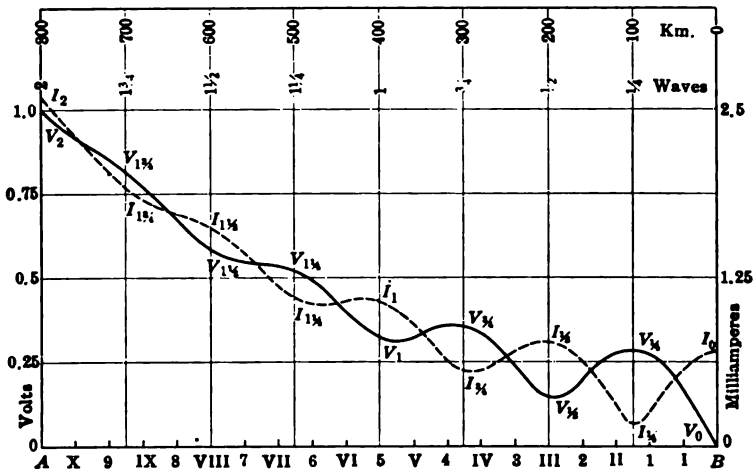


FIG. 185.—Sizes of potentials and currents along smooth line of $\theta = 2 + j8$ and $z_0 = 400\angle 8^\circ$ when grounded at *B* and subjected at *A* to $1.0\angle 0^\circ$ volt.

one are the same as those of the corresponding cosines in the other; or, from (113) and (114),

$$\left| \sinh \left(\alpha + j\frac{\pi}{2} \right) \right| = \left| \cosh \alpha \right| \quad \text{numeric} \quad (454)$$

and

$$\left| \cosh \left(\alpha + j\frac{\pi}{2} \right) \right| = \left| \sinh \alpha \right| \quad \text{numeric} \quad (455)$$

Consequently, the relative sizes of the currents along the line to ground are identical with the relative sizes of the potentials along the line freed, and reciprocally. The same relation can be observed in Fig. 184, which gives the graphs of potential and current along the line, and which may be compared with Fig. 83 for this purpose.

Figs. 185 and 186 are corresponding "size-distance" diagrams of voltage and current for the same line, grounded and freed at *B*, respectively. Referring to Fig. 185, the continuous line $V_2 \dots V_0$ follows the size of potential along the line from 1 to 0; while the broken line $I_2 \dots I_0$ follows the size of the current from 2.59 to 0.689 milliamper. The abscissas are marked off in positions, in kilometer distances, and in wave lengths from *B*. It will be observed that the *V* curve passes through either an

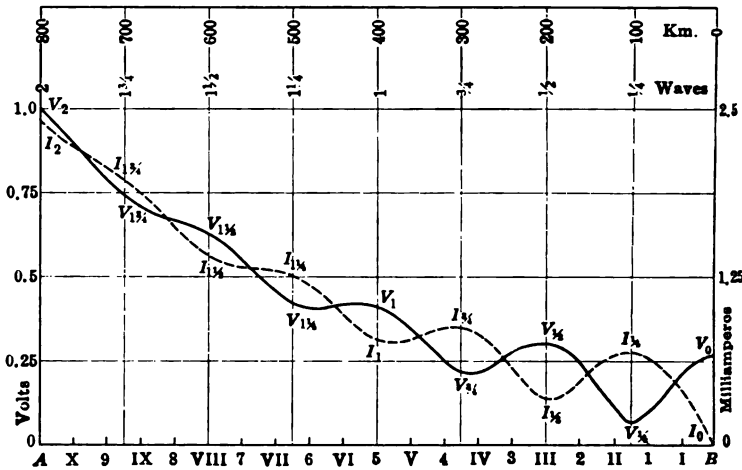


Fig. 186.—Sizes of potentials and currents along smooth line of $\theta = 2 + j\beta$ and $z_0 = 400\sqrt{3}$ when freed at *B* and subjected at *A* to $1.0\angle 0^\circ$ volt.

actual maximum, or a tendency to a maximum size, at each odd quarter-wave distance from *B*. The maximum at the first quarter is the most marked, and the successive subsequent maxima dwindle and gradually disappear. The *I* curve shows on the other hand, minima at the quarter-wave points and maxima at the zero and half-wave points, the oscillation in size being greatest near the *B* end, and gradually disappearing.

Turning now to Fig. 186, where the conditions are represented for an open end at *B*, the *V* line has its minima at odd-quarter wave points and the *I* line its maxima at these points. If the scale of potential and current sizes were suitably selected, the two sets of curves in Figs. 185 and 186 would completely coincide, the *V* curve in one with the *I* curve in the other. With the particular scales shown, the agreement is fairly close.

In the case of a large slope β° in the linear hyperbolic angle α ,

that is, in lines having small linear losses and large linear reactances, as for example a large-conductor aerial line operated at a high frequency, the successive oscillations in the sizes of potential and current continue for a number of waves, with but little damping or diminution. In the case of the line represented in Figs. 185 and 186, the oscillations in size rapidly diminish after the first wave length. In lines of large losses and low linear reactance, even the first oscillation may be imperceptible.

Figs. 185 and 186, show in connection with Tables XX and XXI, that if the line therein considered is open at *B*, a potential of 0.06716 volt at the quarter-wave point 100 km. from *B*, would develop 0.2658 volt at *B*, a resonant *B/A* voltage ratio of nearly 4. At the half-wave point III, 200 km. from *B*, an impressed potential of 0.2997 volt would produce 0.2658 volt at *B*, a drop of 0.1276 per unit, or 12.76 per cent. By proceeding in this way, the ratio of generator to motor end potential or current can be found from these figures for any length of this type of line, at the selected angular frequency of $\omega = 5,000$ ($f = 796\sim$), with the line either open or shorted at the motor end.

If the smooth line considered in Figs. 185 and 186 were replaced by its equivalent *T* or Π line, the graph of potential and current sizes would manifestly be a succession of straight lines. For example, if the artificial line was a Π line of eight sections, each representing a quarter wave at the selected frequency, the potential sizes at terminals and junctions would coincide with those indicated at the points $V_2, V_{1\frac{3}{4}}, V_{1\frac{1}{2}} \dots V_0$, and would fall from one such point to the next in a simple straight line. The current size on the other hand would be in successive horizontal sections with sudden drops at leaks.

Quarter-wave Artificial Lines.—A quarter-wave artificial line, which needs only to be constructed of a single section, has the property of producing a relatively large rise of voltage at the motor free end, when voltage at the generator end with the correct frequency. Such a device becomes, in effect, a frequency-change detector, since if the frequency varies, in either direction, from the normal for which the line section is designed, the motor-end voltage falls off rapidly. Such a quarter-wave artificial line is, however, only a particular set of connections for producing resonance between inductive and condensive reactances at a critical frequency.

TABLE XX
Distribution of Potential and Current over a Uniform Smooth Line of $\theta = 2.0 + j8$ and $z_0 = 400\angle 8^\circ$, when Grounded at B and Voltaged at A

I Position	II r km.	III δ_p hypos.	IV $\sinh \delta_p$ by tables	V V_p volts	VI $\cosh \delta_p$ by tables	VII I_p milliamp.
A	0	$2.0 + j8.0$	$3.62686\angle 0^\circ$	$1.00\angle 0^\circ$	$3.76220\angle 0^\circ$	$2.59328\angle 8^\circ$
X	40	$1.9 + j7.6$	$3.32060\angle 37^\circ.227$	$0.91556\angle 37^\circ.227$	$3.36681\angle 34^\circ.789$	$2.32074\angle 26^\circ.789$
9	80	$1.8 + j7.2$	$3.09206\angle 72^\circ.900$	$0.85255\angle 72^\circ.900$	$2.95835\angle 71^\circ.059$	$2.03919\angle 63^\circ.059$
IX	120	$1.7 + j6.8$	$2.81138\angle 106^\circ.906$	$0.77516\angle 106^\circ.906$	$2.66361\angle 109^\circ.155$	$1.83602\angle 101^\circ.155$
8	160	$1.6 + j6.4$	$2.44721\angle 141^\circ.752$	$0.67475\angle 141^\circ.752$	$2.50955\angle 146^\circ.192$	$1.72983\angle 138^\circ.192$
VIII	200	$1.5 + j6.0$	$2.12928\angle 180^\circ$	$0.58709\angle 180^\circ$	$2.35241\angle 180^\circ$	$1.62151\angle 172^\circ$
7	240	$1.4 + j5.6$	$1.99295\angle 140^\circ.627$	$0.54950\angle 140^\circ.627$	$2.06903\angle 147^\circ.249$	$1.42618\angle 155^\circ.249$
VII	280	$1.3 + j5.2$	$1.94654\angle 105^\circ.642$	$0.53670\angle 105^\circ.642$	$1.72627\angle 110^\circ.659$	$1.18992\angle 118^\circ.659$
6	320	$1.2 + j4.8$	$1.78409\angle 74^\circ.844$	$0.49191\angle 74^\circ.844$	$1.54077\angle 68^\circ.706$	$1.06205\angle 76^\circ.706$
VI	360	$1.1 + j4.4$	$1.45926\angle 42^\circ.227$	$0.40235\angle 42^\circ.227$	$1.56156\angle 30^\circ.182$	$1.07638\angle 38^\circ.182$
5	400	$1.0 + j4.0$	$1.17520\angle 0^\circ$	$0.32403\angle 0^\circ$	$1.54308\angle 0^\circ$	$1.06364\angle 8^\circ$
V	440	$0.9 + j3.6$	$1.18289\angle 45^\circ.407$	$0.32615\angle 45^\circ.407$	$1.30700\angle 27^\circ.493$	$0.90091\angle 19^\circ.493$
4	480	$0.8 + j3.2$	$1.30124\angle 77^\circ.825$	$0.35878\angle 77^\circ.825$	$0.94033\angle 63^\circ.927$	$0.64817\angle 55^\circ.927$
IV	520	$0.7 + j2.8$	$1.21653\angle 101^\circ.110$	$0.33542\angle 101^\circ.110$	$0.81911\angle 118^\circ.263$	$0.56461\angle 110^\circ.263$
3	560	$0.6 + j2.4$	$0.86650\angle 126^\circ.471$	$0.23892\angle 126^\circ.471$	$1.02948\angle 158^\circ.685$	$0.70962\angle 150^\circ.685$
III	600	$0.5 + j2.0$	$0.52110\angle 180^\circ$	$0.14368\angle 180^\circ$	$1.12763\angle 180^\circ$	$0.77727\angle 172^\circ$
2	640	$0.4 + j1.6$	$0.71708\angle 117^\circ.607$	$0.19771\angle 117^\circ.607$	$0.90732\angle 164^\circ.568$	$0.62542\angle 172^\circ.568$
II	680	$0.3 + j1.2$	$0.99862\angle 95^\circ.407$	$0.27534\angle 95^\circ.407$	$0.43385\angle 138^\circ.122$	$0.29905\angle 146^\circ.122$
1	720	$0.2 + j0.8$	$0.97213\angle 86^\circ.331$	$0.26804\angle 86^\circ.331$	$0.36882\angle 31^\circ.277$	$0.25423\angle 30^\circ.277$
I	760	$0.1 + j0.4$	$0.59626\angle 82^\circ.189$	$0.16440\angle 82^\circ.189$	$0.81520\angle 4^\circ.142$	$0.50192\angle 12^\circ.142$
B	800	$0.0 + j0.0$	$0\angle 0^\circ$	$0\angle 0^\circ$	$1.00\angle 0^\circ$	$0.48030\angle 8^\circ$

TABLE XXI
Distribution of Potential and Current over a Uniform Smooth Line of $\theta = 2.0 + j8$ and $z_0 = 400\angle 8^\circ$ when Freed at B and Voltaged at A

I	II	III	IV	V	VI	VII
Position	x km.	δ_p hyas.	$\sinh \delta_p$ by tables	V_p volts	$\cosh \delta_p$ by tables	I_p milliamp.
A	0	$2.0 + j9.0$	$3.76220\angle 90^\circ$	$1.00\angle 0^\circ$	$3.62686\angle 90^\circ$	$2.4101\angle 8^\circ$
X	40	$1.9 + j8.6$	$3.36681\angle 55^\circ.211$	$0.89490\angle 34^\circ.789$	$3.32060\angle 52^\circ.773$	$2.2066\angle 29^\circ.227$
9	80	$1.8 + j8.2$	$2.95835\angle 18^\circ.941$	$0.78634\angle 71^\circ.059$	$3.09206\angle 17^\circ.100$	$2.0547\angle 64^\circ.900$
IX	120	$1.7 + j7.8$	$2.66361\angle 19^\circ.155$	$0.70799\angle 109^\circ.155$	$2.81138\angle 16^\circ.906$	$1.8682\angle 98^\circ.906$
8	160	$1.6 + j7.4$	$2.50955\angle 56^\circ.192$	$0.66704\angle 146^\circ.192$	$2.44721\angle 51^\circ.752$	$1.6263\angle 133^\circ.752$
VIII	200	$1.5 + j7.0$	$2.35241\angle 90^\circ$	$0.62528\angle 180^\circ$	$2.12928\angle 90^\circ$	$1.4149\angle 172^\circ.0$
7	240	$1.4 + j6.6$	$2.06903\angle 122^\circ.751$	$0.54995\angle 147^\circ.249$	$1.99295\angle 129^\circ.373$	$1.3243\angle 148^\circ.627$
VII	280	$1.3 + j6.2$	$1.72627\angle 159^\circ.341$	$0.45885\angle 110^\circ.659$	$1.94654\angle 164^\circ.358$	$1.2985\angle 113^\circ.642$
6	320	$1.2 + j5.8$	$1.54077\angle 158^\circ.706$	$0.40954\angle 68^\circ.706$	$1.78409\angle 164^\circ.844$	$1.1855\angle 82^\circ.844$
VI	360	$1.1 + j5.4$	$1.56156\angle 120^\circ.182$	$0.41507\angle 30^\circ.182$	$1.45926\angle 132^\circ.227$	$0.96969\angle 50^\circ.227$
5	400	$1.0 + j5.0$	$1.54308\angle 90^\circ$	$0.41015\angle 0^\circ$	$1.17520\angle 90^\circ$	$0.78093\angle 8^\circ$
V	440	$0.9 + j4.6$	$1.30700\angle 62^\circ.507$	$0.34740\angle 27^\circ.493$	$1.18289\angle 44^\circ.593$	$0.78604\angle 37^\circ.407$
4	480	$0.8 + j4.2$	$0.94033\angle 26^\circ.073$	$0.24994\angle 63^\circ.927$	$1.30124\angle 12^\circ.175$	$0.86469\angle 69^\circ.825$
IV	520	$0.7 + j3.8$	$0.81911\angle 28^\circ.263$	$0.21772\angle 118^\circ.263$	$1.21653\angle 11^\circ.110$	$0.80840\angle 93^\circ.110$
3	560	$0.6 + j3.4$	$1.02948\angle 68^\circ.685$	$0.27364\angle 158^\circ.685$	$0.86650\angle 36^\circ.471$	$0.57580\angle 118^\circ.471$
III	600	$0.5 + j3.0$	$1.12763\angle 90^\circ$	$0.29973\angle 180^\circ$	$0.52110\angle 90^\circ$	$0.34628\angle 172^\circ$
2	640	$0.4 + j2.6$	$0.90732\angle 105^\circ.432$	$0.24117\angle 164^\circ.568$	$0.71708\angle 152^\circ.393$	$0.47651\angle 125^\circ.607$
II	680	$0.3 + j2.2$	$0.43385\angle 131^\circ.878$	$0.11532\angle 138^\circ.122$	$0.99862\angle 174^\circ.593$	$0.66359\angle 103^\circ.407$
1	720	$0.2 + j1.8$	$0.36882\angle 121^\circ.277$	$0.09803\angle 31^\circ.277$	$0.97213\angle 176^\circ.331$	$0.64599\angle 94^\circ.331$
I	760	$0.1 + j1.4$	$0.81520\angle 94^\circ.142$	$0.21668\angle 4^\circ.142$	$0.59626\angle 172^\circ.189$	$0.39622\angle 90^\circ.189$
B	800	$0.0 + j1.0$	$1.00\angle 90^\circ$	$0.26580\angle 0^\circ$	$0\angle 90^\circ$	$0\angle 8^\circ$

CHAPTER XVI

REGULARLY LOADED LINES

Regular loads on a line are similar loads which recur at regular intervals. They may be either regular series loads (impedance loads) or regular leak loads. Regular series loads are well known and much used in long-distance telephony.

In dealing with series loads, their easiest elucidation is perhaps through the use of the equivalent T ; while in dealing with leak loads, the equivalent Π may be used.

Regular Series Loads.—Let a uniform line, of surge impedance r_0 ohms \angle , be divided into uniform sections of angle θ hyps. \angle . Let an impedance load of

$$\Sigma = 2\sigma \qquad \text{ohms } \angle \quad (456)$$

be inserted between adjacent sections ab , cd , ef , as shown in Fig. 187. The end sections will, by symmetry, terminate in a terminal impedance load of σ ohms \angle . It is required to find the angle and surge impedance which each loaded section AB , CD , EF , appears to possess.

First form the equivalent T of any unloaded section by formulas (246) to (249). These are indicated in Fig. 187 at $a'b'$, $c'd'$, and $e'f'$. These are the artificial-line T sections conjugate to those of the original smooth line. Each has arms of ρ' ohms, and a leak of g' mhos.

Next add to each arm of a T its adjacent semi-load σ ohms \angle , as indicated at $A'B'$, $C'D'$, and $E'F'$. The leaks g' remain unchanged. These T 's, as amended, are clearly equivalent to the loaded sections A_1B_1 , C_1D_1 , E_1F_1 .

Finally revert from the amended T 's to their equivalent smooth lines, using (256) and (257), finding θ_1 and z_0 . This completes the required solution.

In the particular case of Fig. 187, each unloaded section subtends an angle of $\theta = 0.35174$ hyp. with a surge impedance of $z_0 = 1,436.1$ ohms. The nominal T of such a section has, therefore, a total line impedance of $0.35174 \times 1,436.14 = 505.14$ ohms, and a total line admittance of $0.35174/1,436.14 = 0.24492 \times 10^{-3}$ mho. The correcting factor for the T arms is $\tanh 0.17587/0.17587 = 0.98982$, and that for the T staff, $\sinh 0.35174/0.35174 = 1.02077$. Applying these factors, the equivalent T

has a resistance in each arm of $\rho' = 250.0$ ohms, and a staff admittance of 0.250×10^{-3} mho. Adding in the impedance semiloads σ to each arm, the amended T has arms of $C'O, OD' = 350.0$ ohms. In the amended T line, therefore, $r = 700$, and

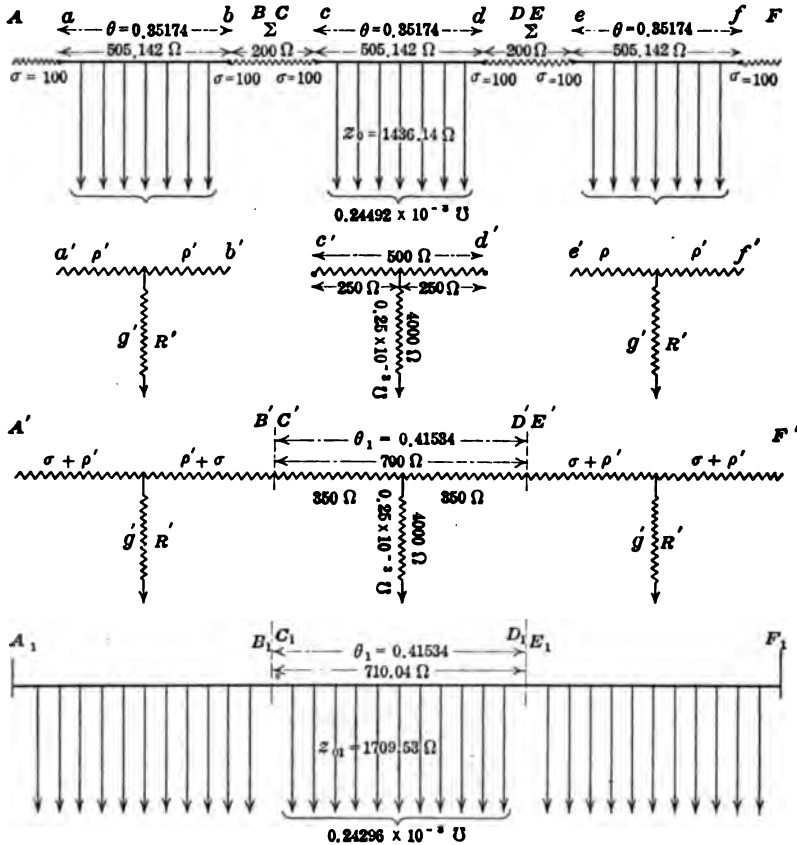


FIG. 187.—Smooth line sections and their equivalents before and after series loading.

$g = 0.25 \times 10^{-3}$. The apparent angle of a half-section is $v = \frac{\theta}{2} = \frac{\sqrt{0.175}}{2} = \frac{0.41833}{2} = 0.209165$ hyp. The corrected semi-section angle is $v = \sinh^{-1}(0.209165) = 0.20767$ hyp. and $\theta = 0.41534$ hyp. The apparent surge impedance of the amended T sections is $z_0 = \sqrt{700/0.25 \times 10^{-3}} = \sqrt{2.8 \times 10^6} = 1,673.32$ ohms, and the corrected value $z_0 = 1,673.32 \cosh$

$0.20767 = 1,673.32 \times 1.02164 = 1,709.53$ ohms. The loading of the line has, therefore, changed the section angles from 0.35174 to 0.41534 hyp. and the surge impedance from 1,436.14 to 1,709.53 ohms. The new sections behave as though they contained 710.04 ohms smoothly distributed resistance and 0.24296×10^{-1} mho smoothly distributed leakance.

It should be observed that whereas before the loading, any section length of the smooth line had the same values of θ and z_0 , after the loading the new values θ , and z_0 , apply only at section junctions, or mid-load points. If we cut into the loaded line at random, we cannot expect to find these values in a section length on either side of the cut.

If we analyze algebraically the steps of the process above indicated, we are led to the following formulas:

If θ be the angle of a smooth line section before loading,

θ , be the angle of the same line section after loading,

z_0 be the surge impedance of the section before loading,

z_0 , be the surge impedance of the section after loading,

then

$$\tanh \left(\frac{\theta}{2} \right) = \sqrt{\tanh \left(\frac{\theta}{2} \right) \cdot \tanh \left(\frac{\theta}{2} + \delta \right)} \quad \text{numeric } \angle \quad (457)$$

where

$$\tanh \delta = \frac{\sigma}{z_0} \quad \text{numeric } \angle \quad (458)$$

or

$$\delta = \tanh^{-1} \left(\frac{\sigma}{z_0} \right) \quad \text{hyp. } \angle \quad (459)$$

Also

$$\cosh \theta, = \cosh \theta + \frac{\sigma}{z_0} \sinh \theta \quad \text{numeric } \angle \quad *(460)$$

$$\frac{z_0}{z_0} = \frac{\sinh \theta}{\sinh \theta} \quad \text{numeric } \angle \quad (461)$$

As an a.c. example, consider the case represented in Fig. 188 of a twisted-pair telephone cable having the linear constants presented in Table XXII and loaded in sections of 2.607 km. (1.62 miles) with $4.535 + j441.5$ ohms per wire. The angle subtended by a section at $\omega = 5,000$ radians per sec., before loading, is $0.20065 + j0.20720$ hyp., as shown at *AB*, Fig. 188,

*"On Loaded Lines in Telephonic Transmissions," by G. A. CAMPBELL, *Phil. Mag.*, series vi, vol. v, p. 313, March, 1903.

the surge impedance being $247.284\angle 43'.16''$ ohms. The nominal T of such a section is indicated at aOb . The equivalent and the amended T , after the addition of a semi-load on one side, are marked at $A'OB'$. The conjugate smooth-line section of the amended T appears at $A''B''$. It will be seen that the loading has changed the section angle from $0.20065 + j0.20720$ to $0.06216 + j0.7384$; while it has changed the surge impedance from $247.284\angle 43'.16''$ to $579.776\angle 4'.25'.48''$.

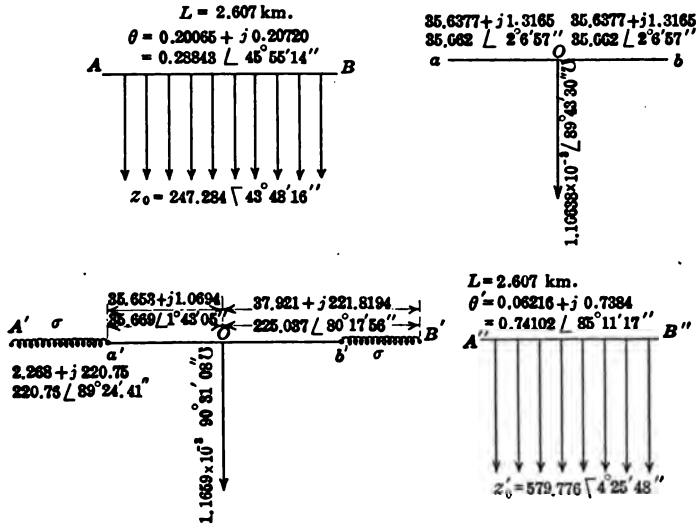


FIG. 188.—Series loaded section of standard telephone cable treated through the substitution of its equivalent T .

Without going through the process indicated in Fig. 188, we may use (457) as follows:

$$\tanh \left(\frac{\theta}{2} \right) = 0.144243\angle 45'.31'.21''$$

$$\tanh \delta = \frac{\sigma}{z_0} = \frac{220.76\angle 89'.24'.41''}{247.284\angle 43'.16''} = 0.89274\angle 133'.12'.57''$$

whence

$$\frac{\theta'}{2} = 0.37051\angle 85'.11'.17''$$

and

$$\theta' = 0.74102\angle 85'.11'.17'' \text{ hyp.}$$

Also by (389)

$$z_0' = 247.284\angle 43'.48'.16'' \times \frac{0.675966\angle 86'.5'.20''}{0.288311\angle 46'.42'.52''} = 579.776\angle 4'.25'.48'' \text{ ohms.}$$

TABLE XXII
Linear Constants of Twisted-pair Cabled Conductor Referred to in Figs. 188 and 192, before being Loaded

Linear quantity	Per loop mile	Per wire mile	Per loop km.	Per wire km.
Conductor resistance, ohms..	$r_{,,} = 88$	$r_s = 44$	$r_{,,} = 54.68$	$r = 27.34$
Conductor inductance, henrys	$l_{,,} = 0.65 \times 10^{-3}$	$l_s = 0.325 \times 10^{-3}$	$l_{,,} = 0.404 \times 10^{-3}$	$l = 0.202 \times 10^{-3}$
Dielectric conductance, mhos.	$g_{,,} = 1.73 \times 10^{-6}$	$g_s = 3.46 \times 10^{-6}$	$g_{,,} = 1.075 \times 10^{-6}$	$g = 2.15 \times 10^{-6}$
Dielectric capacitance, farads	$c_{,,} = 0.072 \times 10^{-6}$	$c_s = 0.144 \times 10^{-6}$	$c_{,,} = 0.04474 \times 10^{-6}$	$c = 0.08948 \times 10^{-6}$

Regular Leak Loads.—If the smooth line AE , Fig. 189, is divided into equal sections, and a leak of Γ mhos is applied at each junction, with half-leaks of γ ; or

$$\Gamma = 2\gamma \quad \text{mhos } \angle \quad (462)$$

at terminals ($A'B'C'D'E'$). Then each smooth section may be replaced by its equivalent Π . To

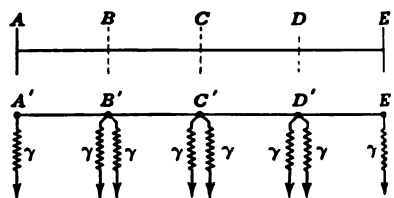


FIG. 189.—Four-section line with leaks at junctions.

each pillar leak of a Π is added the leak γ , thereby producing an amended Π . This amended Π is then reverted to its conjugate smooth line of angle $\theta_{,,}$ and surge impedance, z_0 .

As an example consider the case represented in Figs. 190 and 191. Here a uniform smooth-line section of surge impedance $z_0 = 2,000$ ohms, or surge admittance $y_0 = 0.5 \times 10^{-3}$ mho, and linear hyperbolic angle 0.005 hyp. per km., is loaded at each end A' , B' , with a leak of 0.5 millimho. The unloaded section AB subtends an angle of 0.25 hyp. It contains a total conductor impedance of $0.25 \times 2,000 = 500$ ohms and a total dielectric admittance of

$0.25 \times 0.5 \times 10^{-3} = 0.125 \times 10^{-3}$ mho. These are the values to be inserted in the nominal Π , which has an architrave impedance of 500 ohms, and two leaks each of 0.0625×10^{-3} mho. The correcting factors are $\sinh 0.25/0.25 = 0.25261/0.25 = 1.01044$, and $\tanh 0.125/0.125 = 0.12435/0.125 = 0.99480$. Applying these to the elements of the nominal Π , we obtain the equivalent Π , ab , Fig. 190, with an architrave of 505.22 ohms, and two leaks, each of 0.062175×10^{-3} mho. We now increase

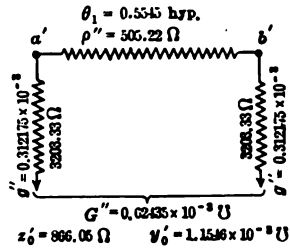
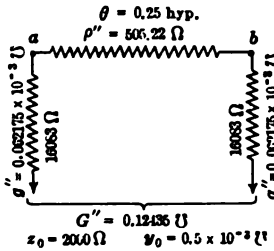
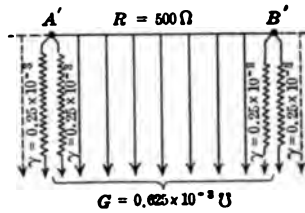
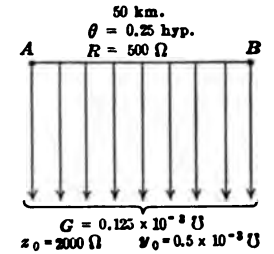


FIG. 190.—Uniform unloaded line and its equivalent Π .

FIG. 191.—Leak loaded-line section and its equivalent Π .

each pillar leak to 0.312175×10^{-3} mho, leaving the architrave unaltered as at $a'b'$, Fig. 191. The total line impedance r of a section is thus 505.22 ohms and the total leak admittance g 0.62435×10^{-3} mho. The apparent angle subtended by half the amended Π is thus

$$\frac{\sqrt{505.22 \times 0.62435 \times 10^{-3}}}{2}$$

$= 0.280818$ hyp. The corrected value is $v = \sinh^{-1} (0.280818)$
 $= 0.27725$ hyp. The apparent surge impedance is $z''_0 =$
 $\sqrt{505.22/624.35 \times 10^{-3}} = 899.552$ ohms. The corrected value

is $z_0 = 899.552/\cosh 0.27725 = 899.552/1.03868 = 866.05$ ohms, and $y_0 = 1.1546 \times 10^{-3}$ mho.

The loaded sections, therefore, behave as though they had a total conductor impedance of $0.5545 \times 866.05 = 505.22$ ohms uniformly distributed, and a total dielectric leakance of $0.5545 \times 1.1546 \times 10^{-3} = 0.62435 \times 10^{-3}$ mho, uniformly distributed.

Instead of going through the steps indicated in Figs. 190 and 191, we may derive the following formulas directly, θ being the unloaded section angle, θ , the loaded section angle, y_0 the surge admittance before loading, y_0 , the surge admittance after loading.

$$\tanh \left(\frac{\theta_c}{2} \right) = \sqrt{\tanh \left(\frac{\theta}{2} \right) \cdot \tanh \left(\frac{\theta}{2} + \delta \right)} \quad \text{numeric } \angle \quad (463)$$

where

$$\tanh \delta = \frac{\gamma}{y_0} \quad \text{numeric } \angle \quad (464)$$

or

$$\delta = \tanh^{-1} \left(\frac{\gamma}{y_0} \right) \quad \text{hyp. } \angle \quad (465)$$

Also

$$\cosh \theta_c = \cosh \theta + \frac{\gamma}{y_0} \sinh \theta \quad \text{numeric } \angle \quad (466)$$

$$\frac{y_{0c}}{y_0} = \frac{\sinh \theta_c}{\sinh \theta} \quad \text{numeric } \angle \quad (467)$$

A remarkable analogy is presented between the groups of formulas (457 to 461) and (463 to 467).

In the case above considered $\delta = \tanh^{-1} (0.25 \times 10^{-3}/0.5 \times 10^{-3}) = \tanh^{-1} 0.5 = 0.549307$ hyp. so that

$$\tanh \left(\frac{\theta_c}{2} \right) = \sqrt{\tanh 0.125 \times \tanh 0.674307}$$

$= \sqrt{0.12435 \times 0.58780} = 0.270357$; whence $\frac{\theta_c}{2} = 0.27725$ and $\theta_c = 0.5545$ hyp., as already found. Again

$$0.5 \times 10^{-3} \frac{y_{0c}}{y_0} = \frac{\sinh 0.5545}{\sinh 0.2500} = \frac{0.58336}{0.25261} = 2.30931.$$

whence $y_{0c} = 1.15466 \times 10^{-3}$ mho, and $z_{0c} = 866.05$ ohms, as above.

The effect of leak leading in this example has been to increase the section angle from 0.25 to 0.5545 hyp. and to diminish the surge impedance from 2,000 to 866.05 ohms.

As an a.c. example, we may consider 2.607-km. sections of smooth standard twisted-pair cable, referred to in Table XXII and* Fig. 188. This line is loaded with leaks of $\Gamma = (0.013332 - j1.3332)10^{-3} = 1.33327 \times 10^{-3} \angle 89^\circ.25'.37''$ mho per wire at junctions, such as would be produced by a reactor of 7.5 ohms and 0.15 millihenry, to ground at each junction. Thus $\gamma = (0.006666 - j0.6666)10^{-3} = 0.666635 \times 10^{-3} \angle 89^\circ.25'.37''$ mho.

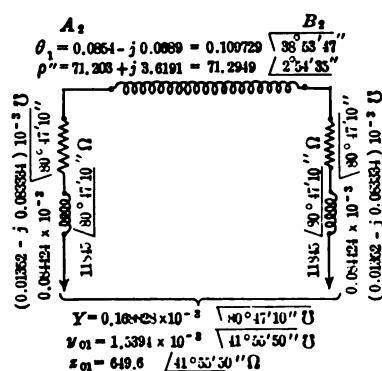
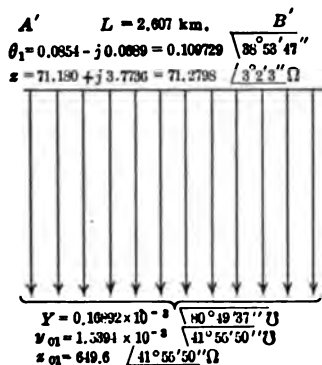
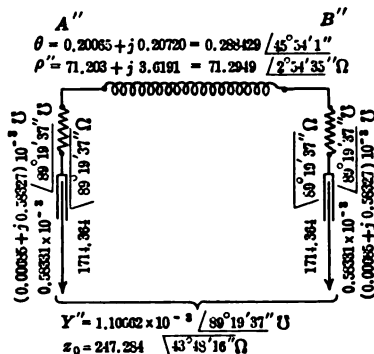
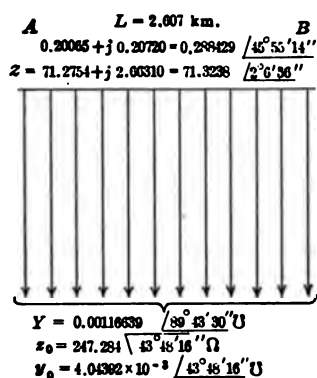


FIG. 192.—Smooth line and its equivalent II before and after regular leak loading.

The unloaded section is indicated at *AB*, Fig. 192, and its equivalent II at *A''B''*. After adding in the leaks, we obtain the amended II, *A₂B₂*, and finally, by reversion, the conjugate smooth section *A'B'*. It will be observed that the loading has

* Further particulars concerning the effects of series loading are given in Chapter VIII of "The Application of Hyperbolic Functions to Electrical Engineering Problems."

changed the section angle from $0.20065 + j0.20720$ to $0.0854 - j0.0689$ hyp., and the surge impedance from $247.284 \sphericalangle 43^\circ .48'.16''$ to $649.6 \sphericalangle 41^\circ .55'.50''$.

Although these leak loads have reduced the real component of the section angle nearly as much as the series loads of Fig. 188, yet, in general, the benefit of reduced attenuation is much more localized toward a critical frequency in leak loading than in series loading. In other words, the benefits of series loading extend in this case over a larger range of frequencies than those of leak loading.

CHAPTER XVII

VARIOUS TYPES OF ARTIFICIAL LINES

Classification of Lines.—If we attempt to classify a.c. artificial lines on the basis of the nature of line impedance and leak admittance, we may assume that there are three ideal types of conductor, namely: (a) resistances; (b) inductances; (c) capacitances.

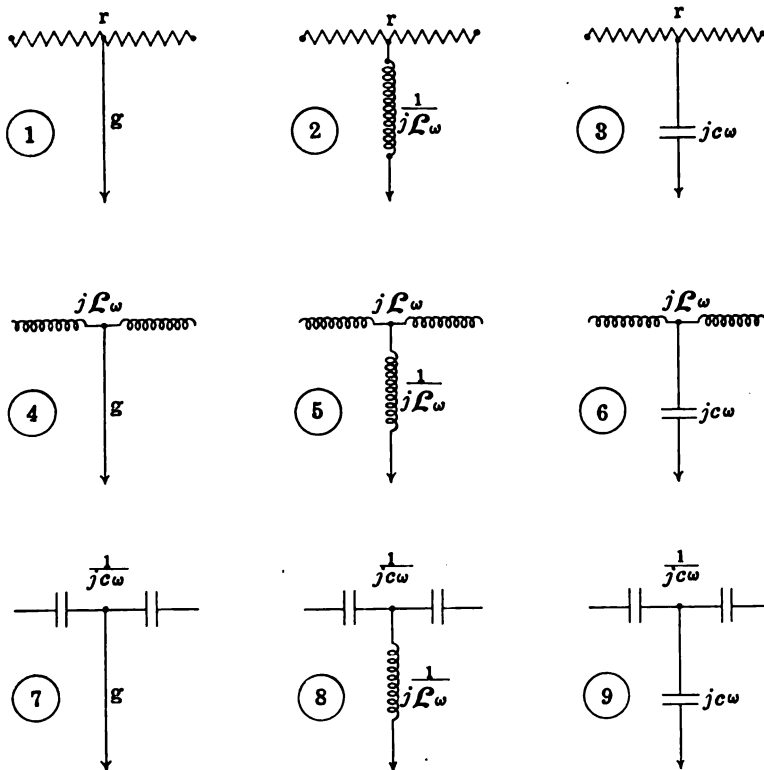


FIG. 193.—Fundamental types of artificial lines.

In practice, it cannot be expected that these three types should be met with in the pure state. There is almost always some admixture, as for example when a resistance is found to be associated with a small amount of inductance, an inductance with a

small amount of resistance, or a capacitance with a small amount of either resistance or leakage. For many purposes, however, the three types can be obtained sufficiently nearly pure, to permit of classification and discussion.

On the foregoing assumption, there are nine fundamental types of artificial line, together with a large number of mixtures, aggregations and subtypes. These nine ideal types are represented as *T* sections in Fig. 193. Numbers 1, 2, and 3 have pure resistance in the line; 4, 5 and 6 have pure inductance in the line; while 7, 8 and 9 have pure capacitance in the line. Any of these types may be described as — series, — shunt. Thus, number 1 is a resistance-conductance type. It will be seen that three types, Nos. 1, 5 and 9 have the same sort of conductor both in series and shunt. These types are all-resistance, all-inductance and all-condensance lines respectively. We may call these three types "homologous types."

The types of line met with ordinarily in engineering practice are Nos. 3 and 6, *i.e.*, the resistance-capacitance and inductance-capacitance types, but the other types deserve to be recognized and examined, even if their present utilities are insignificant. For this purpose, the elementary properties of the nine fundamental types in Fig. 193, in regard to angle and surge impedance, are collected in Table XXIII. It is assumed that the size of the angle θ is so small, that the lumpiness correcting factor of these sections may be ignored. Approximately pure five-section lines of all the types in Fig. 193 have been constructed in the laboratory, and all have been tested* to some extent.

Column III in the table indicates algebraically the nature of the series impedance for each type; and column IV indicates similarly the type of leak admittance. The products of the entries in III and IV give θ^2 in column V; while their ratios give z_0^2 in column VI. The last two columns express θ and z_0 for each of the types of line, uncorrected for lumpiness.

We may note the following deductions from Table XXIII.

1. For all of the nine pure types of line considered, both θ and z_0 are reals, imaginaries, or semi-imaginaries.

2. The three homologous types (Nos. 1, 5, and 9) all have θ real, and independent of ω .

* "Artificial Line Tests," a thesis towards the degree of Master of Science at the Massachusetts Institute of Technology, by CHAS. W. WHITALL, May, 1916.

TABLE XXIII
Fundamental Constants θ and z_0 for short Sections of the various Types of Artificial Line indicated in Fig. 193

I Type No.	II Description	III Series impedance	IV Leak admittance	V θ^2	VI z_0^2	VII θ	VIII z_0
1	Resistance-resistance	r	g	rg	r/g	$\sqrt{rg} \angle 0^\circ$	$\sqrt{\frac{r}{g}} \angle 0^\circ$
2	Resistance-inductance	r	$\frac{1}{jL\omega}$	$\frac{r}{jL\omega}$	$jrL\omega$	$\frac{1}{\sqrt{\omega}} \sqrt{\frac{r}{L}} \angle 45^\circ$	$\sqrt{\omega} \sqrt{\frac{r}{L}} \angle 45^\circ$
3	Resistance-condensance	r	$jC\omega$	$jrC\omega$	$\frac{r}{jC\omega}$	$\frac{1}{\sqrt{\omega}} \sqrt{\frac{r}{C}} \angle 45^\circ$	$\frac{1}{\sqrt{\omega}} \sqrt{\frac{r}{C}} \angle 45^\circ$
4	Inductance-resistance	$jL\omega$	g	$g jL\omega$	$\frac{jL\omega}{g}$	$\sqrt{\omega} \sqrt{gL} \angle 45^\circ$	$\sqrt{\omega} \sqrt{\frac{L}{g}} \angle 45^\circ$
5	Inductance-inductance	$jL_1\omega$	$\frac{1}{jL_2\omega}$	$\frac{L_1}{L_2}$	$j^2\omega^2 L_1 L_2$	$\sqrt{\frac{L_1}{L_2}} \angle 0^\circ$	$\omega \sqrt{L_1 L_2} \angle 90^\circ$
6	Inductance-condensance	$jL\omega$	$jC\omega$	$j^2\omega^2 LC$	$\frac{L}{C}$	$\omega \sqrt{LC} \angle 90^\circ$	$\sqrt{\frac{L}{C}} \angle 0^\circ$
7	Condensance-resistance	$\frac{1}{jC\omega}$	g	$\frac{g}{jC\omega}$	$\frac{1}{jCg\omega}$	$\frac{1}{\sqrt{\omega}} \sqrt{\frac{g}{C}} \angle 45^\circ$	$\frac{1}{\sqrt{\omega}} \sqrt{\frac{1}{Cg}} \angle 45^\circ$
8	Condensance-inductance	$\frac{1}{jC\omega}$	$\frac{1}{jL\omega}$	$\frac{1}{j^2 CL\omega^2}$	$\frac{L}{C}$	$\frac{1}{\omega} \sqrt{\frac{L}{C}} \angle 90^\circ$	$\sqrt{\frac{L}{C}} \angle 0^\circ$
9	Condensance-condensance	$\frac{1}{jC_1\omega}$	$jC_2\omega$	$\frac{C_2}{C_1}$	$\frac{1}{j^2 C_1 C_2 \omega^2}$	$\sqrt{\frac{C_2}{C_1}} \angle 0^\circ$	$\frac{1}{\omega} \sqrt{\frac{1}{C_1 C_2}} \angle 90^\circ$

3. Three types—Nos. 1, 6, and 8—have z_0 real and independent of ω .

Hence it is inaccurate to assume that all types of a.c. artificial lines necessarily involve complex hyperbolic functions, because any homologous type of line carrying alternating currents subtends real hyperbolic angles.

Furthermore, if we take any homologous artificial line of a given number of short sections, in each of which the ratio of the leak impedance to the series impedance is the same real number, *then if the artificial line be grounded at the distant end, and operated at any single frequency, the fall of potential over the line will be the same whether the line is of the all-resistance, all-inductance or all-capacitance type.**

The same proposition holds if the homologous artificial line of constant shunt-series impedance ratio is freed at the *B* end instead of being grounded.

The proposition holds because the position angles at corresponding junction points on all these homologous lines will have the same real values, independent of the value of the impressed frequency. In the first case, the potentials will follow the sines, and in the second case the cosines of these real position angles, and the phases of all these potentials will be the same as the phase of the impressed potential at *A*, assuming that the type of conductor in the artificial line is pure.

We may take, as an example, the three-section homologous lines of unit shunt-series impedance ratio, indicated in Fig. 194. At A_1 and A_2 we have the same all-resistance line of $r = 100$ and $1/g = 100$ ohms per section, with 1.0 volt of d.c. voltage from a voltaic source impressed at (3). The terminal leak impedances are given their proper Π values. In the A_1 case, the line is freed at *B*; while in the A_2 case, it is grounded at *B*. The potentials, currents and line resistances are indicated on the diagrams for these two cases respectively, as derived from Ohm's law deduction. The corresponding values of potential as deduced from hyperbolic functions are set forth in Table XXIV.

The apparent angle subtended by a section of any of the homologous lines in Fig. 194 will be 1 hyp. by (140). The section angle corrected for lumpiness will be, by (170),

* A string of suspension insulators, as used in tower-line construction, furnishes an example of homologous artificial line (Fig. 194A₂) of the all-capacitance type.

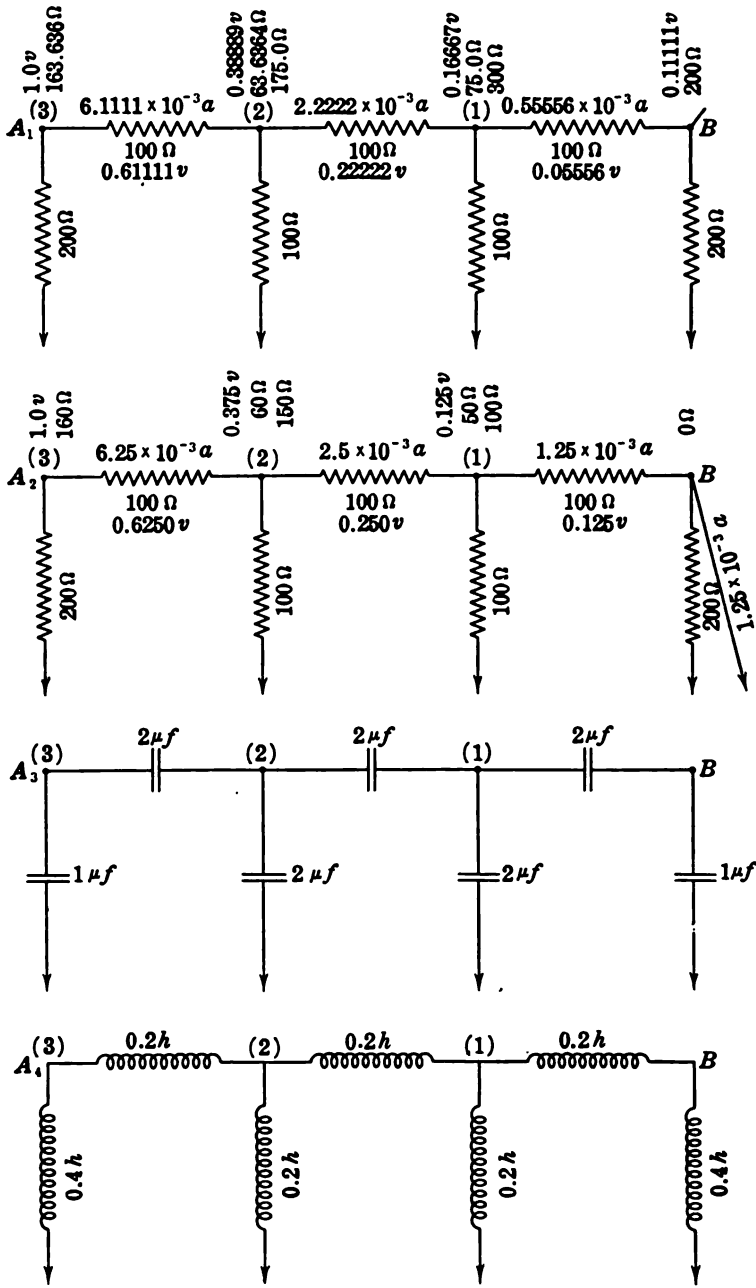


FIG. 194.—Unit-ratio homologous artificial lines, in three II sections.

$$\theta = 2 \sinh^{-1} (0.5) = 0.96243 \quad \text{hyp.}$$

This value of θ would be independent of the impressed frequency, on the assumption that the resistance, inductance or capacitance of any of the elements in Fig. 194 is independent of the frequency.

TABLE XXIV
Distribution of Position Angles and Potentials over a Three-section Homologous Artificial Line Voltaged with 1.0 at A and either Freed or Grounded at B

Position	II Position angle δ_P , hyps.	III $\sinh \delta_P$	IV $\cosh \delta_P$	V VI		VII VIII	
				V_P		V_P	
				B grounded, volts	B freed, volts	B grounded, volts	B freed, volts
3	2.88729	$\sqrt{80} = 8.9443^*$	9.0	1.000	1.000	8	18
2	1.92486	$\sqrt{11.25} = 3.3541$	3.5	0.375	0.388	3	7
1	0.96243	$\sqrt{1.25} = 1.1180$	1.5	0.125	0.166	1	3
B	0	$\sqrt{0} = 0$	1.0	0	0.111	0	2

Columns V and VI of the above table show the potentials at junctions of the artificial line when the B end is respectively grounded and freed. These values are plotted in Fig. 195. They are proportional respectively to the sines and cosines in columns III and IV.

It is to be observed that in Fig. 194, the homologous line at A_3 is an all-capacitance three-section II line, with the same unit shunt-series ratio; *i.e.*, equal impedance in the leaks and line sections at any or all frequencies. Again, at A_3 is depicted an all-inductance three-section II line of unit ratio. Assuming that the capacitances and inductances in the lines A_3 and A_4 are pure,

* It may be noted that the numbers in columns III and VII are in the ratios -8, -3, -1, 0, 1, 3, 8, 21, 55 which constitute what may be called a hyperbolic-sine infinite series of integral numbers, possessing the property that any member is equal to the sum of its next adjacent members on each side, divided by the constant b of the series. Thus $8 = (21 + 3) \div b$; where $b = 3$. Similarly the numbers in columns IV and VIII are in the ratio 18, 7, 3, 2, 3, 7, 18 which constitute what may be called a hyperbolic-cosine infinite series of integral numbers, possessing the same property and constant b . In this case, also $b = 3$. These hyperbolic infinite integral series are infinite in number. They are perhaps unknown. They have some remarkable properties. Theoretically, any of them may be presented by the potentials at the junctions of a homologous artificial line, when either freed or grounded at the distant end, and with the shunt-series impedance ratio appropriately selected. Thus, if as in column VIII, Table XXIV, 18 volts were applied at A_1 , Fig. 194, the junction potentials up the line would be 2, 3, 7, 18 volts, and so on for more sections.

In Table XXIV, the hyperbolic sine series of column VII may be expressed as $0.89443 \sinh (0.96243N)$, where N is the number of the position, or of the term in the series. Similarly, the cosine series of column VIII may be expressed as $2 \cosh (0.96243N)$. Also $b = 2 \cosh 0.96243$.

an impressed alternating potential of $1.0\angle 0^\circ$ at A , would develop the same junction potentials with the B end freed or grounded, as in the corresponding A_1 or A_2 case. Moreover, this condition is independent of the frequency, and of the absolute magnitudes of the resistances, capacitances or inductances used. Thus, in the line A_1 of Fig. 194, all the resistances—except in the terminal elements—have 100 ohms. But the junction potentials de-

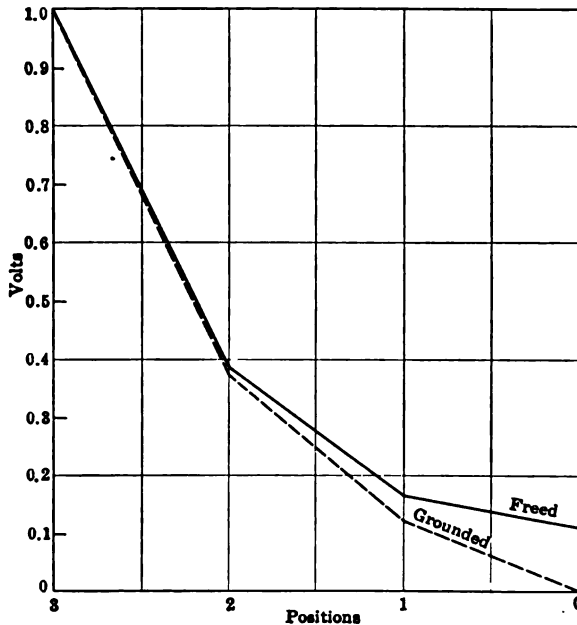


FIG. 195.—Fall of potential along homologous three-section line of unit ratio, when freed and grounded at motor end.

veloped would be the same if they were all 500 ohms, or had any other pure resistance value, provided the shunt-series impedance ratio was maintained at unity.

Series combinations of the different types of line presented in Table XXIII, produce composite groups, some of which possess remarkable properties. These relate more closely, however, to transition or transient phenomena, than to the steady-state phenomena which are here under consideration.

CHAPTER XVIII

MISCELLANEOUS USES OF ARTIFICIAL LINES

In addition to the steady-state uses, described in previous chapters, to which an artificial line may be put, there are two or three others, of an incidental character, to which reference may here be made. These all relate to and depend upon the sensitiveness of such lines to changes in impressed frequency. A suitably selected artificial line may be used:

1. As a frequency filter.
2. As a detector of even-frequency harmonics in a source of alternating e.m.f.
3. As a detector of changes in frequency from the normal.

The Use of an Artificial Line as a Frequency Filter.—We have already seen that when a telephone line is loaded with lumps of inductance, too large or too far apart, the line tends to arrest and suppress frequencies above a certain value by increasing the real component θ_1 of the loaded line angle. In this manner, it is possible to select an artificial inductance-capacitance line of such section elements that it shall offer but little impedance to impressed frequencies below a certain critical value; but shall offer rapidly increasing impedance to frequencies passing beyond that value. Moreover, by selecting a suitable capacitance-inductance line, it is possible to perform the inverse operation, *i.e.*, to have this line offer but little impedance to frequencies above an assigned critical value, but offer rapidly increasing impedances to frequencies below that value. By associating together an inductance-condensance line with a condensance-inductance line, it thus becomes possible to filter through the combination an assigned normal frequency with relatively little absorption, while opposing rapidly increasing impedance to other frequencies diverging from the normal and critical value on either side. This plan was suggested by Mr. G. M. B. Shepherd in 1913.*

* G. M. B. SHEPHERD, "Note on High-frequency Wave Filters," *The Electrician*, June 13, 1913, vol. lxxi, pp. 399-401; see also *Science Abstracts (Engineering)*, August, 1913, No. 833, p. 424.

Upper Harmonic Suppression.—The simplest way of analyzing the matter is perhaps to assume that the artificial line has pure inductance-condensance sections of the type represented at No. 6 in Fig. 193. We know from (170) that the angle subtended by such a section is

$$\frac{\theta}{2} = \sinh^{-1} \left(j \frac{\omega \sqrt{\mathcal{L}C}}{2} \right) \quad \text{hyp. } \angle \quad (468)$$

From an examination of "Tables" or "Charts of Complex Hyperbolic Functions," it is easy to see that so long as $\frac{\omega \sqrt{\mathcal{L}C}}{2}$ does not exceed unity, θ lies between $0 + j0$ and $0 + j2$. That is to say, θ remains purely imaginary, so long as $\omega \sqrt{\mathcal{L}C}$ does not exceed 2. Such a section with a purely imaginary section angle would be able to change the phase of an a.c. passing through it, but could not reduce its size. As soon as $\omega \sqrt{\mathcal{L}C}$ exceeds 2, however, the angle θ develops a rapidly increasing real component θ_1 , which involves loss of energy and attenuation in the traversing current. If, for example, $\omega \sqrt{\mathcal{L}C} = 3$, then

$$\frac{\theta}{2} = \sinh^{-1}(1.5) = 0.9624 + j \frac{\pi}{2}, \text{ or } \theta = 1.9248 + j\pi.$$

Consequently, the critical frequency of this line section, above which it rapidly imposes a barrier to alternating currents is

$$\omega = \frac{2}{\sqrt{\mathcal{L}C}} \quad \frac{\text{radians}}{\text{sec.}} \quad (469)$$

or

$$f = \frac{1}{\pi \sqrt{\mathcal{L}C}} \quad \frac{\text{cycles}}{\text{sec.}} \quad (470)$$

Thus, if the section capacitance were $C = 2 \times 10^{-6}$ farad, and the section inductance $\mathcal{L} = 0.18$ henry, then the critical frequency of an artificial line containing one, two, or more such sections would be

$$f = \frac{10^3}{\pi \times 0.6} = \frac{1,000}{1.885} = 530.5 \sim.$$

In practice, the presence of resistance associated with the inductance in the series elements of the line would exercise a modifying influence, in detail, on the computation, the steps of which could, nevertheless, be carried out with the precision afforded by the measurements of the impedances, by the use of

(170); but the approximate formula (470) would probably suffice for many purposes.

Under Harmonic Suppression.—Again, if the artificial line were of the pure capacitance-inductance type, as indicated at (8) Fig. 193, then the angle subtended by the section would be (Table XXIII)

$$\frac{\theta}{2} = \sinh^{-1} \left(\frac{j}{2\omega} \cdot \frac{1}{\sqrt{LC}} \right) \quad \text{hyp. } \angle \quad (471)$$

So long as the bracketed quantity $\frac{1}{2\omega} \frac{1}{\sqrt{LC}}$ does not exceed unity, θ is purely imaginary, and lies between 0 and $j2$. As soon as the bracketed quantity exceeds unity, θ develops a rapidly increasing real component, with accompanying attenuation and energy loss. The critical value of impedance, therefore, is, when ω falls below the angular frequency,

$$\omega = \frac{1}{2\sqrt{LC}} \quad \frac{\text{radians}}{\text{sec.}} \quad (472)$$

or

$$f = \frac{1}{4\pi\sqrt{LC}} \quad \frac{\text{cycles}}{\text{sec.}} \quad (473)$$

With $L = 0.18$ henry, and $C = 2 \times 10^{-6}$ farad, as before, $\sqrt{LC} = 0.6 \times 10^{-3}$, and $f = \frac{10^3}{7.542} = 132.6\sim$. Frequencies above this critical value would pass attenuated only in phase or slope. Below this value, they would pass attenuated both in size and in slope. The value of \sqrt{LC} in a condensation – inductance section necessary for the critical value of $530.5\sim$, would be four times less than in an inductance-condensation section.

Theoretically, therefore, a C - L section of $C = 0.5 \times 10^{-4}$ farad, and $L = 0.045$ henry, in series with a L - C section of $L = 0.18$ and $C = 2 \times 10^{-6}$, should produce a composite line, which, with pure resistanceless elements, would offer no impedance to alternating currents of the critical value $530.5\sim$, but would offer rapidly increasing impedance to frequencies deviating on either side from this critical value.

Qualitative experiments have already verified the preceding theory, but published quantitative tests as to the degree of attenuation offered by such opposing composite lines on currents of deviating frequency are still lacking.

In the case of the two-wire artificial line recorded by Shepherd,

the line condensers had each 0.08×10^{-6} farad, and the shunt coils 0.2 henry. Reducing this to the single-wire basis $C = 0.08 \times 10^{-6}$, and $\mathcal{L} = 0.1$. Hence by (473), $f = \frac{1}{j12.57\sqrt{0.8 \times 10^{-8}}} = \frac{10^4}{12.57 \times 0.8944} = \frac{10,000}{11.24} = 889.7\sim$, which agrees with the value reported.

Detection of Even-frequency Harmonics.—We have already seen, in Chapter XV, that a quarter-wave line subtends an angle $\theta_{\frac{1}{4}} = \theta_1 + j\underline{1}$ hyps. For simplicity, we may assume that a certain smooth line has negligible conductor resistance and dielectric leakance; so that when operated at quarter-wave frequency, $\theta_1 = 0$, and $\theta_{\frac{1}{4}} = j\underline{\frac{\pi}{2}} = j\underline{1}$ hyp. The current entering this line at the generator end will be, by (128),

$$I_A = V_A y_0 \coth \delta_A \quad \text{amp. } \angle \quad (474)$$

where $y_0 = \sqrt{\frac{c}{l}}$ ohms, a real conductance. If now the line is first grounded and then freed at B , the corresponding values of δ_A are $j\underline{1}$ and $j\underline{2}$ imaginary quadrants, respectively, and the corresponding entering currents will be $V_A y_0 \coth (j\underline{1})$ and $V_A y_0 \coth (j\underline{2})$. But $\coth j\underline{1} = j\underline{0}$, and $\coth j\underline{2} = j\underline{\infty}$; so that with 60 \sim , say, the entering current will be zero with the line grounded at B , and infinity with the line freed at B .

Moreover, this state of affairs would be presented for all odd harmonic frequencies. Thus, if a triple-frequency e.m.f. were impressed on the line, still with negligible losses, its angle would be $j\underline{3}$ hyps. and $\coth j\underline{3} = \coth j\underline{1}$. As in the preceding case, the line would take zero current at A when grounded at B , and an infinite current at A when freed at B .

But if an even-harmonic frequency were applied at A , the lossless line would develop an angle of corresponding even number of imaginary quadrants. In that case, its cotangent would be infinite when the far end was grounded, and zero when the far end was freed. Thus, if the double-harmonic frequency (120 \sim) were impressed at A , this would be the half-wave frequency, and the line would develop the half-wave angle $j\underline{2}$ hyps. The entering current would now be infinite with B grounded, and zero with B freed. The same would be true for any even-harmonic impressed frequency (240 \sim , 360 \sim , 480 \sim , etc.).

If next a 60~ generator is applied at *A*, with a complex harmonic e.m.f., or containing a number of harmonic frequencies, and the line is grounded at *B*, then the fundamental-frequency current and all the odd-harmonic currents will be zero at *A*; but the even-harmonic currents would be infinite. The line therefore acts as a sieve at the *A* end, suppressing all the odd-harmonic currents, and increasing indefinitely the even-harmonic currents.

In any actual line, there will necessarily be some conductor resistance and dielectric leakance, so that there will be loss in the line when it carries alternating currents of any frequency and the line angle will not be a pure imaginary. It will contain a real component θ_1 . In the case, however, of a well-insulated line of large carrying capacity, this real component may be expected to be relatively small. Consequently, when such a line of quarter-wave length at fundamental frequency, is grounded at the far end *B*, and has a complex or multi-frequency wave of e.m.f. impressed upon it at *A*, the odd-frequency components will not be zero, but may yet be very small, and the even-frequency components will not be infinite, but may yet be very large. Such a quarter-wave line is, therefore, a magnifier of such even-frequency harmonics as exist in the e.m.f. wave, and especially of the first or double-frequency harmonic, since the magnification will be less, the higher the even multiple. A properly constructed a.c. generator is ordinarily supposed to produce no even-harmonic components of e.m.f., and they are admittedly small, but they may be larger than is expected. When the generator is used to excite a quarter-wave line grounded at the distant end *B*, and an oscillograph is inserted at *A*, the resulting current oscillograph will contain magnified even harmonics, and minified odd harmonics including the fundamental.

For the purposes of such a test, the line may conveniently be a quarter-wave artificial line, with as little linear resistance and linear leakance as is practicable. An oscillogram of the current wave at the generator end, when the distant end is grounded, may be expected to reveal the presence of the magnified even* harmonics. If these magnified even harmonics are notably present, they will distort the oscillographed current wave with respect to the zero line, the shape of the positive half-waves being rendered different from that of the negative half-waves.

* "Analyzing Electric Waves for Harmonics," by C. W. RICKER, *Electrical World*, Sept. 18, 1915.

In the case of the artificial line specified in Table XIV and tested by Mr. Ricker as a quarter-wave line, the size of the sending-end impedance, with *B* grounded, was found to be 2,799 ohms at 60~, and 42.0 ohms at 120~, a magnification ratio of 66.7 in favor of the double-frequency harmonic.

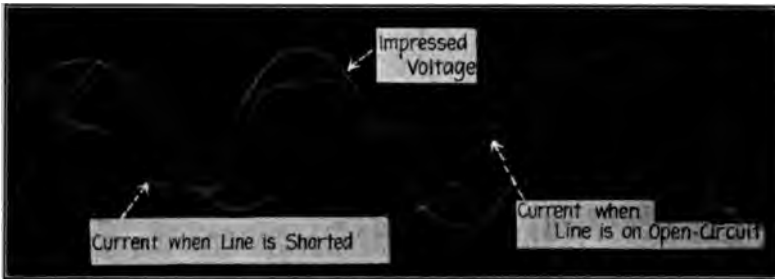


FIG. 196.—Oscillograms of impressed voltage wave (60~) impressed on a quarter-wave artificial line, and also of the generating-end current with the distant end freed and grounded. The apparent phase relations of these three oscillograms are not significant.

Fig. 196 shows the wave forms of the current entering this quarter-wave line, with the distant end *B* freed and grounded respectively, suitable shunts being applied in each case, so as to keep the wave amplitude normal for being photographed. It will be seen that the wave form with *B* on open circuit is sub-

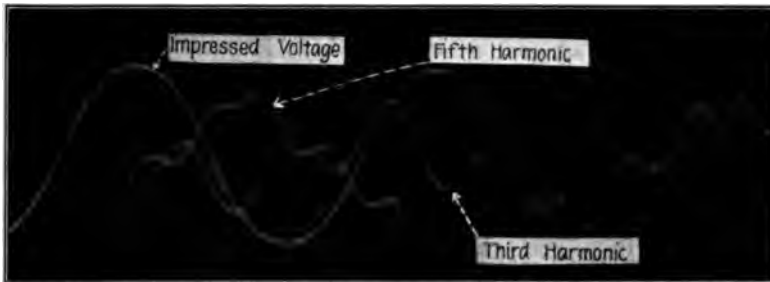


FIG. 197.—Oscillogram of an impressed voltage wave and of magnified third and fifth harmonics contained in it on successive beats with resonant artificial lines.

stantially a smooth sinusoid. Here the fundamental and odd-harmonic components are favored and the even-harmonic components repressed. In the case of *B* end shorted or grounded, when the even harmonics are magnified and the odds repressed, the wave form not only departs from the sinusoidal, but it

is also dissymmetrical on the + and - sides of the mid-line.* This indicates the presence of even-frequency harmonics in the generated wave, which, from its oscillograph in Fig. 196, might not be suspected.

An artificial line may also be used to magnify some particular harmonic frequency, either odd or even. By shortening a line to the amount necessary for resonance to that particular harmonic, an oscillograph may enable this magnified harmonic to be detected or measured. Thus, Fig. 197 shows the oscillograph of the same impressed e.m.f. as in the last preceding case, and also oscillograms of its third and fifth harmonics, as magnified by this process.

Since in all these cases of harmonic magnification, the magnification factor can be computed to a satisfactory degree of precision, from the constants of the artificial line used, they enable such artificial lines to be used as adjuncts to oscillographic measuring apparatus.

Artificial Lines as Detectors of Frequency Variations.—The marked and often objectionably obtrusive influence of variations in the impressed frequency, on the distributions of potential, current and impedance along an artificial line under tests, naturally suggests the use of such a line for the purpose of detecting and manifesting frequency changes. One such use has already been suggested at the end of Chapter XV in relation to quarter-wave lines.

* This mid-line, or zero line, does not appear on the oscillogram.

APPENDIX A—LIST OF IMPORTANT TRIGONOMETRICAL FORMULAS WITH CIRCULAR AND HYPERBOLIC EQUIVALENTS

	Circular	Hyperbolic
	$\sin \beta = \frac{e^{j\beta} - e^{-j\beta}}{j2} = \beta - \frac{\beta^3}{3!} + \frac{\beta^5}{5!} - \frac{\beta^7}{7!} + \dots$	$\sinh \theta = \frac{e^\theta - e^{-\theta}}{2} = \theta + \frac{\theta^3}{3!} + \frac{\theta^5}{5!} + \frac{\theta^7}{7!} + \dots$ (475)
	$\cos \beta = \frac{e^{j\beta} + e^{-j\beta}}{2} = 1 - \frac{\beta^2}{2!} + \frac{\beta^4}{4!} - \frac{\beta^6}{6!} + \dots$	$\cosh \theta = \frac{e^\theta + e^{-\theta}}{2} = 1 + \frac{\theta^2}{2!} + \frac{\theta^4}{4!} + \frac{\theta^6}{6!} + \dots$ (476)
	$\tan \beta = \frac{\sin \beta}{\cos \beta} = \beta + \frac{\beta^3}{3} + \frac{2\beta^5}{15} + \frac{17\beta^7}{315} + \dots$	$\tanh \theta = \frac{\sinh \theta}{\cosh \theta} = \theta - \frac{\theta^3}{3} + \frac{2\theta^5}{15} - \frac{17\theta^7}{315} + \dots$ (477)
	$\sec \beta = 1/\cos \beta = 1 + \frac{\beta^2}{2} + \frac{5\beta^4}{24} + \frac{61\beta^6}{720} + \dots$	$\operatorname{sech} \theta = 1/\cosh \theta = 1 - \frac{\theta^2}{2} + \frac{5\theta^4}{24} - \frac{61\theta^6}{720} + \dots$ (478)
	$\operatorname{cosec} \beta = 1/\sin \beta = \sqrt{\cot^2 \beta + 1}$	$\operatorname{cosech} \theta = 1/\sinh \theta = \sqrt{\coth^2 \theta - 1}$ (479)
	$\cot \beta = 1/\tan \beta = j \frac{e^{j\beta} + e^{-j\beta}}{e^{j\beta} - e^{-j\beta}} = j \frac{e^{2j\beta} + 1}{e^{2j\beta} - 1}$	$\coth \theta = 1/\tanh \theta = \frac{e^\theta + e^{-\theta}}{e^\theta - e^{-\theta}} = \frac{e^{2\theta} + 1}{e^{2\theta} - 1}$ (480)
	$e^{\pm j\beta} = \cos \beta \pm j \sin \beta = 1 \pm j\beta - \frac{\beta^2}{2!} \mp j \frac{\beta^3}{3!} + \frac{\beta^4}{4!} \pm \dots$	$e^{\pm \theta} = \cosh \theta \pm \sinh \theta = 1 \pm \theta + \frac{\theta^2}{2!} \pm \frac{\theta^3}{3!} + \frac{\theta^4}{4!} \pm \dots$ (481)
	$\sin \beta = -j \sinh j\beta = \tanh (gd^{-1} \beta) = -\sin (-\beta)$	$\sinh \theta = -j \sin j\theta = \tan (gd \theta) = -\sinh (-\theta)$ (482)
	$\cos \beta = \cosh j\beta = \operatorname{sech} (gd^{-1} \beta) = \cos (-\beta)$	$\cosh \theta = \cos j\theta = \sec (gd \theta) = \cosh (-\theta)$ (483)
	$\tan \beta = -j \tanh j\beta = \sinh (gd^{-1} \beta) = -\tan (-\beta)$	$\tanh \theta = -\tan j\theta = \sin (gd \theta) = -\tanh (-\theta)$ (484)
	$\sin 2\beta = 2 \sin \beta \cos \beta = \frac{2 \tan \beta}{1 + \tan^2 \beta}$	$\sinh 2\theta = 2 \sinh \theta \cosh \theta = \frac{2 \tanh \theta}{1 - \tanh^2 \theta}$ (485)
	$\cos 2\beta = \cos^2 \beta - \sin^2 \beta = 2 \cos^2 \beta - 1$	$\cosh 2\theta = \cosh^2 \theta + \sinh^2 \theta = 2 \cosh^2 \theta - 1$ (486)
	$\tan 2\beta = \frac{2 \tan \beta}{1 - \tan^2 \beta} = \frac{2 \cot \beta}{\cot^2 \beta - 1} = \cot \beta - \tan \beta$	$\tanh 2\theta = \frac{2 \tanh \theta}{1 + \tanh^2 \theta} = \frac{2 \coth \theta}{\coth^2 \theta + 1} = \coth \theta + \tanh \theta$ (487)
	$\cot^2 \beta - 1 = \frac{2 \cot \beta}{2 \tan \beta} = \cot \beta - \tan \beta$	$\coth^2 \theta + 1 = \frac{2 \coth \theta}{2 \tanh \theta} = \coth \theta + \tanh \theta$ (488)

APPENDIX A

LIST OF IMPORTANT TRIGONOMETRICAL FORMULAS WITH CIRCULAR AND HYPERBOLIC EQUIVALENTS.—(Continued)

Circular

$$\sin \frac{\beta}{2} = \frac{\sin \beta}{2 \cos \frac{\beta}{2}} = \sqrt{\frac{1 - \cos \beta}{2}}$$

$$\cos \frac{\beta}{2} = \frac{\sin \beta}{2 \sin \frac{\beta}{2}} = \sqrt{\frac{1 + \cos \beta}{2}}$$

$$\tan \frac{\beta}{2} = \frac{\sin \beta}{1 + \cos \beta} = \frac{1 - \cos \beta}{\sin \beta} = \sqrt{\frac{1 - \cos \beta}{1 + \cos \beta}}$$

$$\cos^2 \beta + \sin^2 \beta = 1$$

$$\operatorname{cosec}^2 \beta - \cot^2 \beta = 1$$

$$\sec^2 \beta - \tan^2 \beta = 1$$

$$\sin (\beta_1 \pm \beta_2) = \sin \beta_1 \cos \beta_2 \pm \cos \beta_1 \sin \beta_2$$

$$\cos (\beta_1 \pm \beta_2) = \cos \beta_1 \cos \beta_2 \mp \sin \beta_1 \sin \beta_2$$

$$\tan (\beta_1 \pm \beta_2) = \frac{\tan \beta_1 \pm \tan \beta_2}{1 \mp \tan \beta_1 \tan \beta_2}$$

$$\sin \beta_1 + \sin \beta_2 = 2 \sin \frac{\beta_1 + \beta_2}{2} \cdot \cos \frac{\beta_1 - \beta_2}{2}$$

$$\sin (\beta \pm 2n\pi) = \sin \beta$$

$$\cos (\beta \pm 2n\pi) = \cos \beta$$

$$\tan (\beta \pm n\pi) = \tan \beta$$

$$\sin \left(\beta \pm \frac{\pi}{2} \right) = \pm \cos \beta$$

$$\cos \left(\beta \pm \frac{\pi}{2} \right) = \mp \sin \beta$$

Hyperbolic

$$\sinh \frac{\theta}{2} = \frac{\sinh \theta}{2 \cosh \frac{\theta}{2}} = \sqrt{\frac{\cosh \theta - 1}{2}} \quad (489)$$

$$\cosh \frac{\theta}{2} = \frac{\sinh \theta}{2 \sinh \frac{\theta}{2}} = \sqrt{\frac{\cosh \theta + 1}{2}} \quad (490)$$

$$\tanh \frac{\theta}{2} = \frac{\sinh \theta}{1 + \cosh \theta} = \frac{\cosh \theta - 1}{\sinh \theta} = \sqrt{\frac{\cosh \theta - 1}{\cosh \theta + 1}} \quad (491)$$

$$\cosh^2 \theta - \sinh^2 \theta = 1 \quad (492)$$

$$\operatorname{coth}^2 \theta - \operatorname{cosech}^2 \theta = 1 \quad (493)$$

$$\operatorname{sech}^2 \theta + \tanh^2 \theta = 1 \quad (494)$$

$$\sinh (\theta_1 \pm \theta_2) = \sinh \theta_1 \cosh \theta_2 \pm \cosh \theta_1 \sinh \theta_2 \quad (495)$$

$$\cosh (\theta_1 \pm \theta_2) = \cosh \theta_1 \cosh \theta_2 \pm \sinh \theta_1 \sinh \theta_2 \quad (496)$$

$$\tanh (\theta_1 \pm \theta_2) = \frac{\tanh \theta_1 \pm \tanh \theta_2}{1 \pm \tanh \theta_1 \tanh \theta_2} \quad (497)$$

$$\sinh \theta_1 + \sinh \theta_2 = 2 \sinh \frac{\theta_1 + \theta_2}{2} \cdot \cosh \frac{\theta_1 - \theta_2}{2} \quad (498)$$

$$\sinh (\theta \pm 2jn\pi) = \sinh \theta \quad (499)$$

$$\cosh (\theta \pm 2jn\pi) = \cosh \theta \quad (500)$$

$$\tanh (\theta \pm jn\pi) = \tanh \theta \quad (501)$$

$$\sinh \left(\theta \pm j \frac{\pi}{2} \right) = \pm j \cosh \theta \quad (502)$$

$$\cosh \left(\theta \pm j \frac{\pi}{2} \right) = \pm j \sinh \theta \quad (503)$$

LIST OF IMPORTANT TRIGONOMETRICAL FORMULAS WITH CIRCULAR AND HYPERBOLIC EQUIVALENTS.—(Continued)

Circular	Hyperbolic
$\tan\left(\beta \pm \frac{\pi}{2}\right) = \mp \cot \beta$	$\tanh\left(\theta \pm j\frac{\pi}{2}\right) = \coth \theta$ (504)
$\cot\left(\beta \pm \frac{\pi}{2}\right) = \mp \tan \beta$	$\coth\left(\theta \pm j\frac{\pi}{2}\right) = \tanh \theta$ (505)
$a \cos \beta \pm b \sin \beta = \sqrt{a^2 + b^2} \cos\left(\beta \mp \tan^{-1} \frac{b}{a}\right)$	$a \cosh \theta \pm b \sinh \theta = \sqrt{a^2 - b^2} \cosh\left(\theta \pm \tanh^{-1} \frac{b}{a}\right)$ (506) $= \sqrt{b^2 - a^2} \sinh\left(\theta \pm \tanh^{-1} \frac{a}{b}\right)$ $a > b$ $b > a$
$a e^{j\beta} \pm b e^{-j\beta} = (a \pm b) \cos \beta + j(a \mp b) \sin \beta$	$a e^{\theta} \pm b e^{-\theta} = (a \pm b) \cosh \theta + (a \mp b) \sinh \theta$ (507)
$\sin(\beta_1 + \beta_2) + \sin(\beta_1 - \beta_2) = 2 \sin \beta_1 \cos \beta_2$	$\sinh(\theta_1 + \theta_2) + \sinh(\theta_1 - \theta_2) = 2 \sinh \theta_1 \cosh \theta_2$ (508)
$\cos(\beta_1 + \beta_2) + \cos(\beta_1 - \beta_2) = 2 \cos \beta_1 \cos \beta_2$	$\cosh(\theta_1 + \theta_2) + \cosh(\theta_1 - \theta_2) = 2 \cosh \theta_1 \cosh \theta_2$ (509)
$\sin(\beta_1 \mp j\beta_2) = \sin \beta_1 \cosh \beta_2 \pm j \cos \beta_1 \sinh \beta_2$	$\sinh \theta_1 \cos \theta_2 \pm j \cosh \theta_1 \sin \theta_2$ (510)
	$\sqrt{\sin^2 \theta_1 + \sin^2 \theta_2} / \pm \tan^{-1}(\coth \theta_1 \tan \theta_2)$ (511)
	$\sqrt{\cosh^2 \theta_1 - \cos^2 \theta_2} / \pm \tan^{-1}(\coth \theta_1 \tan \theta_2)$ (512)
	$\cosh \theta_1 \cosh \theta_2 \pm j \sinh \theta_1 \sin \theta_2$ (513)
	$\sqrt{\cosh^2 \theta_1 - \sin^2 \theta_2} / \pm \tan^{-1}(\tanh \theta_1 \tan \theta_2)$ (514)
	$\sqrt{\sinh^2 \theta_1 + \cos^2 \theta_2} / \pm \tan^{-1}(\tanh \theta_1 \tan \theta_2)$ (515)
	$\sinh 2\theta_1 \pm j \sin 2\theta_2$ (516)
	$\cosh 2\theta_1 + \cos 2\theta_2$
	$\sinh^{-1}(u \pm jv) = \cosh^{-1} \left\{ \sqrt{(1+v)^2 + u^2} + \sqrt{(1-v)^2 + u^2} \right\}$
	$\pm j \sin^{-1} \left\{ \frac{\sqrt{(1+v)^2 + u^2} - \sqrt{(1-v)^2 + u^2}}{2} \right\}$ (517)

LIST OF IMPORTANT TRIGONOMETRICAL FORMULAS WITH CIRCULAR AND HYPERBOLIC EQUIVALENTS.—(Continued)

Circular	Hyperbolic
$\cos^{-1}(u \pm jv) = \cos^{-1} \left\{ \frac{\sqrt{(1+u)^2 + v^2} - \sqrt{(1-u)^2 + v^2}}{2} \right.$	$\cosh^{-1}(u \pm jv) = \cosh^{-1} \left\{ \frac{\sqrt{(1+u)^2 + v^2} + \sqrt{(1-u)^2 + v^2}}{2} \right.$
$\mp j \cosh^{-1} \left\{ \frac{\sqrt{(1+u)^2 + v^2} + \sqrt{(1-u)^2 + v^2}}{2} \right.$	$\left. \pm j \cosh^{-1} \left\{ \frac{\sqrt{(1+u)^2 + v^2} - \sqrt{(1-u)^2 + v^2}}{2} \right\} \right.$
$\tan^{-1}(u \pm jv) = \left\{ \begin{array}{l} \pi - \tan^{-1} \left(\frac{u}{\pm v - 1} \right) + \tan^{-1} \left(\frac{u}{\pm v + 1} \right) \\ \pm j \frac{1}{2} \log h \sqrt{\frac{(1 \pm v)^2 + u^2}{(1 \pm v)^2 + u^2}} \end{array} \right.$	$\tanh^{-1}(u \pm jv) = \frac{1}{2} \log h \sqrt{\frac{(1+u)^2 + v^2}{(1-u)^2 + v^2}} + j \left\{ \begin{array}{l} \pi - \tan^{-1} \left(\frac{u+1}{\pm v} \right) + \tan^{-1} \left(\frac{u-1}{\pm v} \right) \end{array} \right.$
$\sin^{-1} u = -j \sinh^{-1} ju = -j \log h (ju + \sqrt{1-u^2})$	$\sinh^{-1} u = -j \sin^{-1} ju = \log h (u + \sqrt{1+u^2})$
$\cos^{-1} u = -j \cosh^{-1} u = -j \log h (u + j\sqrt{1-u^2})$	$\cosh^{-1} u = j \cos^{-1} u = \log h (u + \sqrt{u^2-1})$
$\tan^{-1} u = -j \tanh^{-1} ju = -\frac{j}{2} \log h \frac{1+ju}{1-ju}$	$\tanh^{-1} u = -j \tan^{-1} ju = \frac{1}{2} \log h \frac{u+1}{u-1}$
$\frac{d \sin \beta}{d\beta} = \cos \beta$	$\frac{d \sinh \theta}{d\theta} = \cosh \theta$
$\frac{d \cos \beta}{d\beta} = -\sin \beta$	$\frac{d \cosh \theta}{d\theta} = \sinh \theta$
$\frac{d \tan \beta}{d\beta} = \sec^2 \beta$	$\frac{d \tanh \theta}{d\theta} = \operatorname{sech}^2 \theta$
$\int \sin \beta d\beta = -\cos \beta$	$\int \sinh \theta d\theta = \cosh \theta$
$\int \cos \beta d\beta = \sin \beta$	$\int \cosh \theta d\theta = \sinh \theta$

(528)

APPENDIX B

PROPOSITIONS RELATING TO ALTERNATING CONTINUED FRACTIONS

Constant Continued Fractions.—A continued fraction of the type

$$F_n(c) = \cfrac{1}{c + \cfrac{1}{c + \cfrac{1}{c + \cfrac{1}{\ddots}}}} \quad \text{numeric } \angle \quad (529)$$

to n stages

is called a “*constant continued fraction*,” because the quantity c , which may be positive or negative, integral or fractional, real or imaginary, constantly reappears in each denominator.

Let us denote a constant continued fraction of even number n , of stages, by $F_{n,}(c)$, and one of odd number n , of stages, by $F_n(c)$.

Then*

$$F_n(c) = \frac{\cosh n, v}{\sinh \{(n, + 1)v\}} \quad \text{numeric } \angle \quad (530)$$

and

$$F_{n,}(c) = \frac{\sinh n, v}{\cosh \{(n, + 1)v\}} \quad \text{numeric } \angle \quad (531)$$

where

$$v = \sinh^{-1} \left(\frac{c}{2} \right) \quad \text{or} \quad \sinh v = \frac{c}{2} \quad \text{numeric } \angle \quad (532)$$

Let us assume that (530) is true for some particular value of n .

Then

$$F_{n,+1}(c) = \cfrac{1}{c + F_n(c)} = \cfrac{1}{2 \sinh v + \cfrac{\cosh n, v}{\sinh \{(n, + 1)v\}}} = \cfrac{\sinh \{(n, + 1)v\}}{\cosh \{(n, + 2)v\}} \quad \text{numeric } \angle \quad (533)$$

which agrees with (531).

* “The Expression of Constant and of Alternating Continued Fractions in Hyperbolic Functions,” by A. E. KENNELLY. *The Annals of Mathematics*, 2d series, vol. ix, No. 2, January, 1908.

Similarly, assuming that (531) is true for some particular value of $n_{,,}$.

Then

$$F_{n_{,,}+1}(c) = \frac{1}{c + F_{n_{,,}}(c)} = \frac{1}{2 \sinh v + \frac{\sinh n_{,,} v}{\cosh\{(n_{,,} + 1)v\}}} = \frac{\cosh\{(n_{,,} + 1)v\}}{\sinh\{(n_{,,} + 2)v\}} \quad \text{numeric } \angle \quad (534)$$

which agrees with (530).

The entire series of integral values of n from 1 to ∞ is thus ensured in (533) and (534), if we can show that

$$F_1(c) = \frac{\cosh v}{\sinh 2v} = \frac{1}{c}$$

But

$$\frac{\cosh v}{\sinh 2v} = \frac{\cosh v}{2 \sinh v \cdot \cosh v} = \frac{1}{2 \sinh v} = \frac{1}{c} \quad \text{numeric } \angle \quad (535)$$

which completes the demonstration.

When n approaches ∞ , it is evident from (530) or (531) that

$$F_{\infty}(c) = \epsilon^{-v} = \cosh v - \sinh v = \frac{c}{2} \left(\sqrt{1 + \frac{4}{c^2}} - 1 \right) \quad \text{numeric } \angle \quad (536)$$

As an example, we may consider the four-stage constant continuous fraction,

$$1.2375 + \frac{1}{1.2375 + \frac{1}{1.2375 + \frac{1}{1.2375 + \frac{1}{1.2375}}}}$$

The successive convergents of this fraction by ordinary arithmetic, are 0.80808, 0.48886, 0.57925 and 0.55043. Using (530), we have

$$F_4(1.2375) = \frac{\sinh 4v}{\cosh 5v}, \quad \text{where } \sinh v = \frac{1.2375}{2} = 0.61875.$$

By tables, $v = 0.58483$, so that $4v = 2.33934$

and $5v = 2.92417$, so that

$$F_4(1.2375) = \frac{\sinh 2.33934}{\cosh 2.92417} = \frac{5.1390}{9.3363} = 0.55043.$$

The limit of this fraction for an infinite number of stages would be, by (536), $e^{-0.58483} = 0.55720$.

Alternating Continued Fractions.—A continued fraction of the type

$$F_n(a, b) = \cfrac{1}{a + \cfrac{1}{b + \cfrac{1}{a + \cfrac{1}{b + \cfrac{1}{\ddots}}}}} \quad \text{numeric } \angle \quad (537)$$

to n stages

is called an “*alternating continued fraction*.” The example given in (537) is a “*four-stage alternating fraction*” or briefly a “*four-stage alternate*,” denoted by $F_4(a, b)$, a being the first denominator.

It is easy to see by trial that

$$\begin{aligned} d \times F_n(a, b) &= \cfrac{d}{a + \cfrac{1}{b + \cfrac{1}{a + \cfrac{1}{b + \cfrac{1}{\ddots}}}}} = \cfrac{1}{\cfrac{a}{d} + \cfrac{1}{bd + \cfrac{1}{a + \cfrac{1}{b + \cfrac{1}{\ddots}}}}} \\ &= \cfrac{1}{\cfrac{a}{d} + \cfrac{1}{bd + \cfrac{1}{\cfrac{a}{d} + \cfrac{1}{bd + \cfrac{1}{\ddots}}}}} \quad \text{numeric } \angle \quad (538) \end{aligned}$$

The process can manifestly be extended to all of the stages of any alternate. It is evident that the effect of multiplying an alternate $F_n(a, b)$ by a constant d , is to produce a new alternate whose odd denominators are all a/d and whose even denominators are all bd .

In the particular case where the constant d has the value

$$d = \sqrt{\cfrac{a}{b}} \quad \text{numeric } \angle \quad (539)$$

the new alternate has odd denominators $a \cdot \sqrt{\cfrac{b}{a}} = \sqrt{ab}$ and even denominators $b\sqrt{\cfrac{a}{b}} = \sqrt{ab}$. That is, if we multiply any alternate continued fraction of a given number of stages by the square root of the ratio of the first denominators in their order, the new alternate is reduced to a constant continued fraction of the same number of stages; so that

$$\sqrt{\frac{a}{b}} \cdot F_n(a, b) = F_n(\sqrt{ab}) \quad \text{numeric } \angle \quad (540)$$

and

$$F_n(a, b) = \sqrt{\frac{b}{a}} \cdot F_n(\sqrt{ab}) \quad \text{numeric } \angle \quad (541)$$

or, in full,

$$\begin{aligned} \frac{1}{a + \frac{1}{b + \frac{1}{a + \frac{1}{b + \dots}}}} &= \sqrt{\frac{b}{a}} \cdot \frac{1}{\sqrt{ab} + \frac{1}{\sqrt{ab} + \frac{1}{\sqrt{ab} + \dots}}} \\ \text{to } n \text{ stages} & \qquad \qquad \qquad \text{to } n \text{ stages} \\ &= \frac{b}{c} \cdot \frac{1}{c + \frac{1}{c + \frac{1}{c + \dots}}} \\ & \qquad \qquad \qquad \text{to } n \text{ stages} \end{aligned} \quad \text{numeric } \angle \quad (542)$$

where $c = \sqrt{ab}$.

Thus, any alternating continued fraction may be expressed as a coefficient times a constant continued fraction of like number of stages, the constant denominator \sqrt{ab} being the geometric mean of the denominators a, b , in the alternate, and the coefficient being $\sqrt{b/a}$, the square root of the latter in inverse order.

The values assigned to a and b in (537) to (542) may be any whatever, except that if $b = -a$, and $0 < c^2 < 4$, a case which is unlikely to occur in practice, we obtain

$$\begin{aligned} F_n(a, -a) &= \frac{\sin nc}{\sin \{(n+1)c\}} = \frac{1}{a + \frac{1}{-a + \frac{1}{a + \frac{1}{-a + \dots}}}} \\ & \qquad \qquad \qquad \text{to } n \text{ stages} \\ &= \frac{1}{a - \frac{1}{a - \frac{1}{a - \dots}}} \\ & \qquad \qquad \qquad \text{to } n \text{ stages} \end{aligned} \quad \text{numeric } \angle \quad (543)$$

whether n be odd or even. This particular case, solved in terms of circular functions, is known as Strehlke's theorem, and was

published by him in 1864.* Curiously enough, although readily derivable from (530), (531) and (542), it does not lead back to those formulas.

In view then of (530) and (531), it follows that *any alternating continued fraction* $F_n(a, b)$, of n stages in a and b , may be expressed as a constant factor $\sqrt{b/a}$ times the ratio of functions of nv and $(n + 1)v$, where v is an auxiliary hyperbolic angle, or we may write

$$F_n(a, b) = \sqrt{\frac{b}{a}} \cdot \frac{\cosh nv}{\sinh \{(n + 1)v\}} \quad \text{numeric } \angle \quad (544)$$

$$F_{n..}(a, b) = \sqrt{\frac{b}{a}} \cdot \frac{\sinh (n.., v)}{\cosh \{(n.., + 1)v\}} \quad \text{numeric } \angle \quad (545)$$

where $v = \sinh^{-1}\left(\frac{\sqrt{ab}}{2}\right) = \sinh^{-1}\left(\frac{\sqrt{a}}{2} \cdot \frac{\sqrt{b}}{2}\right)$ numeric \angle (546)

As an example, consider the three-stage alternate

$$F_3(a, b) = \cfrac{1}{0.00025 + \cfrac{1}{500 + \cfrac{1}{0.00025}}}$$

Here $a = 0.00025$, and $b = 500$. We transform this into a constant continued fraction, using (542)

$$F_3(a, b) = \sqrt{\frac{b}{a}} \cdot F_3(\sqrt{ab}) = \sqrt{\frac{500}{0.00025}} \times \cfrac{1}{\sqrt{0.125} + \cfrac{1}{\sqrt{0.125} + \cfrac{1}{\sqrt{0.125}}}}$$

By (544) this becomes

$$\begin{aligned} & \sqrt{2,000,000} \cdot \frac{\cosh 3v}{\sinh 4v}, \text{ where } v = \sinh^{-1}\left(\frac{\sqrt{0.125}}{2}\right) \\ & = \frac{0.353554}{2} = 0.176777. \end{aligned}$$

We find in tables, that the angle whose sine is 0.176777, is 0.17586 hyp. Hence

$$F_3(0.00025, 500) = 1,414.214 \times \frac{\cosh 0.52758}{\sinh 0.70344} = 2,117.7.$$

* A. B. STREHLKE, Grunert's *Archiv der Mathematik und Physik*, 1864, vol. xlii, p. 343.

Terminally Loaded Alternating Continued Fractions.—If an alternating continued fraction $F_n(a, b)$, of n stages in denominators a followed by b , terminates in a denominator m , where m has any value real, imaginary or complex, it is called a *terminally loaded continued fraction*, and the fraction $1/m$ is the *terminal load*.

That is

$$F_n(a, b)_1 = \cfrac{1}{a + \cfrac{1}{b + \cfrac{1}{a + \dots + \cfrac{1}{b + \cfrac{1}{a + \cfrac{1}{m}}}}} \quad \text{numeric } \angle \quad (547)$$

n stages

In dealing with terminally loaded alternates, it is convenient to use an ascending notation, thus:

$$F_0(a, b)_1 = \cfrac{1}{m} \quad \text{numeric } \angle \quad (548)$$

$$F_1(a, b)_1 = \cfrac{1}{a + \cfrac{1}{m}} \quad \text{numeric } \angle \quad (549)$$

$$F_2(b, a)_1 = \cfrac{1}{b + \cfrac{1}{a + \cfrac{1}{m}}} \quad \text{numeric } \angle \quad (550)$$

etc. See (148) to (153) and (180) to (191).

Then it is easily shown from (544) and (545) that

$$F_n(a, b)_1 = \sqrt{a} \cdot \cfrac{\sinh(nv + v')}{\cosh\{(n+1)v + v'\}} \quad \text{numeric } \angle \quad (551)$$

$$F_{n+1}(a, b)_1 = \sqrt{b} \cdot \cfrac{\cosh(nv + v')}{\sinh\{(n+1)v + v'\}} \quad \text{numeric } \angle \quad (552)$$

where v is the same as before, see formula (546) and v' is a new auxiliary hyperbolic angle, obtained as follows:

If m is less than $\epsilon^r \cdot \sqrt{\frac{b}{a}}$, then

$$v' = \tanh^{-1} \left(\cfrac{m\sqrt{\frac{a}{b}} - \sinh v}{\cosh v} \right) \quad \text{hyps. } \angle \quad (553)$$

If, on the contrary, m is greater than $\epsilon^v \cdot \sqrt{b/a}$,

$$v' = v'' + j \frac{\pi}{2} \quad \text{hyps. } \angle \quad (554)$$

and

$$v'' = \tanh^{-1} \left(\frac{\cosh v}{m \sqrt{b/a} - \sinh v} \right) \quad \text{hyps. } \angle \quad (555)$$

In that case (551) and (552) become

$$F_{n,}(a, b)_{\frac{1}{m}} = \sqrt{b/a} \cdot \frac{\cosh(n, v + v'')}{\sinh\{(n, + 1)v + v''\}} \quad \text{numeric } \angle \quad (556)$$

$$F_{n,,}(a, b)_{\frac{1}{m}} = \sqrt{b/a} \cdot \frac{\sinh(n,, v + v'')}{\cosh\{(n,, + 1)v + v''\}} \quad \text{numeric } \angle \quad (557)$$

In the particular case when $m = \epsilon^v \cdot \sqrt{b/a}$

$$v' = v'' = \alpha \quad \text{hyps. } \angle \quad (558)$$

In the case when $m = b/2$, $v' = 0$ by (553) and

$$F_n(a, b)_{1/2} = \sqrt{b/a} \cdot \frac{\sinh n, v}{\cosh\{(n, + 1)v\}} \quad \text{numeric } \angle \quad (559)$$

and

$$F_{n,,}(a, b)_{1/2} = \sqrt{b/a} \cdot \frac{\cosh n,, v}{\sinh\{(n,, + 1)v\}} \quad \text{numeric } \angle \quad (560)$$

It may also be noted that if

$$F_n(a, b)_{\frac{1}{m}} = \sqrt{b/a} \cdot \frac{f(nv)}{f'\{(n + 1)v\}} \quad \text{numeric } \angle \quad (561)$$

then

$$F_n(b, a)_{\frac{1}{m}} = \sqrt{a/b} \cdot \frac{f(nv)}{f'\{(n + 1)v\}} \quad \text{numeric } \angle \quad (562)$$

where f and f' are hyperbolic functions determined according to (551) and (552). That is, the inversion of a and b in an alternate, terminally loaded or not, only inverts the coefficient $\sqrt{b/a}$, and does not affect the hyperbolic fraction.

Alternating Continued Fractions Loaded at the Upper Terminal.

—If any quantity q is added to an alternate, it may be described as an upper load to the alternate, and the alternate is said to be

loaded at the upper terminal. Thus $q + F_n(a, b)_m$, is an alternate loaded at both ends.

Thus a three-stage alternate loaded at both ends would be

$$q + F_3(a, b)_m = q + \frac{1}{a + \frac{1}{b + \frac{1}{a + \frac{1}{m}}}}$$

If $q = b/2$, the alternate becomes, by (551),

$$\begin{aligned} \frac{b}{2} + F_n(a, b)_m &= \sqrt{\frac{b}{a}} \left\{ \frac{\sqrt{ab}}{2} + \frac{\sinh(n, v + v')}{\cosh\{(n, + 1)v + v'\}} \right\} \\ &= \sqrt{\frac{b}{a}} \left\{ \sinh v + \frac{\sinh(n, v + v')}{\cosh\{(n, + 1)v + v'\}} \right\} \\ &= \sqrt{\frac{b}{a}} \cdot \cosh v \cdot \tanh\{(n, + 1)v + v'\} \end{aligned}$$

numeric \angle (563)

and

$$\begin{aligned} \frac{b}{2} + F_n(a, b)_m &= \sqrt{\frac{b}{a}} \left\{ \frac{\sqrt{ab}}{2} + \frac{\cosh(n, v + v')}{\sinh\{(n, + 1)v + v'\}} \right\} \\ &= \sqrt{\frac{b}{a}} \cdot \cosh v \cdot \coth\{(n, + 1)v + v'\} \end{aligned}$$

numeric \angle (564)

If m exceeds $e^v \cdot \sqrt{b/a}$, then, as before, $j\frac{\pi}{2} + v''$ must be substituted for v' , see (556), and this will lead to the mutual inversion of \tanh and \coth in (563) and (564).

LIST OF SYMBOLS EMPLOYED

- A, B sizes of complex numbers (numeric); also resistances of a pair of bridge arms (ohms).
- $A_r, A', A'',$ arbitrary constants in solution of line differential equations (volts \angle).
- A_i, A'_i, A''_i arbitrary constants in solution of line differential equations (amperes \angle).
- a, b successive denominators of an alternating continued fraction (numeric \angle).
- α a hyperbolic angular velocity (hyps. per sec.).
- α linear hyperbolic angle (hyps. per km. \angle).
- $\tau_0 = \sqrt{-j^2 \pi \gamma \mu \omega} = \alpha_1 - j \alpha_2 = \sqrt{2 \pi \gamma \mu \omega} - j \sqrt{2 \pi \gamma \mu \omega}$ (cm.⁻¹ \angle).
- α_1, α_2 linear hyperbolic angle per wire km. and per loop km. respectively (hyps./km. \angle).
- α_1, α_2 real and imaginary components of linear hyperbolic angle (numeric/km.).
- B_r arbitrary constant in solution of line differential equations (volts \angle).
- B_i arbitrary constant in solution of line differential equations (amperes \angle).
- B susceptance of an a.c. line (mhos).
- $b = c\omega$ linear susceptance of an a.c. line (mhos/wire km.).
- β, β_1, β_2 circular angles (radians or degrees); also slopes of complex quantities (degrees).
- C capacitance of a condenser or of a section conductor (farads).
- c_0 linear capacitance of pair of round parallel wires (stat-farads/loop cm.).
- $c_{,,}$ linear capacitance of pair of round parallel wires (farads/loop km.).
- c linear capacitance of pair of round parallel wires (farads/wire km.); also a constant quantity forming the successive denominators of a constant continued fraction (numeric \angle).
- γ admittance of a leak (mhos \angle).
- $\gamma = 1/\rho$ conductivity of a substance (abmhos per cm.); also the slope of the radius vector of an equiangular spiral (degrees).
- $\Gamma = 2\gamma$ admittance of a leak load (mhos \angle).
- D interaxial distance between two parallel cylindrical conductors (cm.).
- $d = v/V$ depression factor of a leak applied to a line (numeric \angle); also in theory of alternating continued fractions the ratio $\sqrt{a/b}$ (numeric \angle).
- Δ', Δ'' auxiliary hyperbolic angles (hyps. \angle).
- $\delta_A, \delta_B, \delta_C, \delta_P$ position angles at generator end A , at motor end B and at points C and P , on a line (hyps. \angle).

- δ_N, δ_N position angle of junction N or leak N of an artificial line (hyp. \angle).
- E electromotive force (r.m.s. volts).
- $e = 2.71828$. . . Napierian base.
- f impressed frequency (cycles/sec.).
- $F_n()$ a continued fraction of n stages.
- $f(nv), f'(nv)$ generic hyperbolic functions of nv in the theory of alternating continued fractions (numeric \angle).
- G total dielectric admittance of a line (mhos \angle); in the d.c. case total dielectric conductance.
- G_1, G_2, G_3 line admittances to ground on each side of a leak respectively, and their sum (mhos \angle).
- G_P, G_C line admittance beyond any point P and a reference point C of a line (mhos \angle).
- G_N, G'_N line admittance at leak N excluding and including that leak respectively (mhos \angle).
- G''_N line admittance at junction N of a Π line including the half leak $g/2$ only (mhos \angle).
- G_{CN}, G_{CN} line admittance at position of junction N , or of leak N on a conjugate smooth line (mhos \angle).
- g linear dielectric admittance of a line (mhos/wire km. \angle), in the d.c. case linear dielectric conductance.
- g_1, g_2 linear dielectric admittance per wire km. and per loop km. respectively (mhos/km. \angle).
- g_1, g_2 pillar leak admittances of an equivalent Π (mhos \angle).
- $g_0 = 1/r_0$ surge admittance of a line, in the d.c. case surge conductance (mhos \angle).
- $g''_0 = \sqrt{g/r}$ apparent surge admittance of a Π section, uncorrected for lumpiness (mhos \angle).
- g leak admittance per section of artificial line (mhos \angle).
- g' admittance in the staff of an equivalent T (mhos \angle).
- g'' admittance in the pillar of an equivalent Π (mhos \angle).
- Θ angle subtended by a line comprising a plurality of sections (hyp. \angle).
- θ_a apparent angle subtended by a T or Π section, uncorrected for lumpiness (hyp. \angle).
- $\theta_1, \theta_2, \theta_3$ hyperbolic angles (hyp. radians or hyp. \angle), angles subtended by successive sections of a composite line (hyp. \angle).
- θ_1, θ_2 real and imaginary components of a hyperbolic angle (numerics).
- $\theta, d\theta$ hyperbolic angle and element (hyp. radians \angle).
- θ angle subtended by a line (hyp. \angle).
- θ_1, θ_2 hyperbolic angle per wire and per loop (hyp. \angle).
- θ' angle subtended by a terminal impedance load at motor end of line (hyp. \angle).
- θ section angle after regular loading (hyp. \angle).
- θ'' auxiliary hyperbolic angle of a sending-end impedance.
- I line current at any point of a smooth line (amperes \angle).

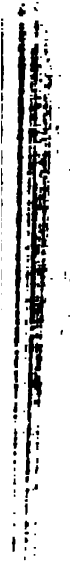
- I_1 line current at a point 1 km. beyond the reference point (amperes \angle).
 I_A line current at generator end A of a line (amperes \angle).
 I_B line current at motor end B of a line (amperes \angle).
 I_C line current at point C on a line, where the electrical conditions are known (amperes \angle).
 I_P line current at point P on a line, where the electrical conditions are known (amperes \angle).
 I_m maximum cyclic current strength (amperes).
 $I_N, I_{\mathbb{N}}$ line current at junction N and leak \mathbb{N} of an artificial T line (amperes \angle).
 $I_{cN}, I_{e\mathbb{N}}$ line current at position of junction N and leak \mathbb{N} on a conjugate smooth line (amperes \angle).
 i_1, i_2 changes in line current on each side of a leak due to its admittance (amperes \angle).
 I_a, I_x active and reactive components of a stationary vector current I (r.m.s. amp.).
 $J_0(\alpha_0 x)$ Bessel function of $(\alpha_0 x)$ of zeroth order (numeric \angle).
 $J_1(\alpha_0 x)$ Bessel function of $(\alpha_0 x)$ of first order (numeric \angle).
 $j = \sqrt{-1}$.
 $k = V/v$ correcting factor for a leak applied to a line (numeric \angle); also the ratio σ/r_0 of a terminal load to the surge impedance (numeric).
 k_v correcting factor for the semi-section angle v of an artificial line section (numeric \angle).
 k_ρ correcting factor for line branches of a nominal T (numeric \angle).
 k_σ correcting factor for staff leak of a nominal T (numeric \angle).
 $k_{\rho,,}$ correcting factor for architrave of a nominal Π (numeric \angle).
 $k_{\sigma,,}$ correcting factor for pillar leaks of a nominal Π (numeric \angle).
 κ permittivity of a dielectric (nominal numeric).
 L length of a line (km.).
 L_1, L_2 distances of a point on a line from the generator and motor ends respectively (km.).
 \mathcal{L} inductance of a coil or of a line (henrys).
 l linear inductance of a line (henrys/wire km.).
 l_0 linear inductance of a pair of parallel wires (abhenrys/loop cm.).
 $l_{,,}$ linear inductance of a pair of parallel wires (henrys/loop km.).
 λ wave length on an a.c. line (km.).
 M complex multiplier of $z_1 \sinh \delta_A$ in the theory of composite line equivalent Π architrave (numeric \angle).
 $m = \frac{r}{2} + \sigma$ impedance beyond leak I of a T line (ohms \angle); also the denominator of the terminal load of an alternating continued fraction (numeric \angle).

- m_v transmission coefficient of voltage wave at transition from z_1 to z_2 (numeric \angle).
- m_c transmission coefficient of current wave at transition from z_1 to z_2 (numeric \angle).
- $\mu = \frac{g}{2} + \gamma$ admittance beyond motor end terminal of a Π line, including terminal leak (mhos \angle); also in theory of composite lines $\mu = 1/\sigma$ admittance of a terminal load (mhos \angle); internal permeability of a wire (gausses/gilberts per cm.).
- N, \bar{N} number of a junction and of a leak, respectively, in an artificial line, starting from the motor end (numeric).
- n number of sections in a multi-section line (numeric); also number of stages in a continued fraction; also exponent of a number (numeric); also ratio of voltage transformation in a transformer (numeric).
- n_o, n_e odd and even numbers of stages in a continued fraction.
- $\nu = 1/\rho''$ admittance of a Π architrave (mhos \angle).
- ν_1, ν_2 architrave admittances on each side of a leak load (mhos \angle).
- P_a active component or real component of complex power (watts).
- P_x reactive component or imaginary component of complex power (j watts).
- P_P, P_C volt-amperes or size of complex power at selected point P , and at reference point C of a line (volt-amperes); volt-amperes or size of complex power.
- $P_{cN}, P_{c\bar{N}}$ volt-amperes at position of junction N or leak \bar{N} on a conjugate smooth line (volt-amperes).
- Π a delta connection of three impedances simulating a line at an assigned frequency.
- $\pi = 3.14159 \dots$
- q the imaginary component of a complex hyperbolic angle expressed in quadrants instead of in radians.
- R_N impedance at junction N , especially in c.c. case (ohms \angle).
- $R_{\bar{N}}, R'_{\bar{N}}$ impedance at leak \bar{N} , excluding and including that leak respectively (ohms \angle) especially in c.c. case.
- R_{fA}, R_{gA} line impedances at generator end A , when respectively freed and grounded at far end (ohms \angle).
- R_{fN}, R_{gN} corresponding line impedances at and beyond junction N (ohms \angle).
- R_f, R_g impedance offered by a line when freed and grounded respectively at the distant end (ohms \angle).
- $R' = 1/G$ impedance equivalent of a total line leakance G (ohms \angle).
- R_i receiving-end impedance of a line, in c.c. case receiving-end resistance (ohms \angle).
- R total conductor impedance of a line (ohms \angle); in the d.c. case, total conductor resistance.
- R_o, R_e total conductor impedance per wire and per loop respectively (ohms \angle).

- R''_N line impedance at junction N of a Π line, including a half-leak only (ohms \angle).
- R_B, R_C, R_P line resistance beyond a generator end A , a motor end B , a reference point C and a selected point P (ohms \angle).
- $Y'' = 1/g''$ impedance in pillar leak of an equivalent Π (ohms \angle).
- $R_{cN}, R_{c\bar{N}}$ line impedances at positions of a junction N and leak \bar{N} , respectively, on a conjugate smooth line (ohms \angle).
- r linear conductor impedance of a line (ohms/wire km. \angle); in the c.c. case linear conductor resistance.
- r' linear resistance of a round wire as influenced by skin effect (ohms/wire km).
- r , linear resistance per wire km. (ohms/w. km.).
- r_l , linear resistance per loop km. (ohms/l. km.).
- $v = \sqrt{r/g}$ surge impedance of a line (ohms \angle).
- r_0', r_0'' surge impedance of wire line and of loop line, respectively (ohms \angle).
- r'_0 apparent surge impedance $\sqrt{r/g}$, uncorrected for lumpiness (ohms \angle).
- r line impedance per section of an artificial line (ohms \angle).
- ρ length of a radius vector in polar coordinates (cm.); also size of a complex quantity (numeric); also radius of a wire (cm.); also virtual internal resistance of a condenser (ohms); also resistivity of a substance (abohm-cm.).
- ρ' resistance in branch of an equivalent T (ohms \angle).
- ρ'' resistance in architrave of an equivalent Π (ohms \angle).
- s, ds arc and arc element (cm. or circular radians).
- σ impedance load to ground or zero potential at motor end of a line (ohms \angle).
- $\Sigma = 2\sigma$ regular impedance load (ohms \angle).
- T a star connection of three impedances simulating a line at an assigned frequency; also the time of single transit of a voltage or current wave over a line (sec.).
- t elapsed time (seconds).
- $v = \theta/2$ semi-section angle (hypos.); also apparent velocity of propagation along a line (km./sec.).
- v', v'' auxiliary hyperbolic angles in theory of continued fractions (hypos. \angle).
- v_0 apparent semi-section angle of a T section, uncorrected for lumpiness (hypos. \angle).
- V potential at any point on a line (volts \angle).
- V_1 potential at a point 1 km. beyond the reference point (volts \angle).
- V_A potential at generator end A of a line (volts \angle).
- V_B potential at motor end B of a line (volts \angle).
- V_C potential at a point C of a line, where the electrical conditions are known (volts \angle).
- V_P potential at a point P on a line (volts \angle).
- V_X potential at an unknown point X on a line fed from both ends (volts \angle).

- V_N, V_N potential at junction N and leak N of an artificial line (volts \angle).
- V_{cN}, V_{cN} potential at position of junction N and of leak N , respectively, on a conjugate smooth line (volts \angle).
- v potential at a leak in the presence of its admittance (volts \angle).
- $V'_1, V'_2, V'_3 \dots$ Fourier sine component amplitudes of a complex harmonic voltage wave (volts).
- $V''_1, V''_2, V''_3 \dots$ Fourier cosine component amplitudes of a complex harmonic voltage wave (volts).
- $V_{r1}, V_{r2}, V_{r3} \dots$ Fourier resultant component amplitudes of a complex harmonic voltage wave (volts).
- $V_0, V_1, V_2, V_3 \dots$ Fourier resultant r.m.s. component amplitudes of a complex harmonic voltage wave (volts).
- φ phase angle of a condenser (defect from 90°) (degrees).
- W maximum cyclic energy in a.c. circuit or conductor (joules).
- W_a active or real component of W (joules).
- W_s reactive or imaginary component of W (joules).
- $W_m = 2W_s$ maximum cyclic magnetic energy in a.c. circuit or conductor (joules).
- X reactance of a coil or of a line (ohms); also in the theory of skin effect, the radius of a conducting wire (cm.).
- x Cartesian coördinate on X axis; also distance along a line from a reference point in a down-energy direction (km.); also radius of a point in the cross-section of a wire (cm.).
- Y dielectric admittance of a line (mhos \angle).
- Y_{fA}, Y_{gA} line admittance at A , with motor end freed and grounded (mhos \angle).
- y Cartesian coördinate on Y axis.
- $y_0 = 1/z_0$ surge admittance of a line (mhos \angle).
- y_0' surge admittance of a line after regular leak loading (mhos \angle).
- $y = g + jb$ linear dielectric admittance of a line (mhos/wire km. \angle).
- y'' linear dielectric admittance of a line (mhos/loop km. \angle).
- $y_{00} = 1/z_{00}$ limiting value of surge admittance of a line neglecting losses (mhos).
- $Z = R + jX$ impedance of a coil or of a line conductor (ohms \angle).
- Z_{fA}, Z_{gA} line impedance at A with motor end freed and grounded (ohms \angle).
- z' linear impedance of a round wire due to skin effect (ohms/wire km. \angle).
- z_0 surge impedance of a line (ohms \angle).
- $z_{0''}$ surge impedance of a two-wire line (loop ohms \angle).
- z'_0 apparent surge impedance $\sqrt{r/g}$ of a T line (ohms \angle).
- z''_0 apparent surge impedance $\sqrt{r/g}$ of a Π line (ohms \angle).
- $z = r + jx$ linear conductor impedance of a line (ohms/wire km. \angle).
- $z_{,,} = r_{,,} + jx_{,,}$ linear conductor impedance of a line (ohms/loop km. \angle).
- z_r impedance of a motor-end load (ohms \angle).
- $\omega = 2\pi f$ angular velocity or angular frequency (radians per sec.).

- $\omega_g = 4f$ angular velocity or angular frequency (quadrants per sec.).
 $z_{00} = \sqrt{l/c}$ limiting value of surge impedance ignoring losses (ohms).
 z_1, z_2, z_3 in theory of composite lines, surge impedance of successive sections (ohms \angle).
 z_0 , surge impedance of a line section after loading (ohms).
 α sign of infinity.
 \angle sign of a complex quantity or of the slope of a complex quantity.
 $|\alpha|$ size of the complex quantity α (numeric).
 α slope of the complex quantity α (degrees or radians).
 \sim sign for "cycles per second."
 Ω sign for ohms impedance.
 \mathfrak{U} sign for mhos admittance.
 \cong sign for "nearly equals," or approximate equality.
 f sign for farads capacitance.
 μf sign for microfarads capacitance.
 $m\mu f$ sign for millimicrofarads.
 $\mu\mu f$ sign for micromicrofarads.
 \log_h hyperbolic logarithm to base e .
 \log common logarithm to base 10.
 hyp. contraction for "hyperbolic radian."
 r.m.s. contraction for "root mean square."
 a.c. contraction for "alternating-current."
 c.c. contraction for "continuous-current."



INDEX

- Abhenry or C.G.S. magnetic unit of inductance, 143
 Active conductance, 129
 resistance, 125
 Actual velocity of propagation, 153
 Addition and subtraction of vectors, 117
 Admittance, linear wire, 149
 Aggregate conductor resistance R of a line, 16
 dielectric leakage G of a line, 16
 Ahlborn, G. H., 213
 All-capacitance artificial line, 312
 All-inductance artificial line, 312
 All-resistance artificial line, 312
 Alternating continued fractions, 327
 Alternating-current artificial lines, fundamental properties of, 164
 simple circuits, 124
 Anderson bridge, 234
 Angle hyperbolic of a line, 16
 Angles, real circular, 6
 real hyperbolic, 6
 Apparent velocity of propagation, 152
 Archtrave admittance, 242
 Artificial line, as frequency filter, 316
 definition of, 1
 homologous types of, 310
 principal purposes of, 1
 sections, unrealizable, 167
 various types of, 309
 lines and duplex telegraphy, 2
 historical outline of, 2
 Attenuation constant of a.c. line, 151
 of a line, 16
 factor, normal a.c., 156
 normal of a line, 18
 Axis of imaginaries, 114
 of reals, 114
 Becker, G. F., 120
 Bedell and Crehore, 127
 Bessel functions, 147
 Bifurcating composite lines, 275
 Bouton, C. L., 123
 Cable circuit, pure, 156
 Campbell, A., 236
 Campbell bridge, 234
 Campbell, G. A., 110, 302
 Campbell mutual-inductance bridge, 235
 Cantilevers, 252
 Casual loads, 254
 Changes in archtrave formula with casual loads, 276
 Characteristic resistance of a line, 19
 Chrystal, G., 123
 Circuit, distortionless, 154
 Circular angles, real, 6
 and hyperbolic formulas list of, 323
 Clerk-Maxwell, 141
 Cohen, B. S., and Shepherd, G. M. B., 181
 Cohen, B. S., 233
 Complex harmonic waves, 192
 hyperbolic angles, 119
 quantities defined, 113
 Composite line, a.c. example, 261
 of impedance terminal loads 268
 archtrave and casual loads, 276
 impedance, second method, 250
 attenuation in miles, 286
 definition of, 15
 equivalent Π of, 249
 intermediate leak loads in, 272
 impedance loads in, 269
 laboratory tests of, 280
 terminal series loads of, 254

- Composite line, leak loads in, 271
 transformer in, 278
 lines, 240
 bifurcating, 275
 line-current distribution over, 247
 position-angle distribution over, 245
 power distribution over, 247
 Condensive susceptance, 129
 Conjugate smooth line, 62, 64
 Constant, attenuation, of a line, 16
 continued fractions, 327
 propagation, of a line, 16
 wave-length, 152
 Constants, linear of a real line, 15
 Contacting polygons, internal and external, to equiangular spiral, 169
 Continued fractions, alternating and constant, 327
 Correcting factor for a leak load, 111
 factors for T and Π sections, 91
 Cosine of complex hyperbolic angle, 120
 Cosines of real circular and hyperbolic angles, 9
 Crab addition or perpendicular summation, 194
 Cunningham, J. H., artificial line design, 5
 Current at point along line in terms of position angle, 39
 Cycloid, 136

 Depression factor of a leak load, defined, 111
 Design and construction of artificial a.c. lines, 196
 Detection of even-frequency harmonics, 319
 Detectors of frequency variations, artificial lines, 322
 Distortionless circuit, 154
 Distribution of c.c. line tests among observers, 106
 Disturbances in potential and current due to a leak, 106
 Division of vectors, 118

 Double surge impedance, T and Π sections of, 211
 Douglas, J. F. H., 292
 Drysdale, C. V., 158, 224
 Drysdale-Tinsley potentiometer, 222
 Duplex telegraphy and artificial lines, 2

 Even-frequency harmonics, detection of, 319
 Equiangular spiral, 157
 polygon, 169
 Equivalent circuits defined, 89
 Π defined, 89
 of composite line, 249
 T defined, 89
 Estwick, C. F., 215
 Exponential case, 45
 Exponentials, geometrical interpretation of, 12, 13
 External contacting polygon to equiangular spiral, 169
 linear loop and external linear wire inductance, 141, 142

 Factor, normal attenuation, of a line, 18
 Feldmann and Herzog, 92
 Fictitious impedance diagrams, 140
 Filter of frequencies, artificial line for, 316
 Fleming, J. A., 115, 116, 224, 235
 Four-wire artificial lines, 56
 Fractions, alternating continued, 327
 Frequency filter, 316
 limitations of artificial lines, 239
 measurements, 238
 Frequencies, range of, 125
 Functions, Bessel, 147
 Fundamental and secondary constants of a line, 22
 differential equation of line, complete solution of, 28
 of a smooth line, 24

 Gati, B., 233
 General Railway Signal Co., artificial track circuit, 215

- Generator end of line defined, 30
 Graphical relation between potential and current spirals, 159
 Gray, A., 110
 Greenhill, A. G., 135, 157
 Grover, F. W., 237

 Half-wave and quarter-wave lines, 288
 Harmonic suppression, under, 318
 upper, 317
 Harmonics, detection of even-frequencies, 319
 sine and cosine, 193
 Heaviside, O., 24, 29, 154, 163, 243
 Herzog and Feldmann, 92
 Historical outline of artificial lines, 2
 Homologous types of artificial line, 310
 Huxley, R. D., 204
 Hyperbolic and merger II of composite line, 243
 angle, linear, of a line, 16
 angles, complex, 119
 real, 6
 Hyperbolic-cosine, infinite series of integers, 314
 radians, 7, 16
 -sine infinite series of integers, 314

I Sections of artificial line defined, 166
 Imaginary axis, 114
 component of rectangular vector, 114
 Impedance graphs on artificial and a.c. conjugate smooth lines, 184
 model of a.c. line, 231
 tests, 219
 Inductive reactance, 125
 susceptance, 129
 Infinite series of numbers, hyperbolic-sine and cosine, 314
 Infr surge impedance, 51
 Initial current at sending end, 161
 Intermediate impedance load in composite line, 269

 Intermediate, leak loads in composite line, 272
 Internal contacting polygon to equiangular spiral, 169
 linear impedance of a wire, 148
 loop and internal linear wire inductance, 141, 142
 Involution and evolution of vectors, 119
 Iterative resistance of a line, 19

 Jahnke and Emde, 147

 Laboratory tests of composite line, 280
 Laws, F. A., and Pierce, P. H., 147
 Leak loads, 254
 regular, 304
 Leblanc, M., 163
 Lewis, L. V., 215
 Line admittance, 48
 current tests by ammeter, 232
 impedance, 48
 reactors, design of, 197
 resistance in unsteady state, 51
 Lines regularly loaded, 300
 Linear and total hyperbolic angles of a line, 21
 complex hyperbolic angle of line or section, 149
 constants of a line, 15
 dielectric leakage and admittance of a real line, 15
 hyperbolic angle of a line, 16, 17
 impedance, internal, of a wire, 148
 inductance, 141
 loop capacitance, 142
 inductance, 141
 reactance, 145
 susceptance, 147
 resistance and impedance of a real line, 15
 wire admittance, 149
 capacitance, 144
 impedance, 147
 inductance, 142
 reactance, 145
 susceptance, 145

- Loaded lines, regularly, 300
 Loads, casual, 254
 leak, 254
 regular, 254
 leak, 304
 Loop capacitance, linear, 142
 inductance, linear, 141
 -kilometer or loop-mile constants, 21
 reactance, linear, 145
 surge impedance, 161
 susceptance, linear, 147
 Lossless line, 154
 Lumpy artificial lines classified, 55
 lines, definition of, 2

 Magnusson, C. E., Gooderham, J.,
 and Rader, R., 204
 and Burbank, S. R., 204, 291
 McCready, Harold, 213
 Measurement of individual induc-
 tances, 233
 Merger II, 243
 Motor end of line defined, 30
 Muirhead, Alex, artificial submarine
 cable, 3
 Multiplication of vectors, 117

 Natural resistance of a line, 19
 Negligible line leakage and reduc-
 tion to Ohm's law, 36
 Nominal II, defined, 91
 T defined, 90
 Normal a.c. attenuation, 156
 defined, 45
 factor, 45
 of a line, 18
 graphs on a. c. lines, 167
 spiral, 157
 waves, 161
 Numbers, hyperbolic-sine and cosine,
 infinite series of, 314

O Sections of artificial line defined,
 166
 Orthogonal projection, 13
 Osborne, H. S., and Pender, H., 144
 Overhead aerial lines and their leaks,
 28

 Pender and Huxley design of reactor,
 144, 205
 and Osborne, 144
 Perpendicular summation or crab
 addition, 194
 II-line admittance on each side of a
 junction, 74
 currents at junctions, 77
 at mid-sections, 84
 defined, 57
 distributions worked out, 78, 79,
 80
 impedances at junctions, 69
 at mid-sections, 84
 junction potentials, 76
 lumpiness correction factor, 73
 potential at mid-sections, 83
 powers at mid-sections, 84
 section angle, 72

 Plane vectors defined, 113
 polar, 115
 rectangular, 114
 Plug contact piece, 209
 Plural frequencies on a.c. lines,
 192
 Position angle, definition of, 37
 distribution on composite
 line, 245
 angles, solution in terms of, 37
 Potentials in terms of position
 angles, 38
 Potentiometer and voltmeter meth-
 ods compared, 230
 tests of c.c. artificial line, 103
 Power at any point of a line, 53
 on a.c. lines, 187
 Primitive of fundamental differen-
 tial equations of line, 28
 Prolate trochoid, 136
 Projection orthogonal, 13
 Propagation constant of a line, 16
 Properties of real circular and hyper-
 bolic angles, 7
 Pupin, M. I., artificial lines, 4
 Pure cable circuit, 156

 Quadrant measure for circular
 angles, 123

- wave and half-wave lines, 288
 hyperbolic, 7, 16
 of frequencies, 125
 of formula for skin effect, 148
 of surge impedance, 163
 of circuit, 155
 of, non-ferric, 204
 of wire frame, 202
 of angles, 114
 of similar and hyperbolic angles, common properties of, 7
 of numerical values of sines, and cosines, 8
 of angles, 6
 of component of rectangular vector, 114
 of hyperbolic angles, 6
 of quantities defined, 113
 of sending-end impedance defined, 52
 of angles of vectors, 119
 of similar plane vectors, 114
 of formulas from circular to hyperbolic trigonometry, 10
 of coefficients for individual waves, 243
 of leak loads, 304
 of, 254
 of γ loaded lines, 300
 of β , characteristic, 19
 of α , 19
 of θ , 18
 of transition from T or Π section to conjugate smooth line, 93
 of J. W., 320
 of H. D., 238
 of power diagram, 134
 of vector diagrams, 132
 of A., 144
 of γ and fundamental constants of a line, 22
 of angle, uncorrected, 58
 of capacitances, measurements of, 236
 of Semi-imaginary quantities, 154
 of Sending-end impedance measurements, 220
 of Sending end, initial current at, 161
 of Series-resistance method of measuring capacitances, 237
 of Shepherd, G. M. B., 197, 316
 of Shepherd, G. M. B., and Cohen, B. S., 181
 of Silsbee, F. B., 144
 of Similarity of sectors in normal attenuation spiral, 160
 of Simple alternating-current circuits, 124
 of Sine and cosine harmonics, 193
 of of complex hyperbolic angle, 121
 of Sines of real circular and hyperbolic angles, 9
 of Single-wire and two-wire line constants, 20
 of artificial lines, 55
 of Size of vector defined, 115
 of Skin-effect in round wires, 147
 of Slope of vector defined, 115
 of Smooth lines, definition of, 1
 of Splash, 161
 of Square-frame reactors, 202
 of Standard twisted-pair telephone cable, 150
 of Statfarad or C.G.S. electrostatic unit of capacitance, 143
 of Stationary vector diagrams, 132
 of Steinmetz, C. P., 127, 279
 of Strehlke, A. B., 331
 of Super surge impedance load, 42
 of Surge admittance, 162
 of impedance, 160
 of reactanceless, 163
 of uncorrected, of a section, 59
 of resistance of a line, 18
 of T and Π sections of double surge impedance, 210
 of Tangent of complex hyperbolic angle, 123
 of Tangents and antitangents, 41
 of of real circular and hyperbolic angles, 9

